PB82-196544

REPORT NO.
UCB/EERC-80/42
DECEMBER 1980

EARTHQUAKE ENGINEERING RESEARCH CENTER

EVALUATION OF A SHAKING TABLE TEST PROGRAM ON RESPONSE BEHAVIOR OF A TWO STORY REINFORCED CONCRETE FRAME

by

J. MARCIAL BLONDET
RAY W. CLOUGH
STEPHEN A. MAHIN

Report to the National Science Foundation

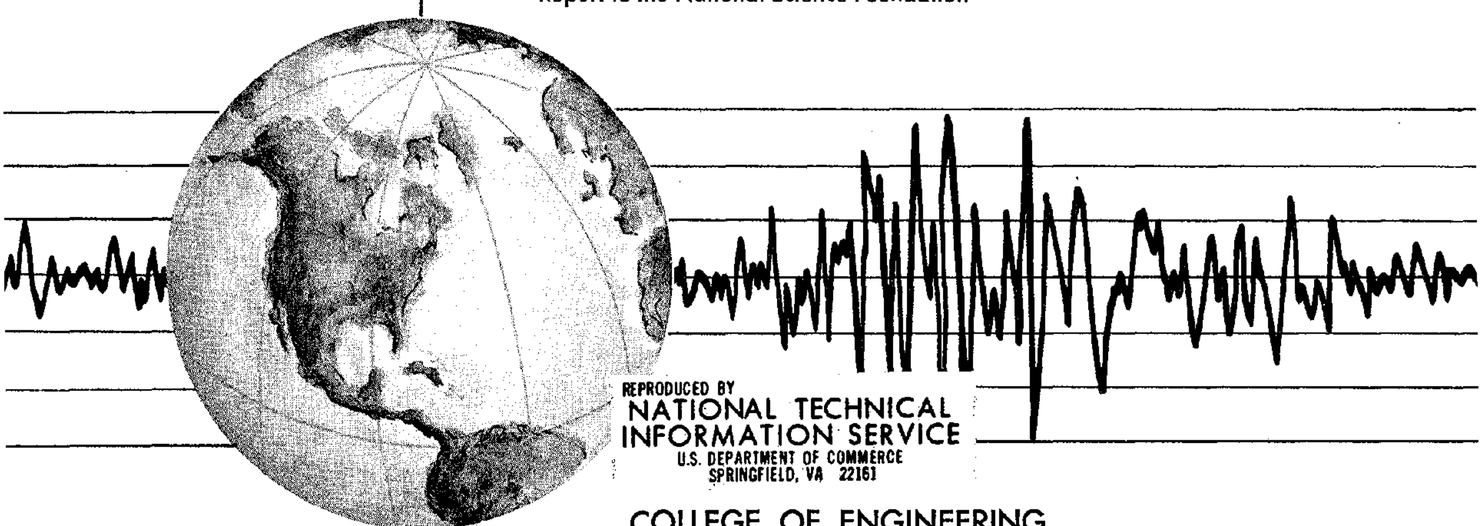

REPRODUCED BY
NATIONAL TECHNICAL INFORMATION SERVICE
U.S. DEPARTMENT OF COMMERCE
SPRINGFIELD, VA 22161

COLLEGE OF ENGINEERING
UNIVERSITY OF CALIFORNIA · Berkeley, California

For sale by the National Technical Information Service, U.S. Department of Commerce, Springfield, Virginia 22161.

See back of report for up to date listing of EERC reports.

DISCLAIMER

Any opinions, findings, and conclusions or recommendations expressed in this publication are those of the authors and do not necessarily reflect the views of the National Science Foundation or the Earthquake Engineering Research Center, University of California, Berkeley.

REPORT DOCUMENTATION PAGE	1. REPORT NO. NSF/RA-800547	2.	3. Recipient's Accession No. PB82 196544
4. Title and Subtitle: Evaluation of a Shaking Table Test Program on Response Behavior of a Two Story Reinforced Concrete Frame			5. Report Date: December 1980
			6.
7. Author(s): J. Marcial Blondet, Ray W. Clough, Stephen A. Mahin			8. Performing Organization Rept. No.: UCB/EERC-80/42
9. Performing Organization Name and Address: Earthquake Engineering Research Center, University of California, Berkeley, 47th Street and Hoffman Blvd., Richmond, CA. 94804			10. Project/Task/Work Unit No.
			11. Contract(C) or Grant(G) No. (C) (G) PFR-7908257
12. Sponsoring Organization Name and Address: National Science Foundation, 1800 G Street, N.W., Washington, D.C. 20550			13. Type of Report & Period Covered
			14.
15. Supplementary Notes			

16. Abstract (Limit: 200 words)

This report presents an evaluation of the different stages involved in an experimental study of the seismic behavior of a reinforced concrete structure, by means of an earthquake simulator (shaking table). The discussion is focused mainly on how representative the test structure and the table input motions are with respect to the actual, "real life" buildings and seismic ground excitations. The design of the structure is then reviewed from the point of view of a current seismic code, and the experimental results are compared with analytical expectations as well as with the design demand levels.

The last chapter summarizes the conclusions obtained and points out areas for future research.

i.a

18. Availability Statement:	19. Security Class (This Report)	21. No. of Pages
Release Unlimited		245
	20. Security Class (This Page)	22. Price

(See ANSI-Z39.18) See Instructions on Reverse OPTIONAL FORM 272 (4-77) (Formerly NTIS-35) Department of Commerce

EVALUATION OF A SHAKING TABLE TEST PROGRAM ON RESPONSE BEHAVIOR OF A TWO STORY REINFORCED CONCRETE FRAME

by

J. Marcial Blondet

Ray W. Clough

and

Stephen A. Mahin

A Report to the National Science Foundation

Report No. UCB/EERC-80/42

Earthquake Engineering Research Center
University of California
Berkeley, California

December 1980

i.b

ABSTRACT

This report presents an evaluation of the different stages involved in a experimental study of the seismic behavior of a reinforced concrete structure, by means of an earthquake simulator (shaking table). The discussion is focused mainly on how representative the test structure and the table input motions are with respect to the actual, "real life" buildings and seismic ground excitations. The design of the structure is then reviewed from the point of view of a current seismic code, and the experimental results are compared with analytical expectations as well as with the design demand levels.

The last chapter summarizes the conclusions obtained and points out areas for future research.

ACKNOWLEDGEMENTS

The research presented in this report has been financially supported by the National Science Foundation whose continuous sponsorship for Earthquake Engineering research is gratefully acknowledged.

The first author is deeply grateful to the Latin American Scholarship Program of American Universities (LASPAU), and to the Pontificia Universidad Católica del Perú, for having provided him with the opportunity to pursue graduate studies at Berkeley.

Many thanks are due to Ruth Canier and Shirley Edwards who typed the manuscript and to Gail Feazell, Mary Edmunds and Gert Weil for their care and dedication in preparing the graphics.

The Computing Center of the University of California, Berkeley provided the computing and plotting facilities.

This report constituted the Master of Engineering Thesis of the first author; the work was supervised by the second and third authors.

TABLE OF CONTENTS

Preceding page blank

Page

LIST OF TABLES

Preceding page blank

LIST OF FIGURES

Preceding page blank

Figure		Page
4.4	Determination of Required Confinement Length for Ideal Model Columns (Section 2626f - UBC79)	105
4.5	Flexural Strength Requirements for Ideal Model Bottom Story Girder	106
4.6	Flexural Strength Requirements for Ideal Model Top Story Girder	107
4.7	Shear Distribution in Girders. Ideal Model Elastic Analysis	108
4.8	Shear Panel Analogy to Determine Shear Stresses at Joints . . .	109
5.1	Displacement Response of RCF2 During Run W1; Solid Line - Bottom Floor; Dashed Line - Top Floor (Relative to Table). . . .	122
5.2	Top Story Drift. Run W1	123
5.3	Bottom Story Shear (from Acceleration Records). Run W1	124
5.4	Top Story Shear (from Acceleration Records). Run W1	125
5.5	Bottom Story Shear vs. Drift Relationship. Run W1	126
5.6	Top Story Shear vs. Drift Relationship. Run W1	127
5.7	Bottom Story Shear vs. Drift Relationship during 5-sec Intervals. Run W1	128
5.8	Top Story Shear vs. Drift Relationship during 5-sec Intervals. Run W1	129
5.9	Actual vs. "Gross Section" Lateral Stiffness. Run W1	130
5.10	Displacement Response of RCF2 During Run W2; Solid Line - Bottom Floor; Dashed Line - Top Floor (Relative to Table). . . .	131
5.11	Top Story Drift. Run W2	132
5.12	Bottom Story Shear (from Acceleration Records). Run W2	133
5.13	Top Story Shear (from Acceleration Records). Run W2	134
5.14	Bottom Story Shear vs. Drift Relationship. Run W2	135
5.15	Top Story Shear vs. Drift Relationship. Run W2	136
5.16	Bottom Story Shear vs. Drift Relationship during 5-sec Intervals. Run W2	137

1. INTRODUCTION

1.1 Objective of Study

During the past few years, a considerable amount of research regarding the behavior of reinforced concrete structures under seismic excitation has been carried out at the University of California, Berkeley. An important part of this research has been done using the shaking table facility at the Earthquake Simulator Laboratory located at the Richmond Field Station, Richmond, California, as part of the research program "Energy Absorption Characteristics of Structural Systems Subjected to Earthquake Excitations," sponsored by the National Science Foundation.

Five reinforced concrete frames, in reduced scale have been tested on the shaking table, and an impressive amount of valuable information regarding various types of structural behavior under different levels of seismic excitations has been obtained from such tests. The results from these experiments have been published in several reports (References [1] to [6]) or are in process of preparation for publication.

However, it has become apparent that a global evaluation of the diverse procedures involved in the development of each phase of the experiments, and of the information obtained from the tests, would be desirable before proceeding with further testing. The main purpose of the evaluation would be to obtain an overall view of what has been learned from the experiments, presenting the acquired knowledge in a systematic way, not as the results of a series of isolated tests. It is expected that the study would provide guidelines for future testing.

In order to fully achieve the stated goal, it would be necessary to evaluate the following aspects of the testing procedure:

1) The design of the test models, and their capability to adequately simulate actual structures subjected to realistic earthquake-induced ground motions and/or to perform according to a selected type of structural behavior.

2) Selection of the test program; this involves the selection of shaking table inputs to the structure, the number of tests to be performed and the instrumentation needed to record the desired information. Of particular interest is whether or not the selected table motions are representative of actual ground motions produced by earthquakes.

3) Prediction of structural behavior; this is necessary in order to verify whether the design of the models and the test program is adequate to obtain the desired structural performance. Both "standard" and "state-of-the-art" techniques to predict response behavior, should be examined.

4) Data reduction and interpretation of results; this is a crucial phase of the process, since it leads to an evaluation of the validity and accuracy of the analytical techniques used to predict the behavior of the test structure. Hence, it identifies areas where more research is needed to provide understanding of the mechanisms responsible for the observed behavior of the models during dynamic excitation.

This report summarizes the first step towards the goal outlined above. Its scope is limited, since only one of the structures tested has been examined, and only some of the factors discussed above are studied. However, it is expected that the results from this study will provide useful guidelines for further evaluations.

The basic aim of this study has been to provide answers to the following questions:

(a) Do the tests adequately simulate the behavior of a real reinforced concrete building subjected to earthquake-induced dynamic excitations?

(b) Does the design of the test structure satisfy current code requirements for structures to be built in regions of high seismic activity? If so, is the observed behavior of the structure adequate from the point of view defined by the code philosophy?

(c) How reliable are "standard," or code-related techniques, for predicting the dynamic behavior of reinforced concrete buildings under seismic excitations?

The second reinforced concrete test frame (RCF2) has been chosen for this study. The principal reasons for having chosen RCF2, among the five structures tested, can be summarized as follows:

1) Its design is simple from the point of view that it is derived directly from a typical two-story office building, basically by means of a dimensional reduction of about 30%. Also its structural behavior was controlled predominantly by flexure, in contrast with RCF3 and RCF4, where significant design distortions were introduced in order to produce models whose behavior would be controlled by shear.

2) Close inspection and control was exercised during its construction process, thus avoiding errors such as those found in RCF1[1], and guaranteeing uniformity in the material properties, and close correspondence with the structural plans.

3) The test program selected for this frame was particularly convenient since it consisted of a strong shaking applied to an essentially undamaged structure (simulating service conditions), followed by a strong aftershock. The table motion was applied along the major axis of the frame, thus simplifying interpretation of the results as compared with RCF5 which was subjected to shaking simultaneously along its two principal axes.

To facilitate and make this study more general, only the global behavior of the test structure is examined. Thus, the parameters used to define the structural performance are the story shears and drifts and the lateral stiffness and strength of the frame; the parameters used to define the table excitation are the peak table acceration, the shape of the acceleration response spectra, and the spectral intensity.

Finally, it should be noted that the conclusions of this investigation can be applied directly only to structures with characteristics similar to those of the prototype from which RCF2 was derived. Specifically, they apply to low rise R/C buildings for which behavior controlled by flexure can be guaranteed, and where the interference of so-called non-structural elements is minimized.

1.2 General Organization of Report

The first problem to be described and analysed in this study arises from the fact that the test structure presents deviations with respect to an ideal model obtained by applying similitude laws to the prototype building. These deviations and their probable effect on correlation between the performance of the test structure and that of the prototype are described in Chapter 2.

Chapter 3 is devoted to evaluation of the input motions, considering whether the table excitation corresponds to possible seismic ground motions, in prototype scale.

In Chapter 4, the design of the model is verified with reference to the Uniform Building Code, 1979[11]. This evaluation is considered necessary because the design of the prototype from which the test structure was derived was based on UCB 1970[9] and ACI 1971[10], codes which no longer are in use.

The overall performance of the structure is described in Chapter 5, and is compared with expected behavior indicated by analyses. Of particular interest is the comparison between the "ultimate" lateral forces specified by the code, and the corresponding inertia forces developed by the structure during the simulated seismic excitations, i.e. the relationship between the design lateral strength and the actual capacity demonstrated by the structure.

General conclusions are drawn in Chapter 6, providing answers to the questions defining the aims of this study, and emphasizing areas of needed research. A number of appendices are included at the end of the report in which the original design of the structure, and the computations of section properties according to several idealizations are presented.

2. PROTOTYPE, IDEAL MODEL AND ACTUAL TEST STRUCTURE

2.1 General Objectives

The test specimen which was the object of the present study can be regarded as the result of a series of modifications performed on a selected prototype structure representative of typical design and construction procedures. The aim of this chapter is to determine if the significant structural and dynamic characteristics of the prototype have been retained in the test structure, in order to ascertain whether the performance of the test structure during the dynamic tests simulates adequately the response of the prototype under strong seismic excitations.

In the following sections, the evolution of the test structure from the prototype building is studied, evaluating the relevance of each phase of the process with regard to the correlation between test structure and prototype.

Most of the information presented here regarding the genesis of the test structure, has been obtained from References [1] and [2], in which the structure design is described in detail.

2.2 The Prototype Structure

One of the basic features sought for the test specimen was that it should be a simple but complete structure, reproducing a "practical situation"[1]. The need for simplicity led to the selection as prototype of a building whose seismic deformations are predominately flexural, and not very sensitive to shear and axial forces. This type of behavior is desirable in framed structures subjected to seismic excitations. In addition it is the most studied- and understood- deformation mechanism in reinforced concrete structures, and a large number of computer programs and analytical techniques are available to predict such behavior.

It appeared suitable to select as a prototype structure a portion of the resisting frame of a narrow two story office building. Its dimensions are shown in Figure 2.1, and the computation of the story weights is summarized in Table 2.1. It should be noted that these values differ slightly from those computed in Reference [1] due to a different estimation of the weights of the girders and columns. It is assumed that the "non-structural" elements (such as walls and partitions) contribute to the weight but are isolated from the resisting frame. Thus, they do not contribute to the structural stiffness and strength of the building.

After having defined the essential characteristics of the building configuration, the resisting frame was designed according to UBC 1970[9] and ACI 1971 [10] codes. Appendix A, which has been taken from Reference [1] summarizes the philosophy and the procedures involved in the design of the prototype structure.

2.3 Scaling Process

When the prototype structure had been defined, further considerations in design of the test specimen were imposed by limitations of the shaking table system, by test convenience, and by economic factors. The limitations of the earthquake simulator facility are discussed extensively in Reference [7], the most significant for the case under consideration being that the specimen had to fit conveniently on the 20 x 20 ft table, with a total weight not in excess of 100 kips. Also it was considered desirable for the fundamental natural frequency to be in the range of 2 to 5 Hz.

Based on these considerations, it was decided to perform a length scale reduction of about 30% on the prototype structure. Accordingly, several other scaling ratios were selected and/or derived using similitude laws to establish the correspondence between model and prototype. A list of the scaling factors employed is presented in Table 2.2.

Strict application of the similitude laws to the prototype structure would lead to an ideal reduced model. Due to several reasons, which are discussed briefly in the next section, the actual test specimen has some significant differences from the ideal model; however, the test structure will be capable of simulating the global behavior of the prototype if its overall performance under lateral loads is comparable to that of the ideal model.

2.4 Ideal Model vs Test Structure

The most relevant discrepancies between ideal model and test structure result from the decision to reduce the distance between longitudinal frames as much as possible. This was done for test convenience and economic reasons, and was permissible because the frame was intended to be excited in one direction only. The term longitudinal refers here to the direction of the shaking table motion.

This reduction of width was performed taking into consideration the need for maintaining the T-beam action of the girders by providing the slab width recommended by the ACI code[10]. However, it should be noted that the ACI specifications concerning T-beam action are based on strength considerations, therefore there is a possibility that the stiffness contribution of the model floor diaphragm might be different from that in the test structure. This problem has not been dealt with in the present study.

Additional masses had to be included on both floors of the test structure, for the following reasons: to simulate the weight of the portion deleted by the reduction in width, to account for the weight of the non-structural elements not included in the test specimen and also to compensate for the fact that the material density was not scaled. Both the prototype and the test specimen were to be made of normal weight concrete.

These additional masses were added to the frame in the form of concrete blocks attached to the longitudinal girders. Their weight was computed to simulate only the dead load condition in the prototype; additional live load was not included for test safety reasons. The fact that the concrete blocks are attached to the longitudinal girders at "discrete" supports, caused the load distribution in the test structure to differ substantially from that of the ideal model, where the slab loads would be distributed over the longitudinal and transverse girders by two-way action. Furthermore, because of its reduced width, the slab in the test structure behaves as one-way slab, transmitting almost all its load to the longitudinal girders. These changes in distribution of the gravity loads acting on the test structure cause changes of the distribution of the internal forces, and hence would lead to a different pattern of cracking under service loads.

The presence of the concrete blocks on the test structure might also have affected the distribution of inertia forces during the dynamic excitation, because the blocks might suffer a "rocking" motion, thus inducing extra dynamic effects on the supporting girders. Since no recordings were made of the block motions during the tests, this effect was not taken into account in evaluating the experimental data, nor in the mathematical idealization of the test structure employed in various analyses made during this study.

Some other test structure features (such as the force transducers located at midheight of the columns to measure internal forces during the tests, the presence of lateral bracing to avoid torsional deformations, and a slight difference in lengths of the test structure columns compared to the ideal model's) might have some effect in the correlation process, but certainly to a much lesser extent than those discussed in the previous paragraphs.

Front and side elevations of the test structure are presented in Figure 2.2, and simplified sketches to compare the geometry and loads of the model and the test structure are shown in Figure 2.3. The original procedure for designing the test structure is presented in Appendix B, which is taken directly from Reference [1]. The details of the reinforcement of the test structure are shown in Figure 2.4; those of the ideal model are very similar. The main differences in reinforcement of the test structure are the use of undeformed #2 bars for the stirrups and the concentration of stirrups near the force transducers. Also there was a slightly inaccurate conversion of the reinforcing bar areas between the prototype and test structure (see Appendix B).

In order to quantify and evaluate the main difference between model and test structure, a number of analyses (elastic and elasto-plastic) were performed for both structures. The basic features to be examined and compared in these calculations are: the distribution of section forces; possible patterns of cracking under gravity loads; the lateral strength, ductility, and stiffness; the mass and lateral elastic flexibility matrices; and the vibration mode shapes and frequencies.

The assumptions made to idealize the structures, the limitations of the analyses performed and a discussion of the results obtained are presented in the following sections. The calculations leading to the numerical values employed in the analyses are detailed in Appendix C for the ideal model, and in Appendix D for the test structure.

2.5 Static and Elastic Vibration Analysis

The computer program ETABS[13] has been used to compute the distribution of section forces due to gravity loads as well as the vibration mode shapes and frequencies of both structures.

The following assumptions have been made, for both structures, for reasons of simplicity or to conform to the limitations of the program.

a) Each structure is a 3-D frame, in which the floor slabs are infinitely rigid in their own plane. The story masses are concentrated at the floor levels.

b) The members are linear elastic. Their stiffness characteristics are based on gross section geometric properties. The contribution of the slabs to the stiffness of the structure is considered by assuming a T-beam section for the girders, using slab widths and modulus of elasticity as recommended by the 1979 UBC code. The geometric characteristics of the transverse sections of the members are presented in Figure 2.5.

c) The joints are infinitely rigid, and the supports are completely fixed.

Figure 2.6 shows a view of the idealized frames in the longitudinal direction. The dimensions shown are center-to-center of members, those of the test structure correspond to the values measured in the laboratory and those of the ideal model were obtained by applying the appropriate scaling factor to the prototype. The computations of story masses and member loads are given in Appendices C and D. The results of these analyses can be summarized as follows:

2.5a Distribution of Internal Forces

The section forces on both structures, induced by gravity loads (dead load only) are presented in Table 2.3. As expected, the distributions of internal forces are very dissimilar, with differences as much as 150%. However, the stress levels associated with these static loads are very small compared with those developed under strong dynamic excitations, hence they would not be expected to significantly affect the overall inelastic behavior of the structures.

The dead load bending moment diagrams for both structures are shown in Figure 2.7, along with the respective cracking moment levels. It can be seen that the patterns of cracking are different, the test structure being cracked in the central regions of the bottom girder and in zones near the ends of the upper columns, whereas the ideal model would be practically uncracked. However, considering the effect of shrinkage, and the possibility of previous loading of the model (due to live load or a mild seismic excitation), it seems reasonable to assume that the levels and patterns of cracking of both structures would be similar, prior to the "strong" shaking simulated by the tests.

The low stress levels associated with shear and axial forces due to gravity loads also demonstrate the predominant role of flexure in the behavior of the structures. For instance, the axial load in the bottom story columns of both structures is about 10 kips, which is well below the balanced load (about 50 kips, computed using "standard" procedures) and produces an average compressive stress of about 200 psi (0.05 f'_c). This indicates that the columns would behave practically as flexural members.

The average shear stresses in the top story columns are

$$v_c = \frac{V}{bd} = \frac{1.20\text{x}1000}{5.66\text{x}6.86} = 30.9 \text{ psi}$$

for the ideal model, and

$$v_c = \frac{V}{bd} = \frac{1.62\text{x}1000}{5.75\text{x}6.75} = 41.7 \text{ psi}$$

for the test structure. Comparing these values with the conservative estimate of the shear strength of the concrete given by $2\sqrt{f'_c}$ (126.5 psi), it can be seen that under gravity loads, the shear forces are of little relevance.

2.5b <u>Dynamic Properties</u>

The natural mode shapes and frequencies of vibration of both structures were calculated; in addition, lateral flexibility matrices were generated by the application of unit lateral forces at each floor level of the structures.

The results of these analyses, which summarize the dynamic characteristics of ideal model and test structure in the elastic range, are presented in Figure 2.8. It can be seen that the differences, although significant (up to 15%), are within acceptable limits; thus the structures have reasonably similar dynamic properties.

2.6 Elasto-plastic Analysis

In order to compare the lateral strength and deformation capacity of the ideal model and the test stucture, a number of elasto-plastic analyses have been performed using the computer program ULARC[14], which is based on simple plastic theory. The basic assumptions used to idealize the structures and the manner of loading are:

a) The structures are assumed to be 2-D frames, composed of linear members, connected at nodal points.

b) The section flexural behavior is elasto-perfectly plastic. The section stiffness is based, as in the case of the elastic analysis, on the gross section characteristics, considering T-beam action for the girders. The flexural capacity is based on the specified material properties, and is computed according to procedures suggested by the UBC and ACI codes. Two sets of flexural capacities have been derived in order to obtain bounds for the lateral strength of the frames. The rotational deformation capacity of the sections is assumed to be sufficient to allow the development of the structural collapse mechanisms.

c) Since the program does not handle distributed loads on the members, only concentrated nodal loads are considered. The distributed loads are simulated by equivalent concentrated loads, computed using the replacement theorem of simple plastic theory. For simplicity of comparison the concentrated loads are assumed to be applied at the same points in both structures; their locations correspond to those of the supports of the concrete blocks on the test structure.

d) The lateral loads applied to both structures are approximately proportional to the inertia forces associated with the first mode of vibration, as computed in the elastic analysis.

e) The loads are applied in two stages. First the gravity loads (dead load only) are applied in full, and then, proportional monotonically increasing lateral forces are applied at the floor level until a mechanism is formed, and the frame collapses.

f) The inelastic deformation is assumed to be concentrated at point plastic hinges, which can develop only at the ends of the members.

g) The following effects are disregarded: strain hardening of the reinforcing steel, spalling and the effect of confinement on the concrete, possibility of shear failure, finite size of the joints and the inelastic regions, $P - \Delta$ effects, and axial force-bending moment interaction for the column capacity.

The idealized frames with the corresponding loads are shown in Figure 2.9, the calculations leading to the numerical values employed in the idealization process are presented in Appendices C and D.

The following results have been obtained:

2.6a Section Strength

In order to obtain bounds for the section strengths (and hence for the structural strength) these have been computed according to two different assumptions. A lower bound (Case I) was estimated using the specified material properties for f'_c (4.0 ksi) and f_y (40.0 ksi) and reducing the nominal strength thus obtained by a factor ϕ. Conservatively, ϕ has been set equal to 0.7 for the columns, and to 0.9 for the girders. An upper bound (Case II) was obtained by considering an increase of the yield stress of the steel of 25%, (thus considering $f_y = 1.25\ f_y$ specified = 50.0 ksi) and deleting the capacity reduction factor ϕ.

The additional assumptions used to estimate the strength of the sections are those recommended by the ACI and UBC codes: linear distribution of strain along the depth of the section, a rectangular block of compressive stress for the concrete (attained when the maximum concrete strain is 0.003), elasto-plastic behavior of the reinforcing steel, and perfect bond between reinforcing steel and the surrounding concrete.

The flexural ("plastic" moment) capacity of the girders has been determined assuming T-beam action of the slab, and considering the contribution of compression reinforcement. The participation of the slab reinforcement has been neglected. The capacity of the columns has been calculated using the computer program RCCOLA[15]; the results are given in the form of axial force-bending moment interaction diagrams (Figure 2.10). However, because the computer program ULARC used to perform the elasto-plastic analysis cannot handle the effect of axial force-bending moment interaction for the section capacity, it has been assumed that the flexural capacity of the columns is constant, and corresponds to the "ultimate" moment that the section can develop if submitted to the axial force resulting from gravity loads acting on the structure. This is a reasonable assumption since the variation of the flexural capacity due to the change in axial force produced by the overturning effect is approximately equal and opposite for the two columns when they are subjected to low gravity axial forces, which is the present case.

The geometric characteristics of the sections of both structures can be seen in Figure 2.5, and the two sets of section strengths used for the analysis of the ideal model and the test structure are listed in Table 2.4. These results show that the capacities of the girders differ by up to 20%; the discrepancy due primarily to the fact that the required area ratio (prototype-model) cannot be obtained with standard reinforcing bars in the prototype and the test structure (see Appendix B). Fortunately this effect is not significant for the columns; the interaction diagrams for the columns of both structures, shown in Figure 2.10, are remarkably similar based on analoguous assumptions of material properties.

2.6b Structural Performance under Lateral Loads.

The overall behavior of the structures under lateral loads was evaluated by studying their story shear-story drift relationships, and the sequence of plastic hinges formation leading to the development of the collapse mechanisms. The lateral deformations of the structure in the inelastic range that occur before formation of collapse mechanism is indicated by the story drift ductilities (μ_δ). The drift ductility is defined for this study as the ratio of the interstory displacement (drift) corresponding to the formation of the last plastic hinge to the drift that would have been obtained if the structure had remained elastic until attaining its lateral capacity. Figure 2.11 illustrates the definition of μ_δ. It should be noted that these ductility ratios are dependent on the relative floor lateral loads and on the idealized section behavior. Therefore, great care should be exercised in comparing the values presented here with those obtained for other structures, under different loading patterns, definitions of ductility and assumptions of section behavior.

The story shears, displacements and drifts are shown in Tables 2.5 and 2.6, for each structure and each set of assumed section strengths. The story shears are plotted versus the story drifts in Figures 2.12 and 2.13; the associated collapse mechanisms and sequence of plastic hinge formation can be seen in Figure 2.14, and the drift ductilities are presented in Table 2.7.

The following observations can be drawn from these results:

1) The results of Case I (lower bound for the section capacities) are highly unrealistic, since the predicted ultimate strength is about 50% lower then the maximum base shear actually developed by the test structure during the dynamic tests (see Chapter 5). The "upper" bound of the lateral strength (computed for Case II) is about 18% lower than the corresponding experimental value; consequently, only the results of Case II are used for the present discussion.

2) The lateral stiffness, strength and ductility of the ideal model and the test structure are reasonably similar, as can be seen in Figures 2.12 and 2.13.

3) The collapse mechanism of both structures is of the soft-story type,

the inelastic deformation being concentrated mainly at the ends of the bottom story columns. This is due to the fact that the capacity of the bottom story girder is about 50% larger than that of the column. Under these circumstances, the overall behavior of the structures in the inelastic range is controlled by the columns' strength and deformation capacities.

To complete this discussion, the distribution of section forces at collapse are presented in Table 2.8, and Figures 2.15 and 2.16. In this case the differences are not as large as in the case of the structural behavior under gravity loads; furthermore, the section forces of the bottom story columns are reasonably similar (particularly, the bending moment distributions are practically identical). As was seen in the previous paragraphs, the global behavior of the frames is controlled by the strength of the lower columns; hence, the observed differences in section forces are not very important for the correlation of the overall behavior of the test structure and the prototype. Regarding local damage in both structures, it is expected to be concentrated in the end zones of the columns, and the bottom story girders. Also, the bending moment in the central region of the bottom story girder of the test structure is very close to its plastic moment, therefore some damage can be expected in that zone of the test structure which would not be present in the ideal model (and prototype). As noted previously, this is due to the fact that the weight of the concrete blocks is concentrated in the central region of the test structure longitudinal girders.

2.7 Conclusions

The most significant differences between the behavior of the test structure and the ideal model (and hence between test structure and prototype) arise from the dissimilar distribution of section forces due to the concrete blocks on the test structure. This fact suggests that forces associated with any particular section would be different for both structures. However, since the model and the test structure have similar global dynamic characteristics and similar global strength, stiffness and ductility capacity, it can be predicted that their overall behavior under dynamic excitations will be similar. Consequently, the overall dynamic behavior of the prototype structure when subjected to seismic excitations will be simulated adequately by the test structure during the shaking table tests, if the dynamic excitations of both structures can be correlated according to appropriate similitude relations.

ITEM	UNIT WEIGHT	DIMENSIONS (ft or ft^2)		WEIGHT (kips)		
		BOTTOM STORY	TOP STORY	BOTTOM STORY	TOP STORY	
SLAB	.05 ksf	408.	408.	20.40	20.40	
CEILING	.001 ksf	408.	408.	.41	.41	
FLOOR	.001 ksf	408.	-	.41	-	
ROOFING	.01 ksf	-	408.	-	4.08	
WALLS ON TRANSVERSE GIRDERS	.207 k/ft	48	-	9.94	-	
PARTITIONS ON LONGITUDINAL GIRDERS	.140 k/ft	34.	-	4.76	-	
COLUMNS & GIRDERS	.100 k/ft	118.	100.	11.80	10.00	TOTAL WEIGHT
TOTAL				47.72k	34.89k	82.61 kips

TABLE 2.1

COMPUTATION OF PROTOTYPE STORY WEIGHTS

MAGNITUDE	DIMENSION	SCALING RATIO	OBSERVATIONS
LENGTH	L	0.707	
AREA	L^2	0.500	
STRAIN	-	1.000	
STRESS	FL^{-2}	1.000	assumed
CONCENTRATED FORCE	F	0.500	
GRAVITY	LT^{-2}	1.000	assumed
ACCELERATION	LT^{-2}	1.000	to have inertia forces scaled by 0.50
DISTRIBUTED LOAD	FL^{-1}	0.707	
MOMENT	FL	0.3536	
MASS	$FL^{-1}T^2$	0.500	
TORSIONAL MASS	FLT^2	0.250	
MOMENT OF INERTIA	L^4	0.250	
DENSITY	FL^2T^2	1.4142	not respected
TIME	T	0.8409	not used in tests

TABLE 2.2

SCALING RATIOS: MODEL TO PROTOTYPE

FORCES ON COLUMNS (kips,in)	AXIAL FORCE (+) Compression		SHEAR FORCE		MAX BENDING MOMENT BOTTOM STORY COL.		MAX BENDING MOMENT TOP STORY COL.	
	Bottom Story Column	Top Story Column	Bottom Story Column	Top Story Column	Bottom of Column	Top of Column	Bottom of Column	Top of Column
IDEAL MODEL	10.16	4.39	0.40	1.20	9.82	18.21	36.50	41.49
TEST STRUCTURE	9.34	3.68	0.96	1.62	22.81	42.41	57.85	52.08
Difference %	-8%	-16%	140%	35%	132%	133%	58%	26%

FORCES ON GIRDERS (kips,in)	AXIAL FORCE (+) Compression		MAX SHEAR FORCE		MAX NEGATIVE MOMENT		MAX POSITIVE MOMENT	
	Bottom Story Girder	Top Story Girder	Bottom Story Girder	Top Story Girder	Bottom Story Girder	Top Story Girder	Bottom Story Girder	Top Story Girder
IDEAL MODEL	-0.79	1.28	3.53	3.38	63.73	48.28	49.18	59.16
TEST STRUCTURE	-0.66	1.62	5.02	3.02	114.74	61.28	120.85	74.56
Difference %	-16%	26%	42%	-11%	80%	27%	146%	26%

TABLE 2.3

SECTION FORCES DUE TO GRAVITY LOADS (DEAD LOAD ONLY) FROM ELASTIC ANALYSIS

Case II f'_c = 4.0 ksi f_y = 5.0 ksi No ϕ	Bottom Story			Top Story		
	Girders		Columns	Girders		Columns
	M_p^+	M_p^-	$M_p^+ = M_p^-$	M_p^+	M_p^-	$M_p^+ = M_p^-$
MODEL	320.5	271.2	207.98	236.5	187.9	192.72
TEST STR.	314.2	313.4	208.7	198.1	226.5	194.17
Difference %	-2%	16%	<1%	-16%	20%	<1%

Case I f'_c = 4.0 ksi f_y = 40.0 ksi ϕ included	Bottom Story			Top Story		
	Girders ϕ=.9		Columns ϕ=.7	Girders ϕ=.9		Columns ϕ=.7
	M_p^+	M_p^-	$M_p^+ = M_p^-$	M_p^+	M_p^-	$M_p^+ = M_p^-$
MODEL	237.9	199.4	132.6	171.3	139.0	118.0
TEST	228.7	230.7	129.9	143.6	167.8	115.9
Difference %	-4%	16%	-2%	-16%	21%	2%

TABLE 2.4

SECTION STRENGTHS (PLASTIC MOMENTS) USED IN ELASTO PLASTIC ANALYSIS

MODEL

Plastic Hinge No.	Load Multiplier λ	SHEAR (kips)		DISPLACEMENT (inches)		DRIFT (inches)
		Bottom Story	Top Story	Bottom Story	Top Story	Top Story
1	4.103	16.66	8.45	.189	.323	.134
2	4.672	18.97	9.62	.231	.400	.169
3	4.785	19.43	9.86	.243	.419	.176
4	5.251	21.32	10.82	.387	.614	.227
5	5.366	21.79	11.05	.477	.723	.246

TEST STRUCTURE

Plastic Hinge No.	Load Multiplier λ	SHEAR (kips)		DISPLACEMENT (inches)		DRIFT (inches)
		Bottom Story	Top Story	Bottom Story	Top Story	Top Story
1	4.019	16.32	8.28	.163	.301	.138
2	4.541	18.44	9.35	.197	.369	.172
3	4.971	20.18	10.24	.236	.436	.200
4	5.564	22.59	11.46	.401	.667	.266
5	5.609	22.77	11.55	.417	.687	.270

TABLE 2.5

STORY SHEARS, DISPLACEMENTS AND DRIFTS OBTAINED FROM ELASTO-PLASTIC ANALYSIS. CASE I: LOWER BOUND OF SECTION STRENGTH

MODEL

Plastic Hinge No.	Load Multiplier	SHEAR (kips)		DISPLACEMENT (inches)		DRIFT (inches)
		Bottom Story	Top Story	Bottom Story	Top Story	Top Story
1	2.746	11.15	5.66	.127	.216	.089
2	2.897	11.76	5.97	.138	.237	.099
3	3.096	12.57	6.38	.158	.270	.112
4	3.401	13.81	7.01	.253	.397	.144
5	3.409	13.84	7.02	.255	.401	.146
6	3.421	13.89	7.05	.260	.408	.148

TEST STRUCTURE

Plastic Hinge No.	Load Multiplier	SHEAR (kips)		DISPLACEMENT (inches)		DRIFT (inches)
		Bottom Story	Top Story	Bottom Story	Top Story	Top Story
1	2.436	9.89	5.02	.099	.183	.084
2	2.616	10.62	5.39	.111	.206	.095
3	2.804	11.38	5.78	.127	.236	.109
4	3.114	12.64	6.41	.157	.294	.137
5	3.119	12.66	6.43	.158	.296	.138
6	3.183	12.92	6.56	.187	.328	.146
7	3.299	13.39	6.80	.351	.587	.236

TABLE 2.6

STORY SHEARS, DISPLACEMENTS AND DRIFTS OBTAINED FROM ELASTO-PLASTIC ANALYSIS. CASE II: UPPER BOUND OF SECTION STRENGTH

	BOTTOM STORY					TOP STORY				
CASE II	V_y (kips)	δ_y (in)	V_u	δ_μ	μ_δ	V_y	δ_y	V_u	δ_u	μ_δ
MODEL	16.66	.189	21.79	.477	1.93	8.45	.134	11.05	.246	1.40
RCF2	16.32	.163	22.77	.417	1.83	8.28	.138	11.55	.270	1.40
Difference %	-2%	-14%	5%	-13%	-5%	-2%	3%	5%	10%	0
CASE I										
MODEL	11.15	.127	13.89	.260	1.64	5.66	.089	7.05	.148	1.34
RCF2	9.89	.099	13.39	.351	2.62	5.02	.084	6.80	.236	2.07
Difference %	-11%	-22%	-4%	35%	60%	-11%	-6%	-4%	60%	54%

TABLE 2.7

COMPUTATION OF STORY DRIFT DUCTILITIES
(ELASTO PLASTIC ANALYSIS)

	MAX AXIAL FORCE IN COLS (kips)		MIN AXIAL FORCE IN COLS (kips)		MAX SHEAR FORCE IN COLS (kips)		AXIAL FORCE IN GIRDERS (kips)		MAX SHEAR FORCE IN GIRDERS (kips)	
CASE II	Bottom Col.	Top Col.	Bottom Col.	Top Col.	Bottom Col.	Top Col.	Bottom Girder	Top Girder	Bottom Girder	Top Girder
MODEL	15.95	6.30	4.33	2.44	5.45	2.98	-.21	+.21	6.24	4.18
RCF2	15.41	5.71	3.27	1.61	5.69	3.69	-.80	+.80	8.77	4.80
Difference %	-3%	-9%	-25%	-34%	4%	24%	280%	280%	41%	15%

CASE I

MODEL	13.84	5.55	6.44	3.19	3.47	2.42	-.66	+.66	4.88	3.43
RCF2	12.81	4.89	5.88	2.43	3.54	2.73	-.84	+1.03	6.99	3.98
Difference %	-7%	-12%	-9%	-24%	2%	13%	27%	56%	43%	16%

TABLE 2.8

SHEAR AND AXIAL FORCES IN ELEMENTS AT COLLAPSE

(ELASTO-PLASTIC ANALYSIS)

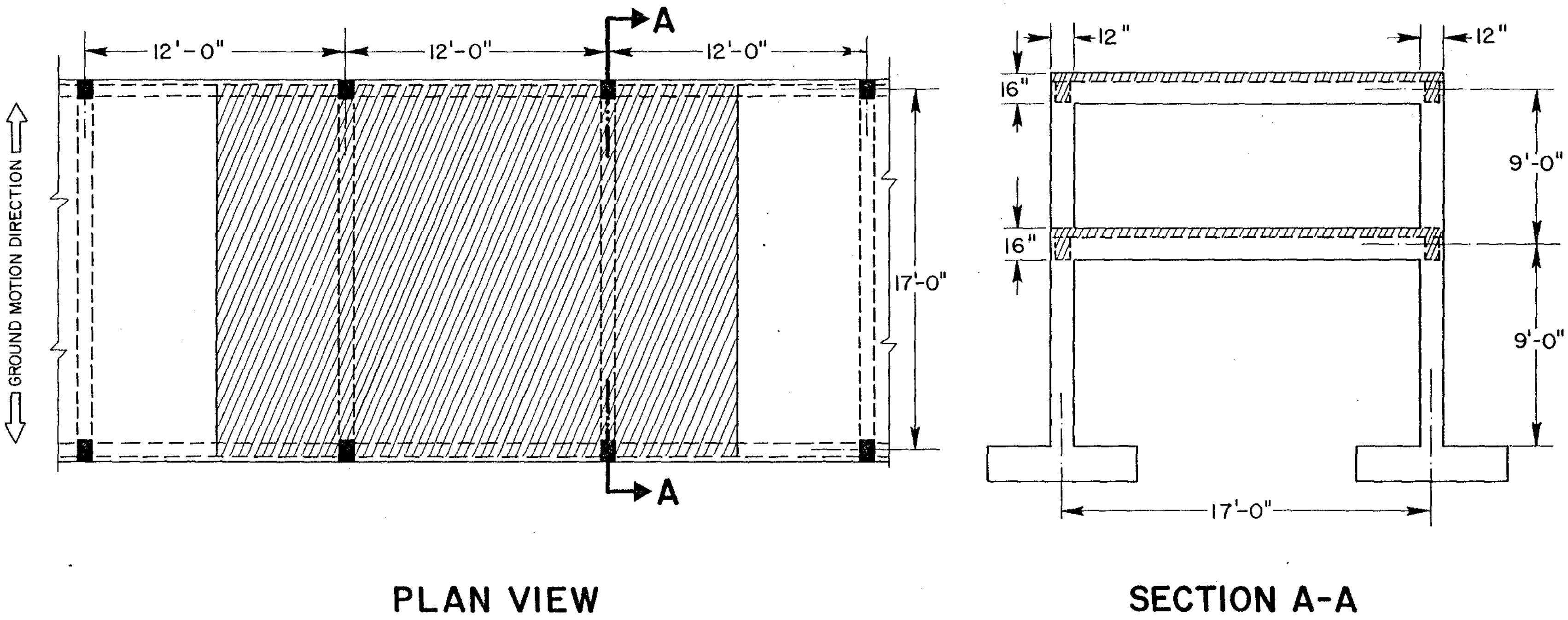

FIG. 2.1 PROTOTYPE OFFICE BUILDING DIMENSIONS

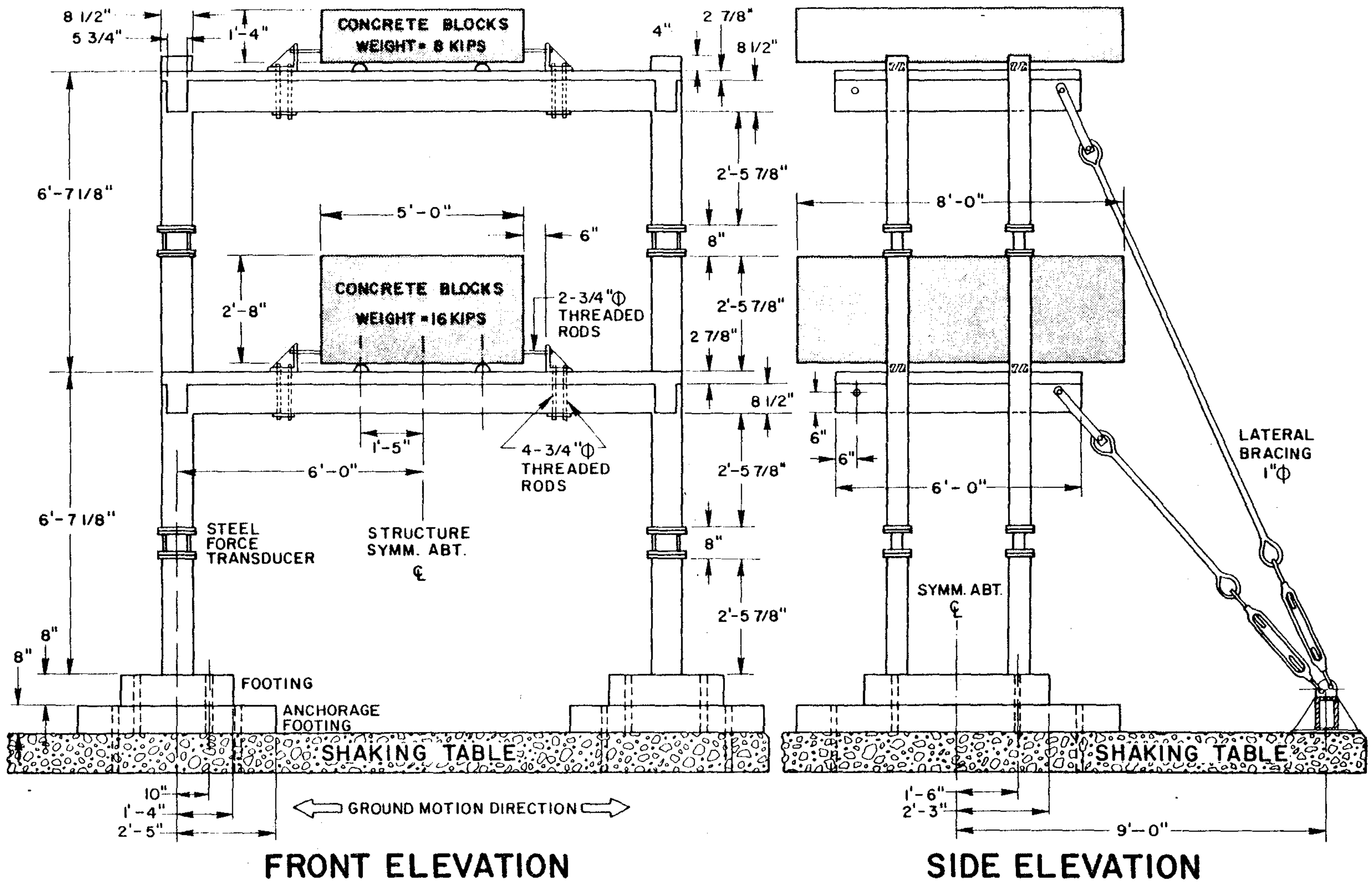

FIG. 2.2 TEST STRUCTURE AND TEST ARRANGEMENT ON SHAKING TABLE

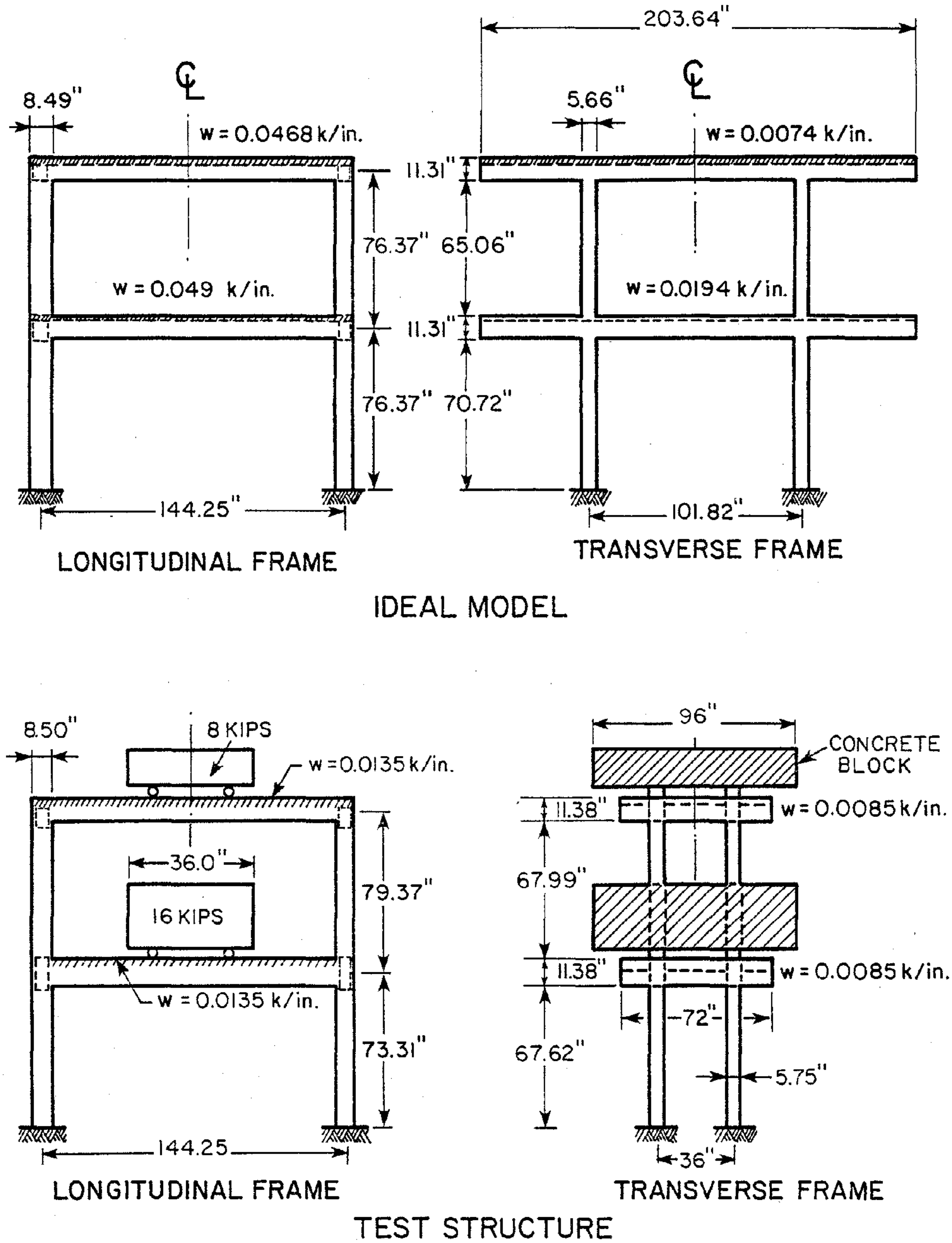

FIG. 2.3 IDEAL MODEL VS. TEST STRUCTURE: DIMENSIONS AND LOADS

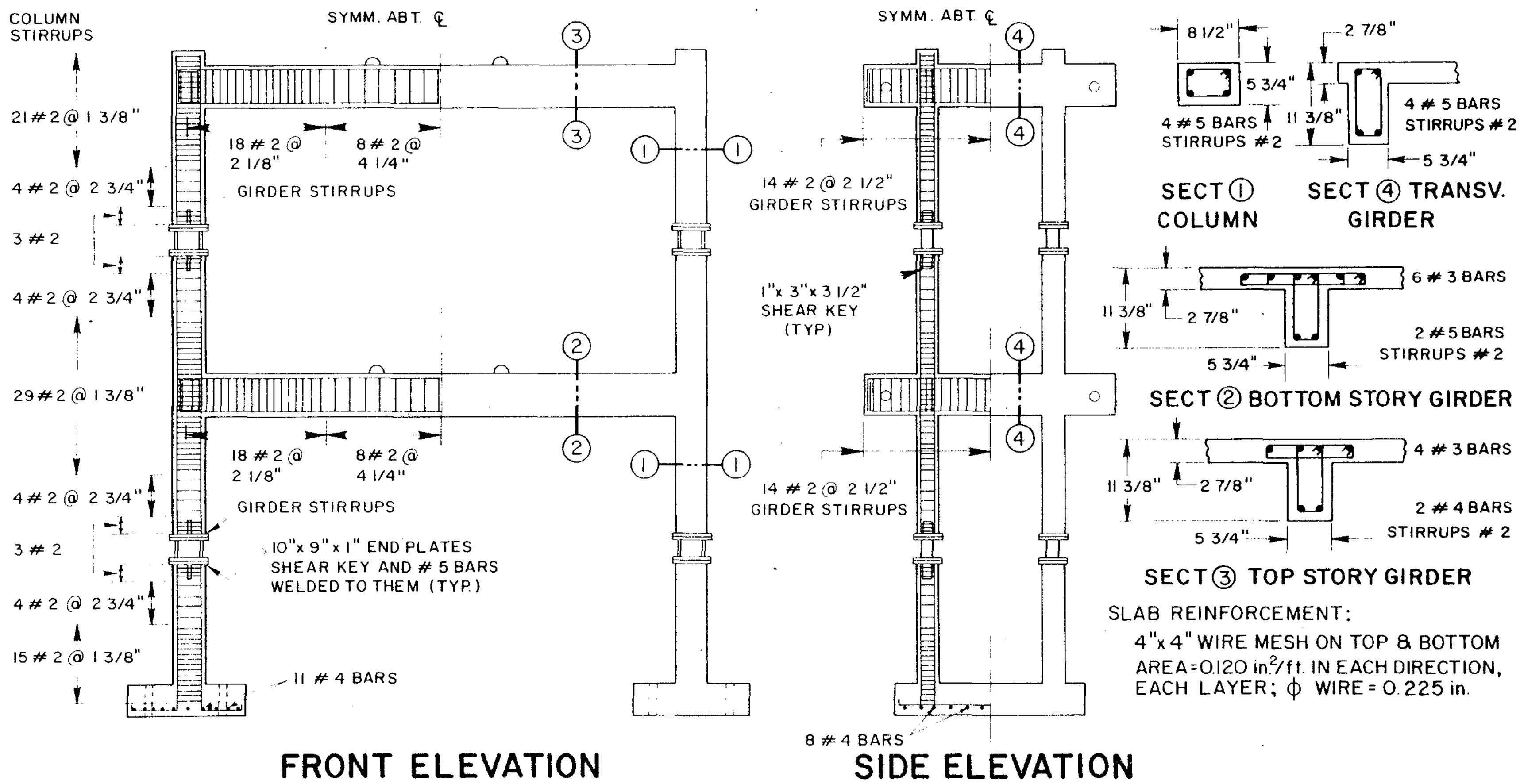

FIG. 2.4 TEST STRUCTURE - DETAILS OF REINFORCEMENT

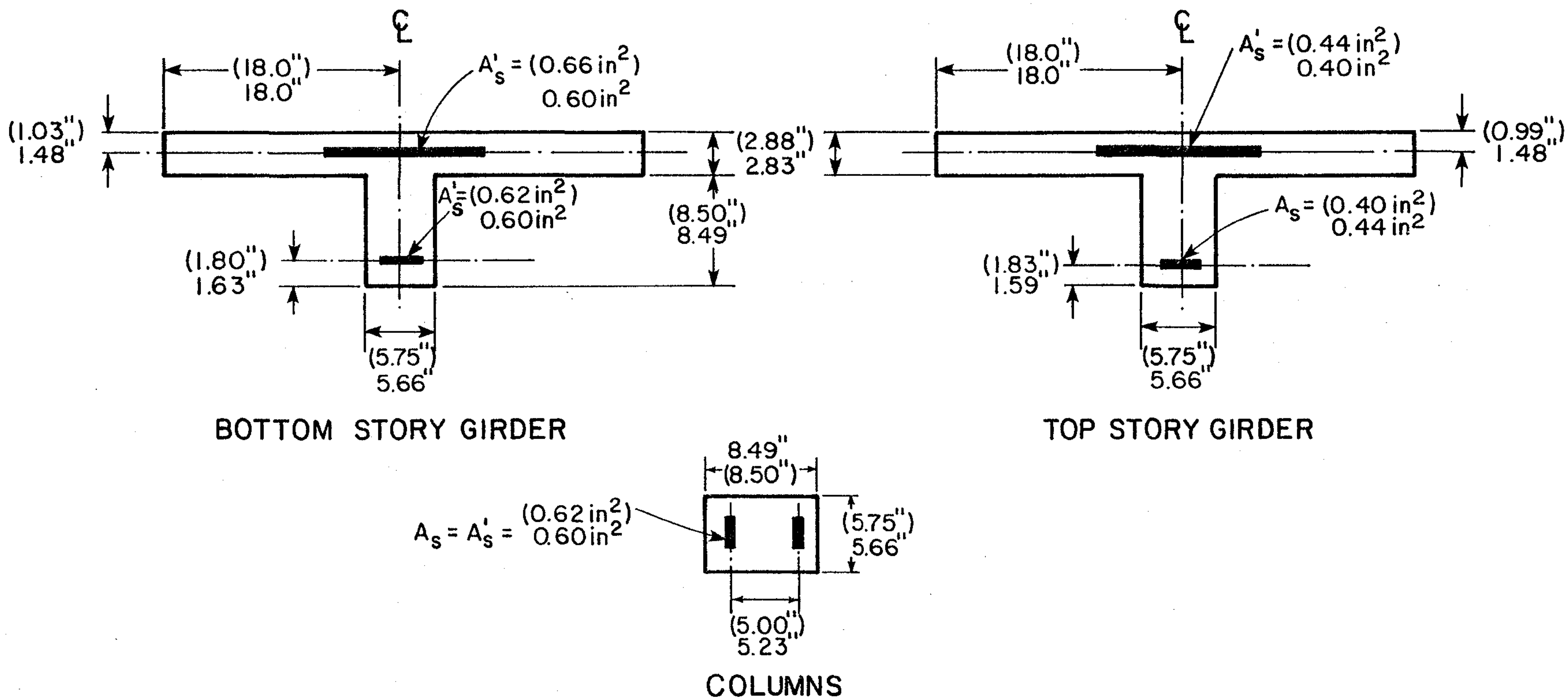

FIG. 2.5 SECTION CHARACTERISTICS OF IDEAL MODEL AND RCF2

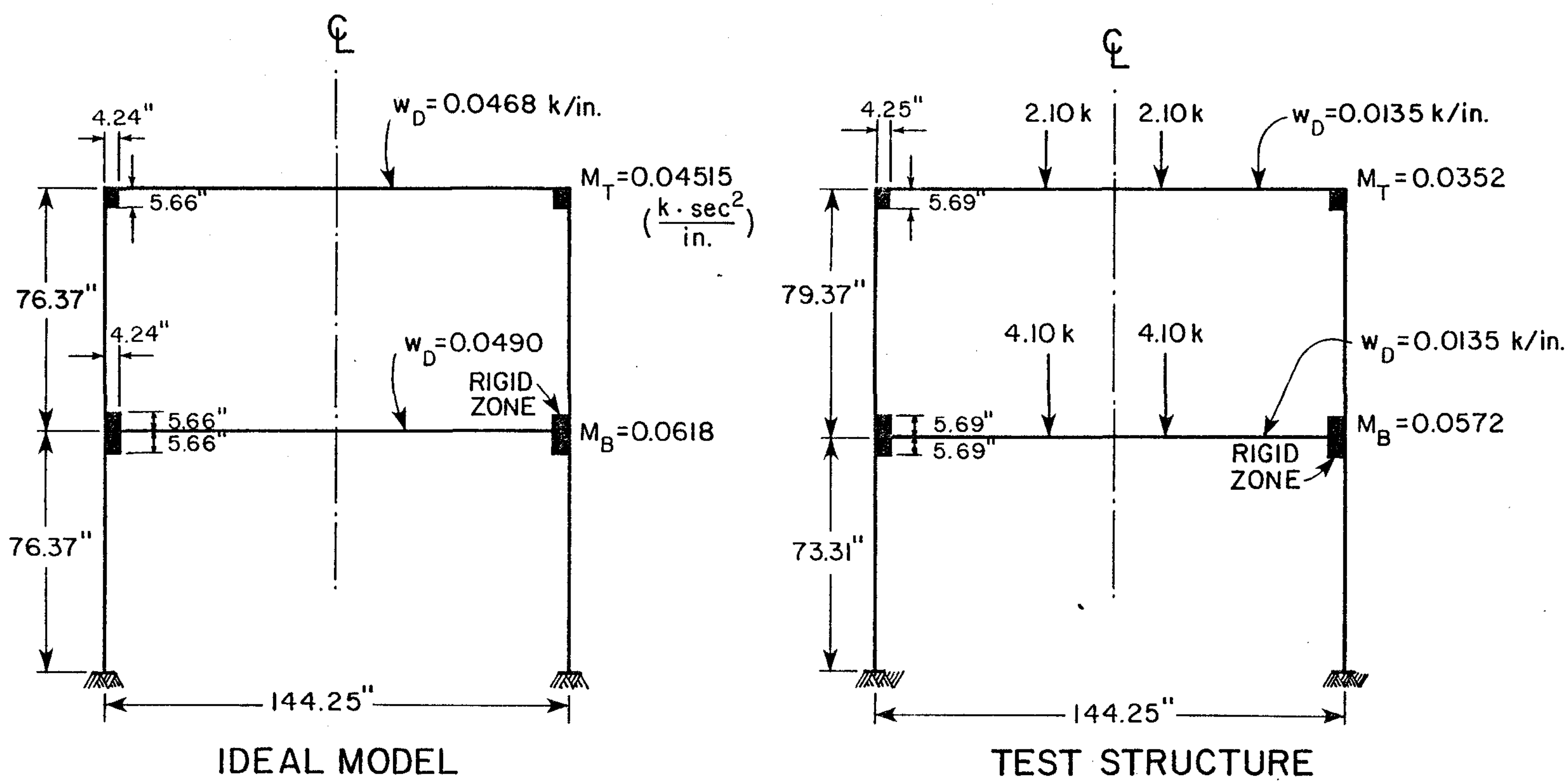

FIG. 2.6 LONGITUDINAL VIEW OF THE IDEALIZED FRAMES - ELASTIC ANALYSIS

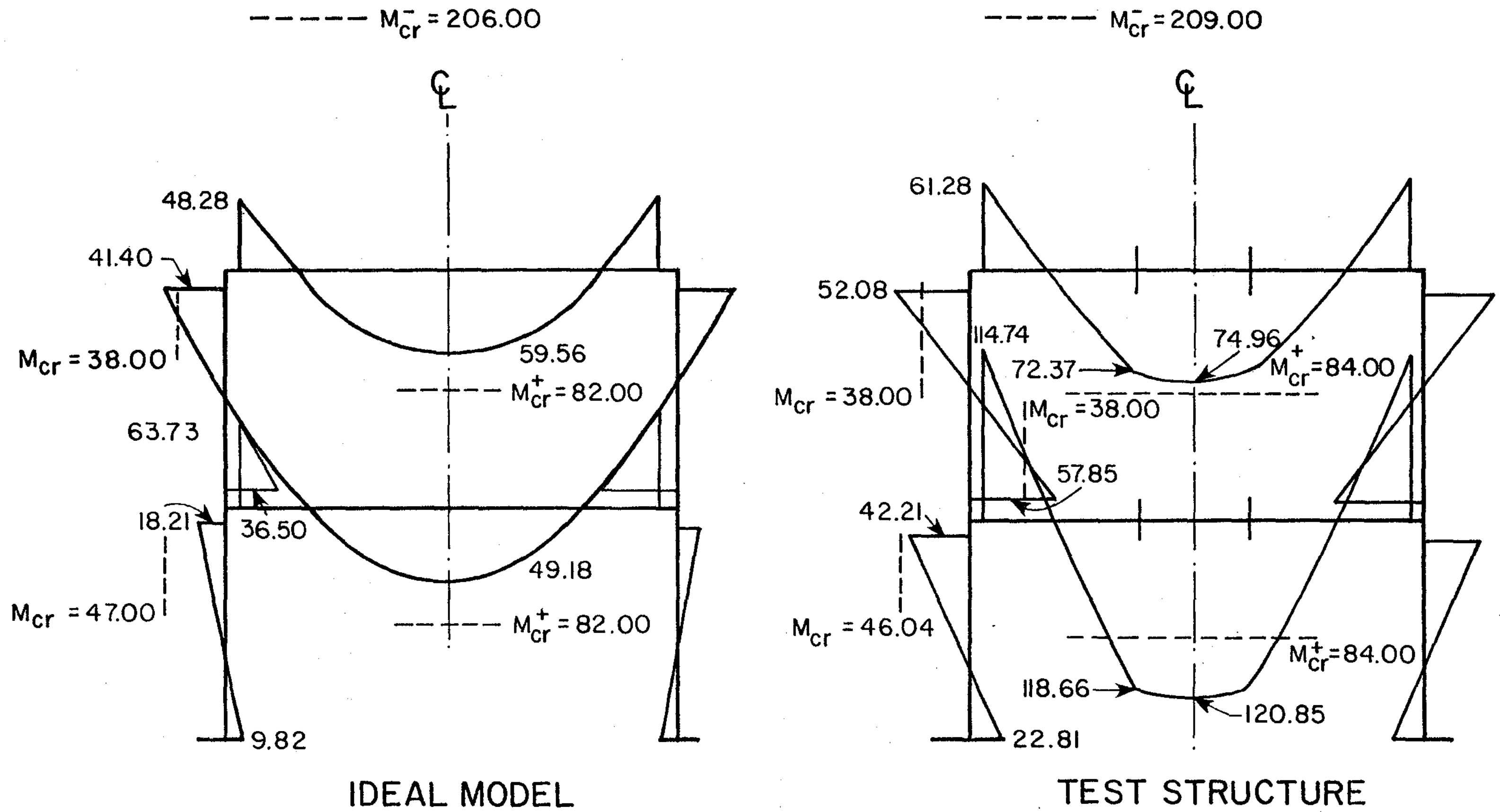

FIG. 2.7 BENDING MOMENT DIAGRAMS DEAD LOAD ONLY - ELASTIC ANALYSIS (KIP INCHES)

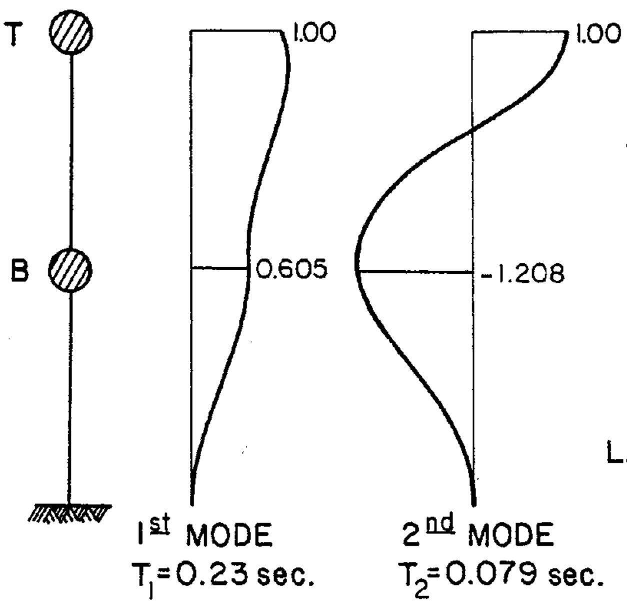

MODEL

$$\underline{m} = \begin{array}{c} \\ \end{array}\begin{array}{cc} T & B \end{array}$$

$$\underline{m} = \left[\begin{array}{cc} 0.04515 & 0.00 \\ 0.00 & 0.618 \end{array}\right]\begin{array}{c} T \\ B \end{array} \left(\frac{k-sec^2}{in.}\right)$$

MASS MATRIX

$$\underline{f} = \left[\begin{array}{cc} 0.02095 & 0.01054 \\ 0.01054 & 0.00896 \end{array}\right]\begin{array}{c} T \\ B \end{array} \ (in/k)$$

LATERAL FLEXIBILITY MATRIX

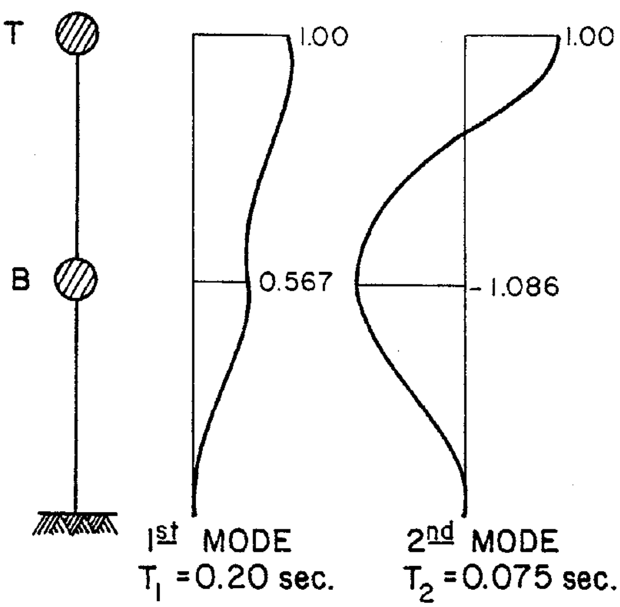

$$\underline{m} = \left[\begin{array}{cc} 0.0352 & 0.0 \\ 0.0 & 0.0572 \end{array}\right]\begin{array}{c} T \\ B \end{array}$$

$$\underline{f} = \left[\begin{array}{cc} 0.02046 & 0.00929 \\ 0.00929 & 0.00776 \end{array}\right]\begin{array}{c} T \\ B \end{array}$$

TEST STRUCTURE

FIG. 2.8 DYNAMIC PROPERTIES OF IDEAL MODEL AND RCF2

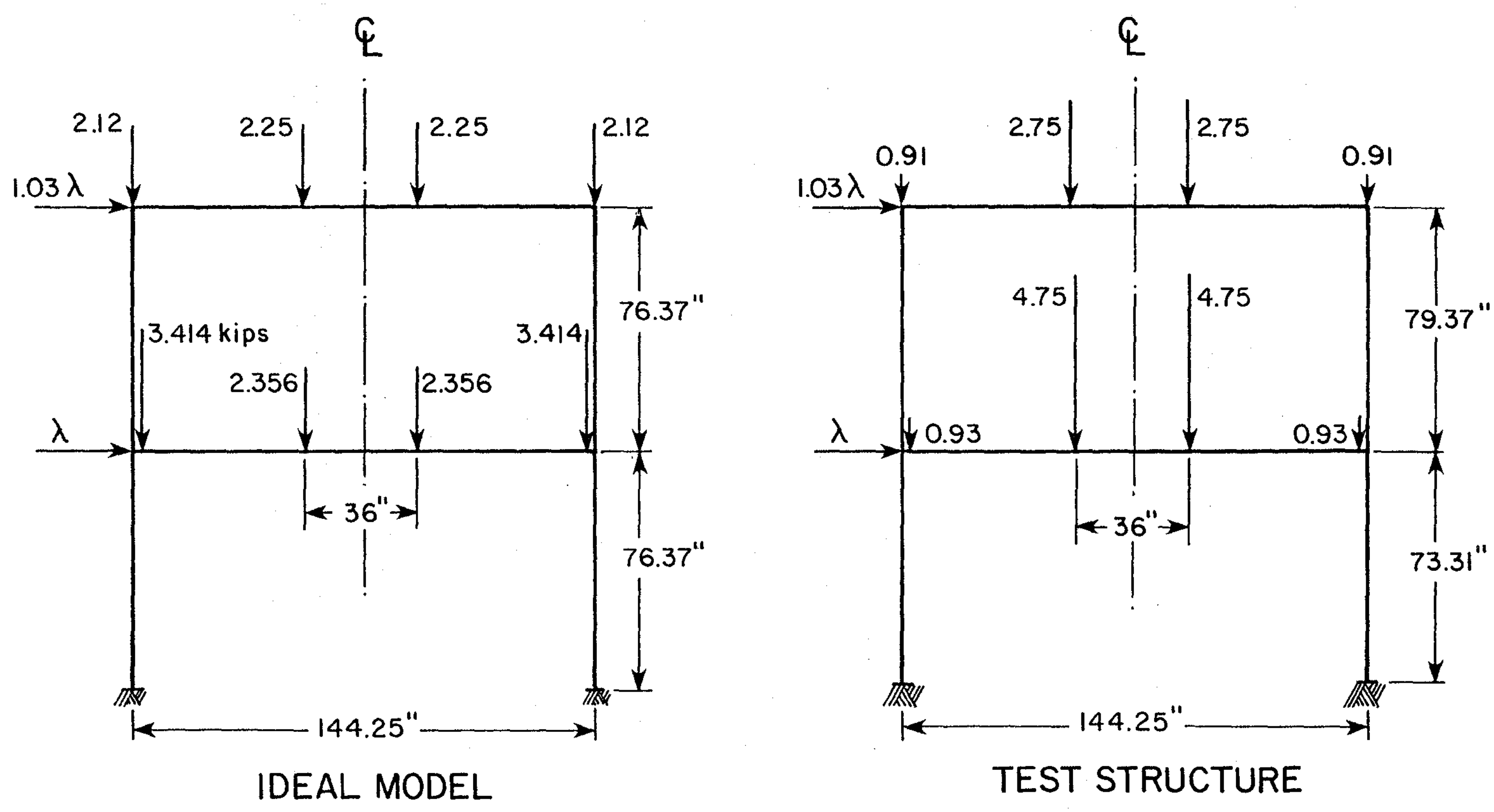

FIG. 2.9 IDEALIZED LONGITUDINAL FRAMES - ELASTO-PLASTIC ANALYSIS

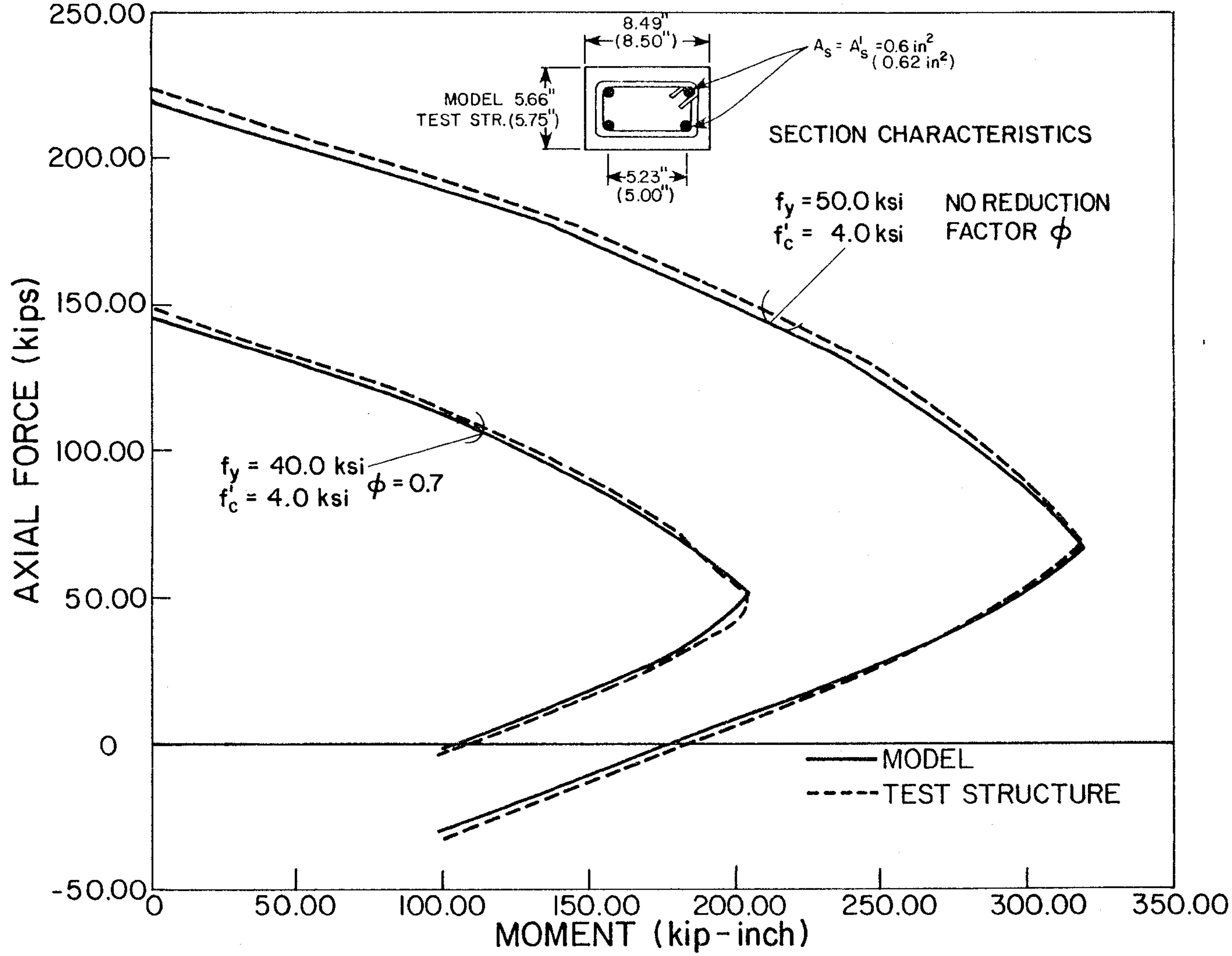

FIG. 2.10 AXIAL FORCE - BENDING MOMENT INTERACTION DIAGRAMS FOR COLUMNS OF IDEAL MODEL AND RCF2

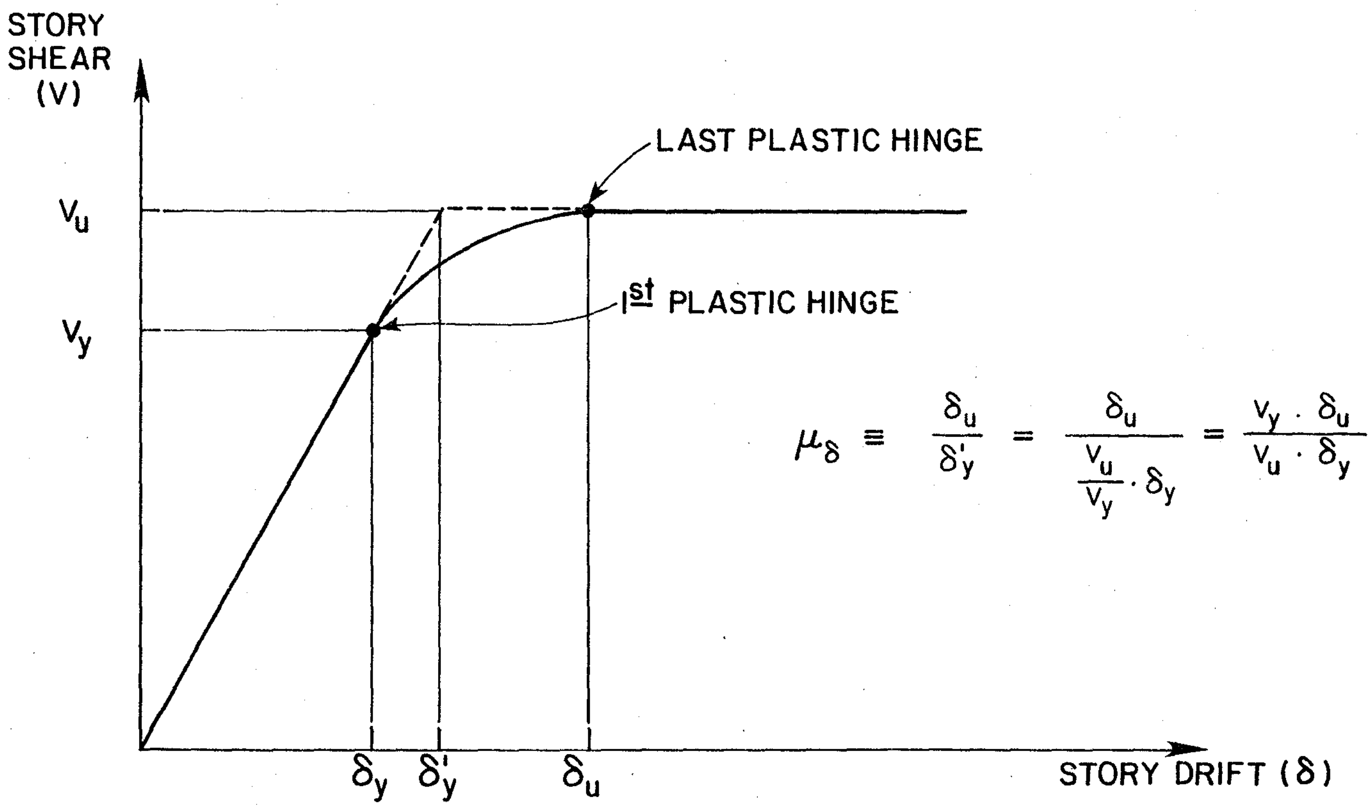

FIG. 2.11 DEFINITION OF DRIFT DUCTILITY

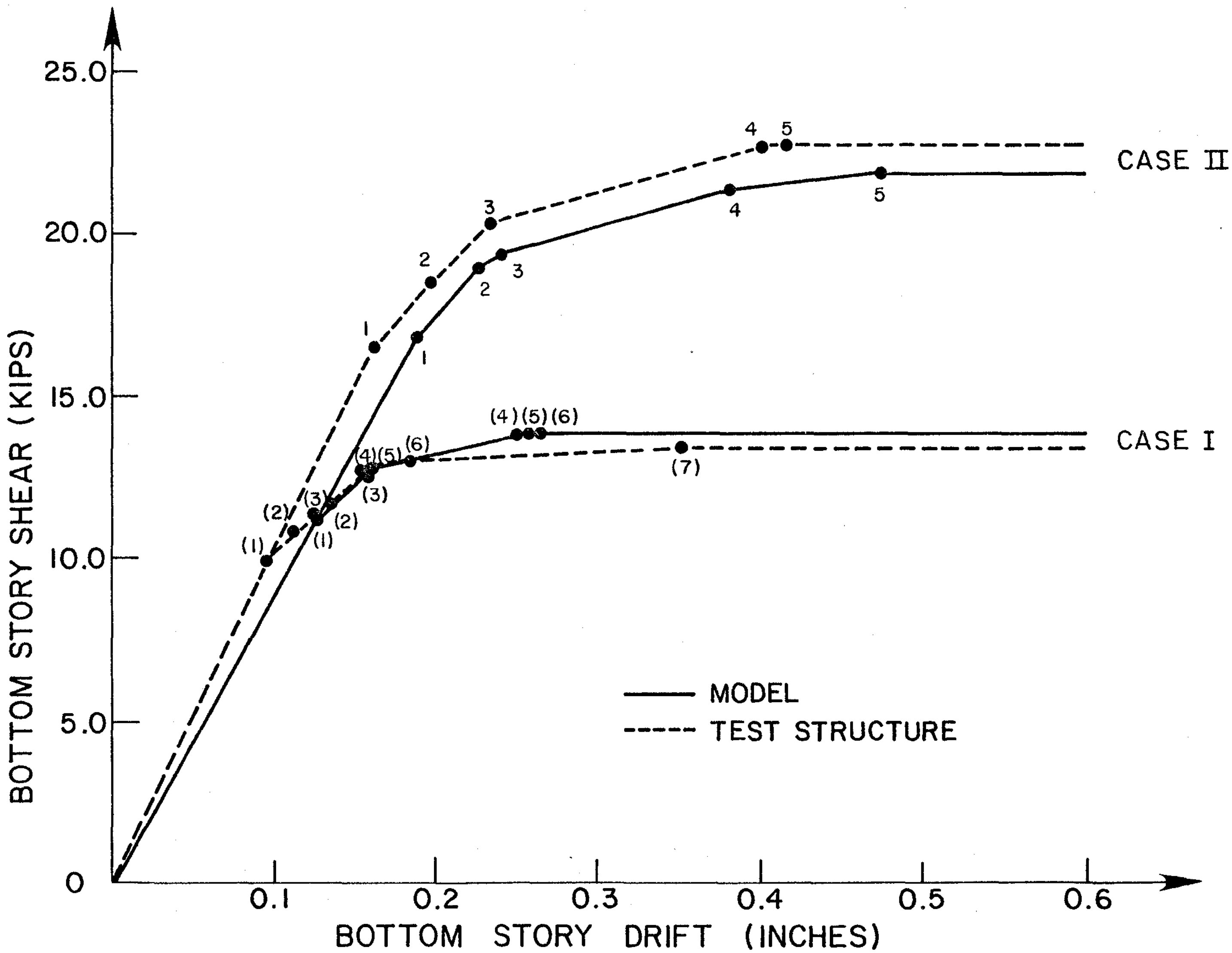

FIG. 2.12 BOTTOM STORY SHEAR VS. DRIFT FROM ELASTO-PLASTIC ANALYSIS. IDEAL MODEL AND RCF2

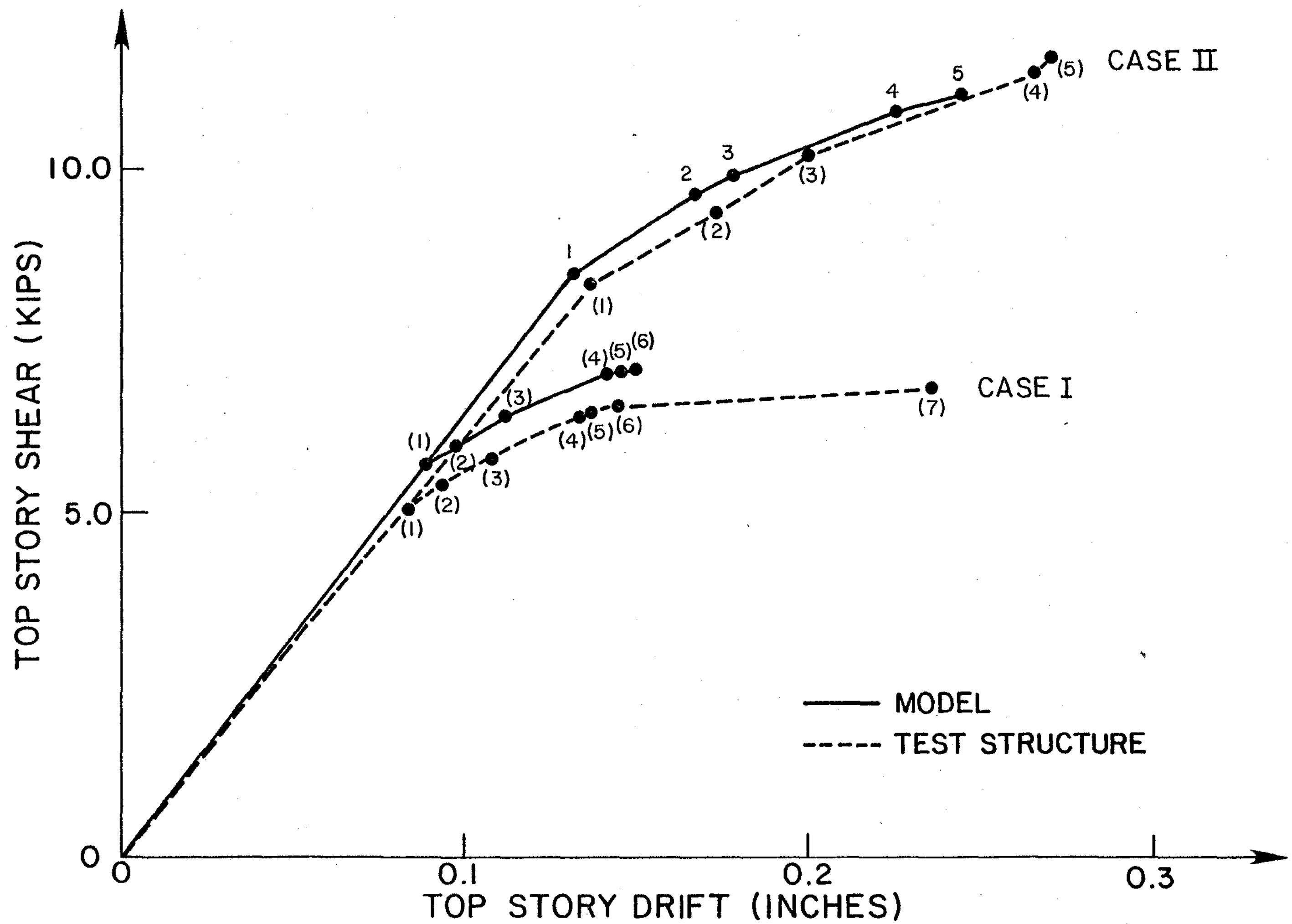

FIG. 2.13 TOP STORY SHEAR VS. DRIFT FROM ELASTO-PLASTIC ANALYSIS. IDEAL MODEL AND RCF2

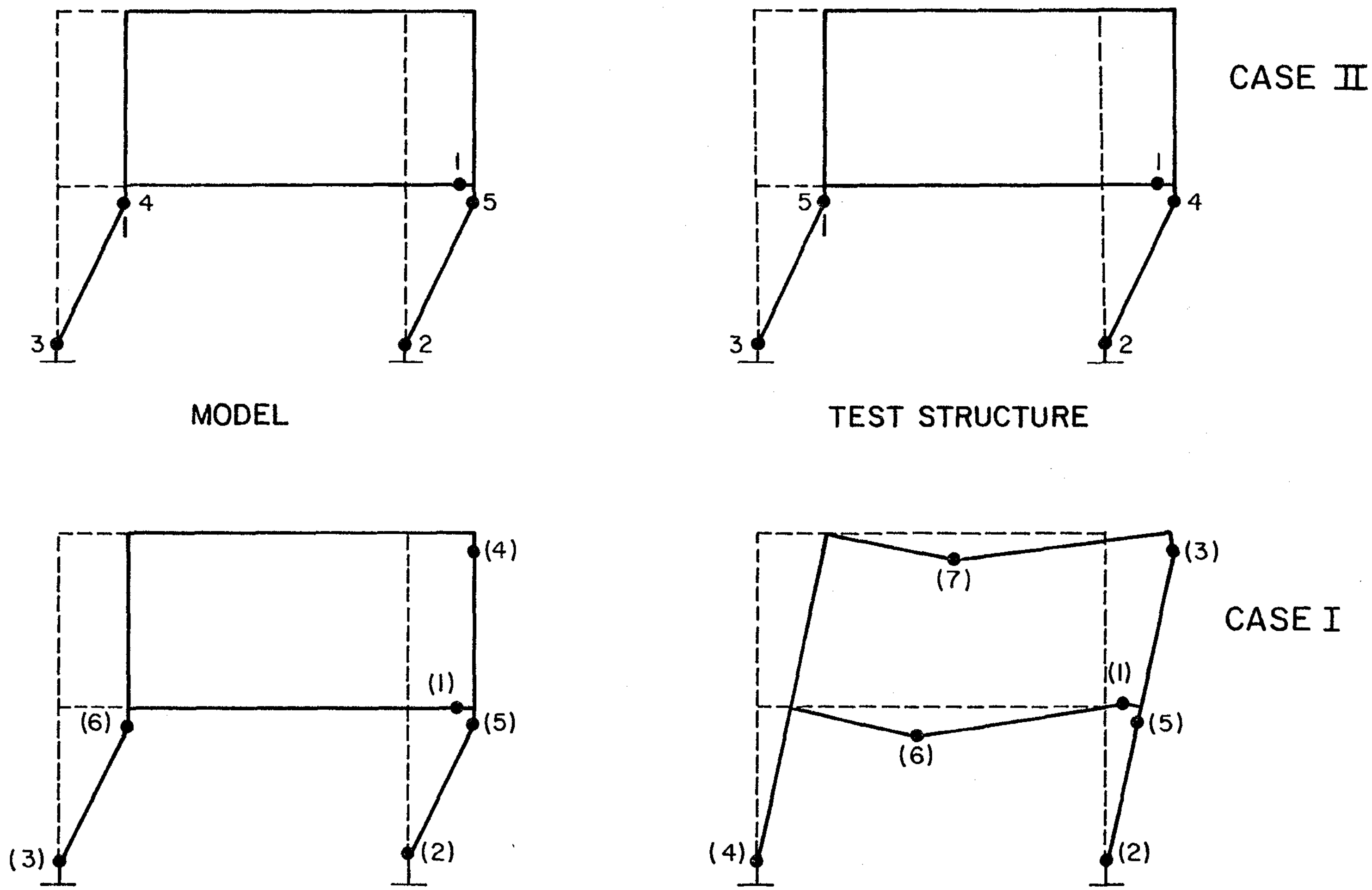

FIG. 2.14 COLLAPSE MECHANISMS AND SEQUENCE OF PLASTIC HINGE FORMATION (FROM ELASTO-PLASTIC ANALYSIS)

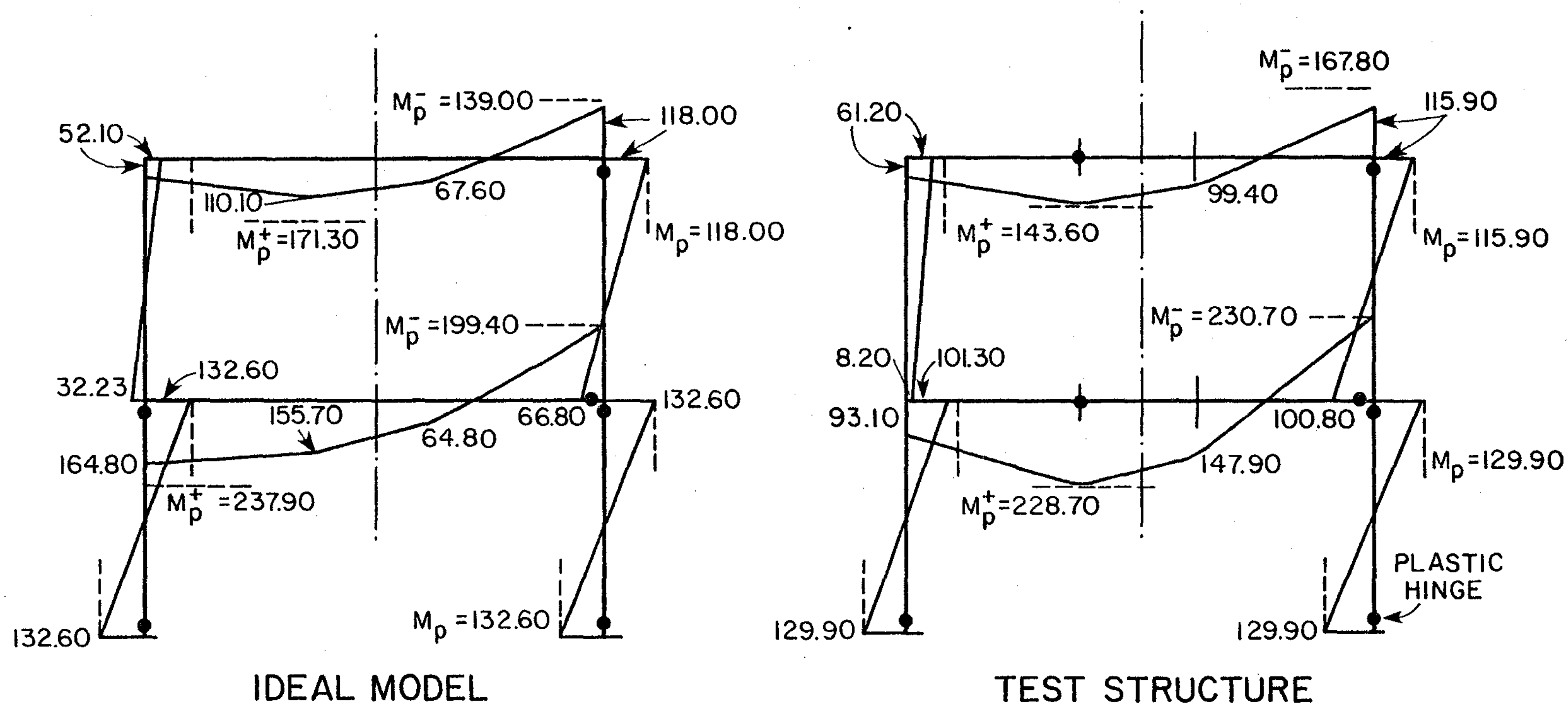

FIG. 2.15 DISTRIBUTION OF BENDING MOMENTS AT COLLAPSE. ELASTO-PLASTIC ANALYSIS, CASE I

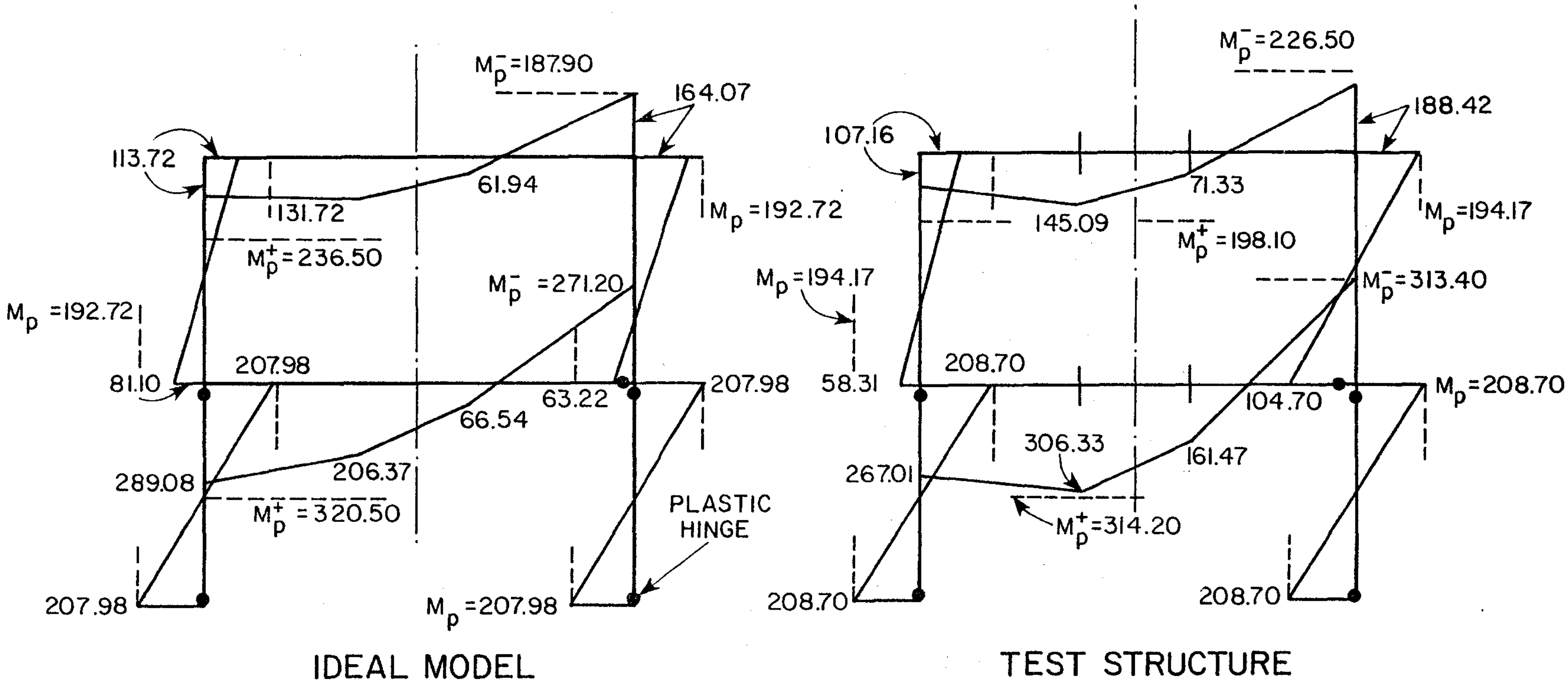

FIG. 2.16 DISTRIBUTION OF BENDING MOMENTS AT COLLAPSE. ELASTO-PLASTIC ANALYSIS, CASE II

Preceding page blank

3. EVALUATION OF THE INPUT MOTIONS

3.1 Preliminary Observations

The first reinforced concrete structure (RCF1) tested on the shaking table was subjected to a series of seismic excitations with increasing intensity[1], consequently, it was significantly damaged before being subjected to the strongest simulated earthquake. For the second structure, RCF2, it was decided to study the behavior of an essentially undamaged structure under a strong seismic excitation, which seemed more representative of typical field conditions. This test concept also provided the opportunity to evaluate the effect of strong previous shaking on the response of reinforced concrete structures.

The signal selected as basic input for the shaking table system, was the N69W accelerogram recorded at Taft during the Arvin-Tehachapi earthquake of July 21, 1952, because it had been used with satisfactory results for the tests performed on RCF1. In order to simulate ground motions with different intensities, the acceleration values of the record were scaled by appropriate factors, which were selected according to the experience gained in the previous tests. However, as in the case of RCF1, the earthquake time scale remained unchanged; hence, the required similitude relations between model and prototype (see Table 2.2) were not satisfied.

The consequence of not time scaling the Taft acceleration record, is that the frequency content of the model test table excitation no longer corresponds to a prototype motion equivalent to that recorded at Taft. Instead, the seismic excitation of the test structure simulates a ground motion in prototype scale with different frequency content. The aim of this chapter is to determine if the shaking table inputs used to excite the test structure are representative of possible earthquake induced ground motions in the field.

3.2 Description of Test Motions

As mentioned in the previous section, the aim of the RCF2 experiments was to simulate the effect of a strong earthquake on a practically undamaged structure. In order to start with a degree of cracking representative of normal field conditions, it was decided to subject the test structure to a preliminary mild seismic excitation having a peak acceleration of about 10 percent of gravity. The structure then was excited with the main strong seismic input, and this earthquake was followed by a simulated aftershock of comparable intensity. After these tests the structure was repaired by epoxy injection and the test sequence was repeated in order to observe the effect of the repairs on the structural performance.

Table 3.1 lists the shaking table control "span" setting with the respective peak table acceleration obtained for each "run." The input table accelerations for the unrepaired structure can be compared with the Taft accelerogram in Fig. 3.1. In addition, elastic response spectra have been computed for selected table motions and for the Taft record using the computer program SPECEQ[17]; the results are shown in Figures 3.2 and 3.3. The spectral values are computed over the range 0.1 to 0.9 seconds since the natural periods of the structure varied between those limits during the tests (see Table 3.2). It can be seen that the spectral shapes corresponding to the table excitations are reasonably similar to that of the Taft record, demonstrating the capability of the shaking table to simulate the selected ground motion.

3.3 Effect of Time Scaling

It has already been noted that the accelerogram recorded at Taft was used as a basic input for the shaking system, modifying the acceleration amplitudes to simulate various seismic intensities but with time scale remaining unchanged.

However, according to the similitude laws, if the length ratio between model and prototype is λ_L, and the acceleration ratio is maintained equal to one, different time scales should be used with the two structures.

The required time ratio can be deduced as follows:

$$\text{if} \qquad \lambda_A = \frac{[\text{acceleration of model}]}{[\text{acceleration of prototype}]} = 1.0$$

then

$$\frac{L_M \, T_M^{-2}}{L_p \, T_p^{-2}} = 1.0$$

hence

$$\lambda_T = \frac{T_M}{T_p} = \left(\frac{L_p}{L_M}\right)^{-1/2} = \left(\frac{L_M}{L_p}\right)^{1/2} = \lambda_L^{1/2} \ .$$

Since the length ratio λ_L is 0.707, the corresponding time ratio is $\lambda_T = \sqrt{0.707} = 0.8409$. Consequently, the shaking table excitation simulates a ground motion in the field (i.e. in prototype time-scale) with a larger content of long periods, because

$$\left(\frac{T_p}{T_M} = \frac{1}{\lambda_T} = 1.189\right) .$$

The pseudovelocity and pseudoacceleration spectra of the original Taft record and of the ground motion in prototype scale simulated by runs W1 (Taft 100) and W2 (Taft 8501(1)) are shown in Figures 3.4 and 3.5, to illustrate the effect of the time scaling on the test signal. It can be seen that the peak spectral values corresponding to the prototype time scale are shifted relative to those of the Taft earthquake. Consequently, the simulated prototype ground motions have a different frequency content than the Taft earthquake.

The spectra of the test structure and the corresponding prototype excitations are compared in Figures 3.6 and 3.7, in which the range of variation of the fundamental period of both structures during each test is shown. The prototype natural periods have been computed from those of the test structure, assuming that they satisfy the similitude time ratio (which is a reasonable assumption, according to the findings of Chapter 2.) It can be observed that the pseudoacceleration spectral values for both structures are the same for each test, which corroborates the assumption of unit acceleration ratio between model and prototype, and points out the similarity of the excitations for both structures. Figure 3.8 shows the acceleration time histories for run W2 and the corresponding time scaled prototype ground motion.

The question that remains to be answered is whether the ground motion simulated by the tests are representative of possible actual earthquake motions in the field.

3.4 The Prototype Ground Motions

From the point of view of structural engineering, the most relevant parameters of a strong ground motion induced by earthquakes are the spectral shape, the maximum ground acceleration and the duration of the event. In this section the ground motions (in prototype scale) simulated by the shaking table tests are analysed with respect to the first two of these parameters. Duration is not evaluated because it is thought that the slight time scaling of the present case does not have a significant effect in this parameter.

Only run W2 (Taft 850(1)) will be analyzed, because run W1 corresponds to a very mild earthquake, and run W3 has the same general characteristics as W2. A first approach (perhaps the most obvious) to evaluate the ground motion simulated by run W2, denoted as time-scaled Taft 850(1), is to compare its response spectra with those of several recorded actual earthquake ground motions.

Four records of different earthquakes were selected for this comparison. Figures 3.9 and 3.10 show their respective response spectra together with that of the time-scaled Taft 850(1) test. The most significant characteristics of the four records used are listed in Table 3.3. A spectral intensity parameter has been computed as the area under the pseudovelocity response spectrum over a region comprising the range of variation of the first mode period of the prototype, as an additional parameter of comparison.

It can be seen in the mentioned figures that the spectra of time-scaled Taft 850(1) do not show any striking difference from those of the other records. Moreover, its pseudovelocity and pseudoacceleration spectra are reasonably close to those of the Pacoima Dam and Managua records, and its spectral intensity is bounded by that of these two records. Hence, a ground motion such as the time scaled Taft 850(1) record apparently could be generated by a seismic event.

However, the spectra shown in Figures 3.9 and 3.10 correspond to ground motions recorded at stations located in regions with different geological and soil conditions (in particular, the Pacoima Dam record was obtained in a very unusual site, not likely to be the location of a reinforced concrete building); hence, with the information provided by these figures it seems difficult to ascertain under which conditions a ground motion such as the time scaled Taft 850(1) could act on a typical building.

It is recognized that the site soil conditions have a significant influence on the character of the ground motions induced by a given earthquake. Seed et al [18] obtained average acceleration spectra (normalized with respect to maximum ground acceleration) for different soil conditions, from a large number of records; these are shown in Figure 3.11. Figure 3.12 shows the correlation of the Taft 850(1)(run W2) spectrum curve, which is similar to that of the Taft record, with the average normalized spectrum for stiff soil conditions (the Taft record was obtained at an alluvium site); it can be seen that the Taft spectrum lies reasonably within the range defined by the mean plus or minus one standard deviation. Comparing the spectral shape of the time-scaled Taft 850(1) (corresponding prototype motion) with the average spectral curves for different sites, it is observed that a similar correlation is established with the average normalized spectrum for sites underlain by deep cohesionless soils (see Figure 3.13), particularly in the period range of interest for this study ($0.1<T<1.0$ sec).

It is apparent, then, that the consequence of not having performed the required time scaling on the Taft signal, is that the test excitations correspond in an average sense, to a ground motion which would be obtained under different site conditions ("softer" soil) than those on which the original ground motion was recorded.

It is also necessary to determine if the levels of acceleration produced in the tests (and hence those which would correspondingly occur in prototype scale) could be caused by a seismic event. Since the peak accelerations of the test and prototype excitations are similar (Figure 3.7), but they correspond to ground motions occurring in sites with different soil conditions, they will also correspond to earthquakes of different magnitude (assuming that these movements correspond to sites located at the same distance of the causative fault).

In order to estimate the magnitude of the earthquakes which could induce the strong ground accelerations produced in the shaking table tests and the corresponding prototype excitations it is necessary to use site-dependant attenuation laws. Trifunac and Brady (1976) have proposed attenuation laws for different soil conditions, which relate peak displacement, velocity and acceleration, with earthquake local magnitude, epicentral distance, and direction of ground motion (horizontal or vertical.) These have been taken from Reference [19], and used to determine the earthquake local magnitude corresponding to Taft 850(1) (run W2 on the test structure) and the corresponding time-scaled signal (prototype ground motion.)

The relationships presented by Trifunac and Brady are of the form

$$\log a = M + \log A_0(R) - \log y_0(M,p,s',v')$$

where

$$\log y_0 = a'_p + b'M + c' + d's' + e'v' + f'M^2$$

in which

a = peak ground acceleration (cm/sec)

M = local magnitude

R = epicentral distance (km)

P = confidence limit (0.5 for mean)

s' = side coefficient (equal to 0 for stiff sites and 1 for "intermediate" sites

v' = direction of ground motion (equal to zero for horizontal components)

and

$$a' = -.898;\ b' = -1.789;\ c' = 6.217;\ d' = 0.060;\ f' = 0.186$$

Using those relationships and assuming that the prototype and test structure are located at a distance (R) of 20 km from the epicenter, the following values are obtained

i) Prototype ground motion:

$$a = .572g = 561\ \text{cm/sec}^2$$

$$-\log A_0 = 1.833;\ a' = 1\ \text{(intermediate site)}$$

then

$$\log y_0 = 5.823 - 1.789M + 0.186M^2$$

and

$$\log 561 = M - 1.833 - (5.878 - 1.789M + .186M^2)$$

which leads to

$$M = 7.0$$

(i) Table motion (run W2)

$$s' = 0\ \text{(stiff site)};\ a = 561/\text{cm/sec}^2$$

in this case

$$\log y_0 = 5.768 - 1.789M + 0.186M^2$$

and

$$\log 561 = M - 1.833 - (5.768 - 1.789M + .186M^2)$$

from which

$$M = 6.75$$

Hence, the ground motion in prototype scale corresponds to an earthquake with a slightly larger local magnitude than that of the shaking table tests.

3.5 Conclusions

From the rather simple analysis described in the preceding sections it may be concluded that the shaking table excitations imposed on the test structure simulate ground motions which could possibly occur in the field due to a seismic event. The diverse modifications performed in the records from which the table input signals are obtained, such as scaling the acceleration values and changing the time scale, can be used to simulate ground motions induced by earthquakes of different magnitude, and affecting sites with different soil conditions.

TEST STRUCTURE CONDITION	RUN NO.	GROUND MOTION ACCELEROGRAM RECORD	SHAKING TABLE SPAN SETTING	SCALED PEAK ACCELERATION	RUN IDENTI-FICATION
WITH CONCRETE BLOCKS WITH LATERAL BRACING	1	TAFT[(1)]	100	0.097g	W1
	2	TAFT	850	0.57g	W2
	3	TAFT	850	0.65g	W3
REPAIRED WITH CONCRETE BLOCKS WITH LATERAL BRACING	4	TAFT	50	0.07g	R1
	5	TAFT	850	0.78g	R2
	6	TAFT	850	0.82g	R3

(1) TAFT = TAFT, JULY 21, 1952 N69W COMPONENT

TABLE 3.1 EARTHQUAKE SIMULATOR TEST PROGRAM

TEST NUMBER	LAST RUN BEFORE TEST	CONCRETE BLOCKS	NATURAL PERIOD (Sec)	
			1st Mode	2d Mode
1	NONE	NO	.152	.049
2	NONE	YES	.263	.102
3	W1	YES	.319	.115
4	W2	YES	.493	.149
5	W3	YES	.532	.162

TABLE 3.2

VARIATION OF NATURAL PERIODS OF TEST STRUCTURE THROUGH TEST HISTORY (From Reference [2])

Earthquake	Recording Station	Horizontal Distance (km)	Magnitude	Component	Max. Ground accel.(g's)	Remarks
San Fernando California 02/9/71	Pacoima Dam Abutment	3 (to fault)	6.5	S74W	1.075	Small building on rocky spine adjacent to dam abutment. Highly jointed diorite gneiss
Managua Nicaragua 12/23/72	Esso Refinery	5 (to fault)	6.2	N-S	0.34	Alluvium
El Centro California 05/18/40	El Centro	6 (to fault)	6.5	N-S	0.32	2-story heavy reinforced concrete building, with massive concrete engine pier. Alluvium
Kern County California 07/21/52	Taft	40 (to epi-center)	7.7	N69W	0.18	In service tunnel between buildings. Alluvium

TABLE 3.3

CHARACTERISTICS OF SELECTED EARTHQUAKES

(Partially obtained from Reference [16])

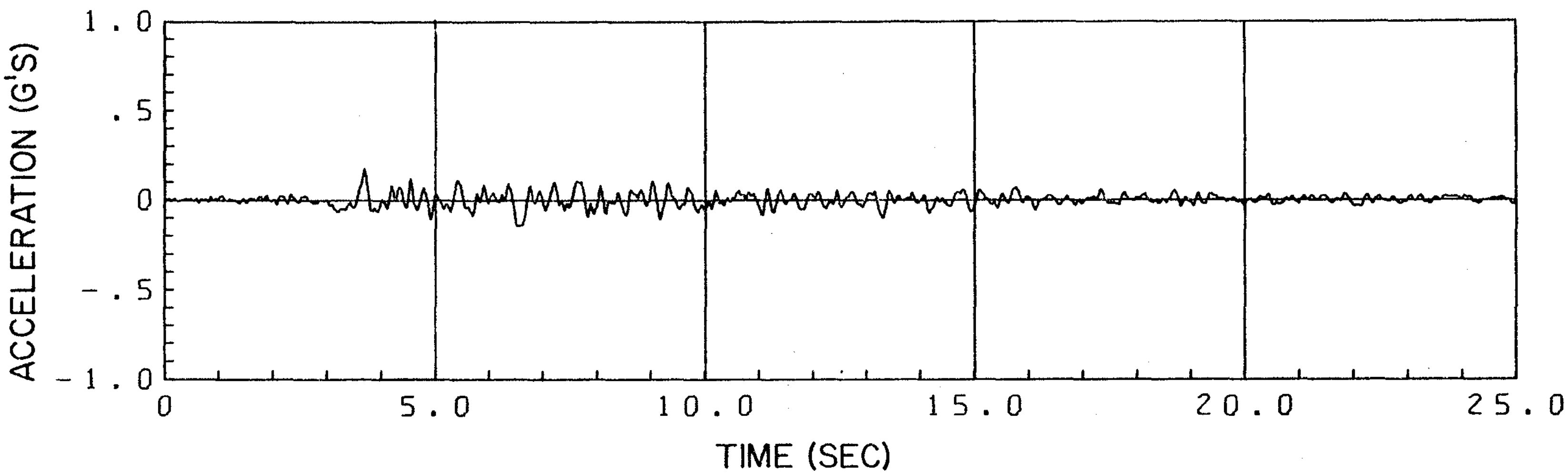

FIG. 3.1(a) TAFT 1952 N69W ACCELERATION RECORD

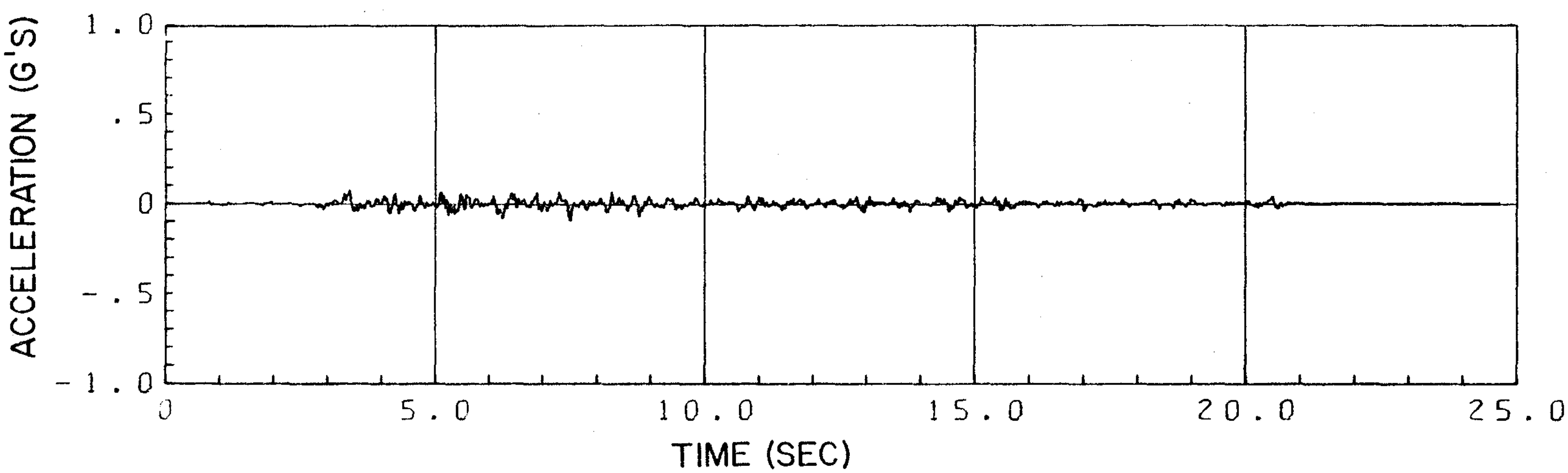

FIG. 3.1(b) HORIZONTAL TABLE ACCELERATION. RUN W1: TAFT 100

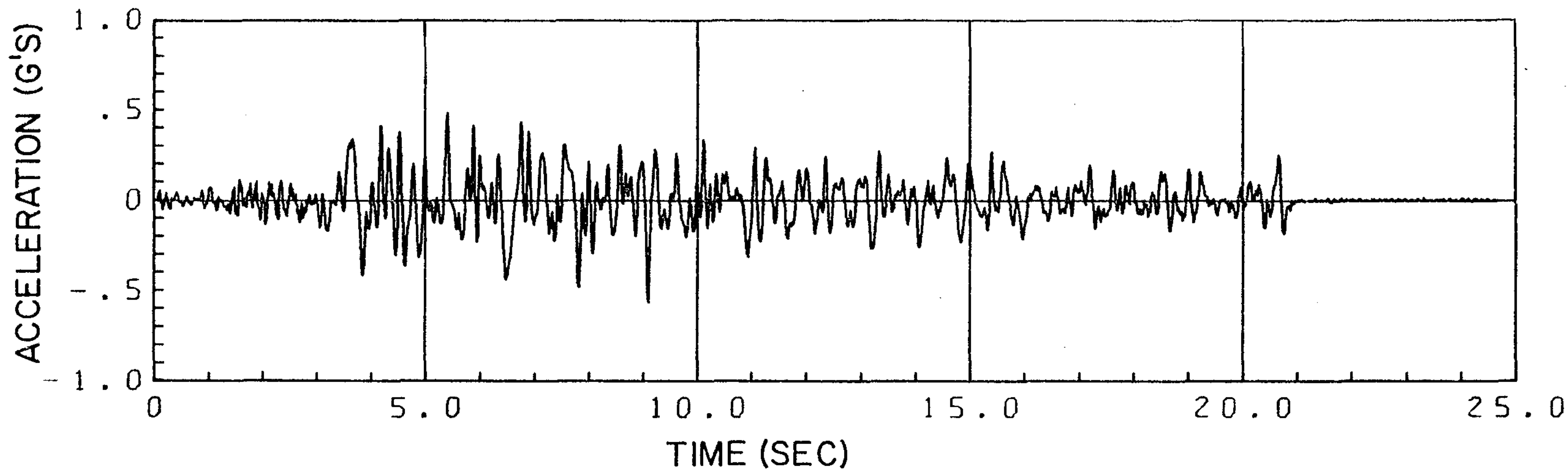

FIG. 3.1(c) HORIZONTAL TABLE ACCELERATION. RUN W2: TAFT 850(1)

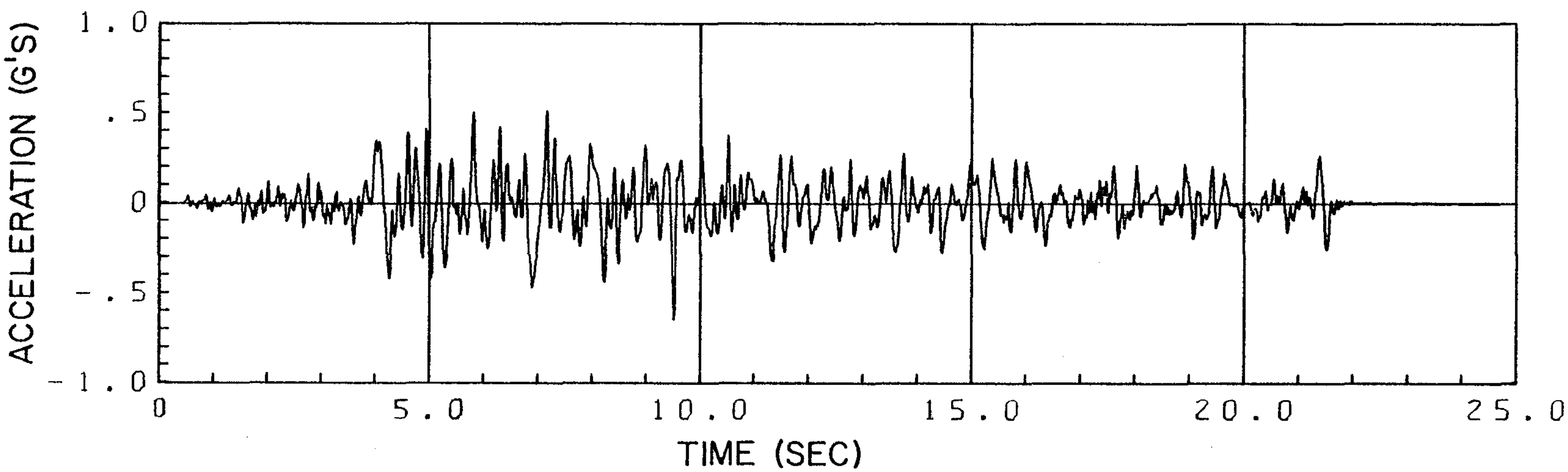

FIG. 3.1(d) HORIZONTAL TABLE ACCELERATION. RUN W3: TAFT 850(2)

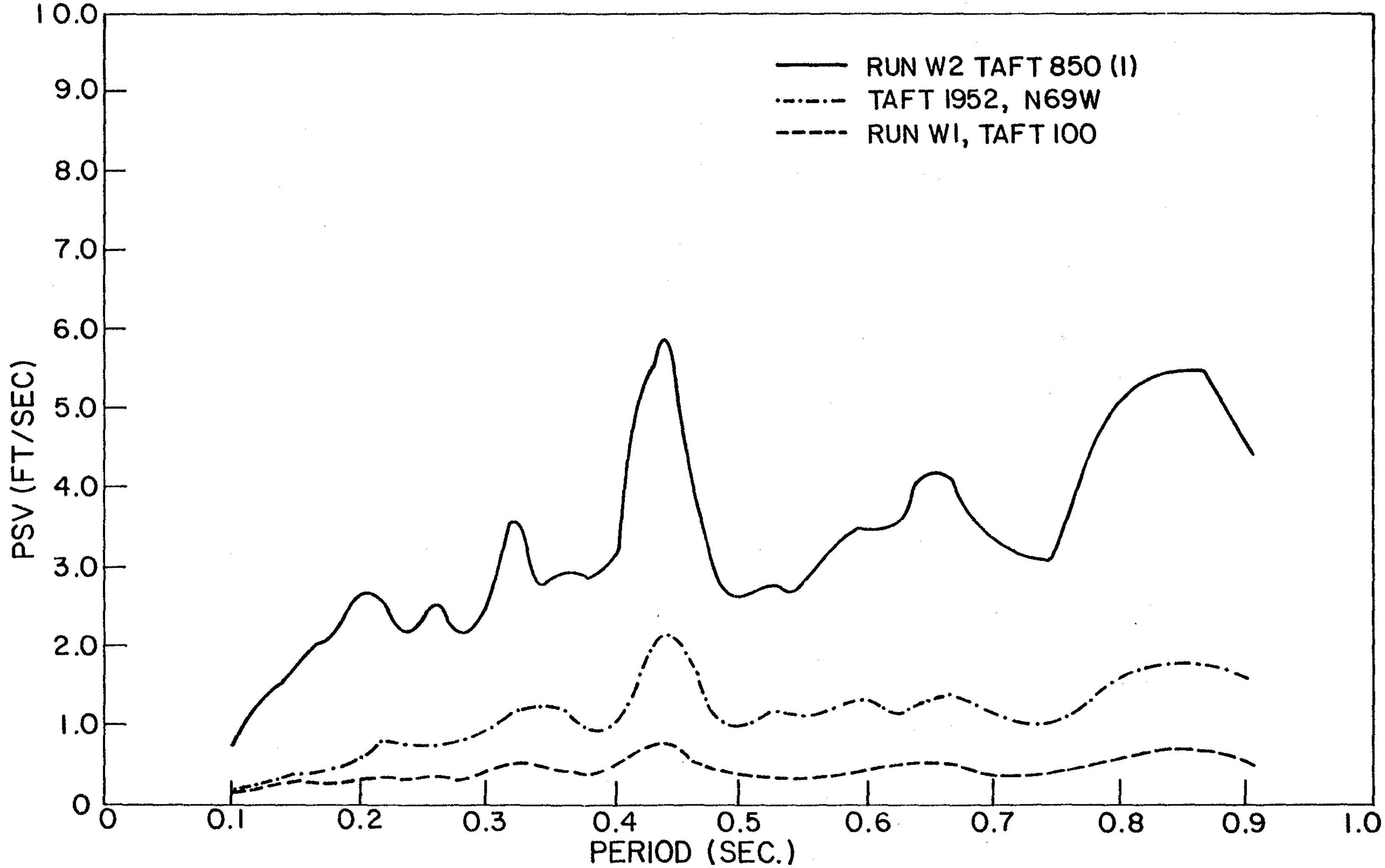

FIG. 3.2 PSEUDO VELOCITY RESPONSE SPECTRA (2% DAMPING) MODEL (TEST STRUCTURE) TIME SCALE. TAFT 1952 N69W AND RUNS W1 and W2

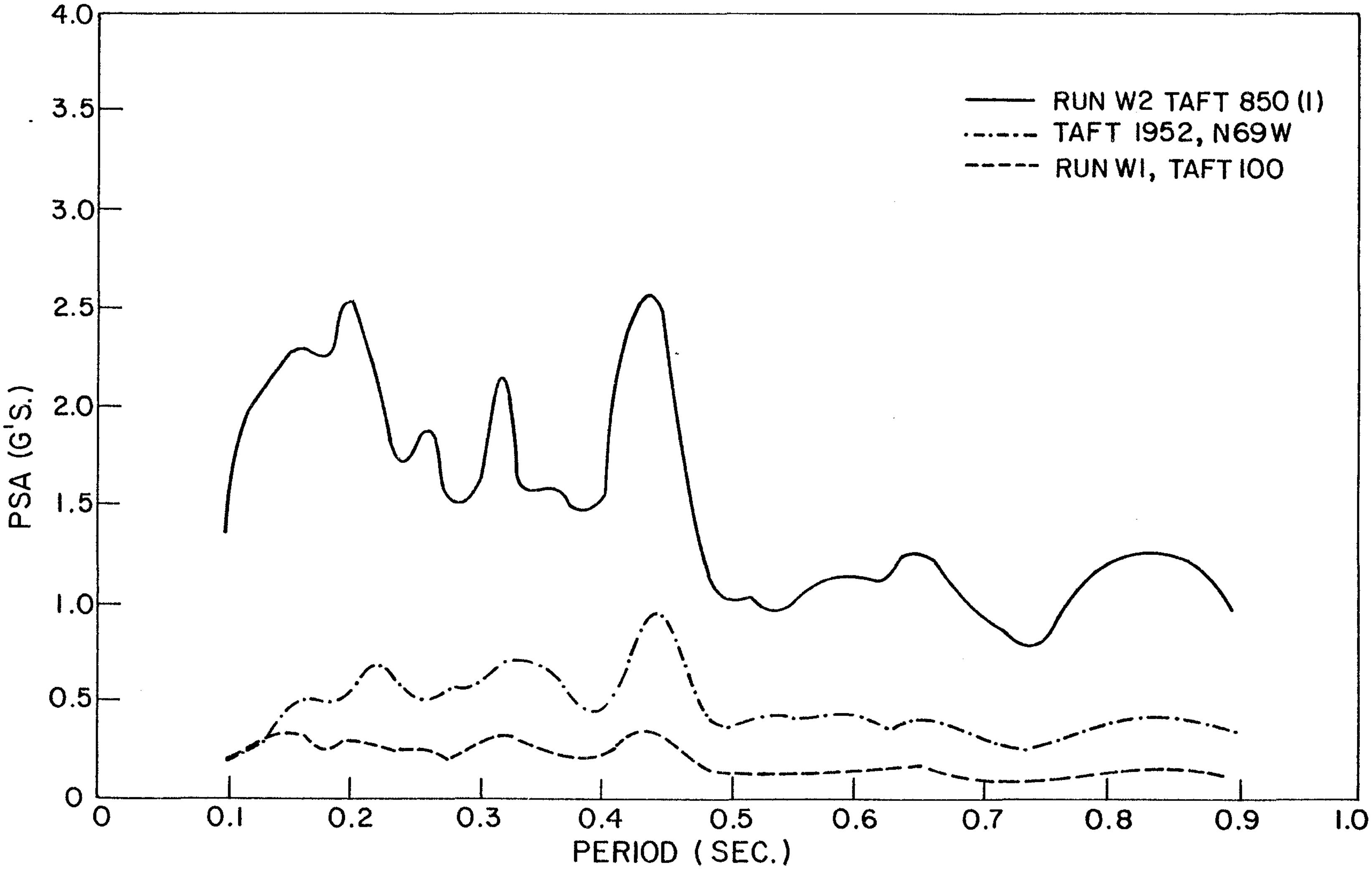

FIG. 3.3 PSEUDO ACCELERATION RESPONSE SPECTRA (2% DAMPING) MODEL (TEST STRUCTURE) TIME SCALE. TAFT 1952 N69W AND RUNS W1 AND W2

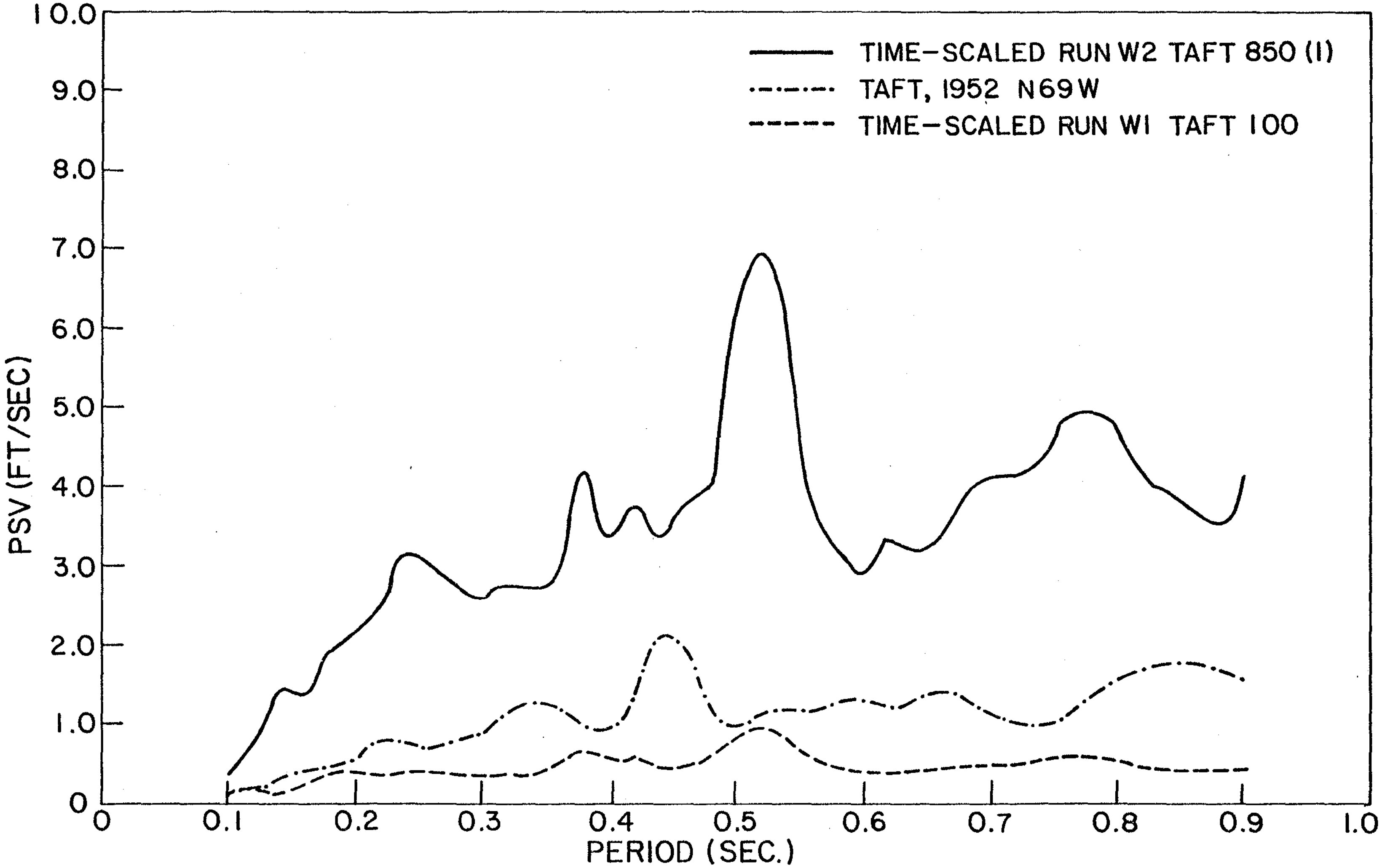

FIG. 3.4 PSEUDO VELOCITY RESPONSE SPECTRA (2% DAMPING) PROTOTYPE TIME SCALE. TAFT 1952 N69W AND TIME-SCALED RUNS W1 AND W2

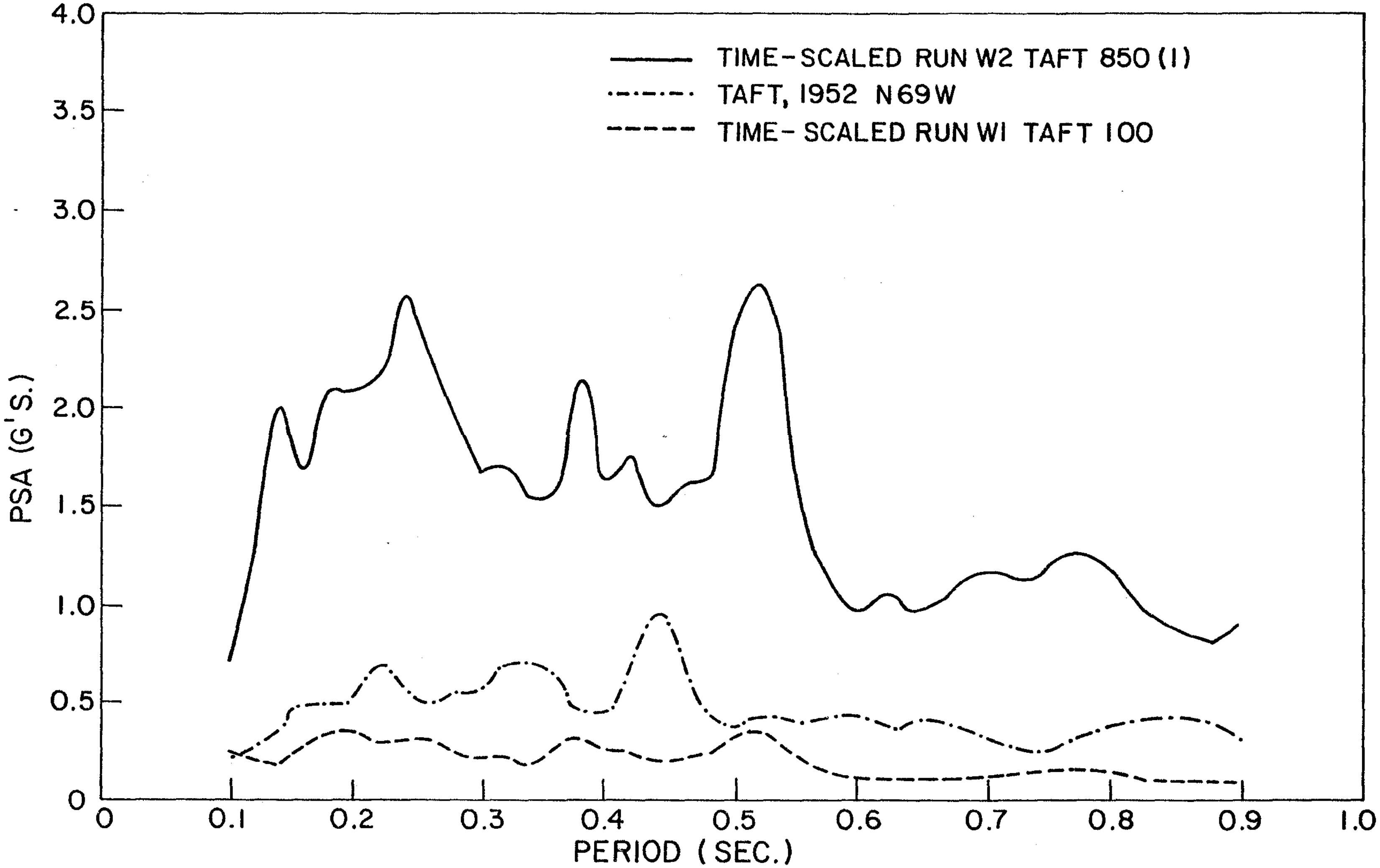

FIG. 3.5 PSEUDO ACCELERATION RESPONSE SPECTRA (2% DAMPING) PROTOTYPE TIME SCALE. TAFT 1952 N69W AND TIME-SCALED RUNS W1 AND W2

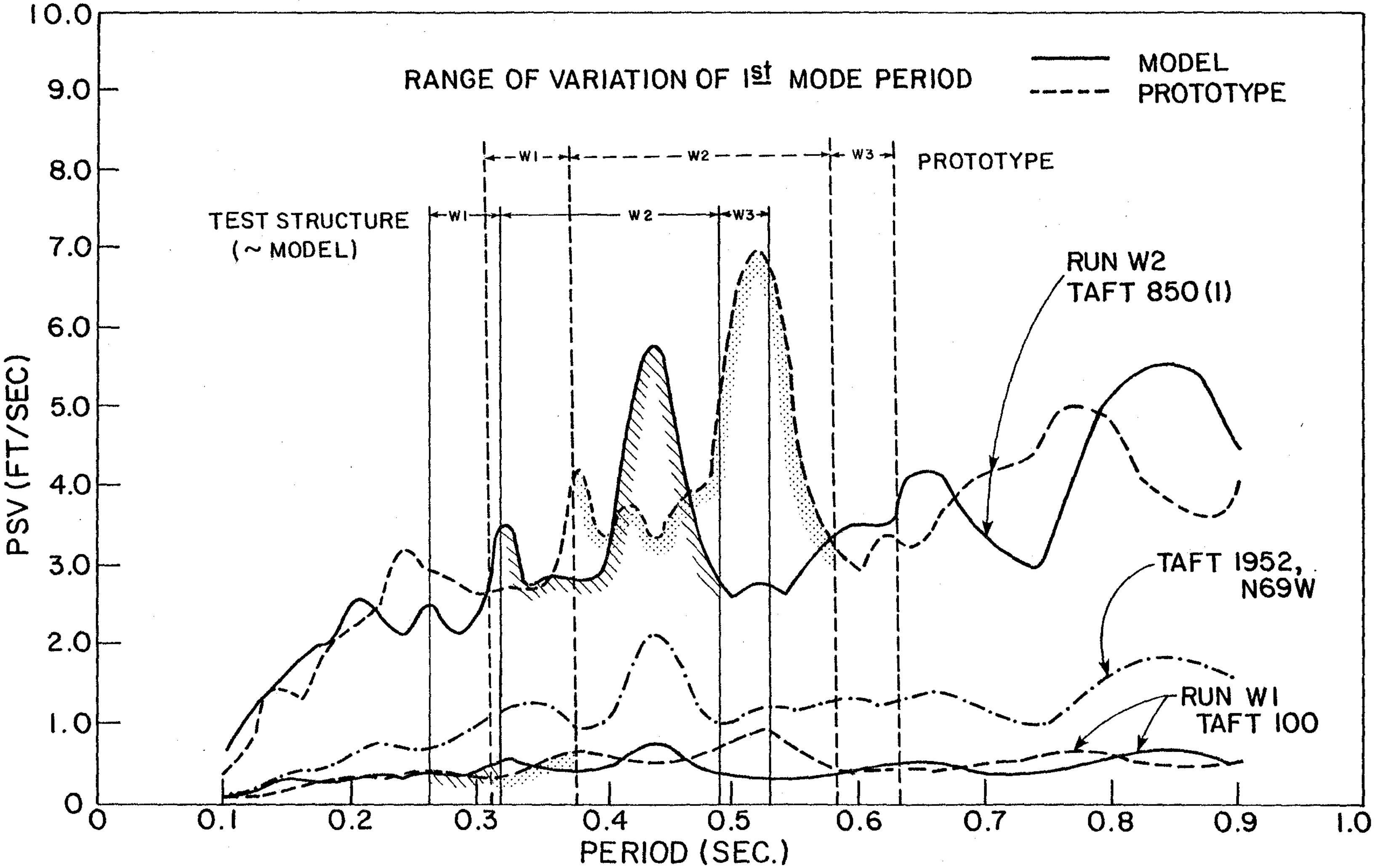

FIG. 3.6 PSEUDO VELOCITY RESPONSE SPECTRA (2% DAMPING) MODEL AND PROTOTYPE TIME SCALES. TAFT 1952 N69W (UNSCALED) AND RUNS W1 AND W2

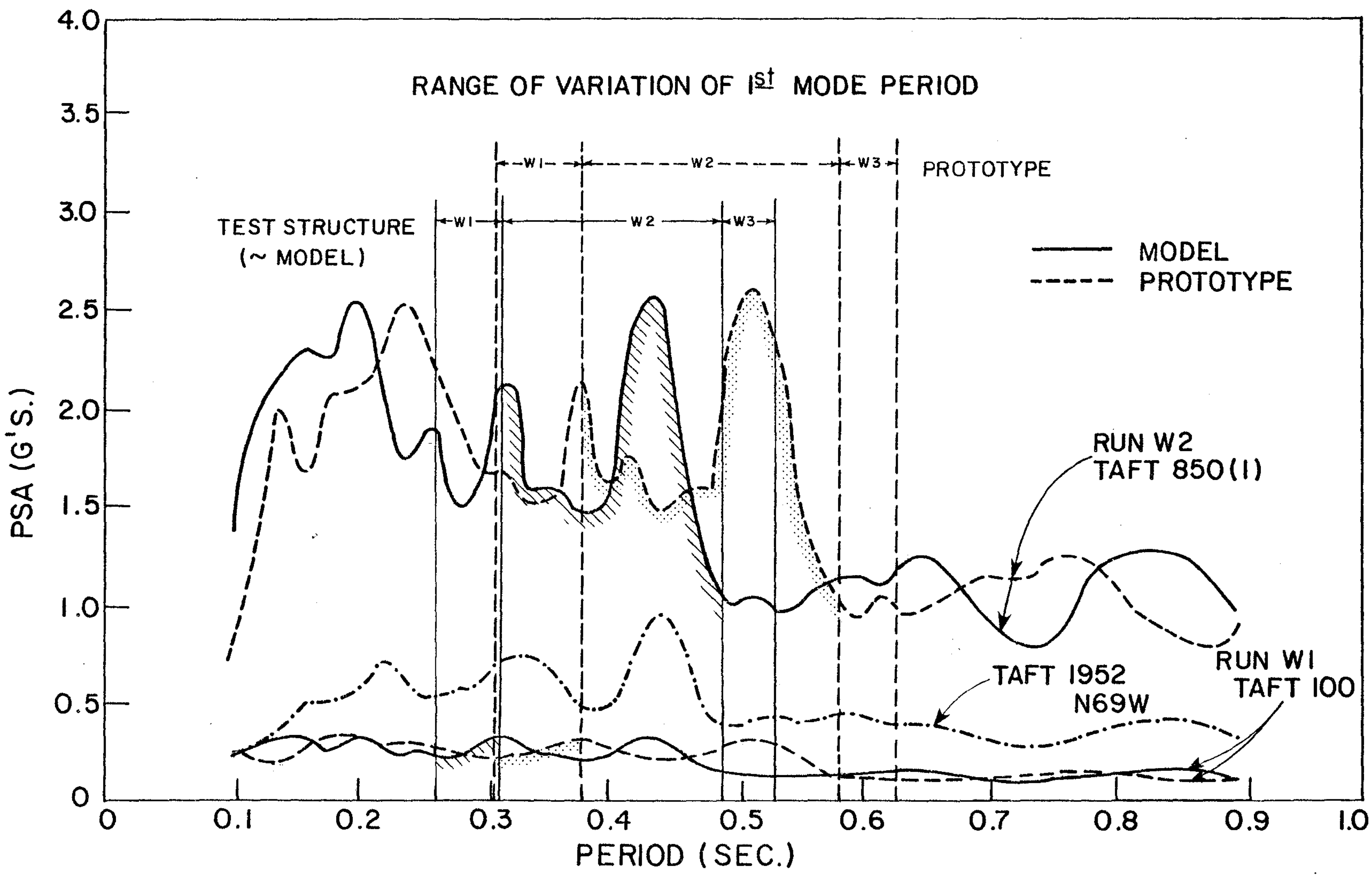

FIG. 3.7 PSEUDO ACCELERATION RESPONSE SPECTRA (2% DAMPING) MODEL AND PROTOTYPE TIME SCALES. TAFT 1952 N69W (UNSCALED) AND RUNS W1 AND W2

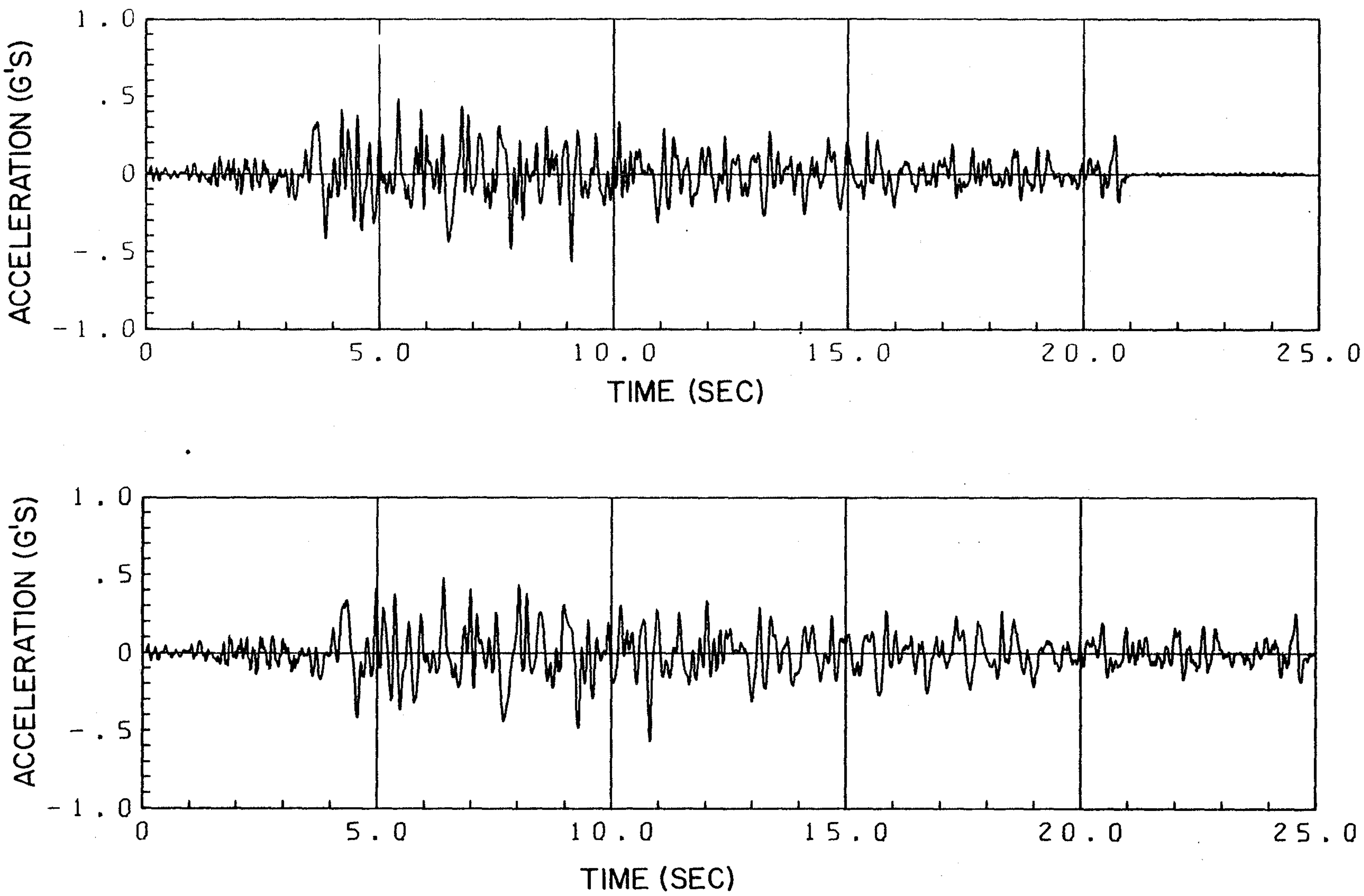

FIG. 3.8 EFFECT OF TIME SCALING ON THE ACCELERATION RECORD OF RUN W2: TAFT 850(1)

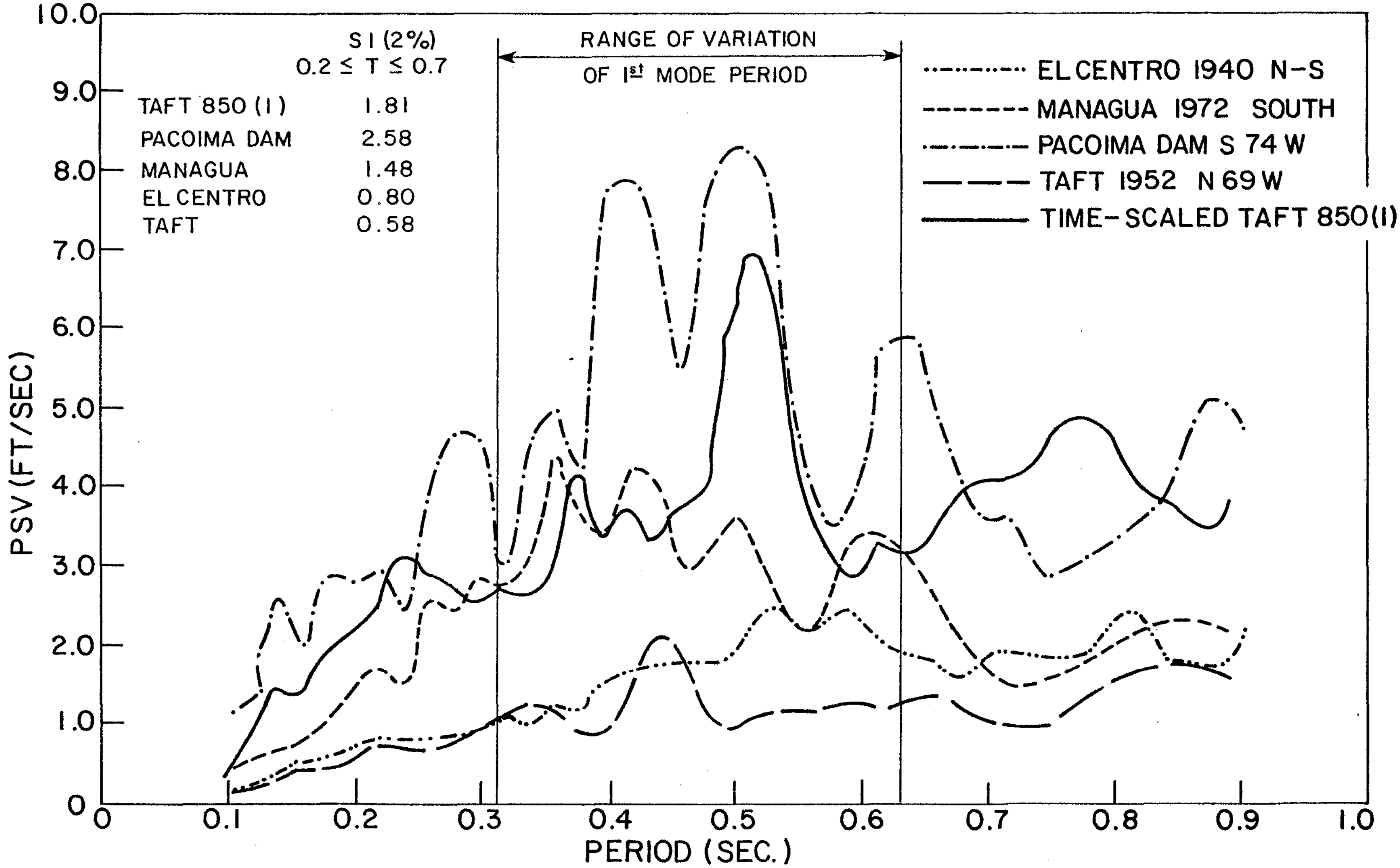

FIG. 3.9 PSEUDO VELOCITY RESPONSE SPECTRA (2% DAMPING) TIME-SCALED RUN W2: TAFT 850(1) AND SELECTED RECORDED SEISMIC EVENTS

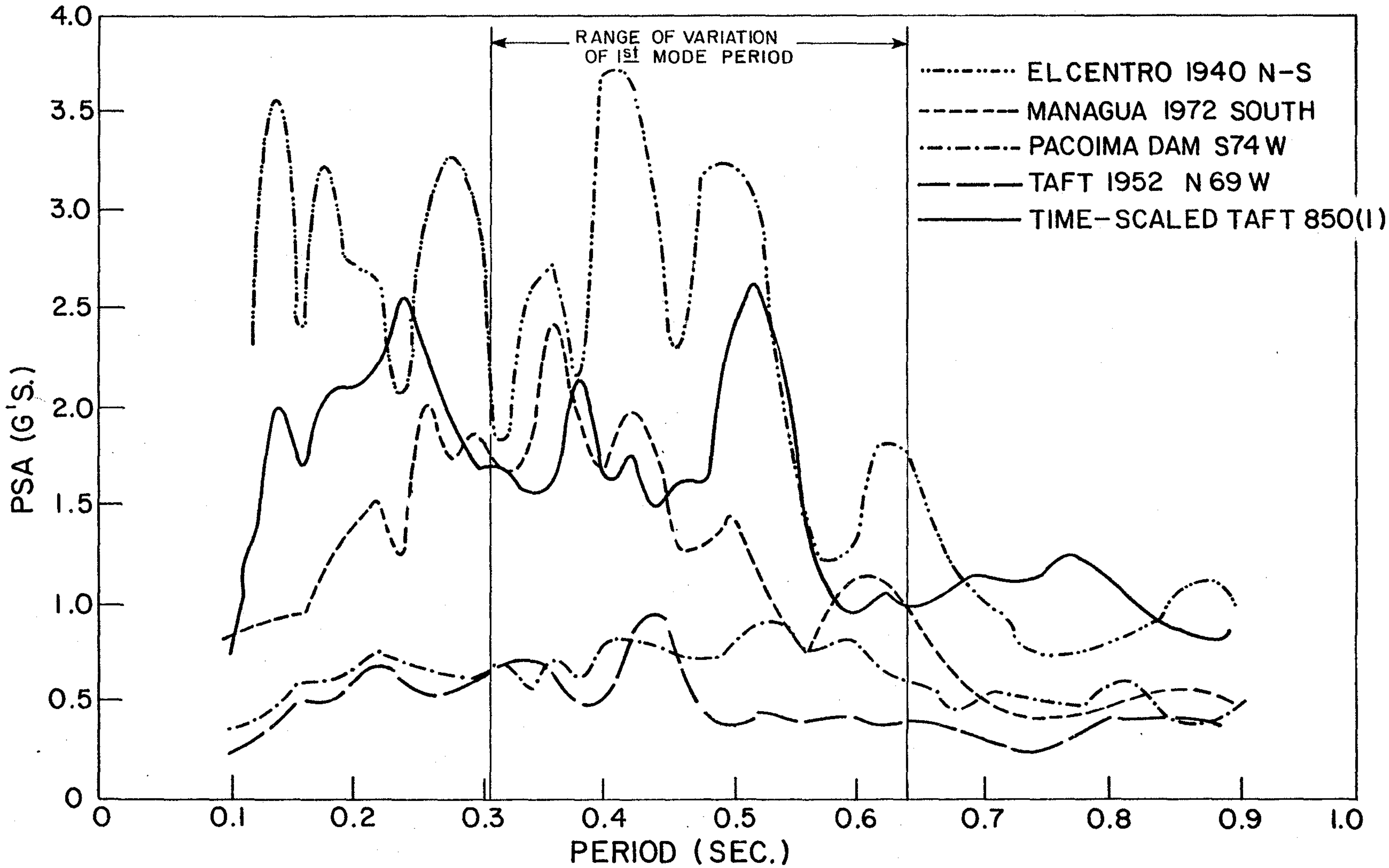

FIG. 3.10 PSEUDO ACCELERATION RESPONSE SPECTRA (2% DAMPING) TIME-SCALED RUN W2: TAFT 850(1) AND SELECTED RECORDED SEISMIC EVENTS

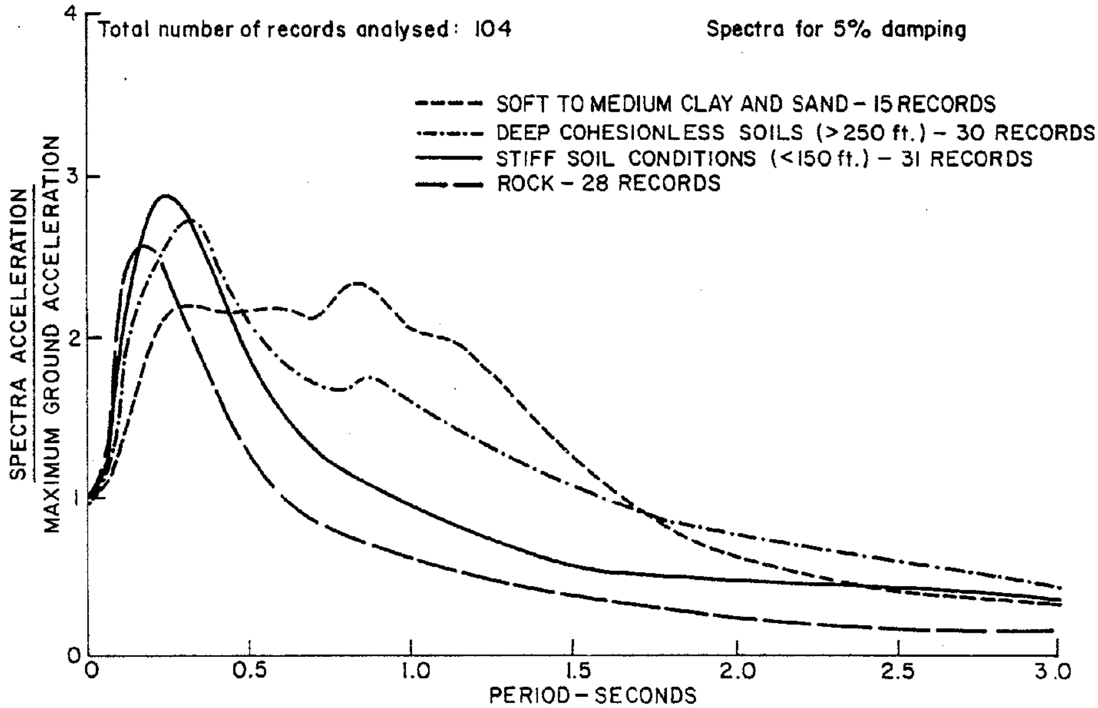

FIG. 3.11(a) AVERAGE ACCELERATION SPECTRA FOR DIFFERENT SITE CONDITIONS (FROM REFERENCE [18])

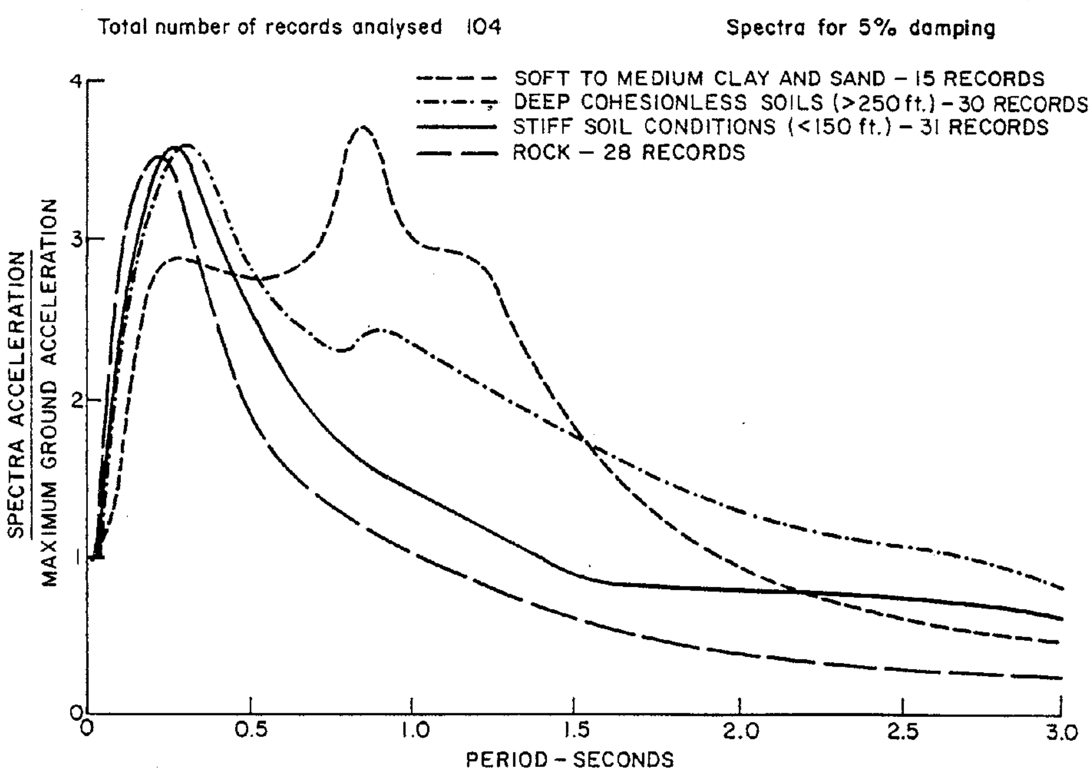

FIG. 3.11(b) 84 PERCENTILE ACCELERATION SPECTRA FOR DIFFERENT SITE CONDITIONS (FROM REFERENCE [18])

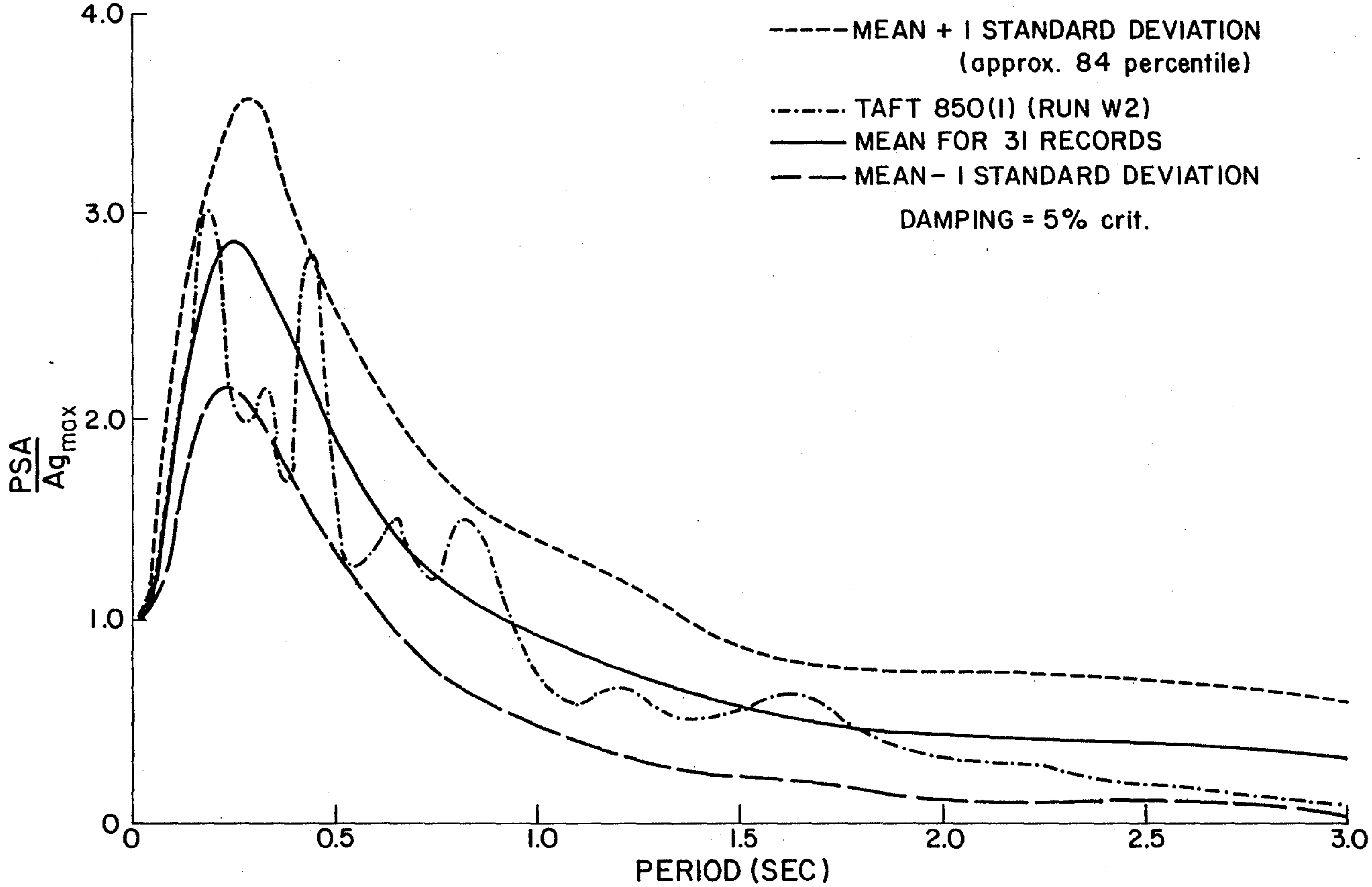

FIG. 3.12 NORMALIZED ACCELERATION SPECTRA FOR STIFF SOIL CONDITIONS AND RUN W2: TAFT 850(1) (BASED ON 31 RECORDS)

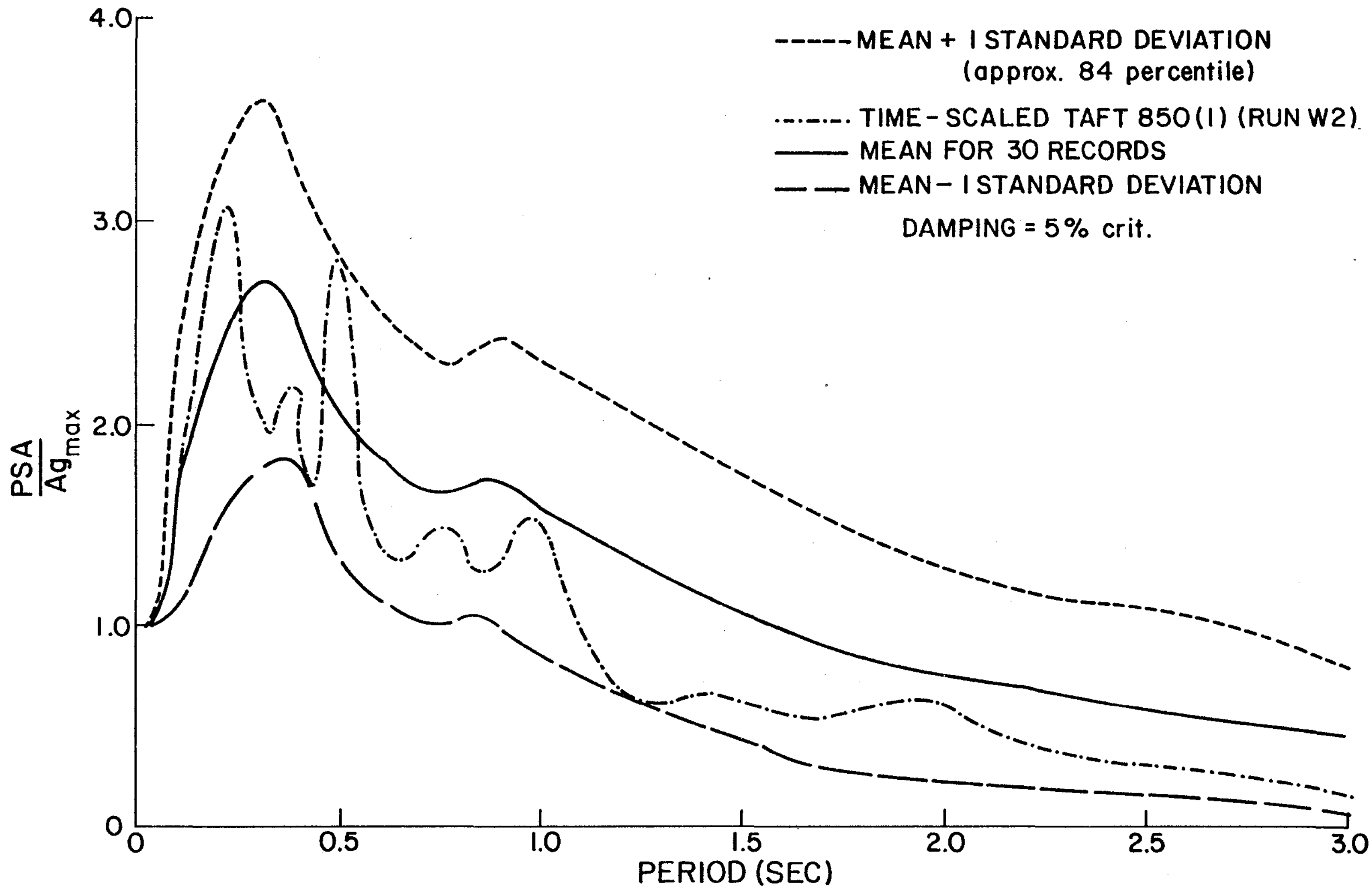

FIG. 3.13 NORMALIZED ACCELERATION SPECTRA FOR SITES UNDERLAIN BY DEEP COHESIONLESS SOILS AND TIME-SCALED RUN W2: TAFT 850(1) (BASED ON 30 RECORDS)

Preceding page blank

4. EVALUATION OF THE DESIGN OF THE TEST STRUCTURE

4.1 Preliminary Considerations

In order to complete the evaluation of the RCF2 test procedure undertaken by this study, it is necessary to determine if the test specimen under consideration corresponds to a normal structure designed for adequate performance in a region of high seismic activity.

The structural design of the ideal model of the prototype two story office building, described in Chapter 2, is examined in the following sections with respect to provisions of the Uniform Building Code, 1979 Edition[11], to determine if it complies with the requirements for ductile moment-resisting space frames (DMRSF) located in zones of the highest seismic activity in the USA (Seismic Zone 4.) The decision to examine the structural design of the model rather than that of the prototype structure and/or the test structure, is based on the results of this study presented in Chapter 2, where it is shown that the test structure and the ideal model have basically the same structural characteristics. Hence, if it is determined that the ideal model can be qualifield as a DMRSF meeting the Code requirements, it will be evident that the test structure (and, of course, the prototype building) are also adequately designed according to the Code philosophy. The ideal model is therefore used as a "link" between the prototype structure and the test specimen, as it was in the previous chapters.

The prototype structure has been designed to meet the requirements provided in the UBC 1970[9] and ACI 1971[10] Codes. The design procedure is presented in Appendix A. For the purpose of determining the design loads corresponding to the current (1979) Uniform Building Code, the distribution of gravity loads in the model has been derived from that used for the design of the prototype, applying the appropriate scaling ratios (Table 2.2); however, the seismic lateral loads do not correspond to those originally employed, due to a different estimate of the total weight of the prototype and to the different expression used in the 1979 UBC to compute the seismic base shear. Furthermore, the load combinations used to produce the ultimate design loads recommended by the current code are slightly different from those used in the original design. As a result, the ultimate design loads used in this study to verify the adequacy of the design of the model do not correspond to those used in the design of the prototype building. Since it is not within the scope of this study to evaluate the effect of the change of Code requirements on the seismic-resistant design of reinforced concrete buildings, these differences will be pointed out only when it is considered convenient for clarification purposes.

4.2 Determination of Seismic Lateral Forces

1) Total base shear

The minimum total lateral force specified by the 1979 UBC, Section 2312(d) to be used for the seismic resistant design of any structure is given by

$$V = Z\ I\ K\ C\ S\ W$$

In which

$Z = 1.0$ for buildings located in Seismic Zone 4

$I = 1.0$ is the occupancy importance factor corresponding to office buildings (non essential facility)

$K = 0.67$ for buildings in which the total lateral force is resisted by a DMRSF

$C = \dfrac{1}{15\sqrt{T}}$ Where T is the fundamental period of the structure in the direction under consideration

S is a numerical coefficient for site - structure resonance,

and

W is the total dead weight (including partitions) of the building.

Hence, in this case

$$V = 1.0 \times 1.0 \times 0.67 \times CS \times W = 0.67CSW$$

In addition, $CS \leqslant 0.14$

and $C \leqslant 0.12$

The fundamental period T has been computed in the elastic analysis described in Chapter 2; its value is

$$T = 0.23 \text{ sec.}$$

In addition, the Code provides two formulas to estimate the natural periods of buildings:

a) $$T = \frac{0.05\ h_n}{\sqrt{D}}$$

Where h_n is the height of the building (ft), and D its base dimension in feet in the direction parallel to the seismic forces, thus

$$T = 0.05 \times \left(\frac{2x76.37}{12}\right) \cdot \frac{1}{\sqrt{\frac{144.25}{12}}} = .18 \text{ sec.}$$

b) $T = 0.1\ N$, for DMRSF where N is the number of stories, hence

$$T = 0.2 \text{ sec.}$$

The highest value of the seismic coefficient C corresponds to the lowest estimate of T, hence, the value T = .18 will be used to estimate conservatively this factor, although the code permits the value obtained by analysis to take precedence.

For T = .18,

$$C = \frac{1}{15\sqrt{.18}} = .157$$

but $C \leqslant .12$; hence C = .12 is used

The coefficient S is taken to be 1.5, since the natural period of the soil underlying the site is unknown.

Consequently,

$$CS = 0.12 \times 1.5 = .18$$

but $CS \leq .14$, hence $CS = .14$ is used.

The total weight of the prototype has been estimated as 82.61 kips. The weight of the model is consequently

$$W = 0.5 \times 82.61 = 41.305 \text{ kips},$$

leading to the total seismic base shear

$$V = 0.67 \times 0.14 \times 41.305 = 3.875 \text{ kips}.$$

This corresponds, in prototype scale, to a total lateral force of 7.75 kips. The seismic base shear used to design the prototype building, required by the 1970 UBC, was 4.7 kips (about 40% less than the load required by the 1979 UBC.)

2) Distribution of lateral forces along height.

The UBC specifies (Section (2312(e))

$$F_x = \frac{(V-F_t)w_x h_x}{\sum_{i=1}^{n} w_i h_i}$$

Where

F_x = lateral force at level x

w_x, w_i = weight corresponding to levels x, i

h_x, h_i = height above the base of levels x, i

and $F_t = 0$ since $T < 0.7$ sec.

The forces thus calculated for each level are presented in the table below. The values of the story weights and heights can be seen in Figure 4.1.

STORY	WEIGHT (kips)	HEIGHT (ft)	$w_i h_i$	F_x (kips)
TOP	17.445	12.77	221.90	2.301
BOTTOM	23.86	6.36	151.75	1.574
TOTAL	41.305		373.65	3.875

In order to compare the design earthquake loads with the lateral strength computed in Chapter 2, and the inertia forces developed in the test structure during the dynamic tests, it was decided to compute the lateral load corresponding to each level as being proportional to the inertia forces associated with the first mode of vibration. This procedure is allowed by the Code (Section 2312(i)). The computation of the ratio between the lateral forces at each level is presented in Appendix C. The lateral forces associated with the Code base shear are listed in the following table

STORY	LOAD MULTIPLIER	LATERAL FORCE (kips)
TOP	1.03λ	1.965
BOTTOM	1.00λ	1.91
TOTAL	2.03λ	3.875

Where λ is determined as follows:

for $V = 3.875$ kips $= 2.03\lambda$,

$$\lambda = \frac{3.875}{2.03} = 1.9088$$

A broad comparison with the loads computed using the formula provided by the Code suggests that in this case a uniform distribution of lateral forces (as used in the original design) seems more rational than the "triangular" distribution provided by the Code formula.

4.3 Determination of Gravity Loads on Girders

The loads acting on the girders due to gravity forces were obtained from those derived in Reference [1], applying the corresponding ratios to reduce them to model scale. It should be noted that the loads due to the two-way action of the floor slabs have been computed using Method 3 in the 1963 ACI recommendations[8] which is not included in the current ACI Code. The equivalent frame method (1979 UBC Section 2613(e)) has also been used to compute the distribution of the slab loads along the girders; a brief discussion of the discrepancies of the two methods mentioned is presented in Section 4.6. Another assumption worth mentioning is that the live loads have been considered acting in full, i.e. no reduction was made, although the UBC recommendations allow for it (Section 2306).

The distribution of dead and live loads on the longitudinal and transverse girders assumed for the model is shown in Figure 4.1.

4.4 Elastic Analysis

In order to determine the required strength for the girders and columns of the ideal model, an elastic analysis using the computer program ETABS[13] was performed using the gravity and seismic loads computed in the previous sections. The assumptions used to idealize the structure have been described in Section 2.5, and the dimensions and loads are summarized in Figure 4.1.

The ultimate design loads were obtained from the following combinations of dead, live and seismic loads, according to UBC Sections 2609(d) and 2626(a)

$$U_1 = 1.4D + 1.7L$$

$$U_2 = 1.4D + 1.4L + 1.4E$$

$$U_3 = 1.4D + 1.4L - 1.4E$$

$$U_4 = 0.9D + 1.4E$$

$$U_5 = 0.9D - 1.4E$$

The results of the elastic analysis for each load condition are summarized in Table 4.1. Only the results concerning the longitudinal frames are presented. The weight of the columns is considered in the computation of the axial loads.

In the next sections, the most revelant Code requirements from the point of view of the structural seismic behavior are examined. Figure 4.2 shows the geometric characteristics and the location and amount of the steel reinforcement. Unless otherwise specified, and in accordance with the assumptions made for the static analysis, the specified material properties (f'_c=4.0 ksi and f_y=40.0 ksi) are used. Numbers within paranthesis refer to the appropriate 1979 UBC sections. The notation used corresponds to that of the 1979 UBC.

4.5 Code Requirements for Columns

1) Dimensional limitations (2626(f)1)

a) $\frac{\text{Minimum column thickness}}{\text{Maximum column thickness}} \geqslant 0.4$

in this case

$$\frac{5.66}{8.49} = 0.67 > 0.4 \quad \text{OK.}$$

b) minimum column dimension $\geqslant$ 12 in.

This requirement is not satisfied. In prototype scale, the minimum dimension of the column is 8 in. However, this fact does not have any significant consequence in the structural behavior of the prototype (or the model) and can be disregarded.

2) Vertical reinforcement limitations

a) $0.01 < \rho = \frac{A_s}{bd} < 0.06$ (2626f2)

the columns have $A_s = 0.60 \text{in}^2$

$$b = 5.66 \text{ in.}, \quad d = 6.86 \text{ in.}$$

hence

$$\rho = \frac{0.60}{5.66 \times 6.86} = .0155$$

which is within the required limits.

b) $\rho \leqslant 0.75\ \rho_b$ corresponding to zero axial load. (2610d2)

$$\rho_b = \frac{0.85\ \beta_1\ f'_c}{f_y} \times \frac{87000}{87000+f_y}$$

hence

$$\rho_b = \frac{.85 \times .85 \times 4}{40} \times \frac{87000}{87000+40000} = .0495$$

and

$$\rho = 0.0154 < 0.75\rho_b = .0371 \quad \text{OK.}$$

3) Approximate evaluation of slenderness effects (2610(1))

These effects will be evaluated in the longitudinal direction only. Since the columns are not braced against sideways, the slenderness effects should be accounted for if the ratio $\frac{k\ell_u}{r}$ is larger than 22, where

ℓ_u = unsupported length = 70.72 in.

r = radius of gyration = 0.3 x h = 0.3 x 8.49 = 2.55 in.

k = effective length factor

This latter factor depends on the end restraints of the column, and the flexural rigidity of the column and of the restraining members. Since the bottom story and top story columns have different restraint conditions, their effective lengths are different, and must be computed separately. The flexural stiffness of the sections (EI) are computed using the expressions proposed by Winter[20], namely

$$(EI)\ \text{beams} = E_c I_{ct}$$

$$(EI)\ \text{columns} = \frac{E_c I_g}{5} + E_s I_{se}$$

where

E_c = elastic modulus of concrete = $57000\sqrt{f'_c}$

= 3605 ksi (2608(c))

E_s = elastic modulus of reinforcing steel

= 29000 ksi (2608(c))

I_{ct} = average moment of inertia of the transformed cracked sections of the girders, corresponding to curvature in opposite senses

I_g = moment of inertia of the column reinforcing steel about the centroidal axis of the section

I_{se} = moment of inertia of the column reinforcing steel about the centroidal axis of the section

For the computation of the moment of inertia of the transformed cracked section, a modular ratio $n = E_s/E_c$ is taken for both the tension and compression reinforcement. The contribution of the slab reinforcement is neglected. See Appendix C.

a) Bottom story column

The average moment of inertia of the transformed cracked section of the bottom story girder is

$$I_{ct} = I^{+}_{ct} + I^{-}_{ct} = \frac{347.1+262.4}{2} = 304.75 \text{ in.}^4$$

hence

$$\frac{E_c I_{ct}}{\ell_n} = \frac{3605\text{x}304.75}{135.77} = 8100 \text{ k-in.}$$

where ℓ_n is the clear height of the girder in inches

The geometric properties of the column are

$$I_g = 288 \text{ in.}^4$$

$$I_{se} = 2 \times 0.6 \times \left(\frac{5.23}{2}\right)^2 = 8.21 \text{in.}^4$$

hence

$$EI_c = \frac{3605\text{x}288}{5} + 2900 \times 8.21 = 446000\text{k}\cdot\text{in.}^2$$

and $$\frac{EI_c}{\ell_u} = \frac{446.000}{70.72} = 6310 \text{ k}\cdot\text{in.}$$

for the bottom column, and

$$\frac{EI_c}{\ell_u} = \frac{446.000}{65.05} = 6860 \text{ k-in.}$$

for the top column

The end restraint of the column is measured by the coefficient

$$\psi = \frac{\sum(\frac{EI}{\ell})\text{cols}}{\sum(\frac{EI}{\ell})\text{beams}}$$

which gives for the top end of the column

$$\psi_{top} = \frac{6310+6860}{8100} = 1.63$$

For the bottom end, ψ_{bottom} is taken equal to zero, assuming fixed-end conditions.

Using the Jackson and Moreland alignment chart for frames unbraced against sidesway, taken from Reference [20], the effective length factor of the bottom story column is found to be

$$k = 1.23$$

Then, the effective height of the column is

$$k\ell_u = 1.23 \times 70.72 = 87.0 \text{ in.}$$

and the slenderness coefficient becomes

$$\frac{k\ell_u}{r} = \frac{87.0}{2.55} = 34.1$$

which is larger than 22.

Therefore the slenderness effects must be accounted for, by magnifying the column design moments by a factor δ given by

$$\delta = \frac{c_m}{1 - \dfrac{P_u}{\phi\, P_c}} \qquad (2610\ 1\ 5)$$

where

$$c_m = 1.0$$

Since the frame is unbraced against sidesway:

$$P_c = \frac{\Pi^2 EI}{(k\ell_u)^2}$$

$$EI = \frac{\dfrac{E_c I_g}{5} + E_s I_s}{1 + \beta_d}$$

and β_d is the ratio of the maximum design dead load moment and the maximum design total moment.

For this case:

$$\beta_d = \frac{1.4x18.21}{90.52} = 0.28$$

where the value of the maximum dead load moment of the column has been taken from Figure 2.7. Consequently,

$$EI = \frac{446000}{1+0.28} = 348400 \text{ k·in.}$$

and the Euler critical load, P_c, results:

$$P_c = \frac{\Pi^2 x348400}{(870)^2} = 454 \text{ k}$$

Hence the moment magnification factor for the bottom column is found to be

$$\delta = \frac{1.0}{1.0 - \frac{20.65}{0.7x454}} = 1.07$$

This value has been computed for the maximum design axial load and for $\phi = 0.7$, and will be used for all load conditions, to be conservative. The capacity reduction factor ϕ has been taken equal to 0.7 since

$$P_u = 20.65 > 0.10\ A_g f'_c = 19.22 \text{ k}$$

$$\frac{h-d'-d_s}{h} = \frac{8.49-1.63-1.63}{8.49} = 0.62 < 0.7 (2609(c))$$

b) Top story column.

In this case

$$I_{ct} = \frac{I^+_{ct} + I^-_{ct}}{2} = \frac{260.0+185.5}{2} = 222.75 \text{ in.}^4$$

then

$$\frac{EI_b}{\ell_n} = \frac{3605x222.75}{135.77} = 5910 \text{ in.}^4$$

Hence, using the values for $\frac{EI}{\ell}$ computed for the bottom story column and girder, the end restraint factors become

$$\psi_{top} = \frac{6860}{5910} = 1.16$$

and

$$\psi_{bottom} = 1.63$$

Hence

$$k = 1.40$$

and

$$k\ell_u = 1.40 \times 65.06 = 91.08 \text{ in.}$$

hence

$$\frac{k\ell_u}{r} = \frac{91.08}{2.55} = 35.7 > 22$$

Again it is necessary to take into account the slenderness effects.

Proceeding as for the bottom column, the following values are obtained:

$$\beta_d = \frac{1.4x41.49}{103.71} = 0.56$$

$$EI = \frac{446000}{1+0.56} = 286000 \text{ k·in.}$$

$$P_c = \frac{\Pi^2 x286000}{(91.08)^2} = 340 \text{ kips}$$

For

$$P_u = 7.96 < 0.10A_g f'_c = 19.22$$

$$\phi = 0.7 + (0.9-0.7) \times \frac{19.22-7.96}{19.22}$$

$$= 0.82$$

Hence

$$\delta = \frac{1.0}{1-\frac{7.96}{0.82x340}} = 1.03$$

i.e., the column design moments of the top story column must be amplified by 1.03

4) Required flexural strength

The design ultimate loads for the bottom and the top story columns, along with their corresponding amplified moments are presented in Table 4.2. These load conditions have been plotted in a bending moment-axial force coordinate system, along with the interaction diagram of the columns, computed according to the requirements of the Code (Fig. 4.3). It is clear that since all the points representing the design load condition lie inside the "safe" regions bounded by the interaction curves, the column is strong enough to withstand all the prescribed load condition.

Moreover, it can be seen that the column core by itself is able to develop the necessary strength to avoid failure under the design load conditions.

5) Required shear strength

a) Minimum reinforcement (2611(b))

The minimum area of transverse reinforcement in square inches is given by

$$A_v = \frac{50 b_w s}{f_y}$$

Where b_w is the width of the section, and s the spacing of the transverse reinforcement. Hence, the maximum spacing of stirrups is:

$$s_{max} = \frac{A_v f_y}{50 b_w}$$

The prototype column transverse reinforcement consists of stirrups made of 3/8" diameter deformed steel, with a transverse area of 0.11 in.^{2}. Correspondingly, the transverse reinforcement of the model has an area of 0.055 in.^{2}, and

$$s_{max} = \frac{2x0.055x40000}{50x5.66} = 15 \text{ in.}$$

The transverse reinforcement of the prototype has a spacing of 4 in. in the central region, and of 2 in. in the end zones of the column. These spacings correspond to 2.88 in. and 1.44 in. respectively for the model structure, and are significantly smaller than the maximum spacing allowed by the Code.

b) Required transverse reinforcement

The required area of shear reinforcement is given by

$$A_v = \frac{(v_u - v_c) b_w s}{f_y} \qquad (2611(g))$$

hence the required spacing becomes

$$s = \frac{A_v f_y}{(v_u - v_c) b_w}$$

where

$$v_u = \frac{V_u}{\phi b_w d} \qquad (2611(c))$$

and, conservatively

$$v_c = 2\sqrt{f'_c} \text{ psi} \qquad (2611(e))$$

The maximum shear on the columns due to the different load conditions imposed on the structure occurs in the top story left column, for load condition 3, 1.4(D+L-E), and for the right column for load condition 2, 1.4(D+L+E), being

$$V_u = 3.10 \text{ kips}$$

Hence, for $\phi = 0.85$ (2609(c)), the maximum shear stress in the columns is

$$v_u = \frac{3.10}{0.95 \text{x} 5.66 \text{x} 6.86} = 0.094 \text{ ksi} = 94 \text{ psi}$$

The stress carried by the concrete, v_c is conservatively given by (2611(e))

$$v_c = 2\sqrt{f'_c} = 2\sqrt{4000} = 126.5 \text{ psi} > v_u$$

Therefore the concrete alone is strong enough to withstand the maximum shear stress induced by the design load conditions.

However, in order to be considered as a DMRSF in Zone 4, the design of the frame has to comply with the requirements of Section

2626. In particular, the required spacing of the transverse reinforcement should satisfy

$$s = \frac{A_v f_y d_c}{\frac{V_u}{\phi} - V_c} \qquad \text{(from formula 26.7)}$$

where V_u corresponds to the maximum possible shear in the column. This maximum value is the shear developed in the columns when plastic hinges form at both ends of the columns; therefore it ensures that failure in shear is avoided. Since the collapse mechanism of the model involves formation of plastic hinges at the ends of all the columns of the bottom story, the fulfillment of this requirement is essential to guarantee ductile behavior of the structure.

The column ultimate moment capacities were determined from the interaction diagram constructed considering a reinforcing yield strength 25 percent larger than the specified yield, and without considering the capacity reduction factor ϕ. The axial load P_e considered to determine the ultimate moment capacity of the columns is taken as the largest design axial load (for the bottom column).

Hence, for P_e = 20.55 kips, the moment capacity of the column is M_{ec} = 234k-in. and

$$V_u = \frac{2M_{ec}}{\ell_u} = \frac{2\text{x}234}{70.72} = 6.62 \text{ kips}$$

Also, since

$$\frac{P_e}{A_g} = \frac{20.65}{566\text{x}8.49} = 0.43 \text{ ksi} < 0.12f'_c = 0.48 \text{ ksi}$$

V_c must be considered zero

Consequently, the required spacing is found to be

$$s = \frac{A_v f_y d_c}{(V_u/\phi)}$$

where d_c is the dimension of the column core in the direction of V_u and $\phi = 0.85$. Hence for $A_v = 0.11$ in.^{2},

$$s = \frac{0.11 \times 40 \times 6.36}{\frac{6.62}{0.85}} = 3.60 \text{ in.}$$

The actual spacing in the test structure is 2.83 in., which is smaller than required; thus the columns are adequately protected against shear failure.

6) Special transverse reinforcement

During a strong earthquake, large compressive forces can be induced in the columns as a result of overturning effects; these forces can produce spalling of the concrete cover of the columns. In order to increase the strain capacity of the remaining core, and to avoid buckling of the reinforcing steel, it is necessary to provide adequate confinement to the section by means of closely spaced stirrups[12]. The intended result of this condition is to guarantee that the spalled section has strength equivalent to that of the complete (unspalled) section, and also has the necessary rotation capacity to develop this strength without suffering severe, irreparable damage.

The minimum required spacing of the special transverse reinforcement must satisfy the following expressions (2626(f))

$$s_h \leqslant \frac{A_{sh}}{0.30 h_c \frac{f'_c}{f_{yh}} \left(\frac{A_g}{A_{ch}} - 1 \right)} \qquad \text{(from formula 26.5)}$$

and

$$s_h \leqslant A_{sh} \frac{f_{yh}}{0.12 h_c f'_c} \qquad \text{(from formula 26.6)}$$

$$s_h \leqslant 4 \text{ inches}$$

where A_{sh} is the total cross-sectional area of hoop reinforcement, having a spacing of s_h, and crossing a section with a core dimension of h_c, expressed in inches, and A_{ch} is the area of the confined core measured out-to-out of the hoop, in square inches.

In this case

$$A_{sh} = 0.11 \text{ in.}^2$$

$$A_g = 48.0 \text{ in.}^2$$

$$A_{ch} = 6.36 \times 3.54 = 22.51 \text{ in.}^2$$

$$h_c = 6.36 \text{ in.}$$

and

$$f_c' = 4.0 \text{ ksi}, \quad f_{yh} = 40.0 \text{ ksi}.$$

hence the requirements are

$$s_h \leqslant \frac{0.11}{0.30 \times 6.36 \times \frac{4.0}{40.0}\left(\frac{48.0}{22.51} - 1\right)} = 0.51 \text{ in.}$$

$$s_h \leqslant \frac{0.11 \times 40}{0.12 \times 6.36 \times 4.0} = 1.44 \text{ in.}$$

and

$$s_h \leqslant 4 \text{ in.}$$

The provided spacing is 1.41 in. (2 in. in the prototype structure.) Consequently the last two requirements are satisfied, but the first requirement is not. However, the Code specifies that formula 26.5 need not be complied with if the column design is based on the column core only. This exception is based on the fact that the purpose of formula 26.5 is to guarantee that the spalled section has the same capacity as the complete section.

Hence, if it is demonstrated that the core has the necessary capacity to withstand all design load conditions, this requirement is not essential. Figure 4.3 shows the P-M interaction diagram for the column core, and it can be seen that all load conditions lie within the interaction curve, consequently the core has enough strength to withstand all load conditions, and the spacing provided for the transverse reinforcement is adequate.

The special transverse reinforcement has to be provided in the end regions of the columns, over a lenth ℓ_c satisfying the following requirements

$$\ell_c \geqslant \text{maximum column dimension} = 8.5 \text{ in.}$$

$$\ell_c \geqslant 1/6 \text{ clear height of the column} = 1/6 \times 70.72 = 12 \text{ in.}$$

and

$$\ell_c \geqslant 18 \text{ in. from either face of the joint.}$$

The confined length provided in the prototype structure is 18 in. which satisfies the third requirement; the equivalent length in the model structure is about 13 in. hence the two other requirements are also satisfied.

The Code also requires that the special transverse reinforcement has to be placed in the region where the capacity of the column is less than the sum of the shears (ΣV_u) corresponding to formation of plastic hinges in the girders framing into the column above the level of consideration.

For each beam, V_u is computed from:

$$V_u = \frac{M_A + M_B}{L_{AB}} + 1.1 \ (\omega_D + \omega_L) \times \frac{L_{AB}}{2}$$

where A,B are the hinge locations. The ultimate capacities M_A, M_B, are computed without the ϕ factor, assuming a reinforcement yield strength 25 percent larger than the specified value.

The most likely collapse mechanism involving formation of plastic hinges in the girders would be similar to that shown in Figure 4.4, according to the results of the elasto-plastic analysis performed previously (Chapter 2). The distribution of bending moments in the most heavily loaded columns can be obtained approximately assuming that the effect of the finite size of the joints and the inelastic region (plastic hinges) is small and can be neglected, and that the plastic moment at the end of the bottom story girder is equally distributed between the top and bottom columns. The position of the plastic hinge in the central region of the girders can be determined by means of an elasto-plastic analysis; for the purpose of the present calculations it will be assumed that the plastic hinges form at a distance of about 90 in. from the right end of the girders (from the results of the elasto-plastic analysis performed previously.) The moment capacity of the column is obtained from the interaction diagram corresponding to the specified material properties, with a conservatively chosen capacity reduction factor ϕ of 0.7.

The region which has to be adequately confined can be identified comparing the moment capacity of the column (for the axial load $P_u = \Sigma V_u$) with the bending moment distribution associated with the assumed collapse mechanism. This process is depicted in Figure 4.4. It can be seen that the column capacity is exceeded at both ends of the top column (especially in the upper 13.1 in.), and in the lower end of the bottom column, where a plastic hinge is formed. The length of special transverse reinforcement that has been provided is 13 in.; thus, all zones of possible plastification are adequately confined.

4.6 Code Requirements for Girders

1) Dimensional limitations (2626(e))

a) $\frac{\text{width}}{\text{depth}} \geqslant 0.3$

In this case

$$\frac{5.66}{11.32} = 0.5 > 0.3 \quad \text{OK}$$

b) width $\geqslant$ 10 in.

In model scale this requirement becomes

width $\geqslant$ 7.07 in.

The girders have a width of 5.66 in., thus, this requirement is not met. As in the case of the columns, it is thought that this violation has no significant influence on the structural behavior.

c) width $\leqslant$ width of column + 3/4 depth of girder

$$\leqslant 5.66 + 3/4 \times 11.32 = 14.15$$

or

$$5.66 \leqslant 14.15 \quad \text{OK}$$

d) T-beam requirements. (2608(g))

The contribution of the slab considered in the elastic analysis to quantify the T-beam action must conform to the following requirements:

i) effective flange width $\leqslant$ 1/4 space length = 1/4 (144.25) = 36 in.

The effective flange width of 36 in. meets this requirement

ii) overhanging width $\leqslant$ 8 x thickness of slab

$$= 8 \times 2.83 = 22.64 \text{ in.}$$

iii) overhanging width $\leqslant$ 1/2 x clear distance to next beam

$$= 1/2 \times (101.82-5.66) = 48.08 \text{ in.}$$

In this case, the overhanging width is

$$1/2(36-5.66) = 15.17 \text{ in.}$$

which meets the above requirements.

Similarly, for the transverse girders, which have a flange in one side only:

i) effective overhanging flange < 1/2 span length

$$= 1/12 \times 101.82 = 8.49 \text{ in.}$$

ii) effective overhanging flange $\leqslant$ 6 x thickness of slab

$$= 16.98 \text{ in.}$$

and

iii) effective overhanging flange $\leqslant$ 1/2 clear distance to next beam

$$= 1/2 \times (144.25-8.49)$$

$$= 67.88 \text{ in.}$$

Accordingly, a overhanging flange width of 8.49 in. was considered in the analysis.

2) Longitudinal reinforcement limitations (2626(e))

The longitudinal reinforcement ratio for top and bottom reinforcement must lie within the following limits

$$\frac{200}{f_y} \leqslant \rho \leqslant 0.025$$

or, for f_y = 40000 psi,

$$0.005 \leqslant \rho \leqslant 0.025$$

where

$$\rho = \frac{A_s}{b_d}$$

The reinforcement ratios provided for the bottom story girder are:

$$\text{Bottom reinforcement} \quad \rho = \frac{0.60}{5.66 \text{x} 9.68} = 0.011$$

$$\text{Top reinforcement} \quad \rho = \frac{0.60}{5.66 \text{x} 9.83} = 0.017$$

and for the top story girder:

$$\text{Bottom reinforcement} \quad \rho = \frac{0.44}{5.66 \text{x} 9.73} = 0.008$$

$$\text{Top reinforcement } \rho = \frac{0.40}{5.66 \times 9.83} = 0.007$$

using the width of the stem of the T-beams (2610(f)) to compute the reinforcement ratios. It can be seen that the provided reinforcement ratios satisfy the Code limitations.

In addition, $\rho \leqslant 0.75\ \rho_b$(2610(d)) where $\rho_b = 0.0495$ for $f_y = 40$ ksi and $f'_c = 4.0$ ksi. Obviously, this requirement is met.

Reinforcement must be provided such that the positive moment capacity at the face of the columns is at least 50 percent of the negative moment capacity (2626(e)).

For the bottom story girder,

$$M_u^+ = 232.9 > \frac{1}{2} M_u^- = \frac{1}{2} \times 199.4 = 99.7 \text{ k-in.}$$

and for the top story girder

$$M_u^+ = 171.3 > \frac{1}{2} \times 139.0 = 69.5 \text{ k-in.} \qquad \text{OK}$$

3) Required flexural strength

The bending moment envelopes obtained from the elastic analysis for the bottom and top story girders are shown in Figures 4.5 and 4.6, respectively. The envelopes represent the required flexural capacity for the girders to withstand all load conditions. Since the frame is not braced against sidesway, the moments at the face of the columns have been magnified by the appropriate factor δ, obtained from the analysis of slenderness effects on columns (2613(e)). In the case of the top story girder, the magnification factor δ has been taken equal to the value obtained for the top story column. For the bottom story girder, δ has been taken equal to the average of the magnification factors obtained for the top and bottom columns,

Thus, $\delta_{\text{Top Girder}} = \delta_{\text{Top Column}} = 1.03$

$$\delta_{\text{Botton Girder}} = \frac{1}{2}\left(\delta_{\text{Stop Column}} + \delta_{\text{Bottom Column}}\right)$$
$$= \frac{1}{2} \times (1.03 + 1.07) = 1.05$$

In addition, the bending moment distribution due to gravity loads (1.4D + 1.7L) computed using the equivalent frame method (2613(e)) is also plotted, for comparison with the results of the "standard" elastic analysis results.

Figure 4.5 shows that the provided flexural strength ϕM_n is adequate for all load conditions, at every section along the span of the top story girder. Furthermore, the bending moment distribution for gravity loads obtained from the elastic analysis and the equivalent frame method show good agreement in the girder midspan, (the maximum positive moment from elastic analysis is 106.12 k-in., and that obtained with the equivalent method is 105.39 k-in.). However, the elastic analysis yields a larger negative moment (97.34 k-in.), hence, at least for this case it is more conservative.

With respect to the bottom story girder, the flexural capacity provides for positive curvature, (ϕM_n^+ = 232.92 k-in. is much larger than is required $M_{u\,max}^+$ = 132.08 k-in. from the elastic analysis or 139.72 k-in. from the equivalent frame method.) However, the strength provided at the face of the column, ϕM_n^- = 199.35 k-in. is about 12% lower than is required, $\delta M_{u\,max}^-$ = 226.26 k-in., hence resulting in a slightly unsafe design.

One the other hand, the negative moment at the face of the column obtained from the equivalent frame method for load condition 1: 1.4D + 1.7L (115.64 k-in.) is about 36% smaller than the corresponding moment obtained from the elastic analysis (157.56 k-in.), and since the moment produced by gravity loads (D+L) in load condition 2: 1.4(D+L+E) is about 70% of the total moment, the flexural strength required at the face of the column would be as much as 20% less than that given by the elastic analysis. Therefore, the design of the bottom story girder might be considered adequate.

In addition, it should be noted that no reduction of live load has been considered (2306) to determine the ultimate design loads, and that the prototype has been designed for ultimate lateral loads (total base shear of 4.7 kips) significantly smaller than those determined for the present study (total base shear of 7.75 kips.)

From these considerations, it is reasonable to assume that the girders have adequate flexural strength.

4) Required shear strength

a) Minimum reinforcement (2611(b))

As for the case of the columns, the maximum spacing of the transverse reinforcement, with a total area in square inches A_v, is

$$s_{max} = \frac{A_v f_y}{50\, b_w}$$

Since the reinforcement that is provided has an area of 0.01 square inches this requirement results in

$$s_{max} = \frac{0.01x40000}{50x5.66} = 15 \text{ in.}$$

The spacing provided at the midspan of the girders is 4.24 in. (Figure 4.2), which is significantly smaller than the maximum allowed spacing.

b) Required transverse reinforcement

The maximum shear force due to the design loads occurs at the right end of the bottom story girder, for load condition 2: 1.4(D+L+E), as shown in Figure 4.7. Hence,

$$V_u = 8.88 \text{ kips}$$

and consequently, the shear stress is

$$v_u = \frac{V_u}{\phi b_w d} = \frac{8800}{0.85x5.66x9.83} \qquad (2611c)$$

$$v_u = 186 \text{ psi}$$

The stress carried by the concrete, v_c, is conservatively given by

$$v_c = 2\sqrt{f'_c} = 126.5 \text{ psi}$$

Hence, the required specing for the transvered reinforcement is (2611(g)):

$$s = \frac{A_v f_y}{(v_u - v_c) b_w} = \frac{0.11 \text{x} 40000}{(186-126.5) \text{x} 5.66} = 13 \text{ in.}$$

which is larger than the spacing provided at any location along the girders, and shear failure is avoided.

Additional requirements with respect to spacing of transverse reinforcement are (2626(e)):

i) $s \leqslant \frac{d}{2} = \frac{9.83}{2} = 4.92$ in.

throughout the length of the girders, and

ii) $s \leqslant \frac{d}{4} = \frac{9.83}{4} = 2.46$ in.

iii) $s \leqslant 8$ bar diameters $= 8 \text{ x } 0.707 \text{ x } (\frac{1}{2}) = 2.83$ in.

corresponding to the smallest bar diameter used in the prototype structure (#4),

iv) $s \leqslant 24$ stirrup-tie diameters $= 24 \text{ x } \frac{3}{8} = 9$ in.

at critical location such as the ends of the girders, along a distance of at least 2d, (20 in.) or wherever plastic hinges may be developed or wherever compression reinforcement is required.

The spacing provided at the girder midspan is 4.24 in., hence requirement (i) is satisfied. The spacing has been reduced to 2.14 in. within 24 in. of the column faces, therefore the other requirements are met. Note that the compression reinforcement that has been provided is not required for strength purposes, and the likelihood of formation of plastic hinges at midspan of the girders is very small, as determined by the elasto-plastic analysis presented in Chapter 2. This demonstrates that the collapse mechanism to be expected in the model structure is of the panel type, involving plastic hinge formations at the ends of the columns.

4.7 Requirements for Joints

As required by the 1979 UBC (2626(g)), special transverse reinforcement has been provided through the entire beam-column connection. In order to determine if the transverse reinforcement provides adequate shear strength in the joints, an approximate analysis based on the shear panel analogy[12] has been performed.

Figure 4.8 shows the assumptions used to determine the shear stresses at the bottom and top story beam-column joints.

Hence, for the top story joint

$$V_u = A_s f_y = 0.40 \times 40000 = 16000 \text{ lb.}$$

and the required spacing, assuming that the concrete does not contribute in resisting the shear stresses, is (from formula 26.7)

$$S = \frac{A_v f_y d_c}{\frac{V_u}{\phi}} = \frac{0.11 \times 40000 \times 6.36}{\frac{16000}{0.85}}$$

$$= 1.49 \text{ in.}$$

The spacing provided is 1.41 in., which is smaller than required, and therefore the joint is properly reinforced.

For the bottom story joint

$$V_u = A_s f_y - V_{col}$$

The shear force, V_{col}, coming from the top story column was computed assuming formation of plastic hinges at both ends of the column, while the maximum earthquake design axial load was acting.

For load condition 3: 1.4(D+L-E), the axial force at the left column is

$$P_e = 7.96 \text{ kips}$$

The moment capacity of the column corresponding to P_e, for $f_y = 1.25\ f_y$ specified, and without capacity reduction ϕ, from the corresponding interaction diagram (Figure 4.3) is

$$M_{ec} = 202 \text{ kip-in.}$$

Hence

$$V_{col} = \frac{2M_{ec}}{\ell_u} = \frac{2x202.0}{65.05} = 6.21 \text{ kips}$$

Therefore

$$V_u = 0.60x40-6.21 = 17.79 \text{ kips}$$

and the required spacing of the transverse reinforcement through the joint is found to be

$$s = \frac{0.11x40000\ x6.36}{\frac{17790}{0.85}} = 1.34 \text{ in.}$$

which is 5% smaller than the 1.41 in. spacing provided. Since the shear panel analogy yields conservative estimates for the shear stresses in the joints, the reinforcement that has been provided is considered adequate.

4.8 Strong Column-Weak Girder Design

The UBC requires that at any beam-column connection where $P_e/A_g \geqslant 0.12\ f'_c$ the sum of the moment strengths of the columns under the design earthquake loads must be greater than the sum of the moment strengths of the framing beams (2626(g)). This requirement is intended to minimize the possibility of formation of plastic hinges at the column ends, and to ensure that most of the inelastic deformation takes place at the critical regions of the beams.

From the analysis for the required transverse reinforcement for the columns:

$$\frac{P_e}{A_g} = 0.43 \text{ ksi} < 0.12\ f'_c = 0.48 \text{ ksi}$$

In consequence, the behavior of the columns is predominantly flexural and the strong column-weak girder requirement is not applicable.

4.9 Drift Limitations

The maximum allowable interstory drift due to the design lateral forces is

$$\delta_{max} = 0.005\ h \qquad (2312(h))$$

where h is the interstory height.

The interstory drift computed from the elastic analysis of the structure should be multiplied by the factor

$$\frac{1}{K} = \frac{1}{0.67} = 1.49 > 1$$

To determine the maximum drift.

The results obtained for the model structure are summarized in the following table

Story	Displacement (in.)	Drift(δ) (in.)	Height(h) (in.)	$\frac{\delta}{Kh}$
TOP	0.0853	0.0324	76.37	0.0006
BOTTOM	0.0529	0.0529	76.37	0.0010

The displacements shown above have been obtained by computing the flexural stiffness of the sections assuming gross area sectional properties. This assumption leads to a somewhat larger structural stiffness compared with that obtained assuming cracked sections. However, noting that the calculated understory drifts are much smaller than the maximum allowable, it may be concluded that the structure complies with the code drift requirements.

4.10 Conclusions

Through the analyses performed in the previous sections it has been demonstrated that the ideal model of the prototype structure satisfies the Uniform Builing Code requirements for earthquake resistant design of reinforced concrete moment-resisting space frames located in Seismic Zone 4.

The fact that the actual test structure also can be regarded as a ductile moment-resisting space frame is based on the following findings from Chapter 2:

1) The model and the test structure have similar overall dynamic characteristics.

2) The detailing of the reinforcement of the model and the test structure are essentially similar. The fact that undeformed #2 bars were used as transverse reinforcement in the test structure is not of great consequence in its dynamic performance, since its behavior is controlled by flexure. As a result the strength and deformation capacities (stiffness and ductility) of the ideal model and test structure are very similar.

3) In spite of the fact that the model and the test structure have different distributions of section forces due to gravity loads (and hence due to design ultimate loads) the test structure can withstand (remaining in elastic condition) lateral loads significantly larger than the ultimate lateral loads specified by the Code for the model structure, and consequently its strength is more than adequate.

As a consequence, it is possible to conclude than the test structure is also a ductile moment-resisting frame, as defined by the Uniform Building Code; therefore, its behavior under seismic excitations should be "adequate" in the sense dictated by the design philosophy on which the Code requirements are based.

LOAD CONDITION		BOTTOM STORY COLUMN (left)				TOP STORY COLUMN (left)			
		AXIAL FORCE	SHEAR FORCE	TOP MOMENT	BOTTOM MOMENT	AXIAL FORCE	SHEAR FORCE	TOP MOMENT	BOTTOM MOMENT
1	1.4D+1.7L	20.29	-1.13	-51.83	-27.95	7.87	-2.58	-82.76	-84.77
2	1.4(D+L+E)	17.78	0.33	-3.83	27.11	7.16	-1.73	-53.11	-59.39
3	1.4(D+L-E)	20.65	-2.38	-90.52	-78.00	7.96	-3.10	-103.71	-98.27
4	0.9D+1.4E	7.71	1.00	26.96	43.72	3.42	-0.39	-12.05	-13.41
5	0.9D-1.4E	10.58	-1.71	-59.73	-61.39	4.23	-1.77	-62.64	-52.29

LOAD CONDITION		BOTTOM STORY GIRDER		TOP STORY GIRDER	
		LEFT MOMENT	RIGHT MOMENT	LEFT MOMENT	RIGHT MOMENT
1	1.4D+1.7L	-157.56	-157.56	-97.34	-97.34
2	1.4(D+L+E)	-75.51	-215.49	-64.62	-119.56
3	1.4(D+L-E)	-215.49	-75.51	-119.56	-64.62
4	0.9D+1.4E	12.63	-127.35	-15.98	-70.93
5	0.9D-1.4E	-127.35	12.63	-70.93	-15.98

TABLE 4.1 SECTION FORCES AT MEMBER ENDS FROM ELASTIC ANALYSIS OF IDEAL MODEL (kips, in.)

Load Condition		Bottom Story Column		Top Story Column	
		P_u (kips)	$M_c=\delta M_u$ (1) (kip-in.)	P_u (kips)	$M_u=\delta M_u$ (kip-in.)
1	1.4D+1.7L	20.29	55.46	7.87	87.31
2	1.4(D+L+E)	17.78	29.01	7.16	61.17
3	1.4(D+L+E)	20.65	96.86	7.96	106.82
4	0.9D+1.4E	7.71	46.78	3.42	13.81
5	0.9D-1.4E	10.58	65.69	4.23	64.52

TABLE 4.2

DESIGN LOAD CONDITIONS FOR IDEAL MODEL COLUMNS

(1) For each axial load, the largest moment in the column has been selected.

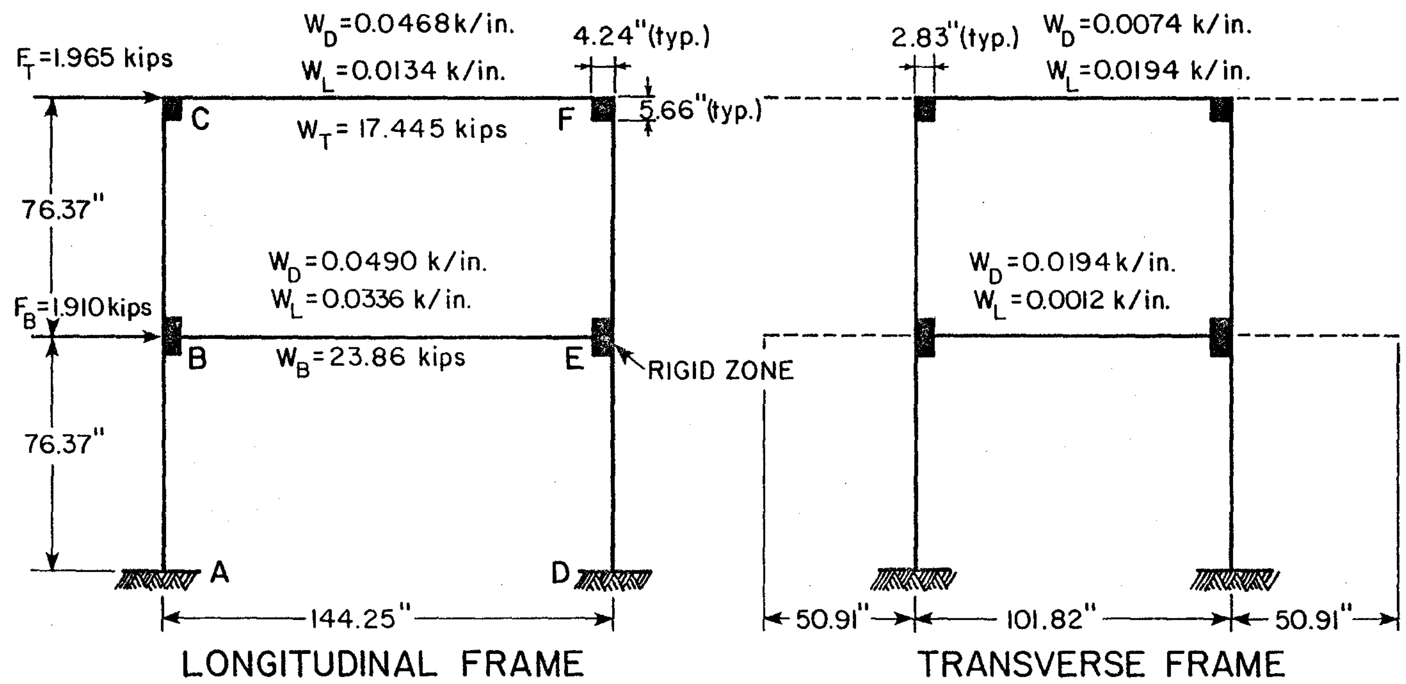

FIG. 4.1 IDEAL MODEL DIMENSIONS AND LOADS FOR ELASTIC ANALYSIS

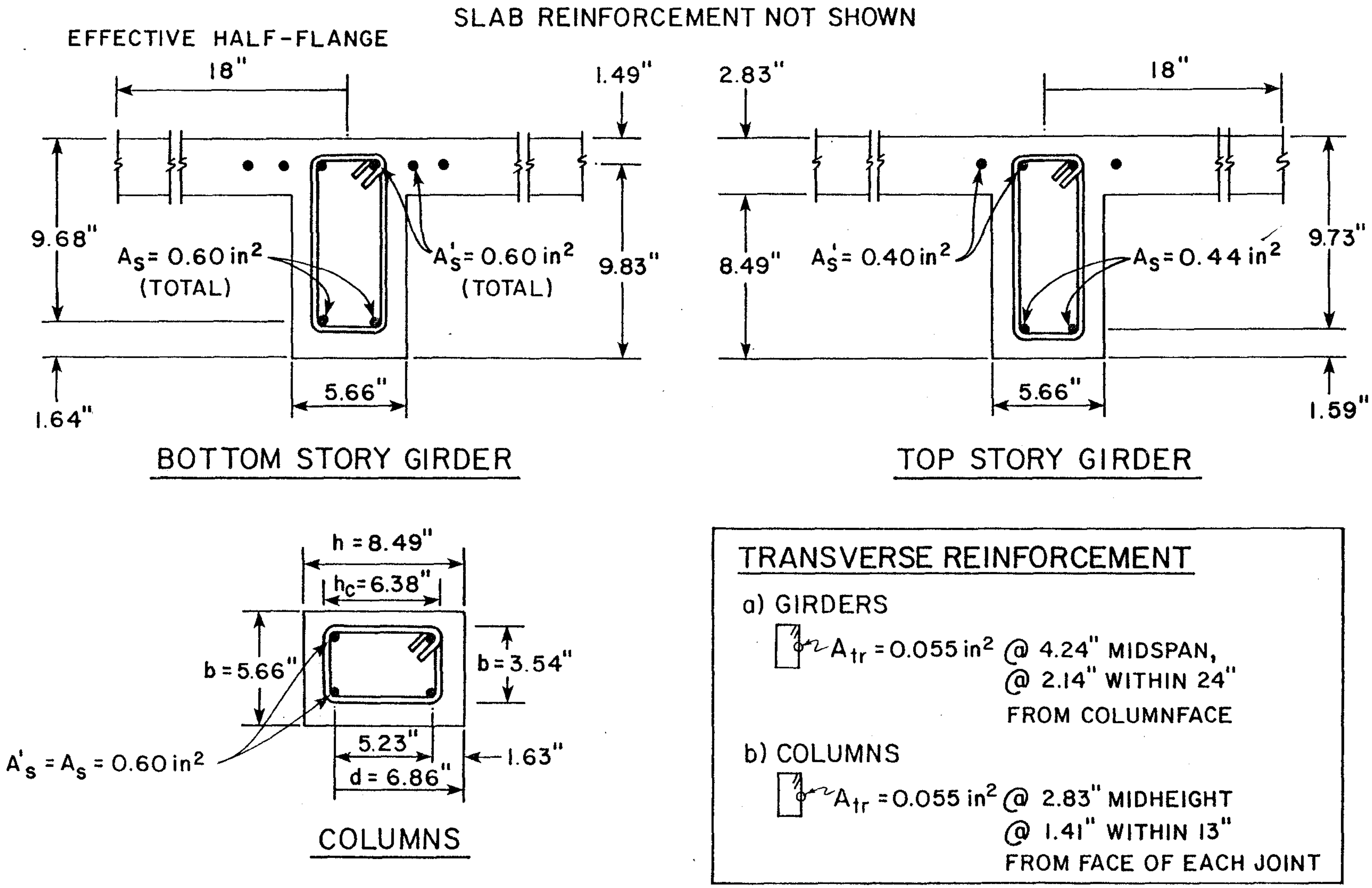

FIG. 4.2 SECTION DIMENSIONS AND PROVIDED REINFORCEMENT. IDEAL MODEL

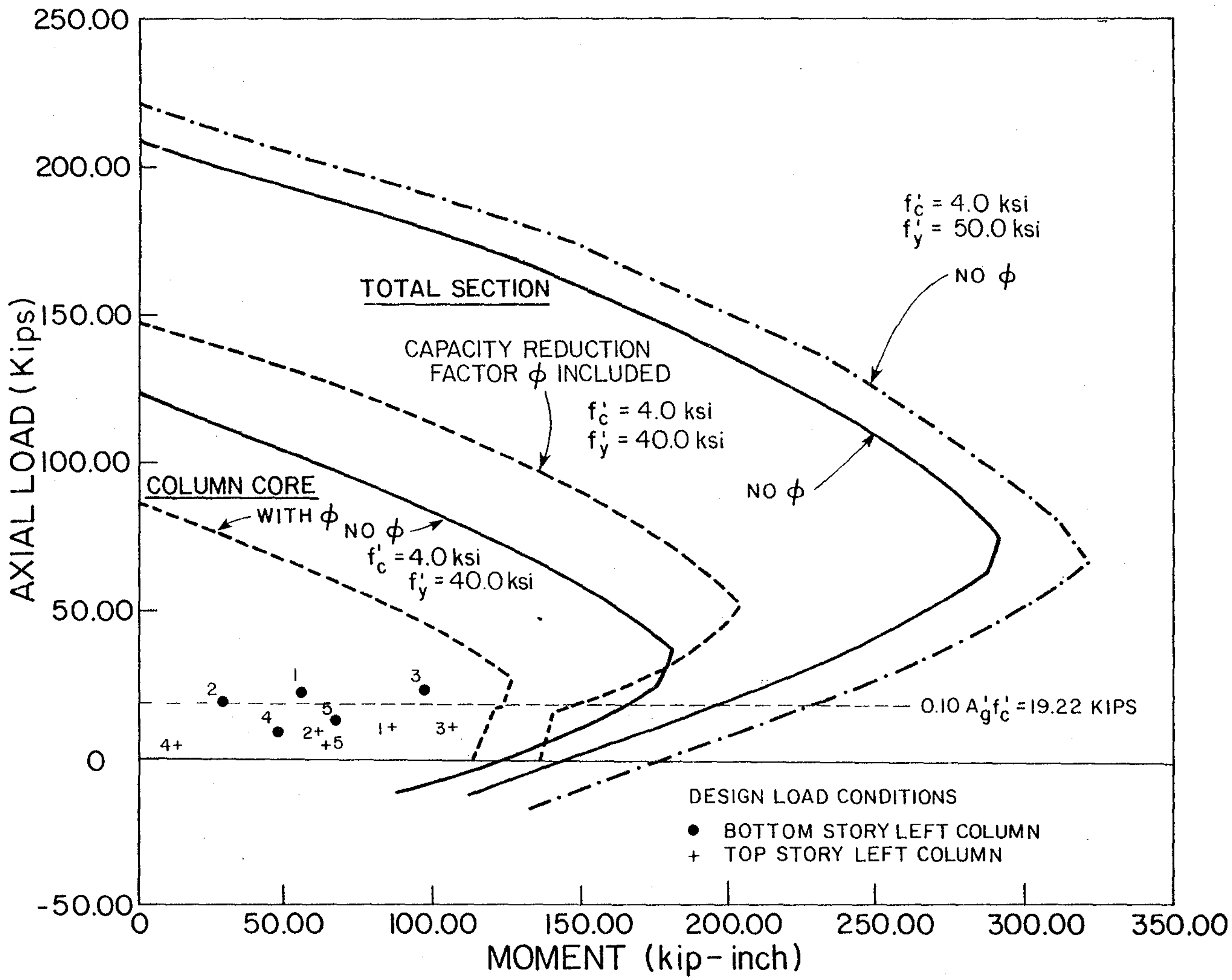

FIG. 4.3 P-M INTERACTION DIAGRAM FOR IDEAL MODEL COLUMNS

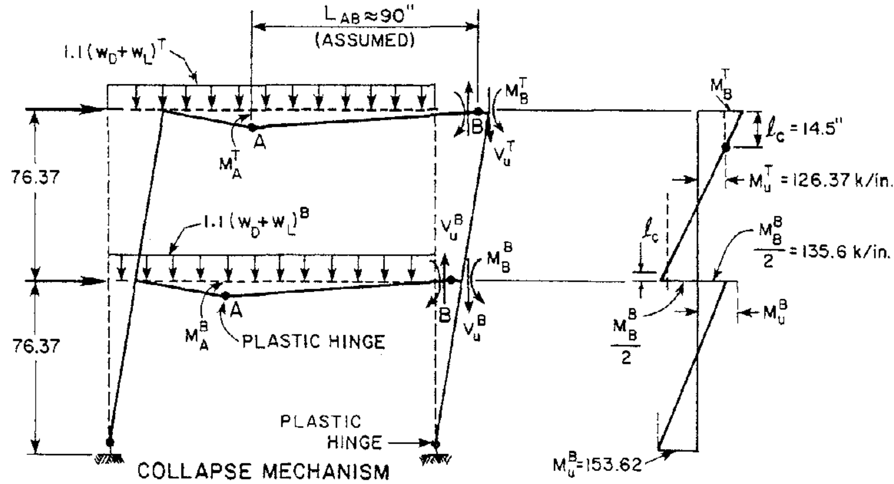

Units, kips, in.	Bottom Story Girder	Top Story Girder
M_A	320.5	236.5
M_B	271.2	187.9
$1.1(W_D+W_L)$	0.091	0.066
V_u	10.67	7.69

$$V_u = \frac{M_A+M_B}{L_{AB}} + \frac{1.1(W_D+W_L)L_{AB}}{2}$$

Special transverse reinforcement is required where $M_{mech.} \geq M_u$; M_u (moment capacity of the column) is computed from the column interaction diagram for $P_u = \sum V_u$ ($f'_c = 4.0$ ksi, $f_y = 40$ ksi, ϕ included)

1) Top story column:

a) Top end

$P_u^T = V_u^T = 7.69$ kips

$M_u^T = 126.37$ k/in.

< 187.90 k/in. $= M_B^T$

within $\ell_c = 14.5$ in.

$= 13.1$ in. from face of joint

b) Bottom end

$M_u^T = 126.37$ k/in.

< 135.60 k/in. $= M_B^T/2$

within $\ell_c = 2.2$ in.

$= 0.8$ in. from face of joint

2) Bottom story column

a) Top end

$P_u^B = V_u^T + V_u^B = 7.69 + 10.67$

$= 18.36$ kips

$M_u^B = 153.62$ k/in.

> 135.60 k/in. $= M_B^T/2$

$\ell_c = 0$

b) Bottom end

$M_{mech.} \equiv M_u$ (plastic hinge)

FIG. 4.4 DETERMINATION OF REQUIRED CONFINEMENT LENGTH FOR IDEAL MODEL COLUMNS (SECTION 2626f - UBC79)

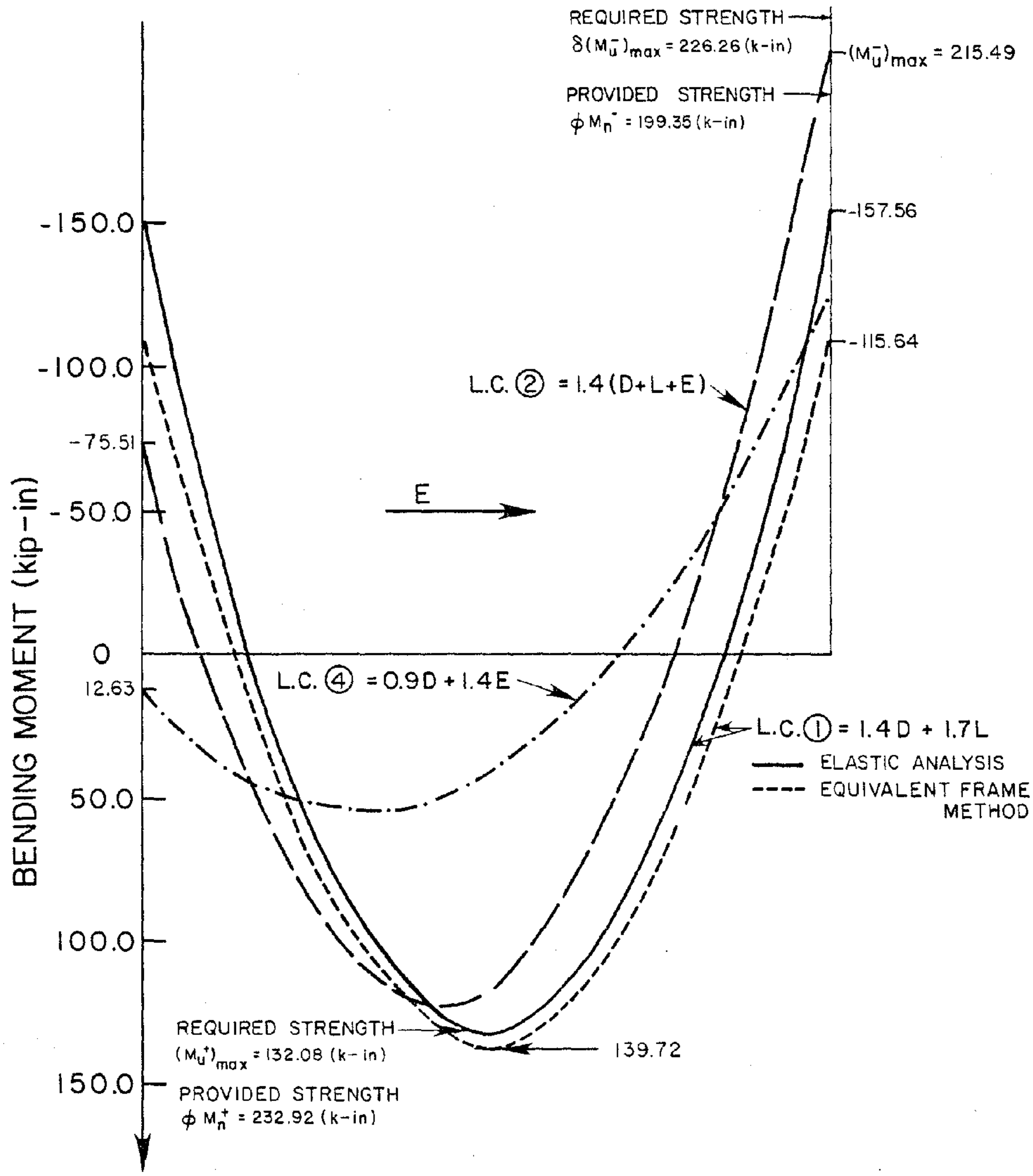

FIG. 4.5 FLEXURAL STRENGTH REQUIREMENTS FOR IDEAL MODEL BOTTOM STORY GIRDER

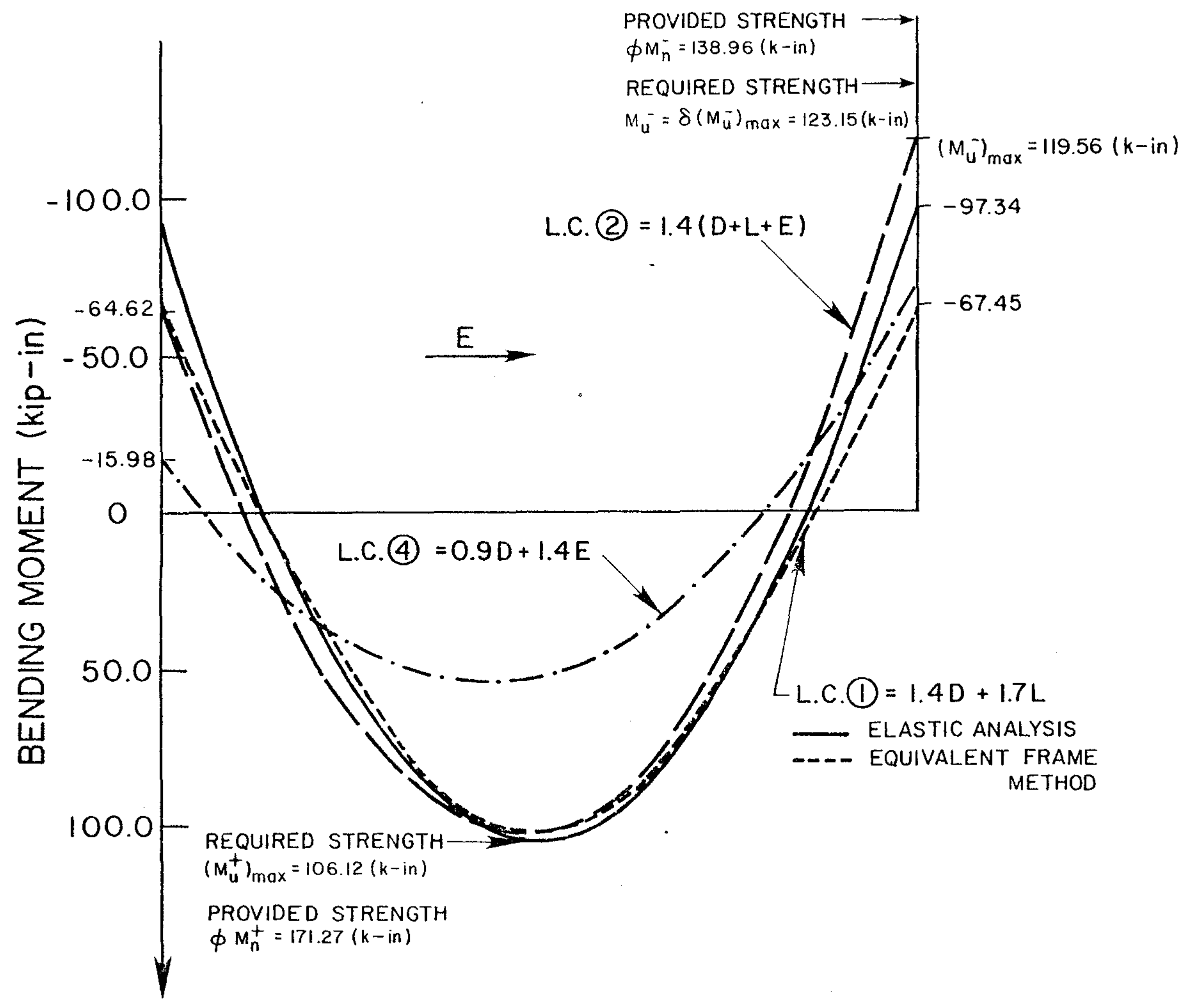

FIG. 4.6 FLEXURAL STRENGTH REQUIREMENTS FOR IDEAL MODEL TOP STORY GIRDER

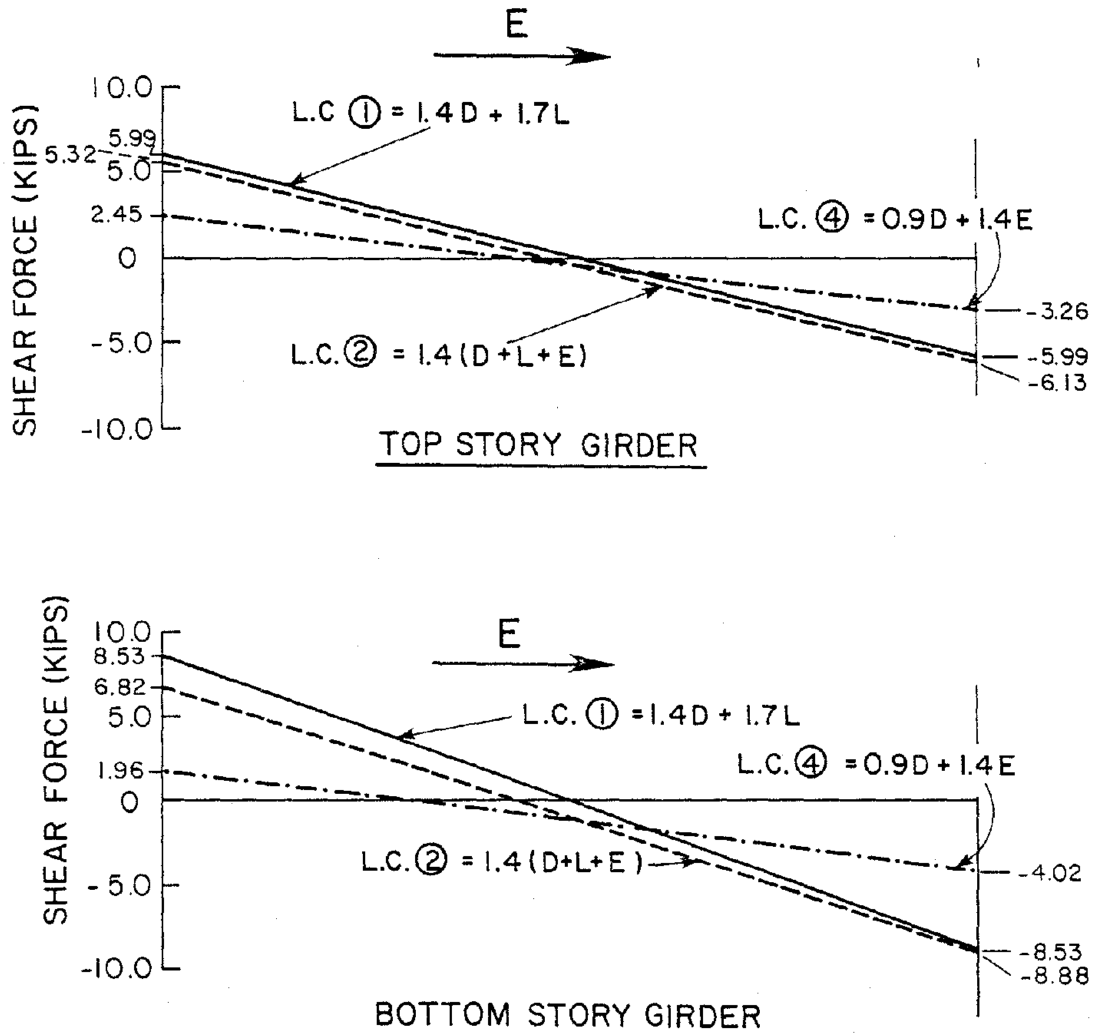

FIG. 4.7 SHEAR DISTRIBUTION IN GIRDERS. IDEAL MODEL ELASTIC ANALYSIS

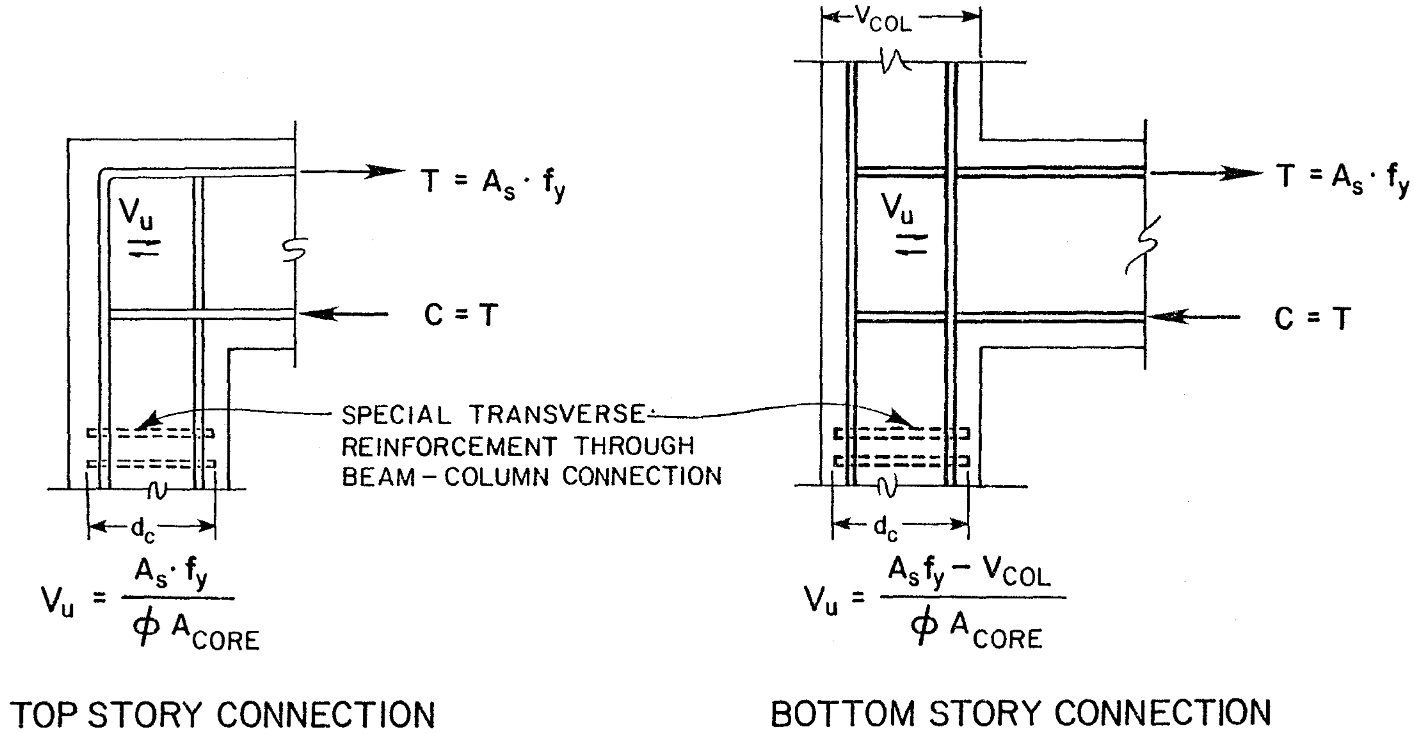

FIG. 4.8 SHEAR PANEL ANALOGY TO DETERMINE SHEAR STRESSES AT JOINTS

5. GLOBAL RESPONSE OF RCF2 DURING TESTS

5.1 Motivation

In the previous chapters of this report, it has been shown that the test structure, RCF2 is representative of a typical low-rise reinforced concrete building, whose design is in accordance with the latest code specifications for earthquake-resistant-construction, and that the excitations to which it was subjected on the shaking table realistically simulate possible seismic ground motions.

The next step in the evaluation process is to examine the actual response of the specimen during the dynamic tests. The motivation for performing such studies arises from the fact that the experiments performed provide an opportunity to verify not only the adequacy of the seismic behavior of the test structure but also the reliability of the analytical techniques on which the design procedure is based.

The overall performance of RCF2 during each "run" in the first phase of the testing sequence (unrepaired structure) is examined in the following sections, with emphasis on correlating the observed behavior with that inferred from the analyses performed previously. A detailed description of the test results, complemented with analytic verifications based on several mathematical models, can be found in Chapter 4 of Reference [2].

5.2 Run W1: Taft 100.

The Taft N69W acceleration was scaled "down" in amplitude to generate a horizontal table motion with peak acceleration of about 0.1 g, which is considered a "mild" excitation, with the purpose of inducing in the virgin structure a level of cracking representative of "normal" service conditions.

The response of the structure to this table motion can be characterized by the time histories of floor displacements with respect to the table. These are plotted in Figure 5.1, in which the dashed line corresponds to the top, and the continuous line to the bottom floor level.

A brief examination of this graph reveals important information about the characteristics of the response of RCF2 during this run. The motion of each floor can be described as a sinusoid with slowly varying amplitude and phase. This type of response is characteristic of resonant-prone systems (like linear elastic, slightly damped structures) to excitations with a wide-band frequency spectrum (such as seismic ground motions)[21]. Also, it is evident that both floors oscillate in phase, following similar patterns. This indicates that the structure is responding basically in the first mode of vibration.

In order to confirm these observations it is necessary to examine the actual force-deformation relationship developed by the structure during the test. This information is available in a global sense since the horizontal floor accelerations were measured during the experiment, permitting the computation of the inertia forces induced at the floor levels, from which the interstory shears could be found. (The force transducers located at the column midheights also provided indications of the shear forces in the column, but since these do not agree with those obtained from acceleration records, they seem to be unreliable, and they have not been used in this investigation.)

The motion of the top floor with respect to the bottom floor level (top story drift) is presented in Figure 5.2, and the bottom and top story shears in Figures 5.3 an 5.4, respectively. These graphs show basically the same characteristics of linear elastic behavior as those in Figure 5.1.

The interstory shear-drift relationship shown by the structure during the test under considerstion is plotted in Figures 5.5 and 5.6 for the bottom and top stories, respectively. From a "practical" point of view it can be said that the behavior of RCF2 during this test was basically linear, however, some nonlinearities were present.

It seems evident that since the main reinforcement in the elements was stressed well below its yield point (the strain in the reinforcement at critical points was monitored) the main cause for the mild nonlinear, hysteretic behavior by the structure was the development of cracks in the concrete and their subsequent opening and closing as the structure oscillated around its equilibrium configuration. This observation suggests that the overall stiffness of the frame had to decrease during the test, from that corresponding to a virgin, uncracked specimen, to that of an elastic but moderately cracked structure.

In order to confirm the previous statement, the interstory shear-drift relationship shown by the structure during consecutive 5 second time intervals has been plotted in Figures 5.7 and 5.8 (a) through (e), which show that basically, the nonlinear effects (and thus the cracking) were significant mainly in the first story members, and that the most noticeable change in stiffness took place in the time interval from 5 to 10 sec after the beginning of the test.

In summary, the response of RCF2 to this mild first excitation can be described as that of an elastic, underdamped, single-degree-of-freedom system.

The findings of the analyses performed in the initial stage of this study (Chapter 2) are substantially in accordance with the experimental results. The effective modal masses[22] associated with the vibratory parameters (mass and flexibility matrices, mode shapes and frequencies) presented in Figure 2.8, for the test structure, are

$$M_{e1} = 0.92\ M_{TOT} \qquad \text{for the first mode}$$

and

$$M_{e2} = 0.08\ M_{TOT} \qquad \text{for the second mode of vibration}$$

(M_{TOT} is the total mass of the structure)

This result indicates that the response of RCF2 should be highly "dominated" by the first mode of vibration, as was observed.

The maximum level of lateral forces which the structure can withstand in an elastic regime, as predicted by the elastoplastic analysis, correspond to a horizontal ground acceleration of about .46g; this result agrees with the observed "elastic" behavior shown by the structure when subjected to a (dynamic) excitation with peak acceleration of about 0.10g.

It seems worth noting that, as is widely accepted, the stiffness predicted under the assumption of "gross section" geometry and elastic modulus given by the Code formula is unrealistically large with respect to the actual structural stiffness. This is dramatically demonstrated in Figure 5.9 (a) and (b) where the predicted lateral stiffness can be compared with the initial stiffness corresponding to a practically uncracked structure-and the "average" stiffness developed by the structure during a 5-second interval. The gross section-and the "code" elastic modulus-formulation to compute stiffness is clearly very unrealistic, and should not be used as a basis for prediction of structural displacements. This formulation was used in Chapter 2 because of its computational convenience and because the analytical results were to be used in a "relative" way, to compare the characteristics of two structures.

5.3 Run W2: Taft 850(1).

The objective of this test was to study the effects of a violent seismic base motion on a well-built structure without significant previous seismic history. For that purpose, the Taft signal was amplified to yield a table motion with peak acceleration of 0.5 to 0.6g, which according to the experience gained with the first structure tested[1] would be strong enough to produce significant damage on the specimen.

The lateral floor displacement response of the structure during this test is presented in Figure 5.10. It shows noticeable differences from the displacement response during the previous run, indicating the presence of significant nonlinear behavior.

The most relevant feature of the behavior of the frame revealed by this graph is that in this case the structure did not oscillate with respect to a fixed position ("equilibrium" configuration.) The position of the "center" of oscillation varied during the first half of the test, but it stabilized about 15-seconds after the beginning of the base excitation, showing that the bottom story suffered a permanent deformation with respect to its original position on the shaking table. The fact that, as in the previous run, both floors oscillated in phase, following similar displacement patterns shows that the nonlinear effects occurred mainly in the first story members, and that the structure can still be considered (globally) as a single degree of freedom system.

In addition, it is possible to observe an increase in the period of the oscillations at the end of the test with respect to the initial period, which is evidence of significant stiffness deterioration.

In order to study the actual force-deformation developed by the specimen during this test, the time histories of the second story drift (the first story drift is the displacement of the first floor with respect to the table) and the interstory shears have been computed and plotted.

Figure 5.11 shows the variation of the second story drift during the test. It can be described as an "irregular" oscilatory motion (compared with a sinusoid, or with the drift response of the structure during run W1.) There is no indication of significant displacement of the center of the oscillations, therefore no permanent drift was produced. However, the irregularity of the time history curve indicates the nonlinearity of the response.

The interstory shear time histories can be seen in Figures 5.12 (bottom story) and 5.13 (top story). The top story shear curve seems to have more high frequency components than the corresponding bottom story curve. A possible explanation for this phenomenon is that the small second modal component (if it is still possible to describe the system in these terms) is more noticeable in the acceleration response than in the displacement response.

The interstory shear versus drift relationships developed by the specimen have been plotted on Figures 5.14 and 5.15 for the bottom and top stories, respectively. They show, as expected, a significant nonlinear hysteretic behavior, especially in the first story. In order to observe with greater detail the force-deformation response of the structure, these curves have been presented in consecutive five second intervals for the whole duration of the test, and then for 1-second intervals during the "strongest" part of the shaking (in Figures 5.16 and 5.17(a) through(f) for the bottom story and in Figures 5.18 and 5.19(a) through(f) for the top story.)

The behavior of both stories can be compared in Figure 5.20, which shows their shear-drift relationship during the time interval 5 to 10-seconds after the beginning of the test.

The main features of the response of the specimen are clearly demonstrated in the mentioned figures. For example, it is evident that the frame suffered a significant lateral stiffness degradation, caused by the occurrence of a few cycles of large inelastic deformation during the first 10-seconds of shaking. Afterwards, its behavior became more regular, ("almost" linear) but with "pinched" force-deformation curve indicative of the occurrence of undesirable phenomena (in earthquake resistant construction) such as deterioration of bond between steel reinforcement and concrete, which is responsible for the slippage of the rebars as the cracks on the surrounding concrete open and close.

It is also evident that most of the energy input to the structure through the shaking table motion was dissipated by the bottom story members, as demonstrated by Figure 5.20 and by the distribution of structural damage after the test: the steel reinforcement of the first story columns was strained beyond its yield point near the columns end zones; noticeable flexure cracks appeared at both ends of the first story columns, the bottom end of the second story columns, and in the longitudinal girder near the column joints. Minor cracking was also observed on top of the first floor slab; and, of course, the permanent drift of the first story was evident.

Now the performance of the test structure will be evaluated in terms of the "adequacy" of its seismic behavior. This seems a difficult task, in the sense that there is not an universally accepted quantifiable parameter to measure quality of structural response. However, the fact that the structure "survived" a test comparable to a major seismic event not only without collapsing, but remaining in a "repairable" condition even after a similarly strong "aftershock" is the best proof of the adequacy of its performance and therefore of its design.

Some other factors can be pointed out which also show that the test specimen had indeed desirable structural characteristics, like, for example, its ability to dissipate seismic energy through stable hysteretic behavior, and its capacity for developing large inelastic deformation. With respect to the last concept, a rough attempt to quantify it is presented in Figure 5.21. This graph shows that the maximum lateral bottom story drift is about three times the "yield" drift (as defined in Figure 2.11); similarly, the maximum top story drift is about two times this "yield" drift. The parameter "interstory drift ductility" μ_δ[23] reached a value of about 3 for the bottom story and about 2 for the top story. These numbers represent in a very crude (but very popular) way a lower bound for the capacity of the frame to withstand lateral inelastic deformations, and, from a practical point of view, they are representative of "adequate" design.

The correlation between expected and observed performance, and between design and "actual" seismic excitations is summarized in Figures 5.21 and 5.22

in which the interstory shear-drift relationships as predicted by the elasto-plastic analysis can be compared with the envelopes of the actual story shear-drift relationship developed by RCF2 during the test under consideration. The levels of "ultimate" interstory shear corresponding to the 1970 UBC (used in the design of RCF2) and the 1979 UBC Codes (1.4E) are also shown, for comparison with the analytical ("collapse") and experimental story shears experienced by the structure. As a reference for stiffness comparison, a straight line representing the initial lateral stiffness of the frame also is drawn in these figures.

The main conclusions that can be drawn from these figures are:

1) The strength of the structure computed using specified material properties and Code-related procedures is substantially below the capacity shown by the structure during the test.

2) The design ultimate lateral loads (1.4E) are disproportionally low with respect to the inertia forces induced over the structure by the dynamic base excitation. The lateral loads proposed by the Code are in this case, totally unrealistic, in the sense that if the shear capacity provided to the structure had been equal to the design ultimate shears, the behavior of the structure would have been highly unsatisfactory under the (simulated) seismic excitations.

3) As expected from results of previous tests, the lateral stiffness of the structure, corresponding to gross section geometry and elastic modulus computed using the formula proposed by the Code, is unreallistically large, as compared with the stiffness shown by the structure, even at the initial stages of the test.

These results appear as a consequence of the assumptions and limitations of the analytical techniques and of the design philosophies involved in the design process. For example, it is obvious that the computation of stiffness based on gross section is inconsistent with the very nature of reinforced concrete behavior; therefore the discrepancy in the analytical and experimental lateral stiffness values are not surprising. In the case of the prediction of lateral strength, the "upper bound" found using the code formulations (specified concrete strength, 25% increase over specified reinforcement strength, and no ϕ capacity reduction factor) proved to be significantly lower than the capacity demonstrated by the structure during the test (which is in turn a lower bound for the actual structural capacity.) This fact demonstrates the conservatism in the design procedures, and thus their limitation for accurate prediction of structural strength.

Finally, the fact the structure showed a large overcapacity with respect to the design ultimate loads can be due to the conservatism of the design techniques (which produces members with larger strength than the "target" design value) and to the fact that the design ultimate gravity forces are "dominating" in the computation of the section capacity demand, therefore when actual (non-magnified) gravity loads are acting there is a "reserve" of structural capacity.

Before presenting the concluding remarks, the performance of RCF2 during the "aftershock" shaking table test is examined in the next section.

5.4 Run W3: Taft 850(2)

A severe "aftershock" was simulated in this test, by repeating the shaking table motion with the same "span" setting as in the previous run. The resulting base excitation was slightly stronger than in the previous case (peak acceleration of 0.65g versus 0.57g) but with the same general frequency and duration characteristics.

The response of the structure is presented in Figures 5.23 to 5.33, which are arranged in the same sequence as for run W2 (Figures 5.10 to 5.20.) In addition, Figures 5.34 and 5.35 show the response of the test specimen (as characterized by its force-deformation curves) to the last two tests (runs W2 and W3), in five-second intervals, to facilitate comparison.

The information contained in these figures can be summarized briefly, by comparing the response of the test specimen to these similar excitations.

In general, the response of RCF2 during run W3 has the same characteristics as in the previous run: the structure suffered several cycles of significant inelastic deformation at the beginning of the test, mainly in the bottom story, followed by a more "regular" type of response. Therefore the structure, even after having been significantly damaged by the first strong test, showed that its strength and deformation capacities were not diminished. It should be mentioned however, that due to the fact that the structure was already damaged before test W3, its degradation in lateral stiffness was not so dramatic as compared to that in run W2 (it did not have as much stiffness to lose.) Also the effect of shear cracking, bond deterioration, and concrete spalling were more important this time. These undesirable phenomena contributed to the more pronounced "pinched" characteristics of the force-deformation relationship shown by the structure in this test.

Another interesting fact is that the top story behavior was similar in both runs (Figure 5.35), since most of the damage (source of nonlinearities) was concentrated in the bottom story members.

To summarize, the performance of the test structure during this second very strong excitation was satisfctory, since it showed a great capacity to dissipate energy through ductile behavior.

5.5 Conclusions

The information obtained during the earthquake simulator experimentation proved to be extremely useful for the study of the seismic performance of the test specimen. It provided significant insight on the limitations and reliability of "standard" analytical techniques and the accepted philosophies involved in design of a seismic-resistant structural system.

The most important conclusion that can be drawn from the test results is that even though the Code requirements for seismic safety of framed reinforced concrete structures contain inconsistencies with respect to the specification of the (design) seismic excitation, the resulting design proves to be effective. This is due,of course, to the very strict reinforcement detailing requirements, which guarantee ductile, flexural behavior of the structural members, as was observed during the experiments.

Another important point that deserves to be mentioned is that in order to predict with satisfactory accuracy the dynamic behavior of reinforced concrete structures, it is necessary to utilize more sophisticated and realistic analysis and modelling techniques than those employed in the "standard practice" of structural design.

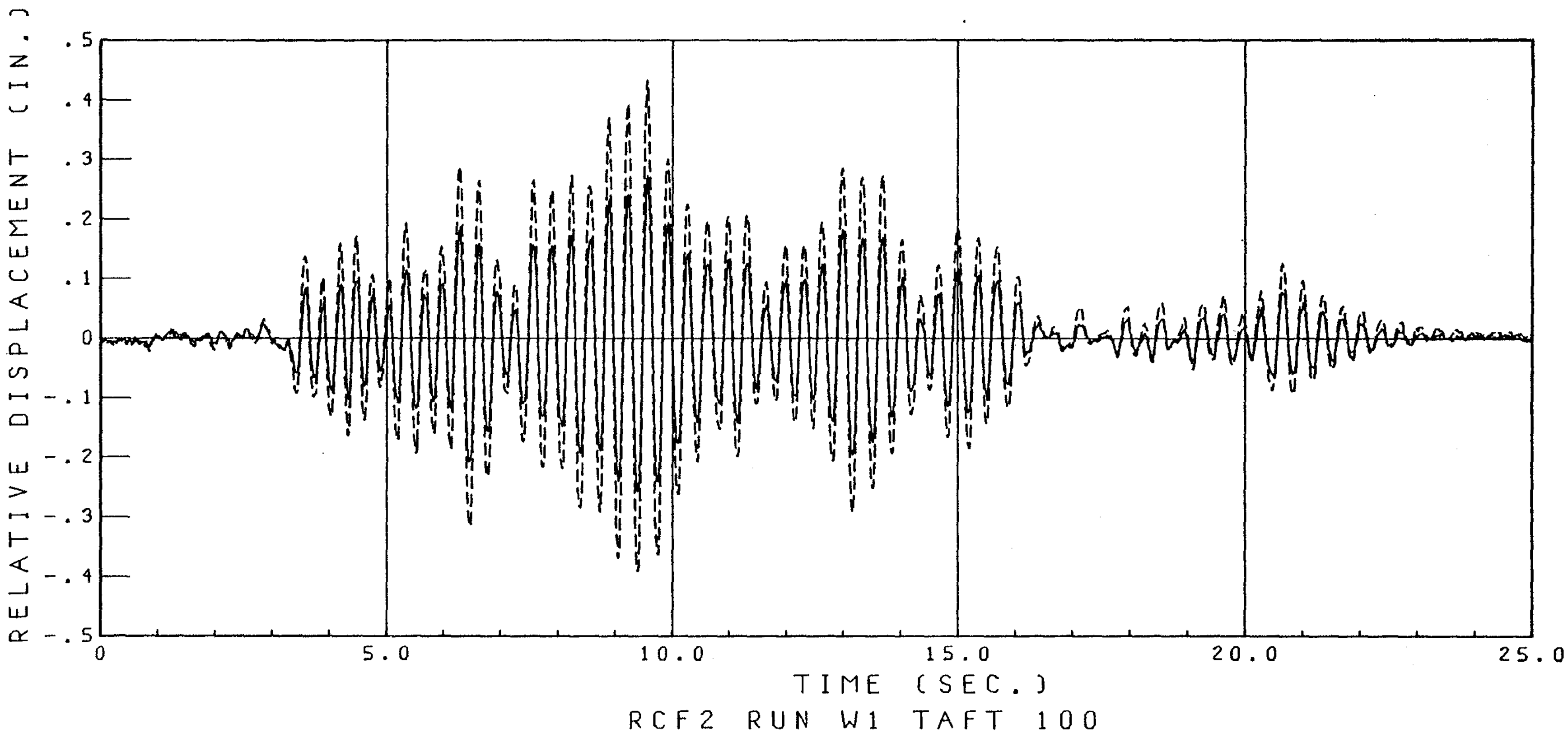

FIG. 5.1 DISPLACEMENT RESPONSE OF RCF2 DURING RUN W1 (RELATIVE TO TABLE)
SOLID LINE - BOTTOM FLOOR: DASHED LINE - TOP FLOOR

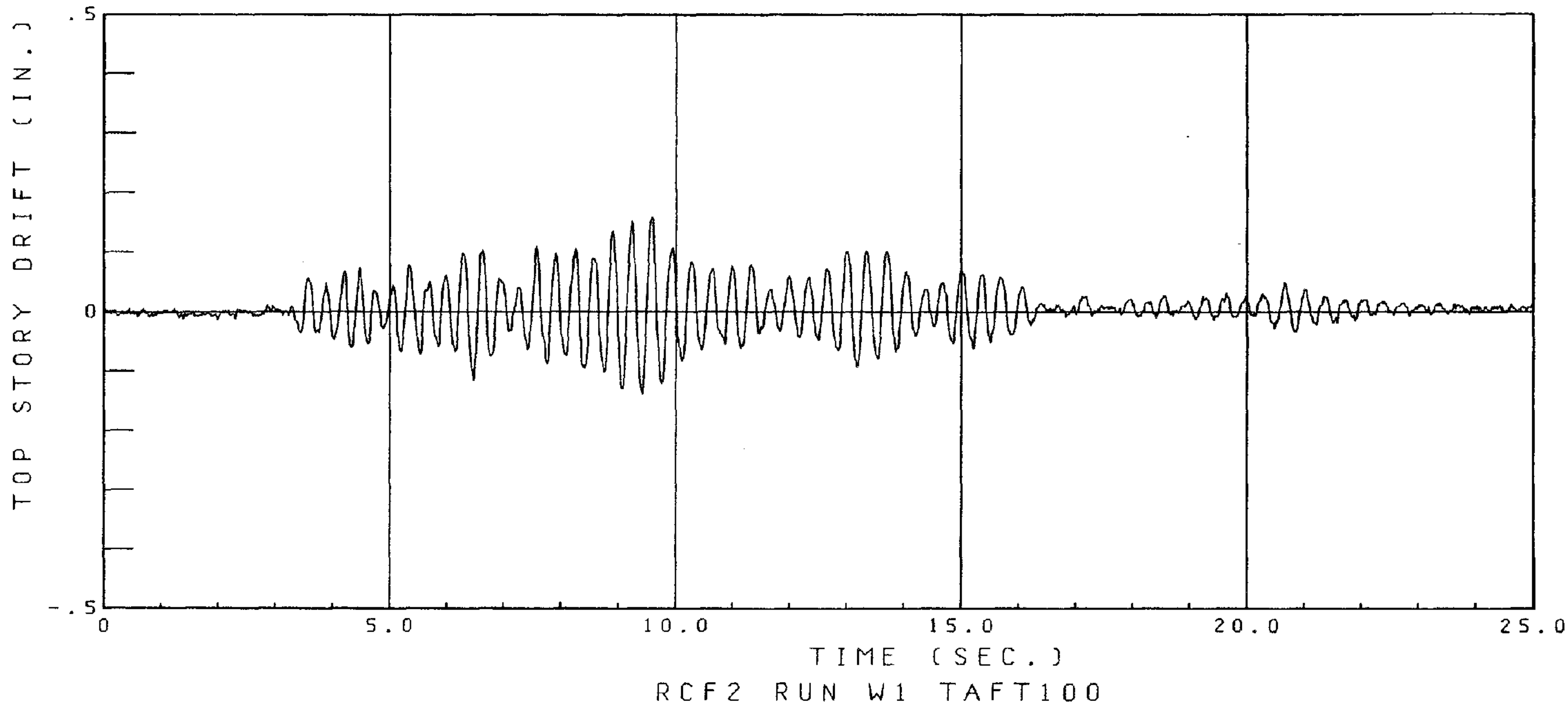

FIG. 5.2 TOP STORY DRIFT. RUN W1

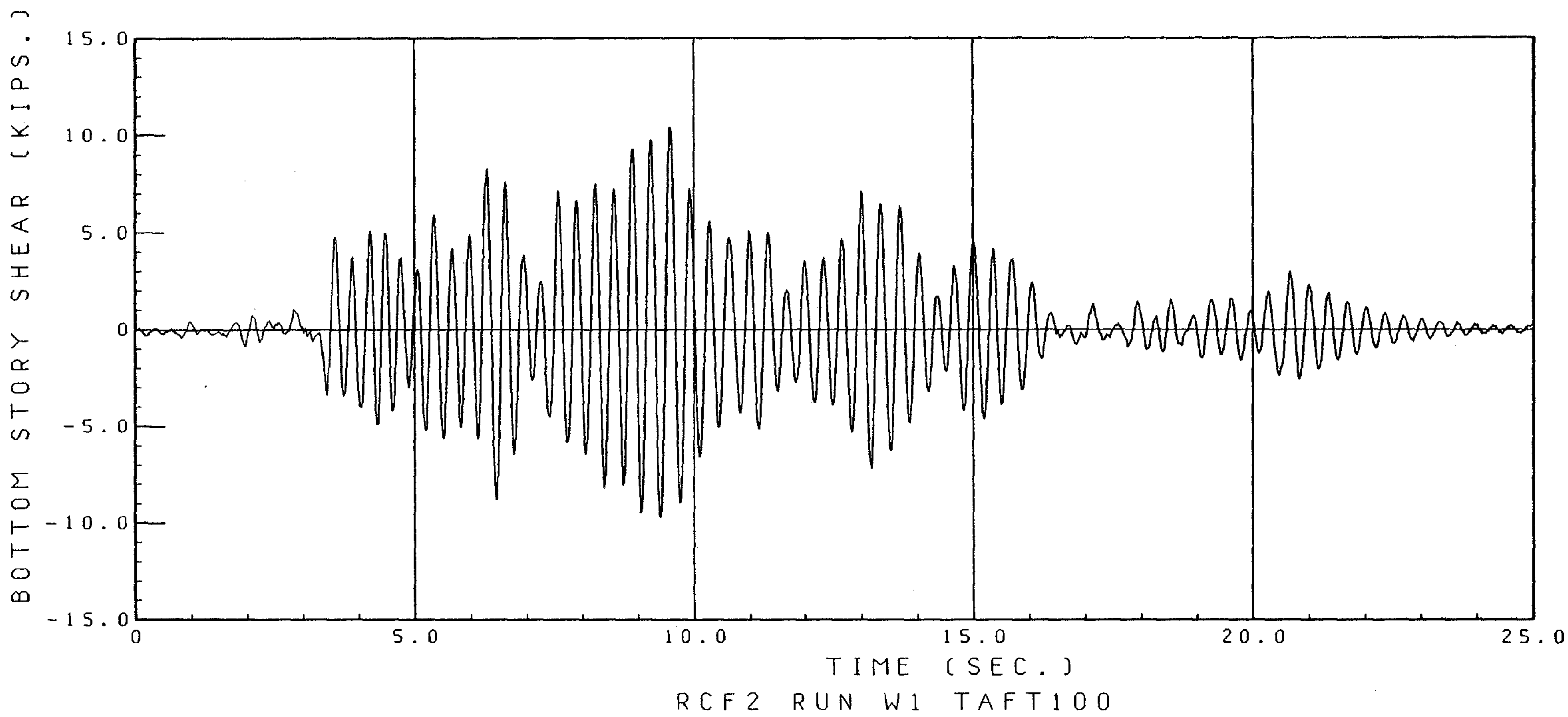

FIG. 5.3 BOTTOM STORY SHEAR (FROM ACCELERATION RECORDS). RUN W1

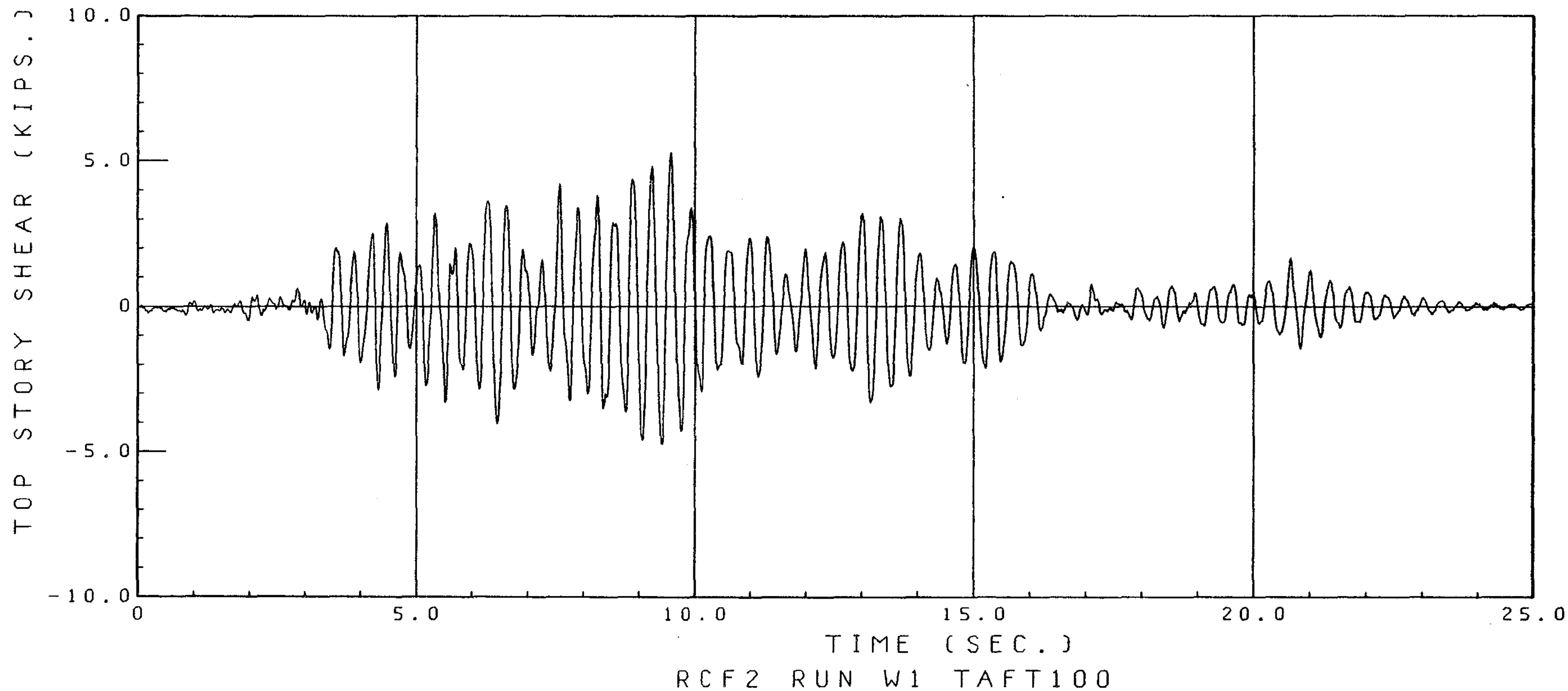

FIG. 5.4 TOP STORY SHEAR (FROM ACCELERATION RECORDS). RUN W1

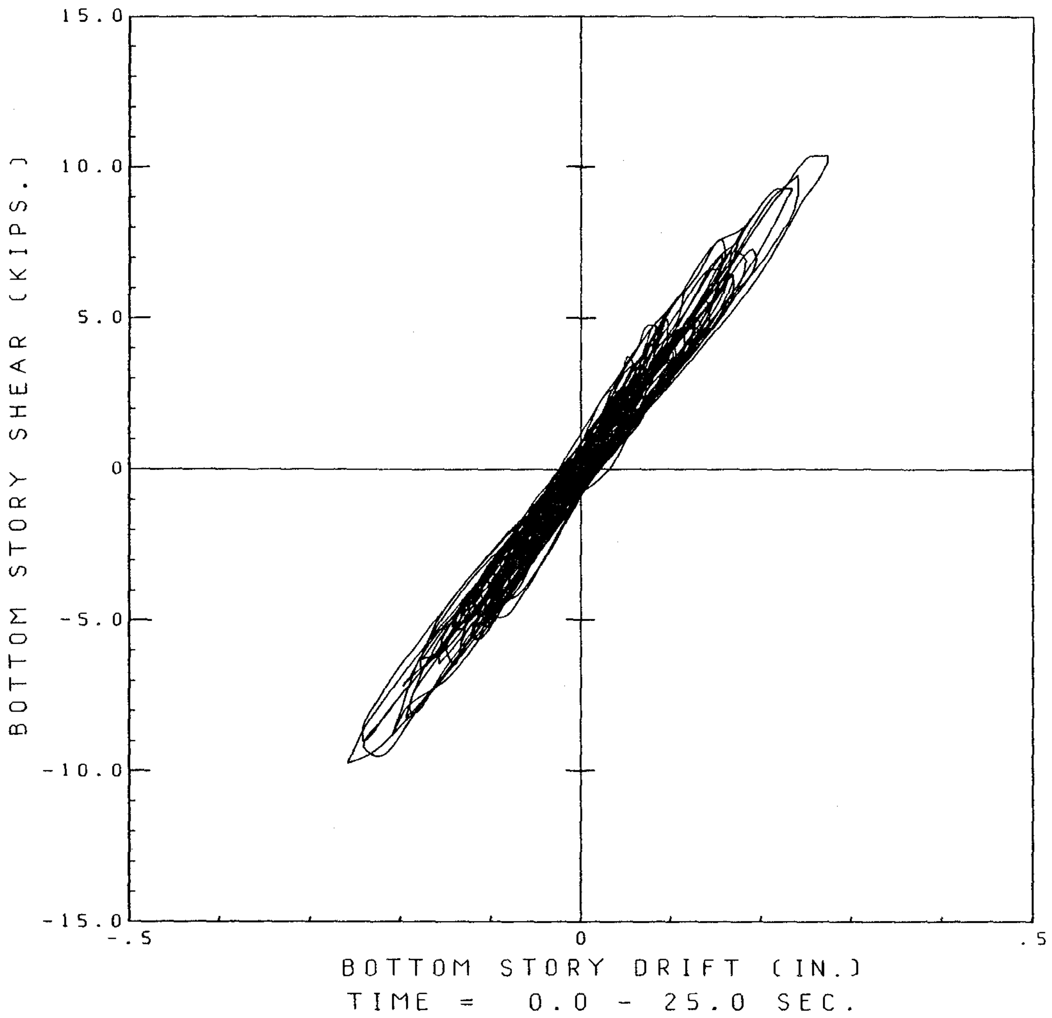

FIG. 5.5 BOTTOM STORY SHEAR VS. DRIFT RELATIONSHIP. RUN W1

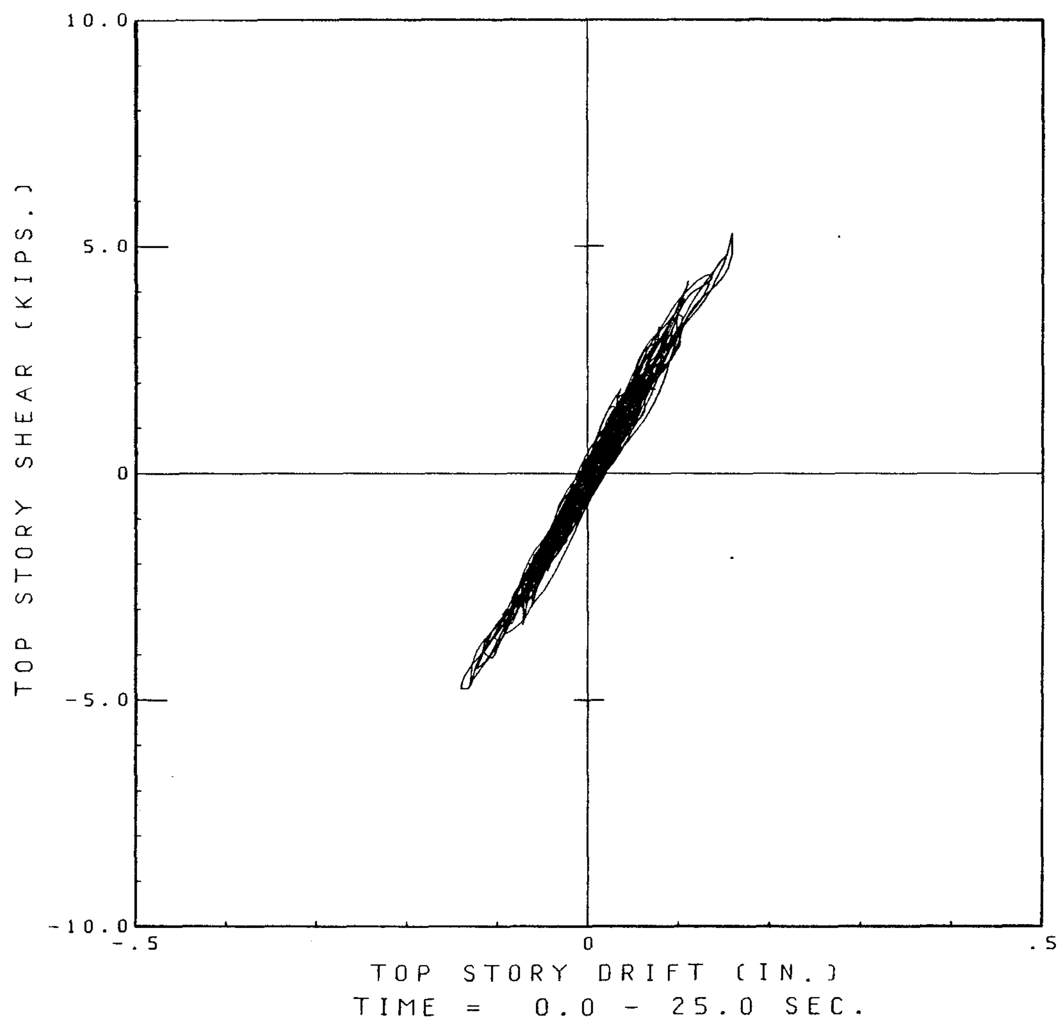

FIG. 5.6 TOP STORY SHEAR VS. DRIFT RELATIONSHIP. RUN W1

Reproduced from best available copy.

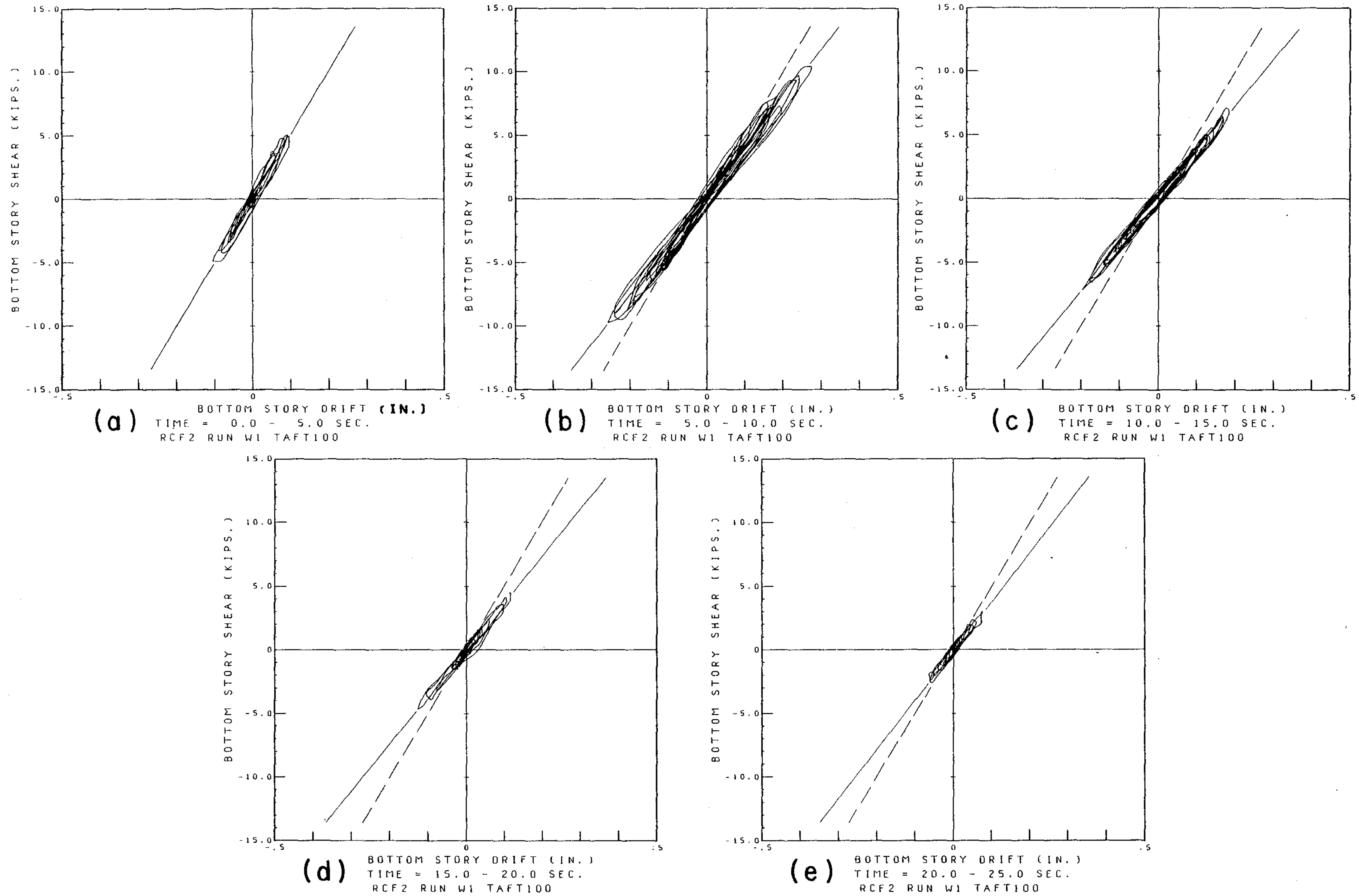

FIG. 5.7 BOTTOM STORY SHEAR VS. DRIFT RELATIONSHIP DURING 5-SEC INTERVALS. RUN W1

Reproduced from best available copy.

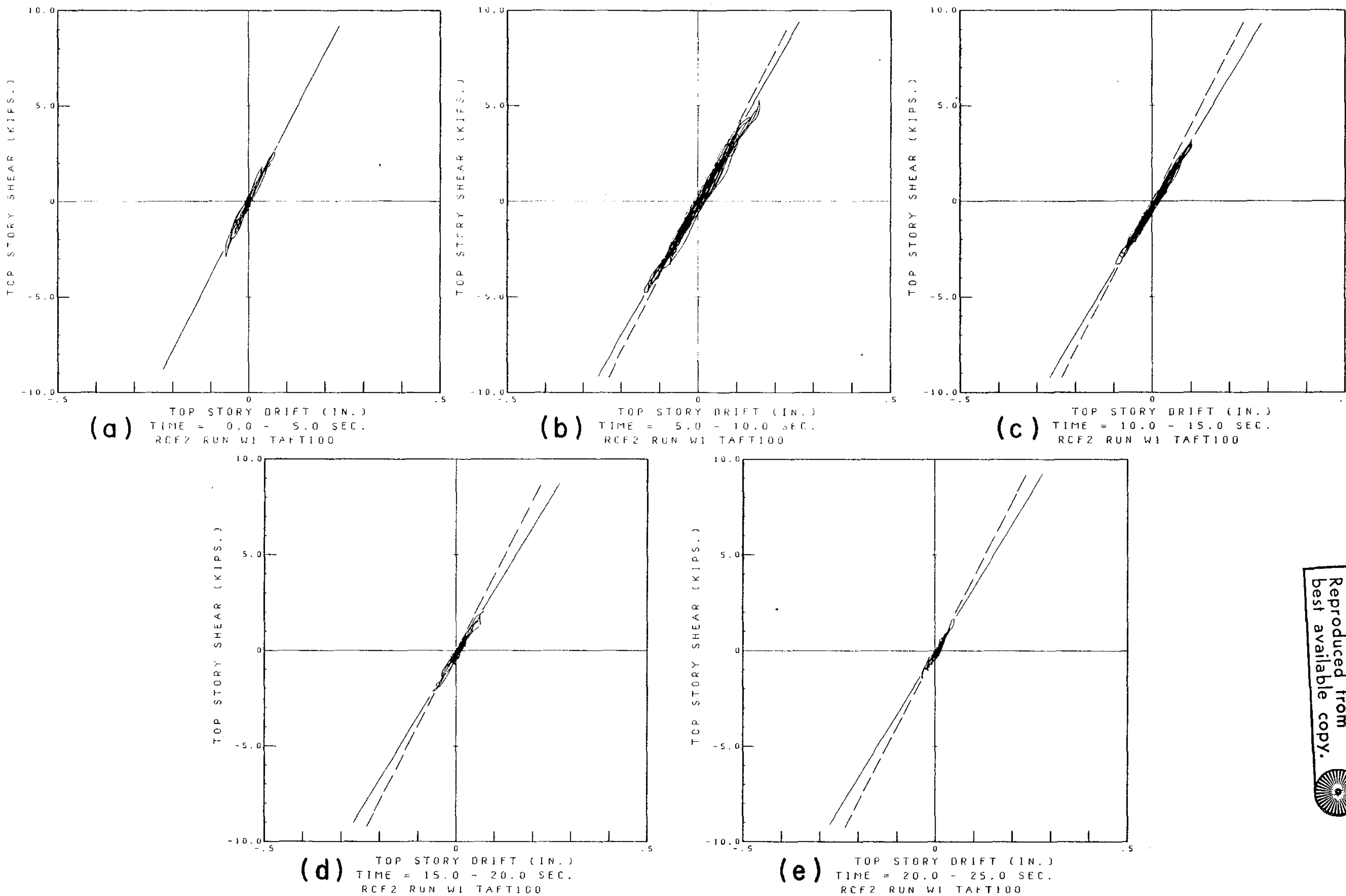

FIG. 5.8 TOP STORY SHEAR VS. DRIFT RELATIONSHIP DURING 5-SEC INTERVALS. RUN W1

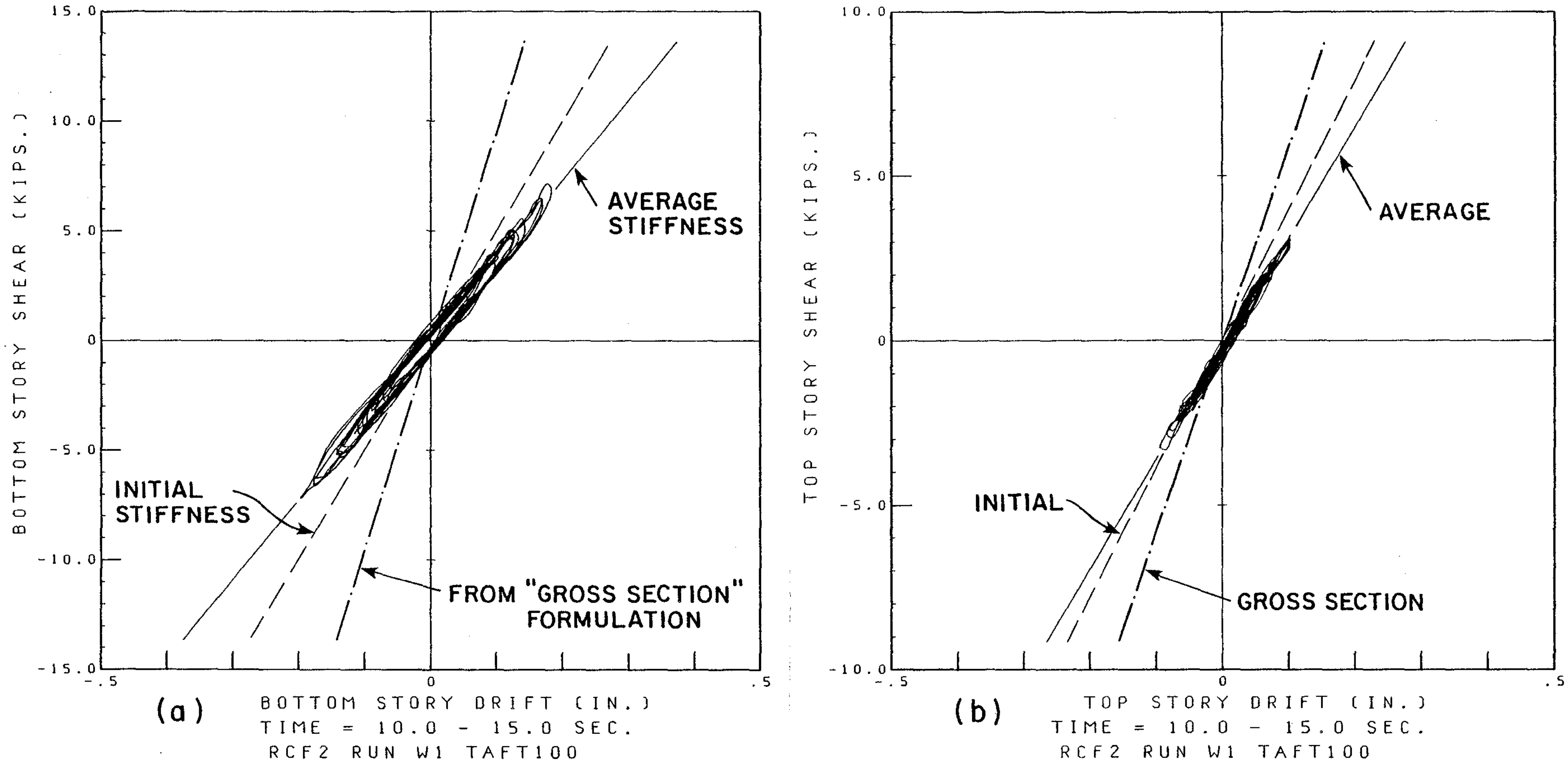

FIG. 5.9 ACTUAL VS. "GROSS SECTION" LATERAL STIFFNESS. RUN W1

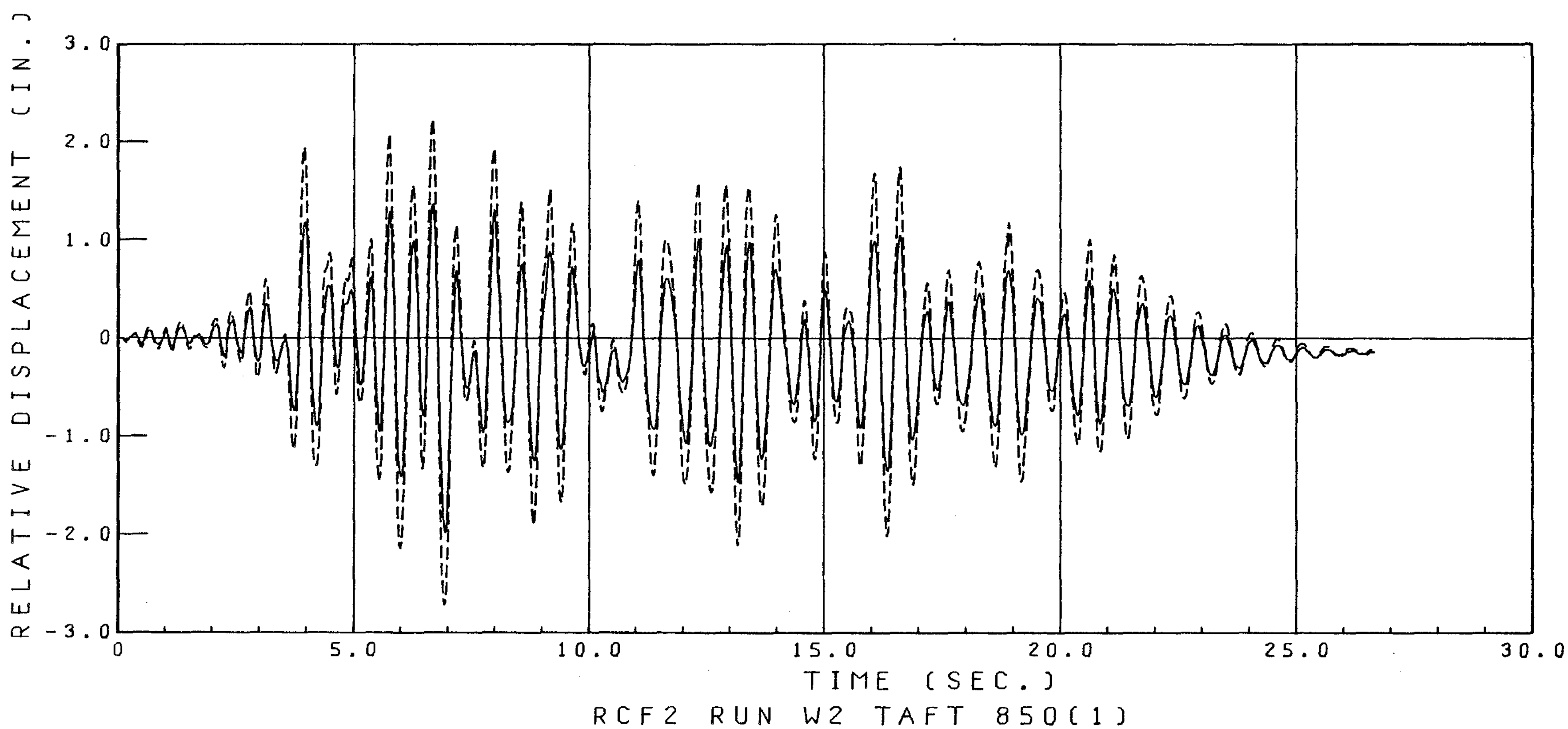

FIG. 5.10 DISPLACEMENT RESPONSE OF RCF2 DURING RUN W2 (RELATIVE TO TABLE)
SOLID LINE - BOTTOM FLOOR; DASHED LINE - TOP FLOOR

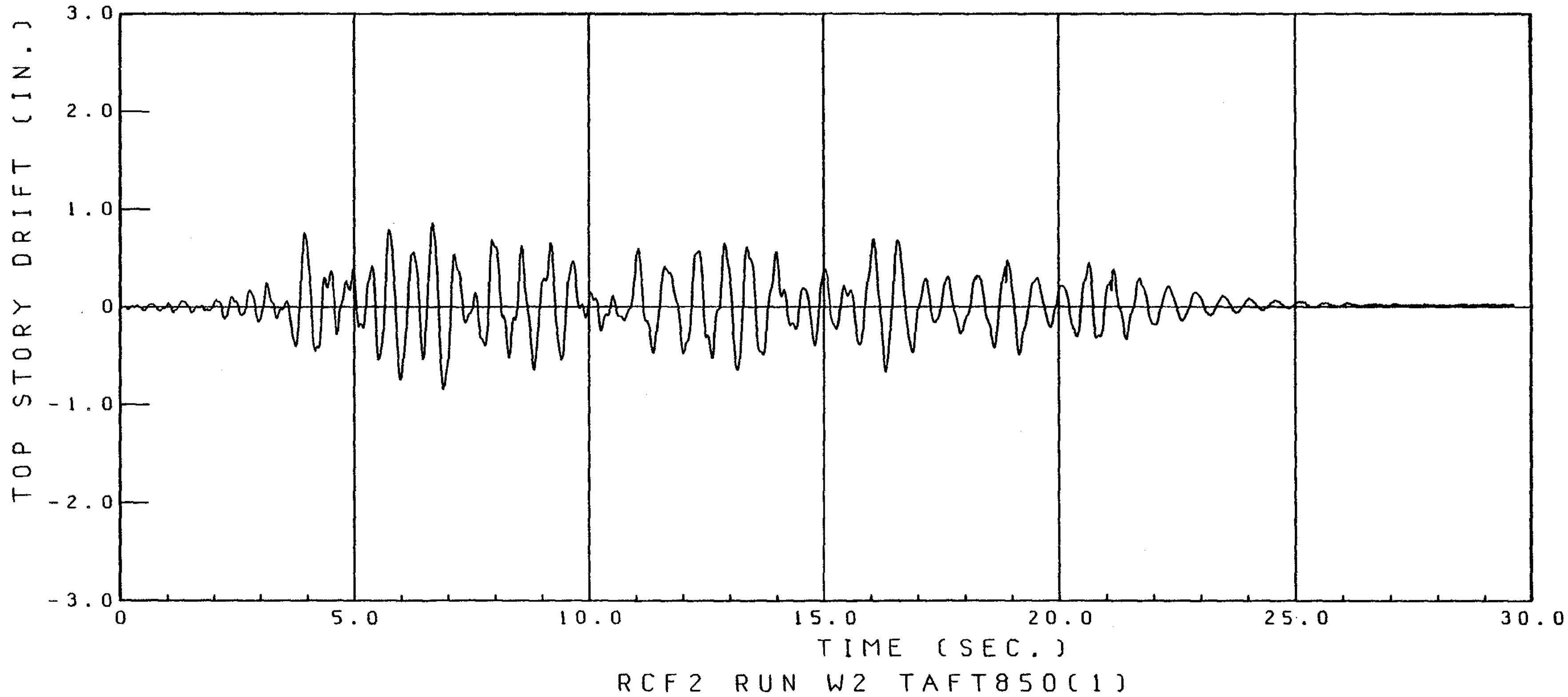

FIG. 5.11 TOP STORY DRIFT. RUN W2

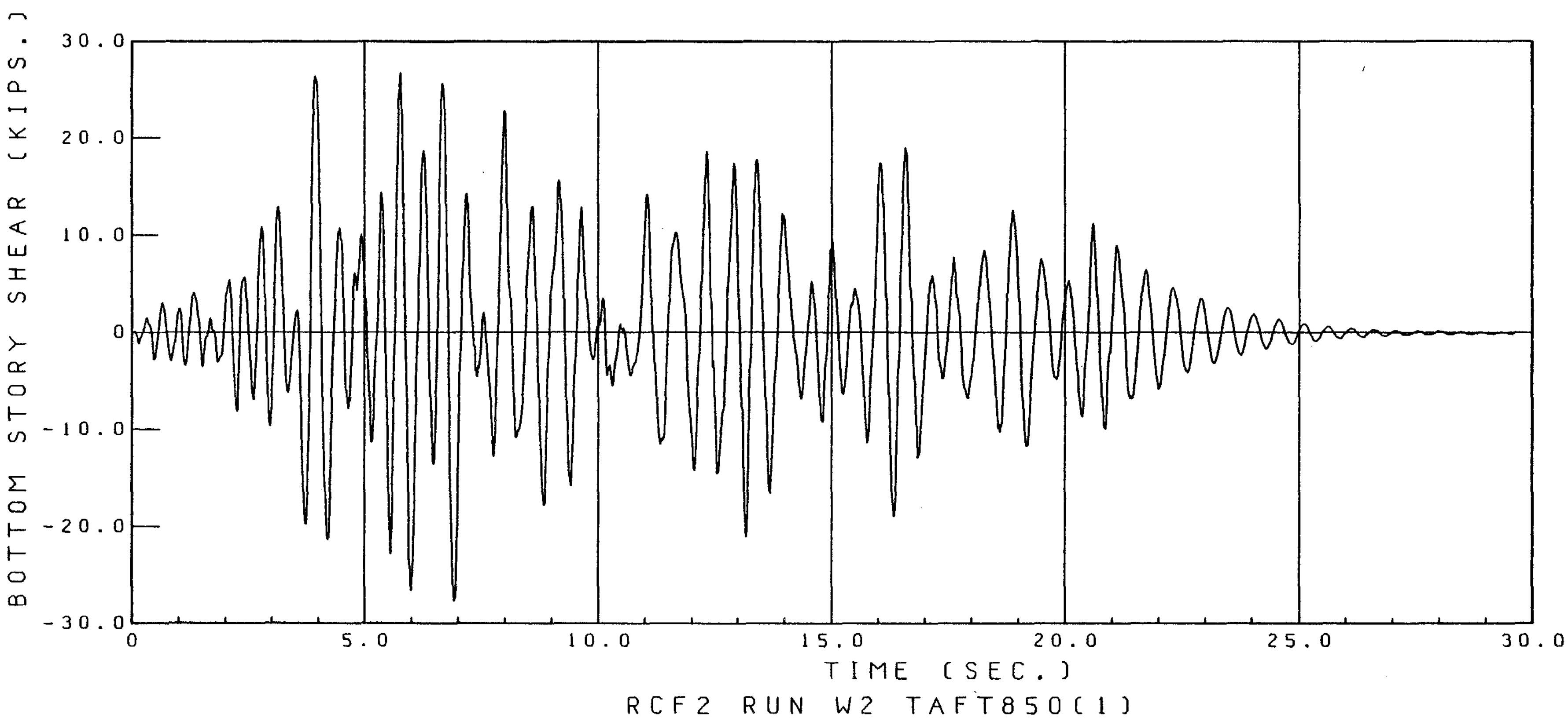

FIG. 5.12 BOTTOM STORY SHEAR (FROM ACCELERATION RECORDS). RUN W2

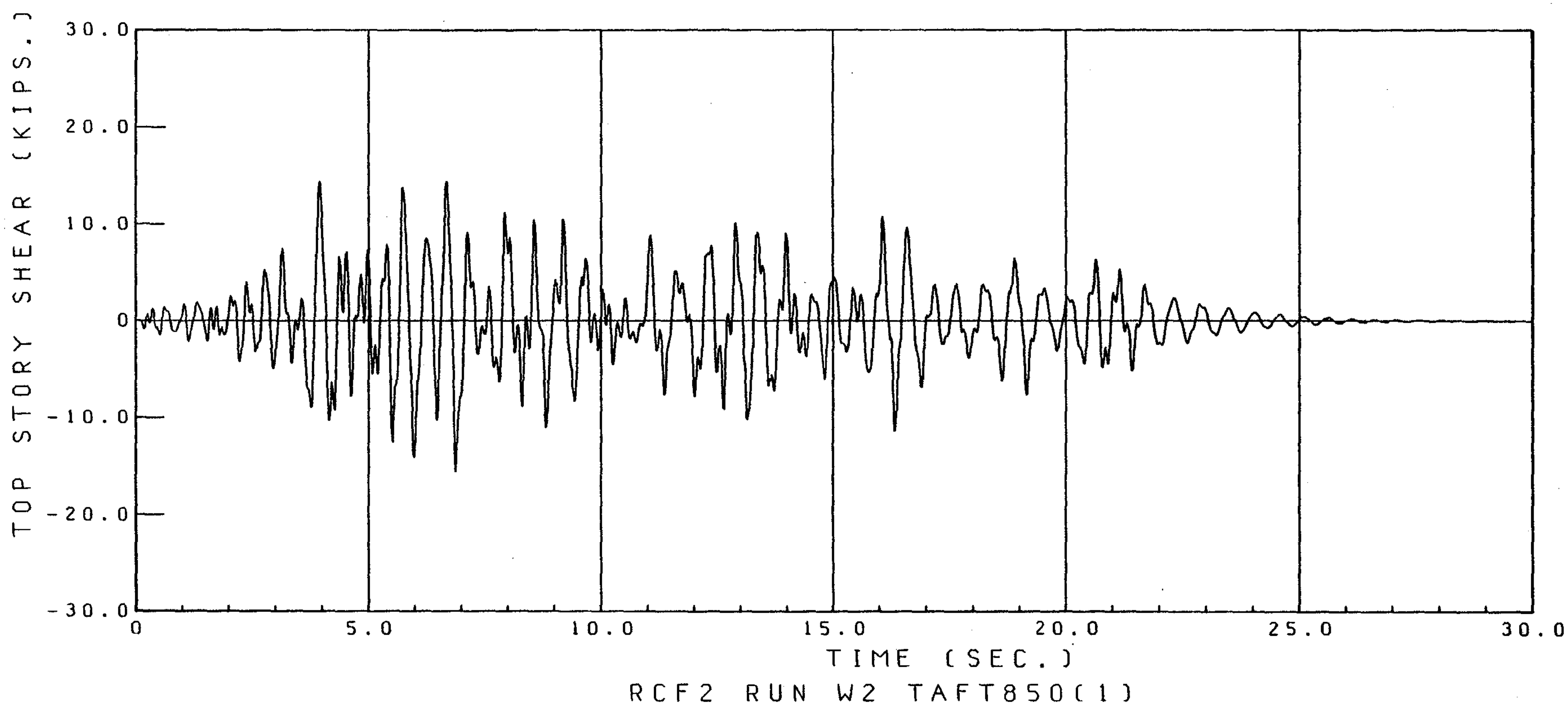

FIG. 5.13 TOP STORY SHEAR (FROM ACCELERATION RECORDS). RUN W2

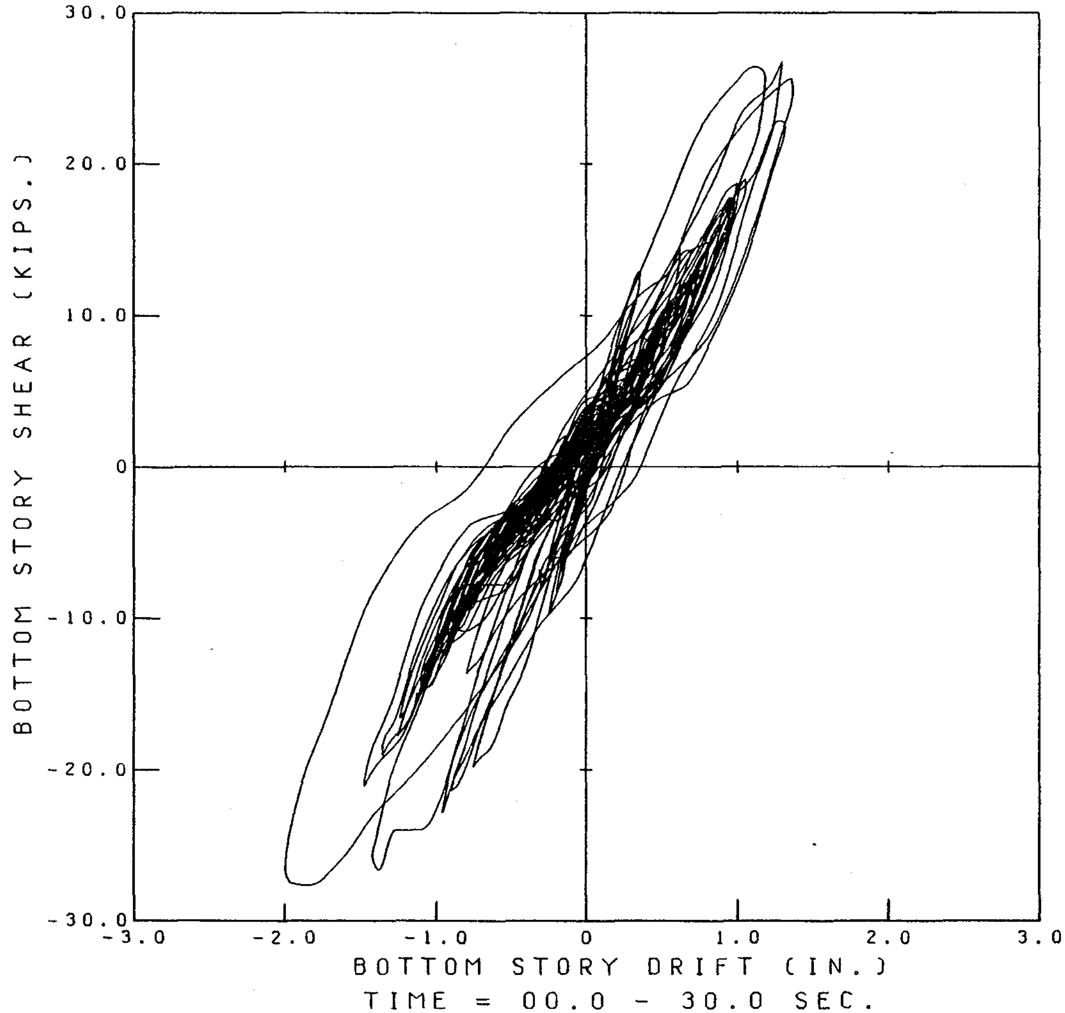

FIG. 5.14 BOTTOM STORY SHEAR VS. DRIFT RELATIONSHIP. RUN W2.

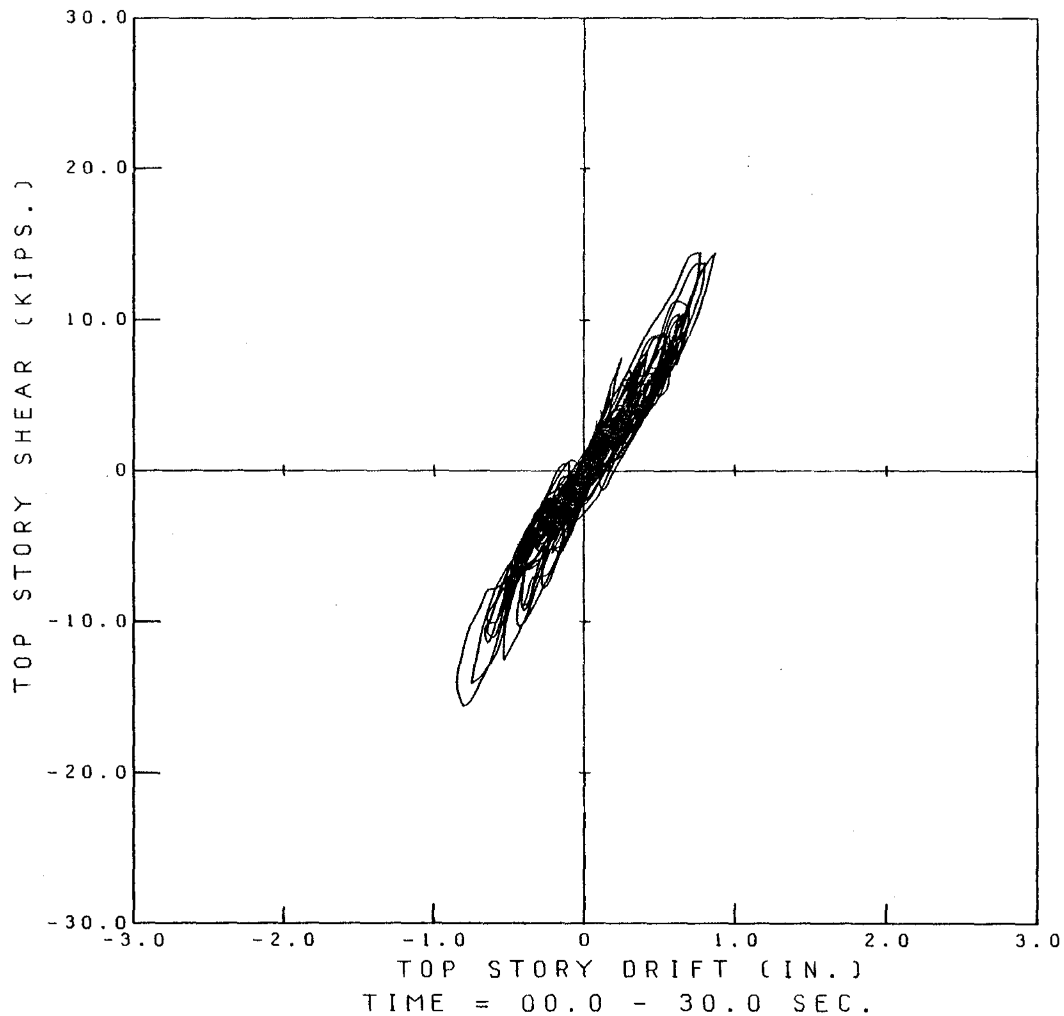

FIG. 5.15 TOP STORY SHEAR VS. DRIFT RELATIONSHIP. RUN W2

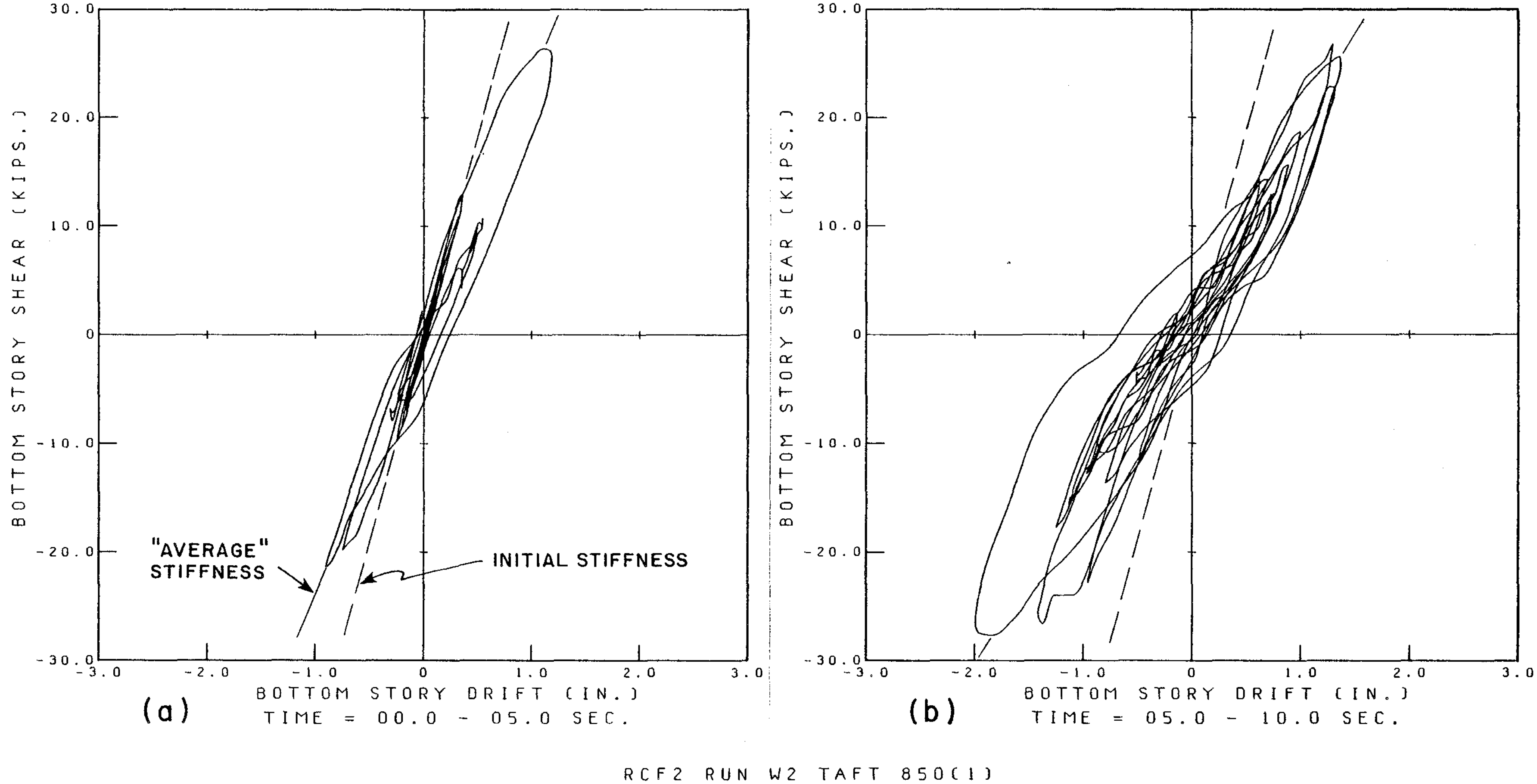

FIG. 5.16 BOTTOM STORY SHEAR VS. DRIFT RELATIONSHIP DURING 5-SEC INTERVALS. RUN W2

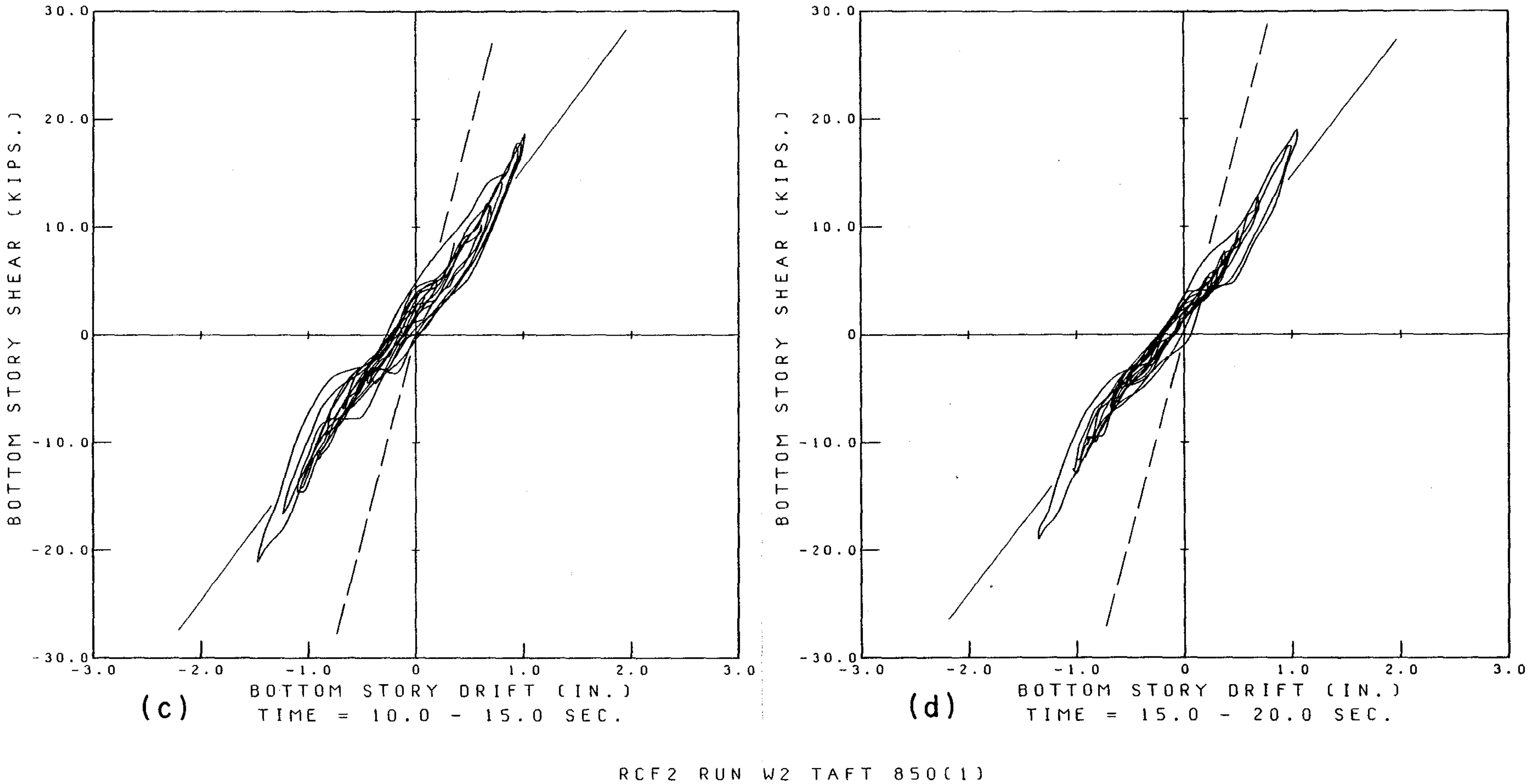

FIG. 5.16(CONT.) BOTTOM STORY SHEAR VS. DRIFT RELATIONSHIP DURING 5-SEC INTERVALS. RUN W2

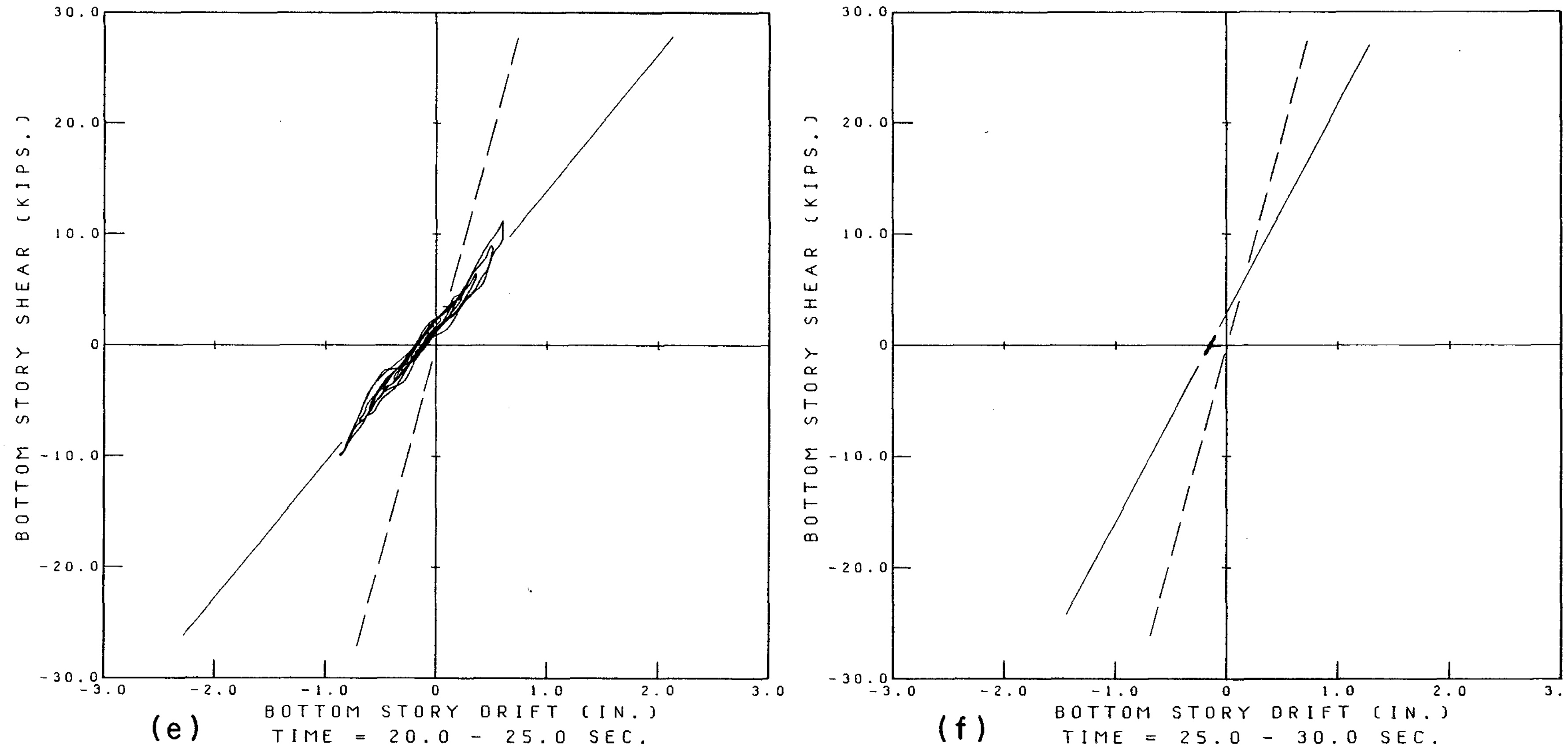

RCF2 RUN W2 TAFT 850(1)

FIG. 5.16(CONT.) BOTTOM STORY SHEAR VS. DRIFT RELATIONSHIP DURING 5-SEC INTERVALS. RUN W2

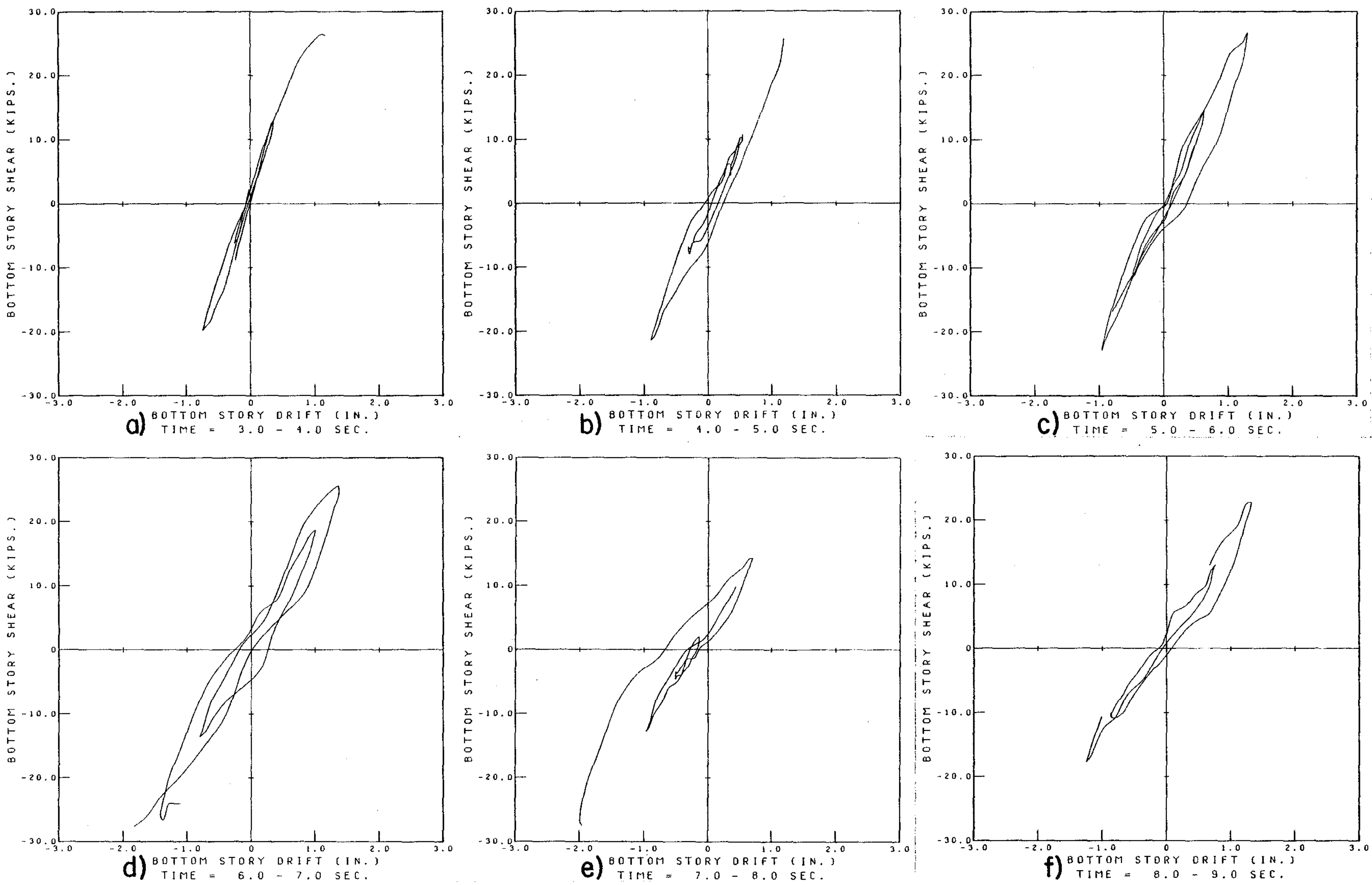

FIG. 5.17 BOTTOM STORY SHEAR VS. DRIFT RELATIONSHIP DURING STRONGEST SHAKING OF RUN W2

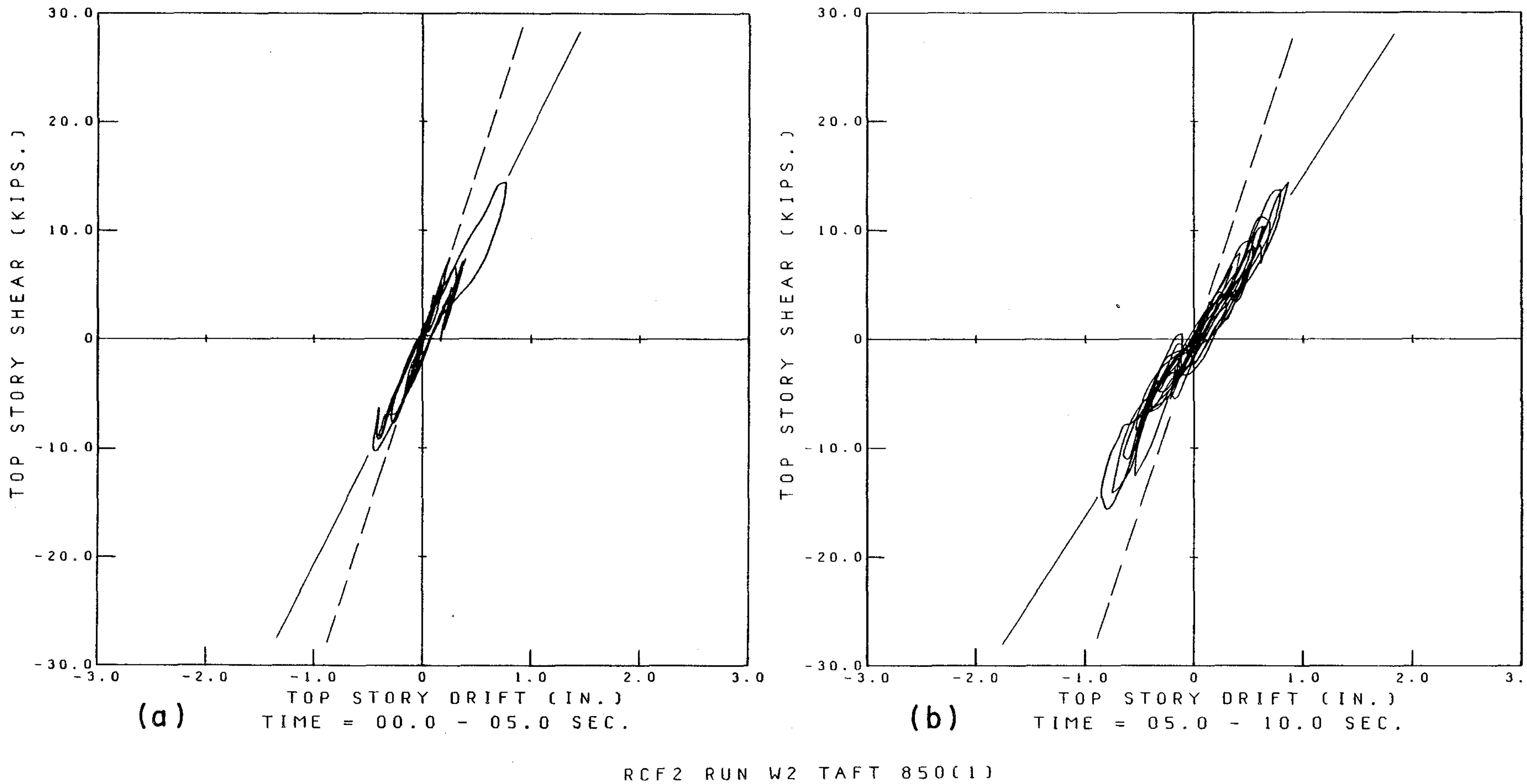

FIG. 5.18 TOP STORY SHEAR VS. DRIFT RELATIONSHIP DURING 5-SEC INTERVALS. RUN W2

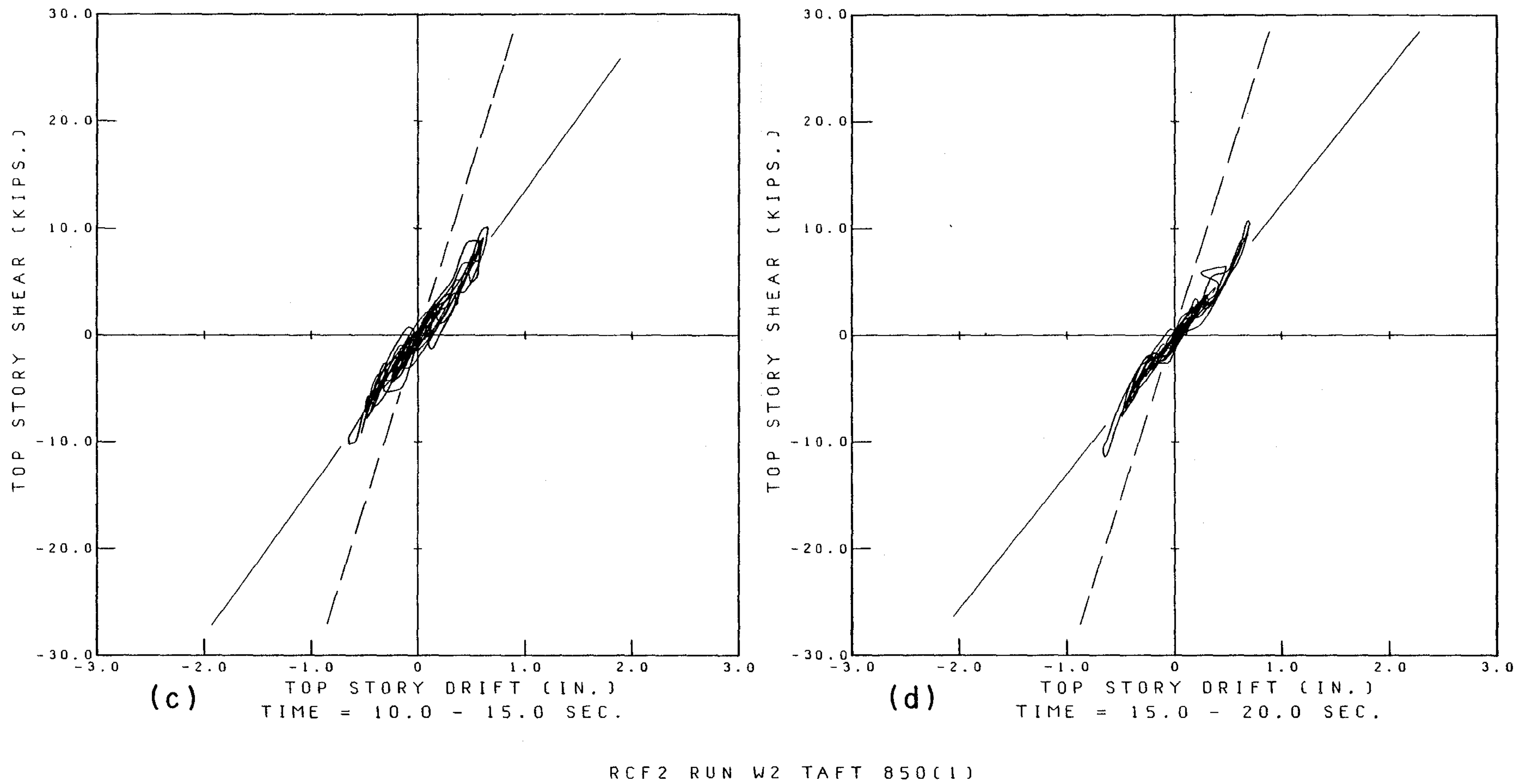

FIG. 5.18(CONT.) TOP STORY SHEAR VS. DRIFT RELATIONSHIP DURING 5-SEC INTERVALS. RUN W2

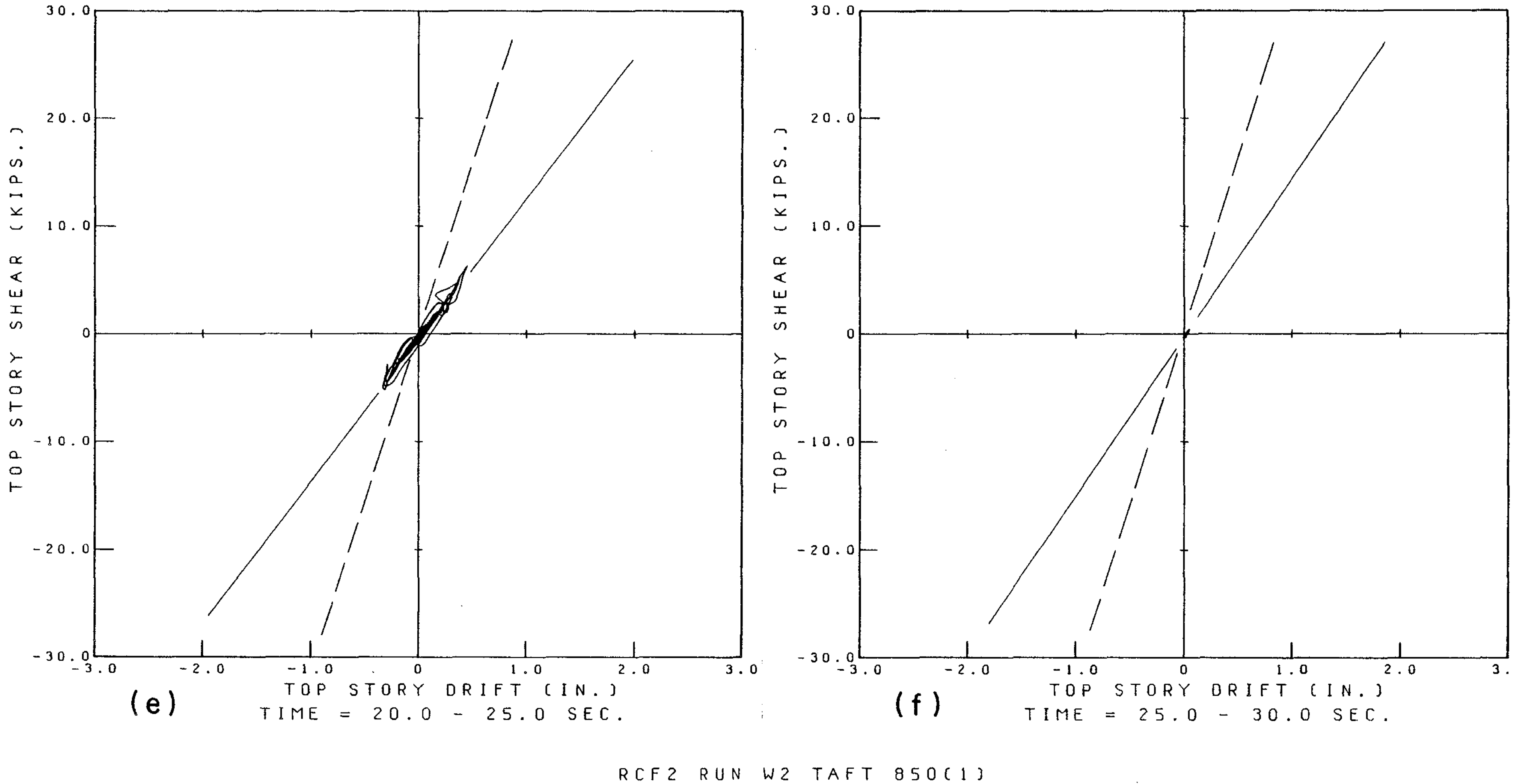

FIG. 5.18(CONT.) TOP STORY SHEAR VS. DRIFT RELATIONSHIP DURING 5-SEC INTERVALS. RUN W2

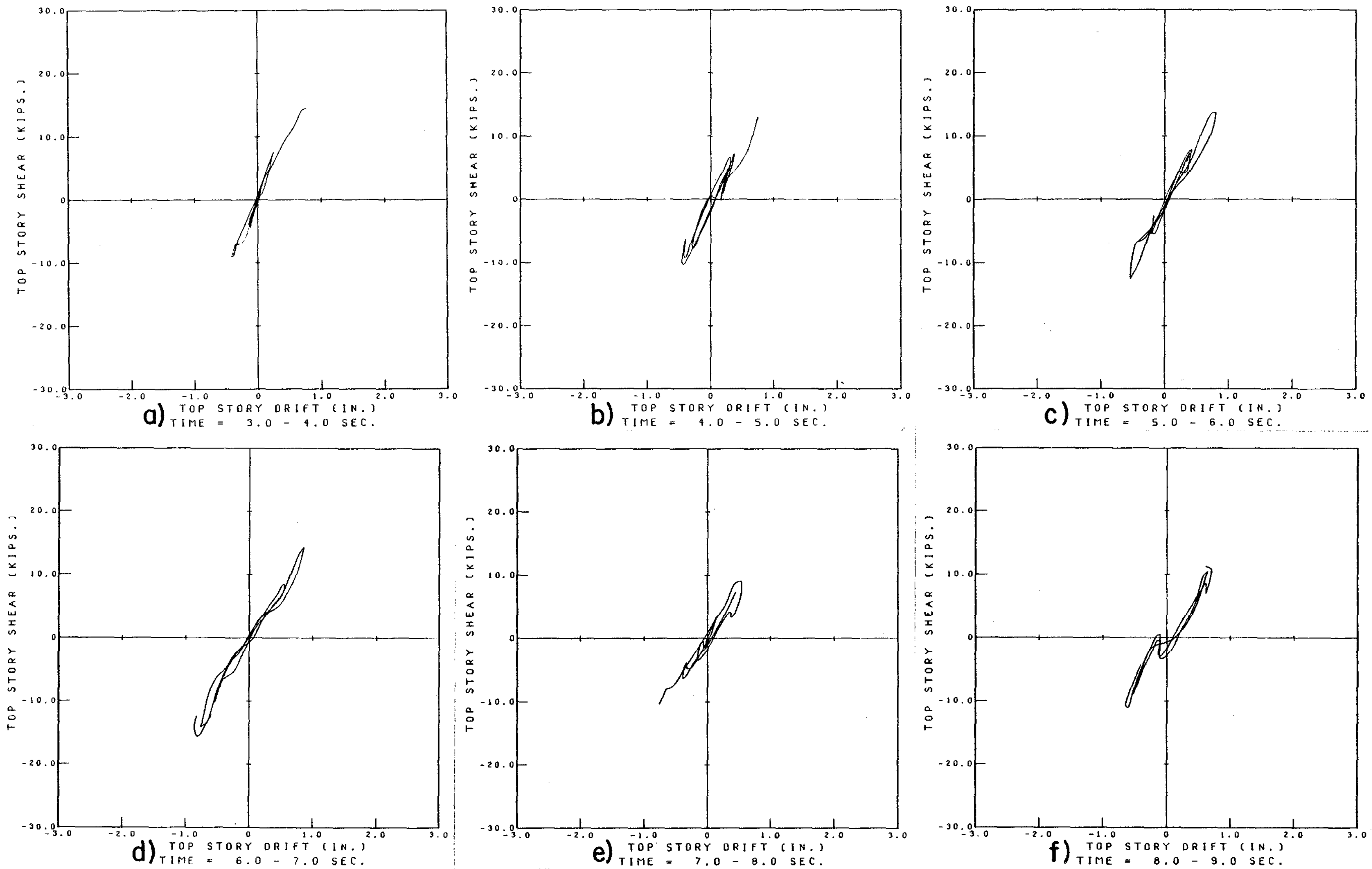

FIG. 5.19 TOP STORY SHEAR VS. DRIFT RELATIONSHIP DURING STRONGEST SHAKING OF RUN W2

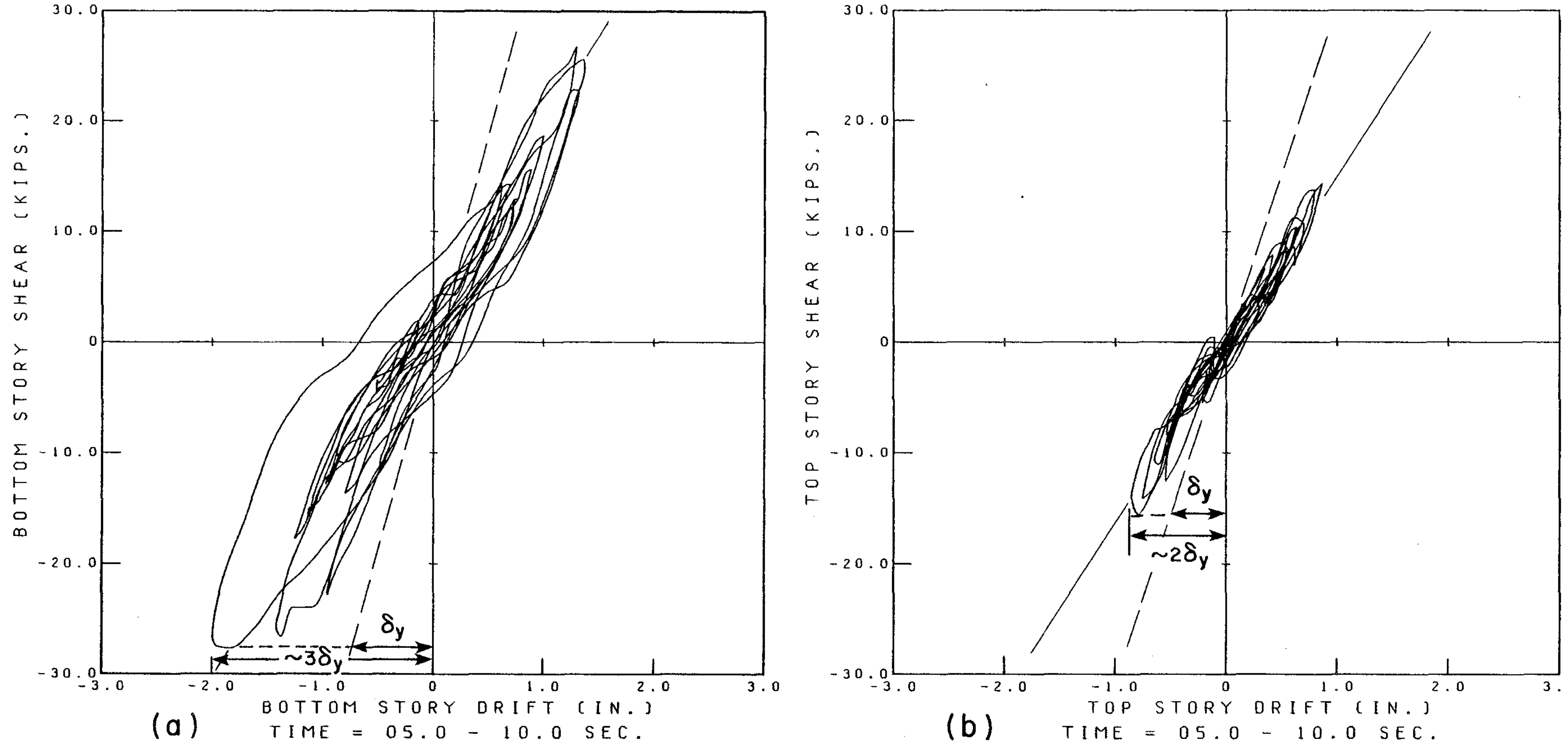

RCF2 RUN W2 TAFT 850(1)

FIG. 5.20 COMPARISON BETWEEN BOTTOM AND TOP STORY BEHAVIOR DURING PART OF RUN W2

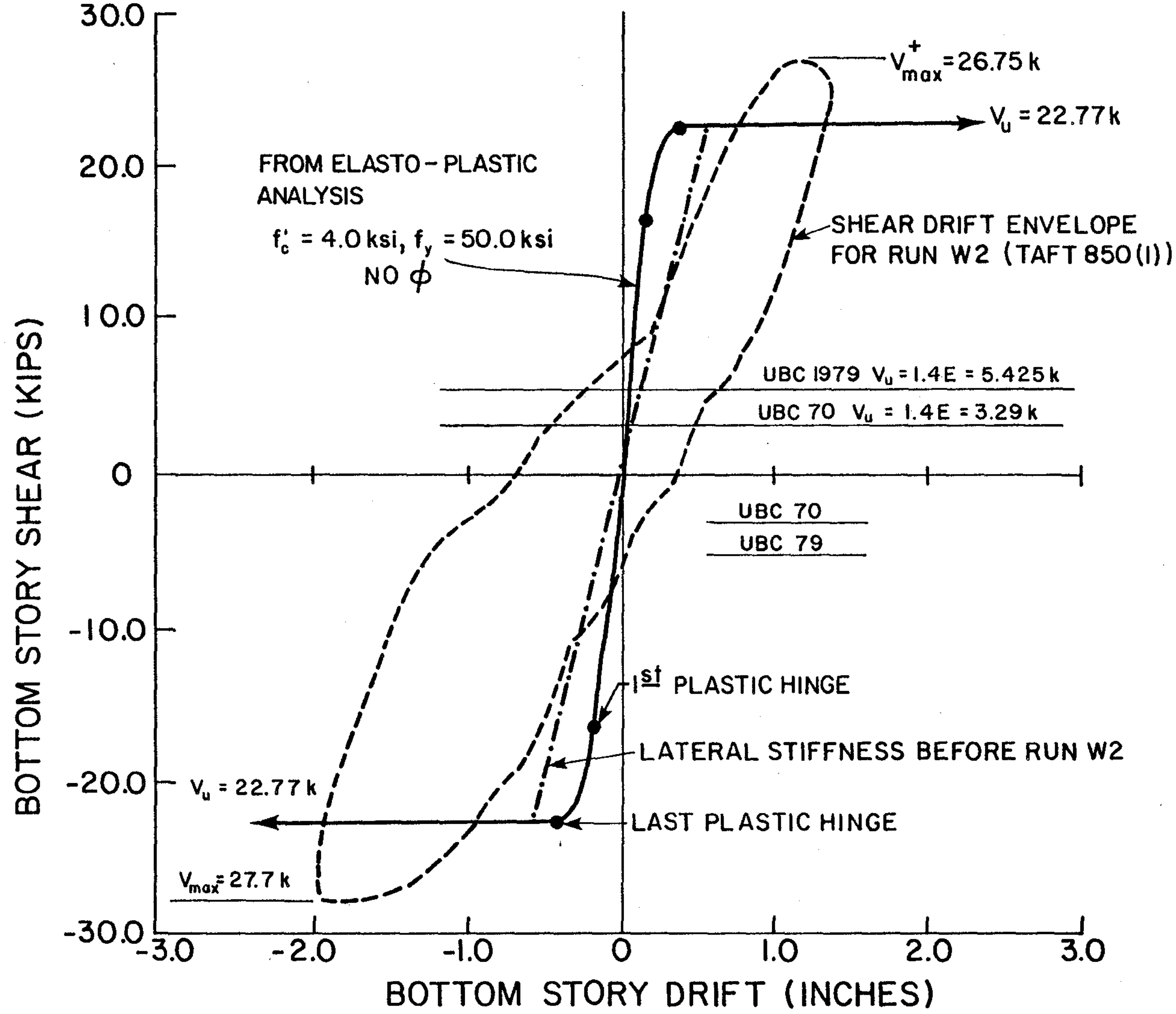

FIG. 5.21 TEST RESULTS VS. EXPECTED PERFORMANCE. BOTTOM STORY. RUN W2

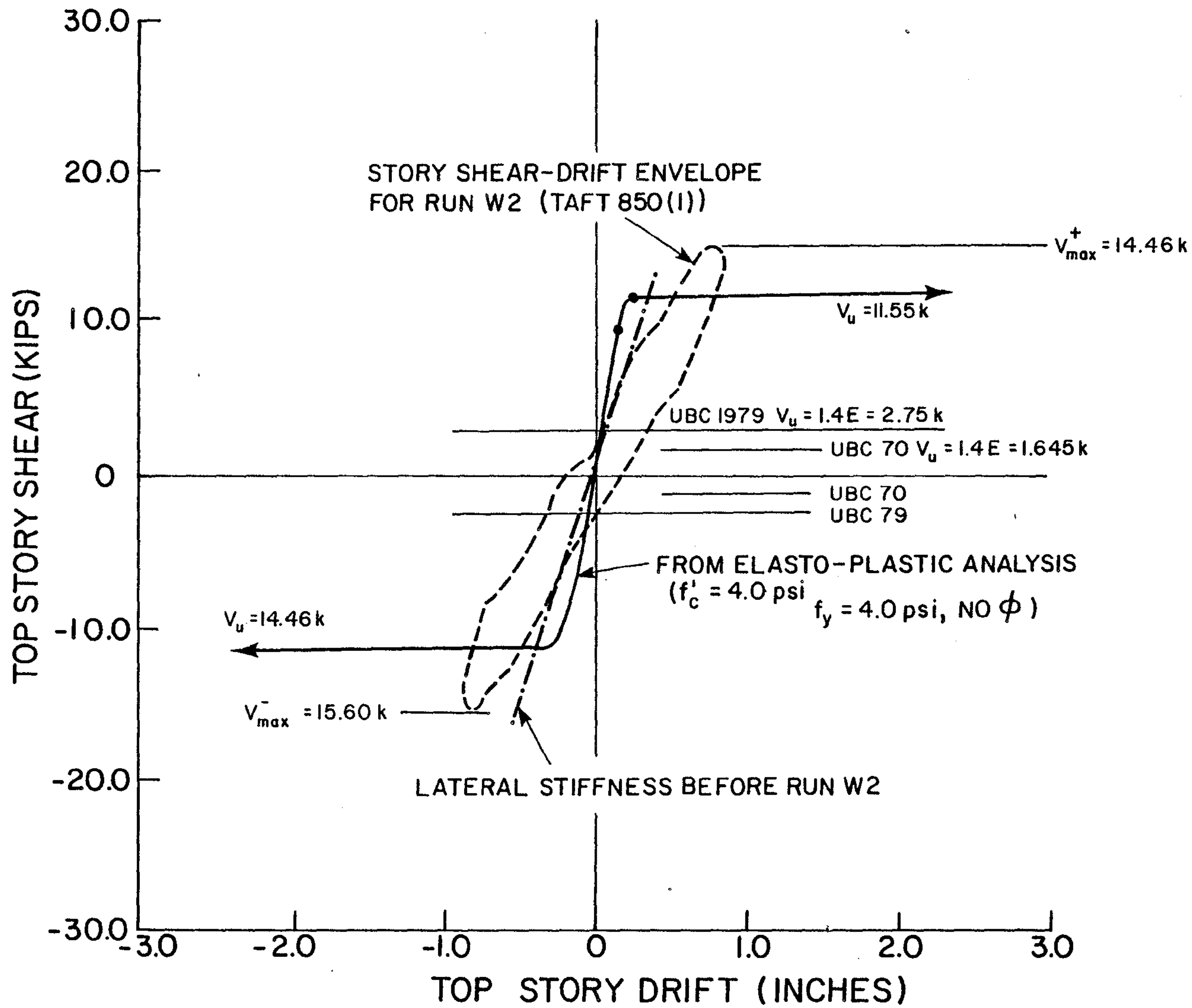

FIG. 5.22 TEST RESULTS VS. EXPECTED PERFORMANCE. TOP STORY. RUN W2

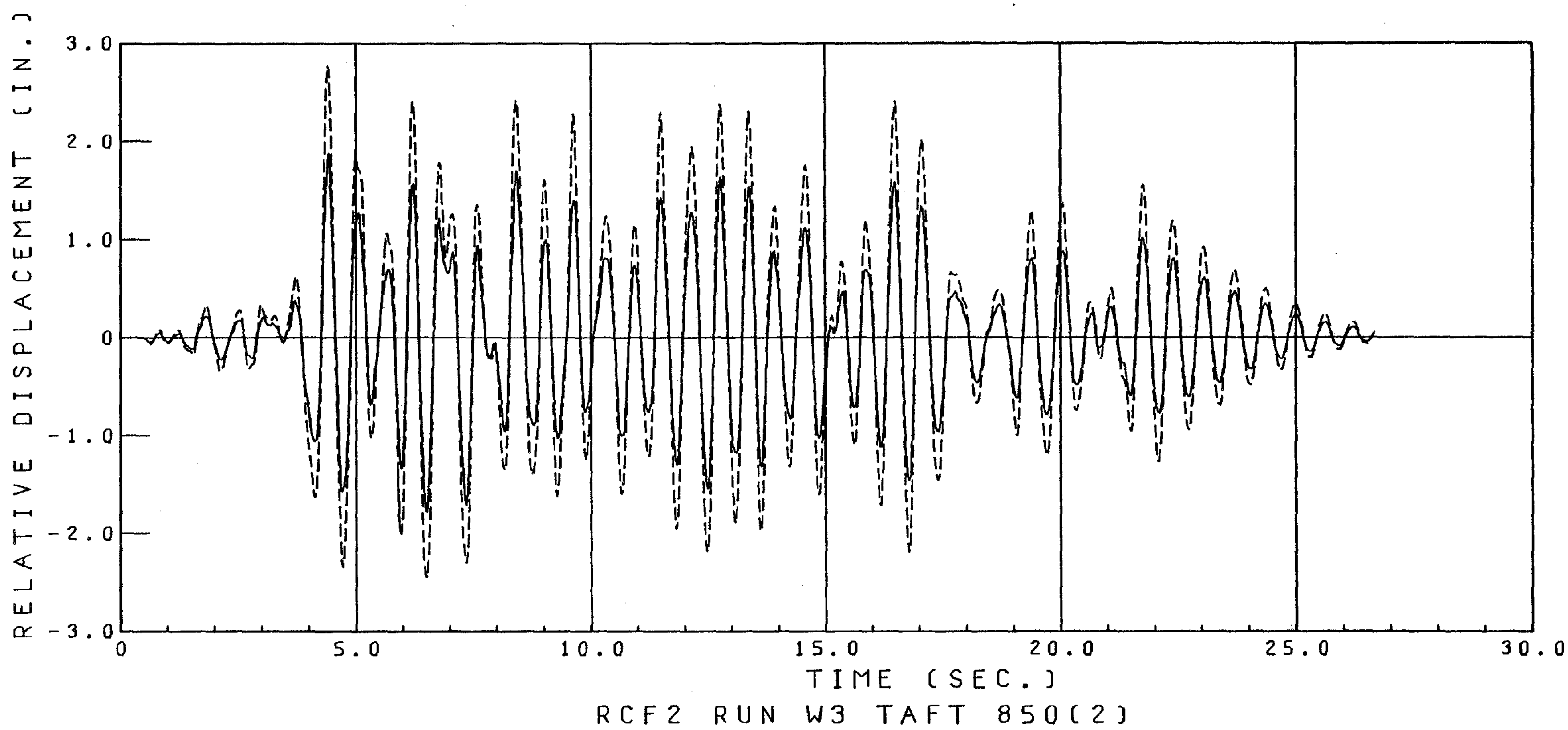

FIG. 5.23 DISPLACEMENT RESPONSE OF RCF2 DURING RUN W3 (RELATIVE TO TABLE)
SOLID LINE - BOTTOM FLOOR; DASHED LINE - TOP FLOOR

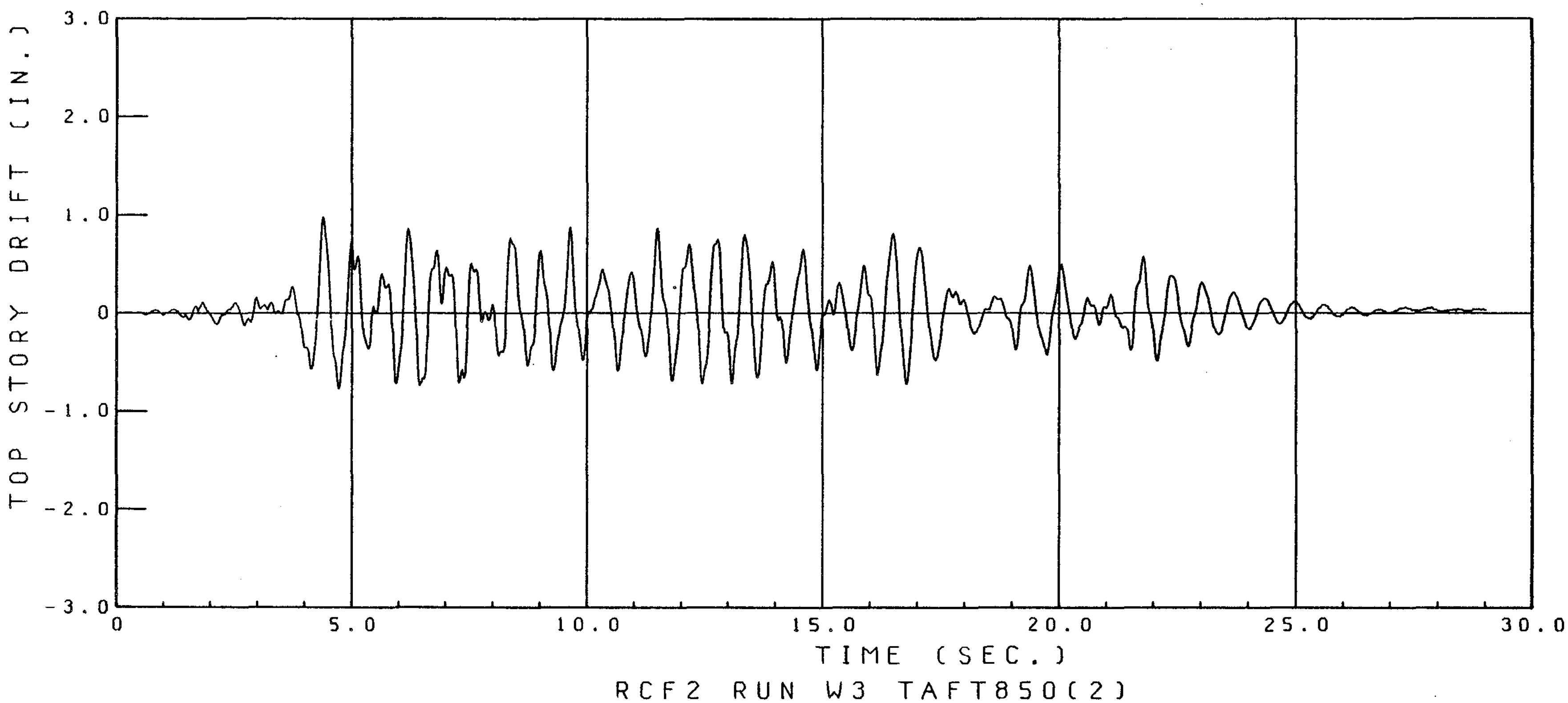

FIG. 5.24 TOP STORY DRIFT. RUN W3

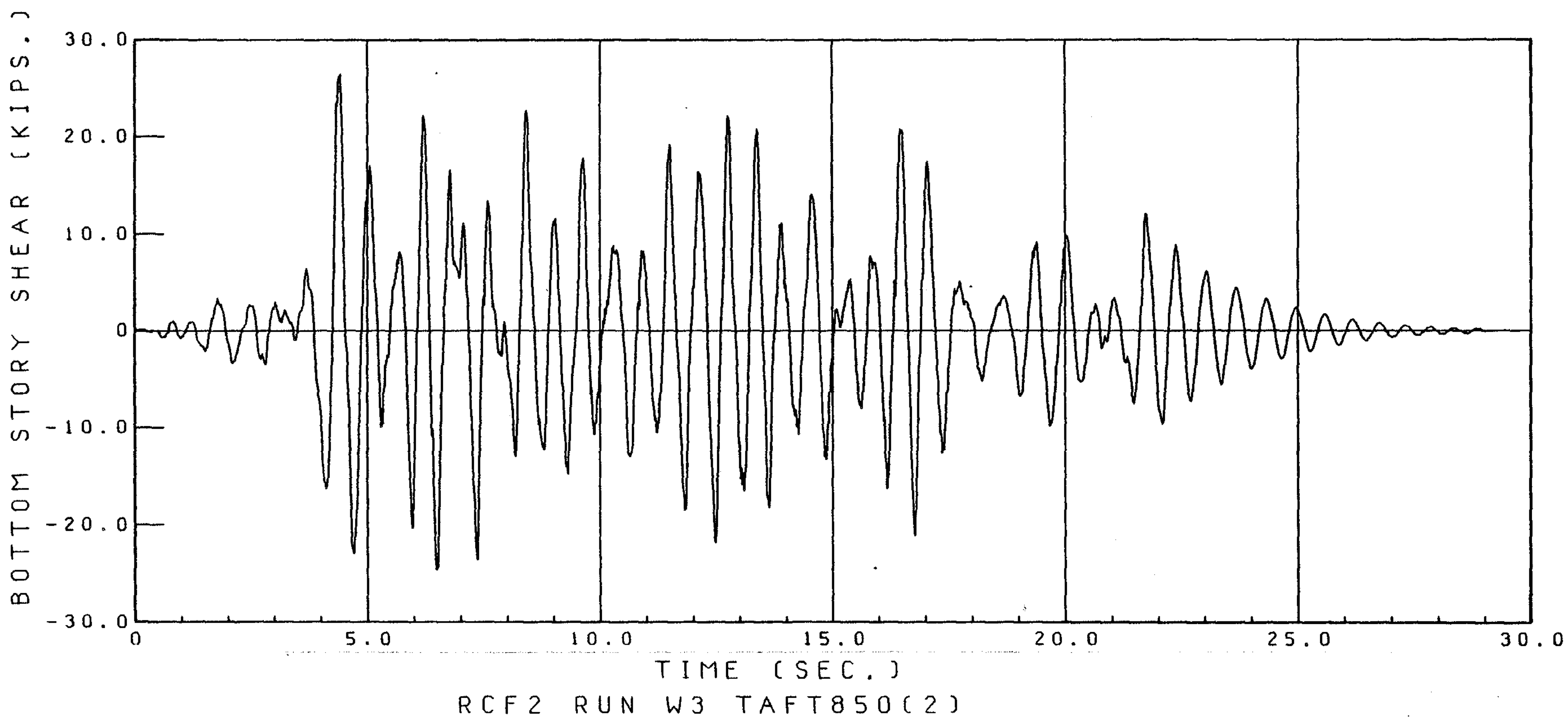

FIG. 5.25 BOTTOM STORY SHEAR (FROM ACCELERATION RECORDS). RUN W3

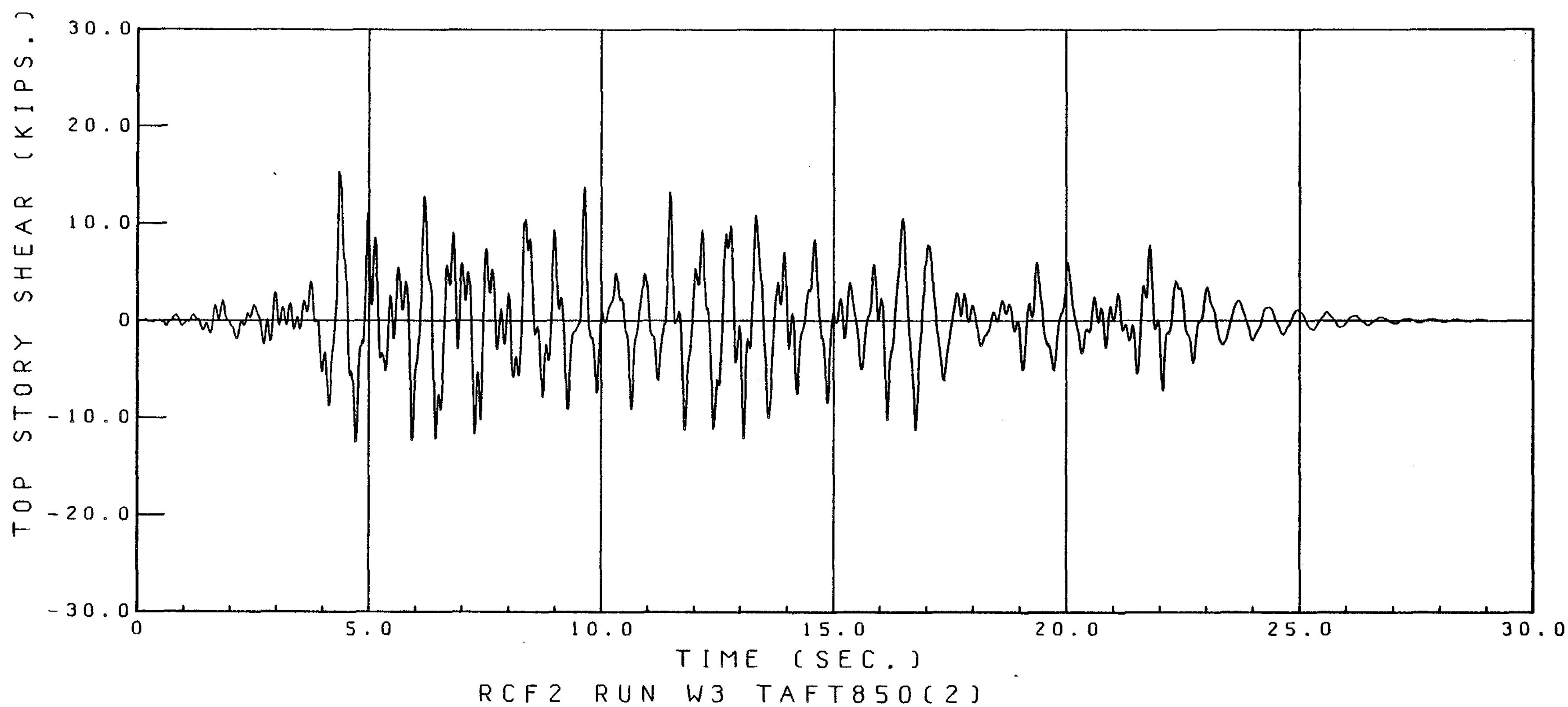

FIG. 5.26 TOP STORY SHEAR (FROM ACCELERATION RECORDS). RUN W3

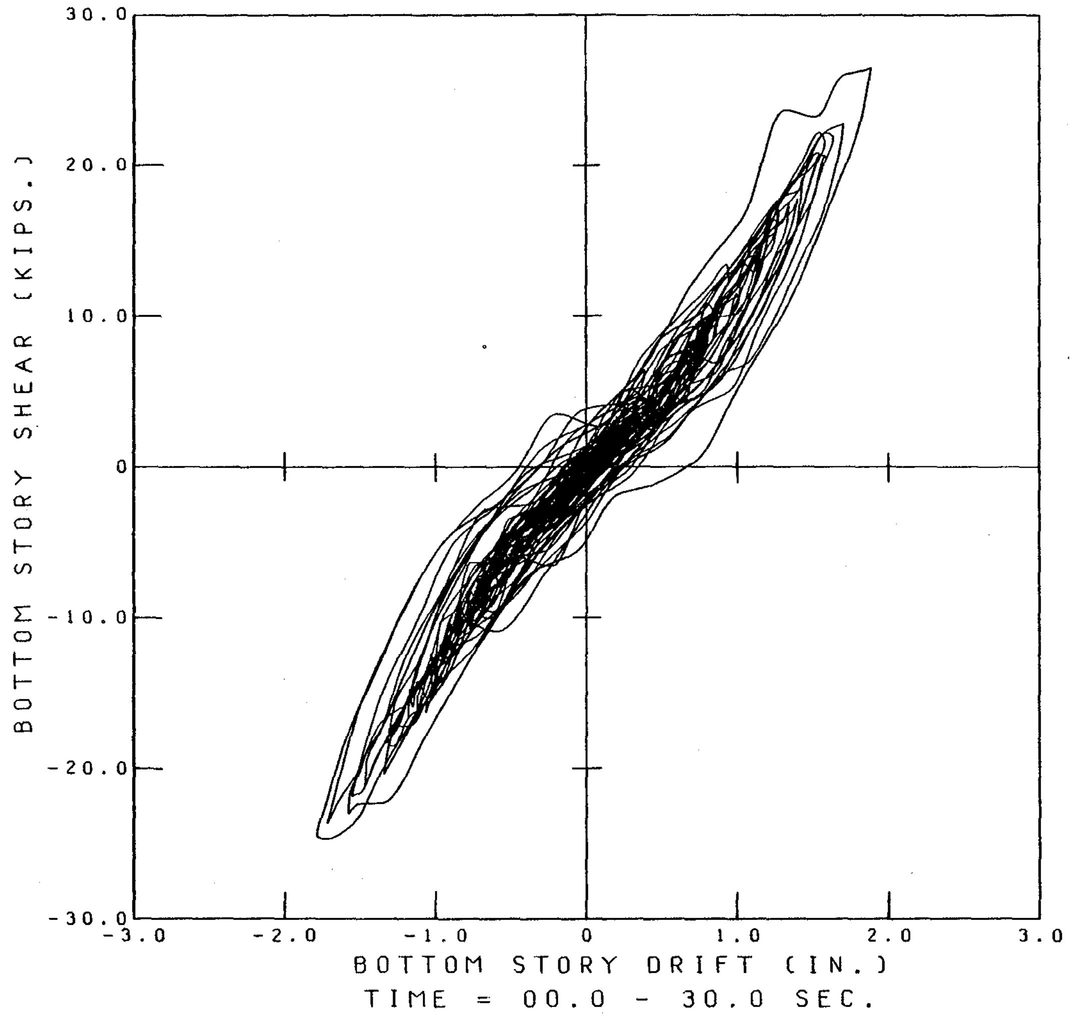

FIG. 5.27 BOTTOM STORY SHEAR VS. DRIFT RELATIONSHIP. RUN W3

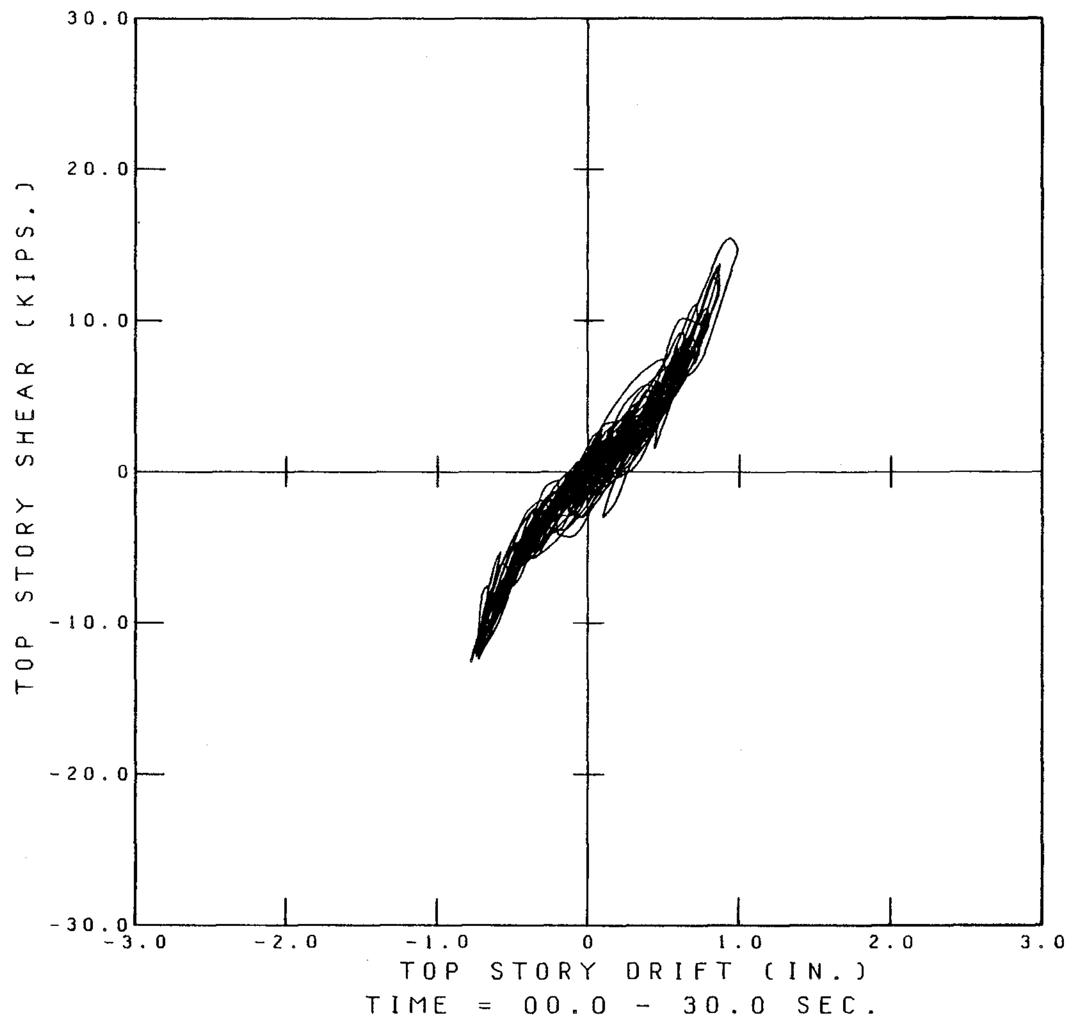

FIG. 5.28 TOP STORY SHEAR VS. DRIFT RELATIONSHIP. RUN W3

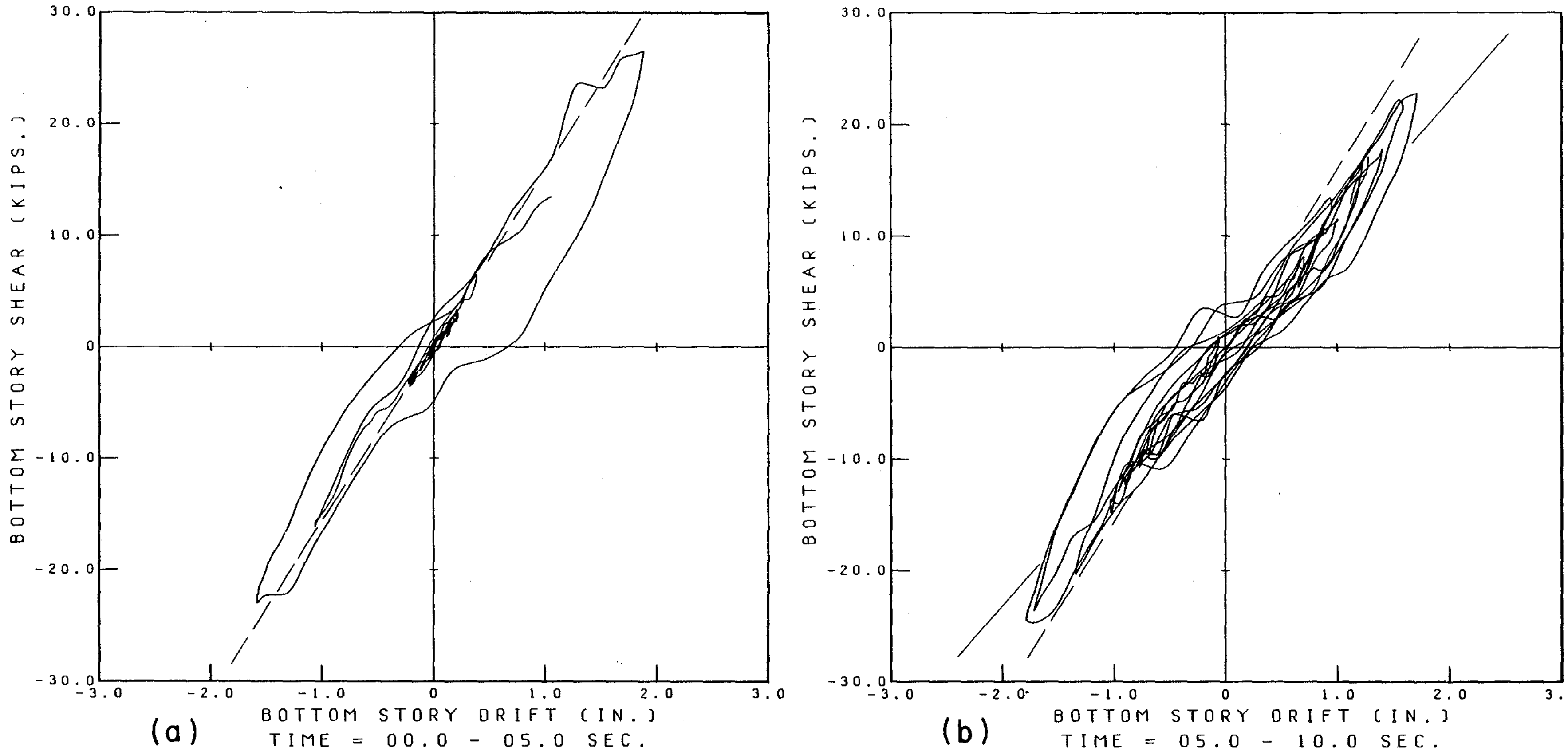

RCF2 RUN W3 TAFT 850(2)

FIG. 5.29 BOTTOM STORY SHEAR VS. DRIFT RELATIONSHIP DURING 5-SEC INTERVALS. RUN W3

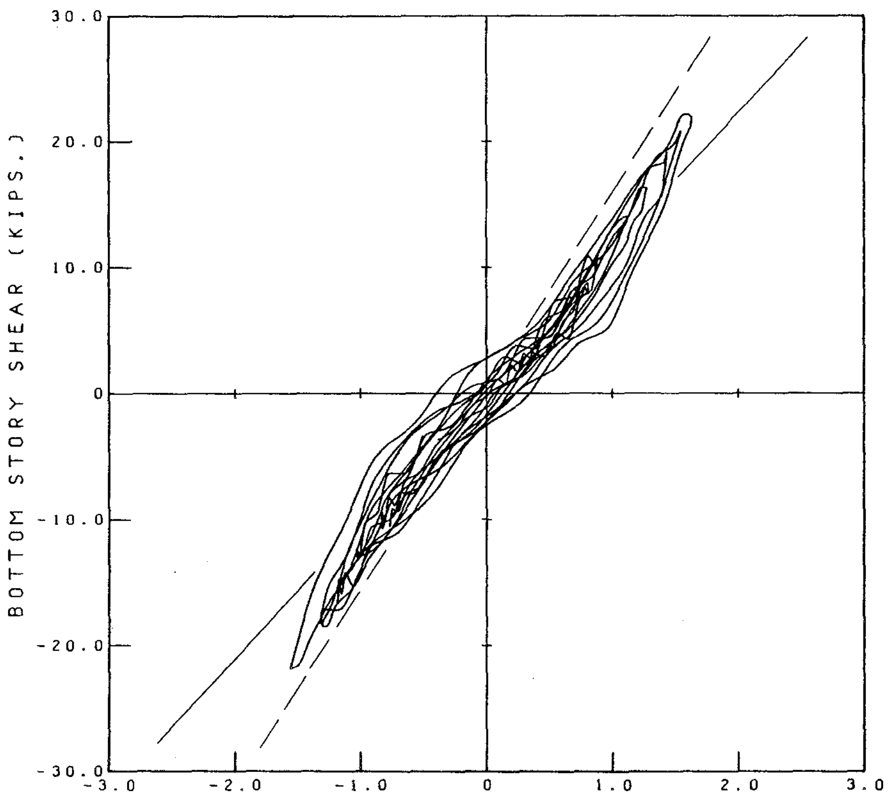

(c)

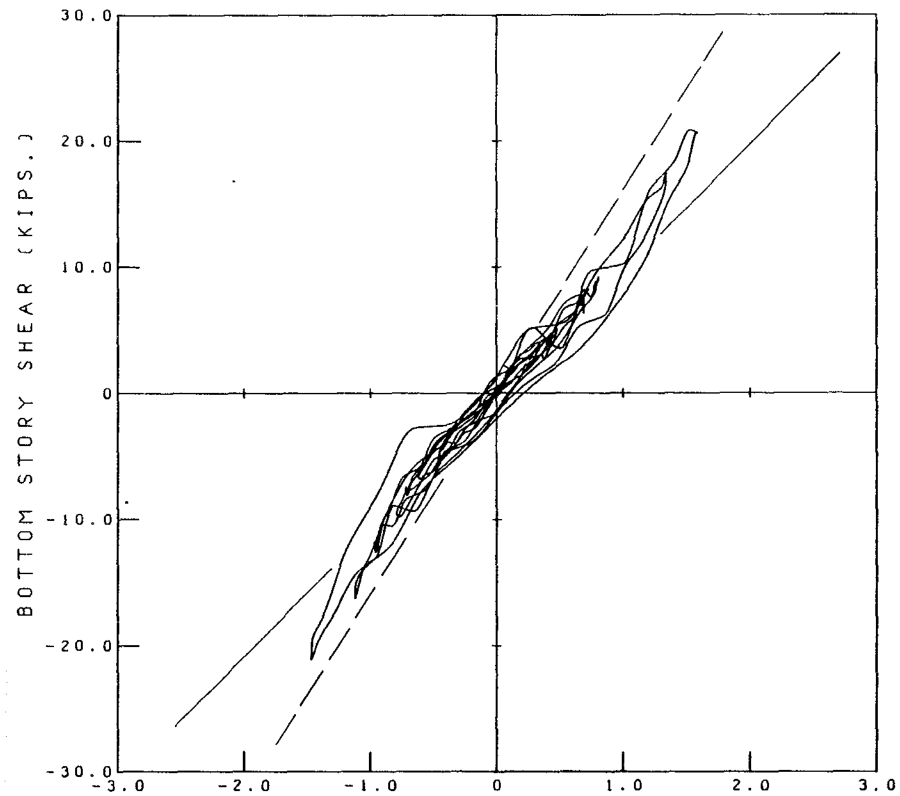

(d)

RCF2 RUN W3 TAFT 850(2)

FIG. 5.29(CONT.) BOTTOM STORY SHEAR VS. DRIFT RELATIONSHIP DURING 5-SEC INTERVALS. RUN W3

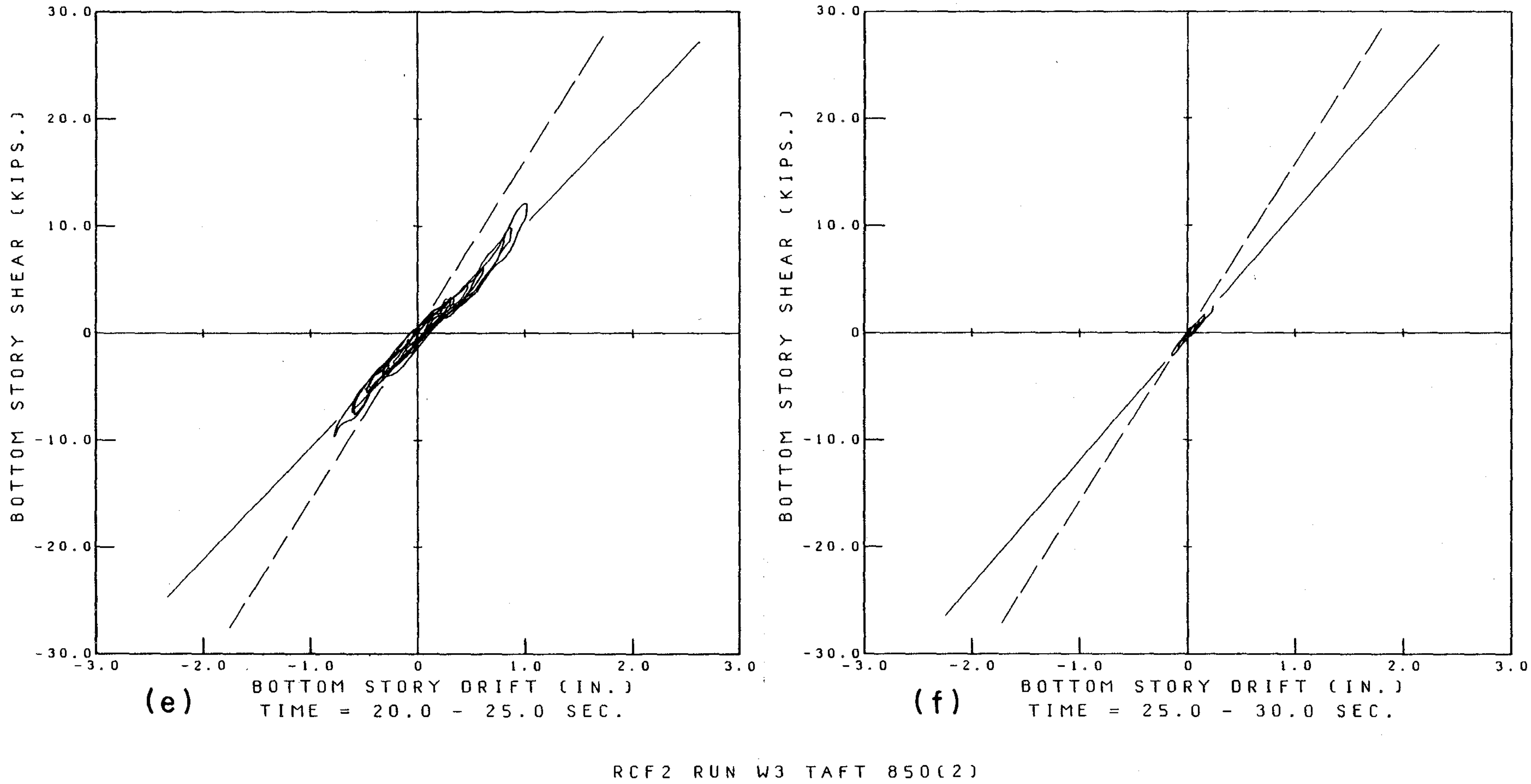

FIG. 5.29(CONT.) BOTTOM STORY SHEAR VS. DRIFT RELATIONSHIP DURING 5-SEC INTERVALS. RUN W3

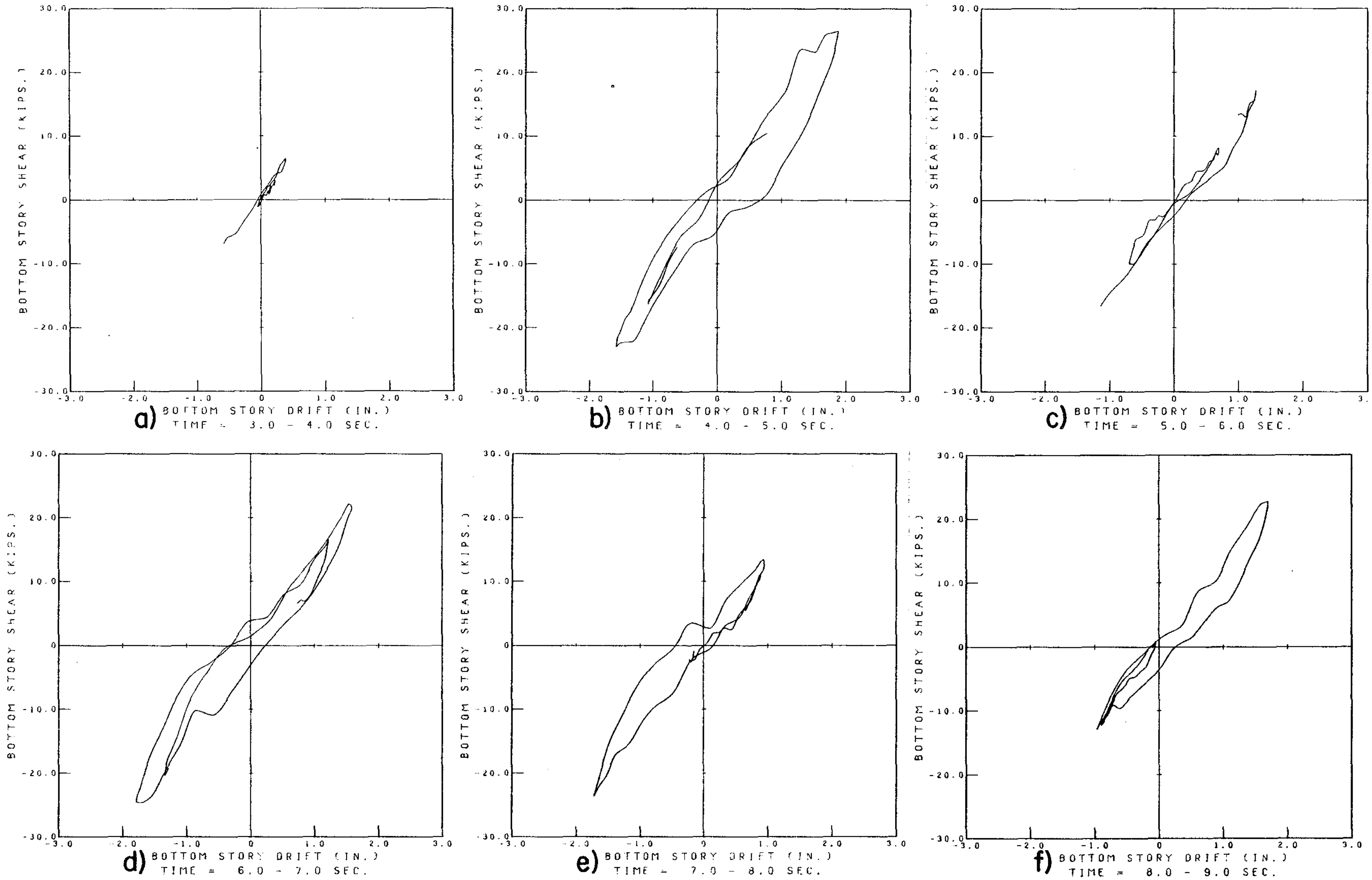

FIG. 5.30 BOTTOM STORY SHEAR VS. DRIFT RELATIONSHIP DURING STRONGEST SHAKING ON RUN W3

Reproduced from best available copy.

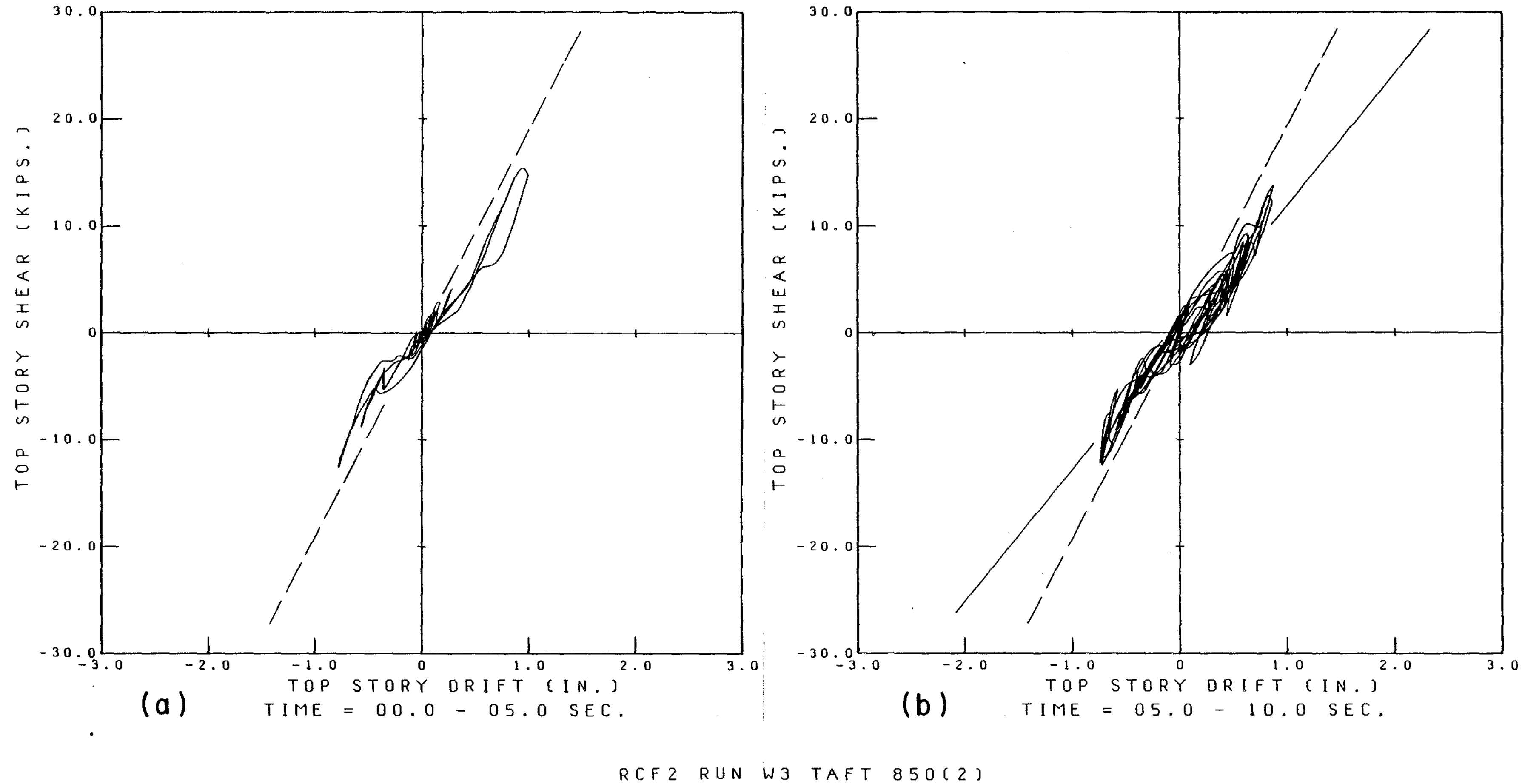

FIG. 5.31 TOP STORY SHEAR VS. DRIFT RELATIONSHIP DURING 5-SEC INTERVALS. RUN W3

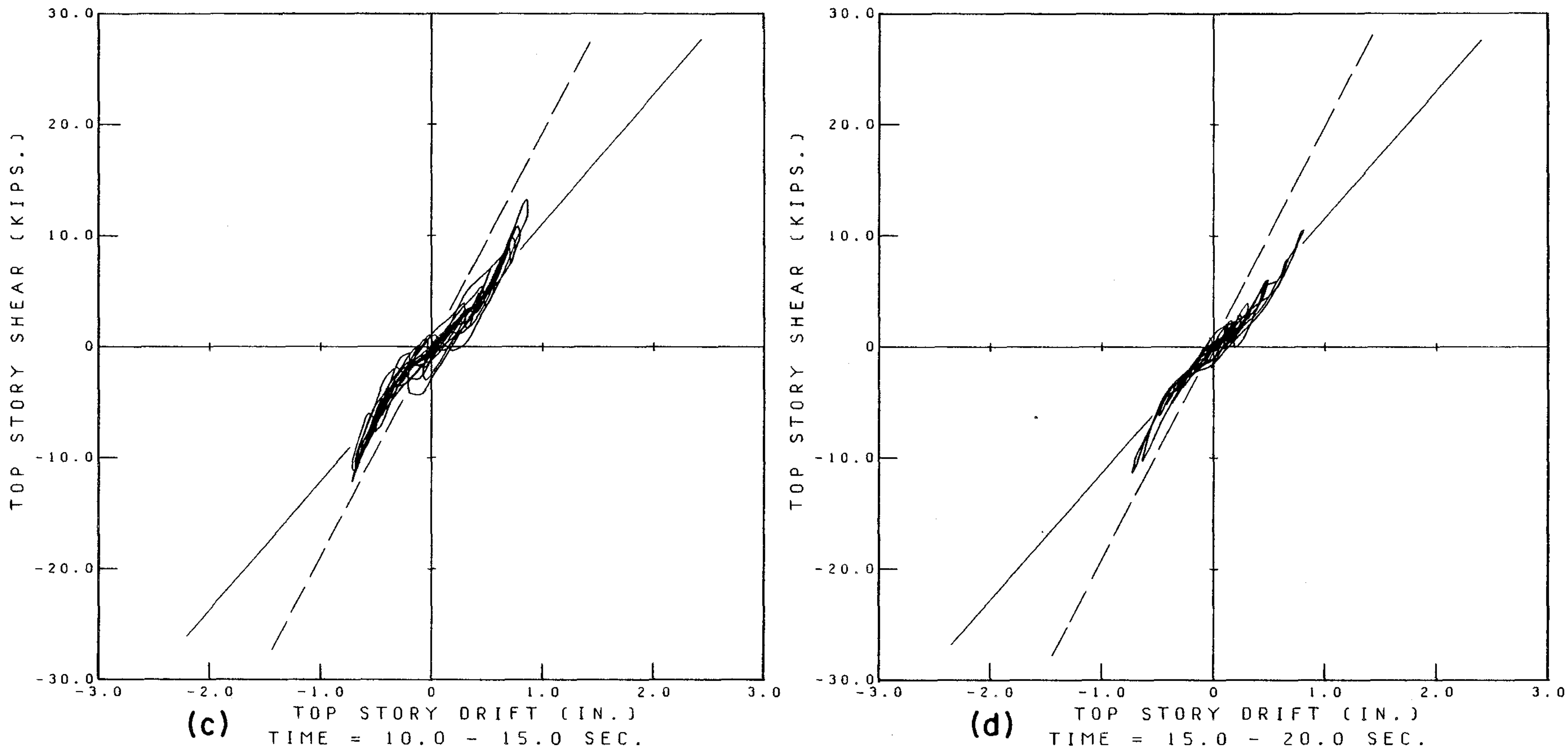

RCF2 RUN W3 TAFT 850(2)

FIG. 5.31(CONT.) TOP STORY SHEAR VS. DRIFT RELATIONSHIP DURING 5-SEC INTERVALS. RUN W3

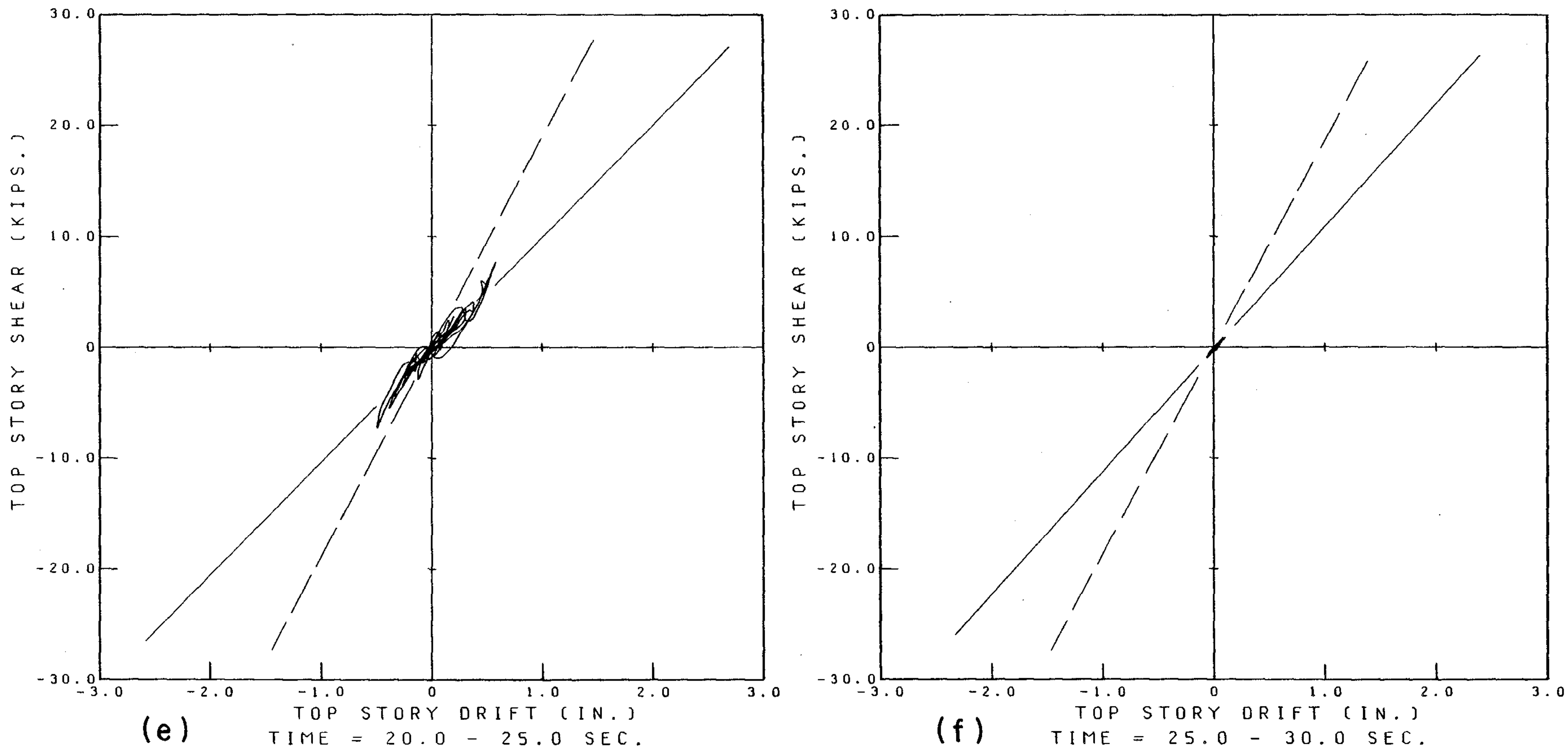

RCF2 RUN W3 TAFT 850(2)

FIG. 5.31(CONT.) TOP STORY SHEAR VS. DRIFT RELATIONSHIP DURING 5-SEC INTERVALS. RUN W3

Reproduced from best available copy.

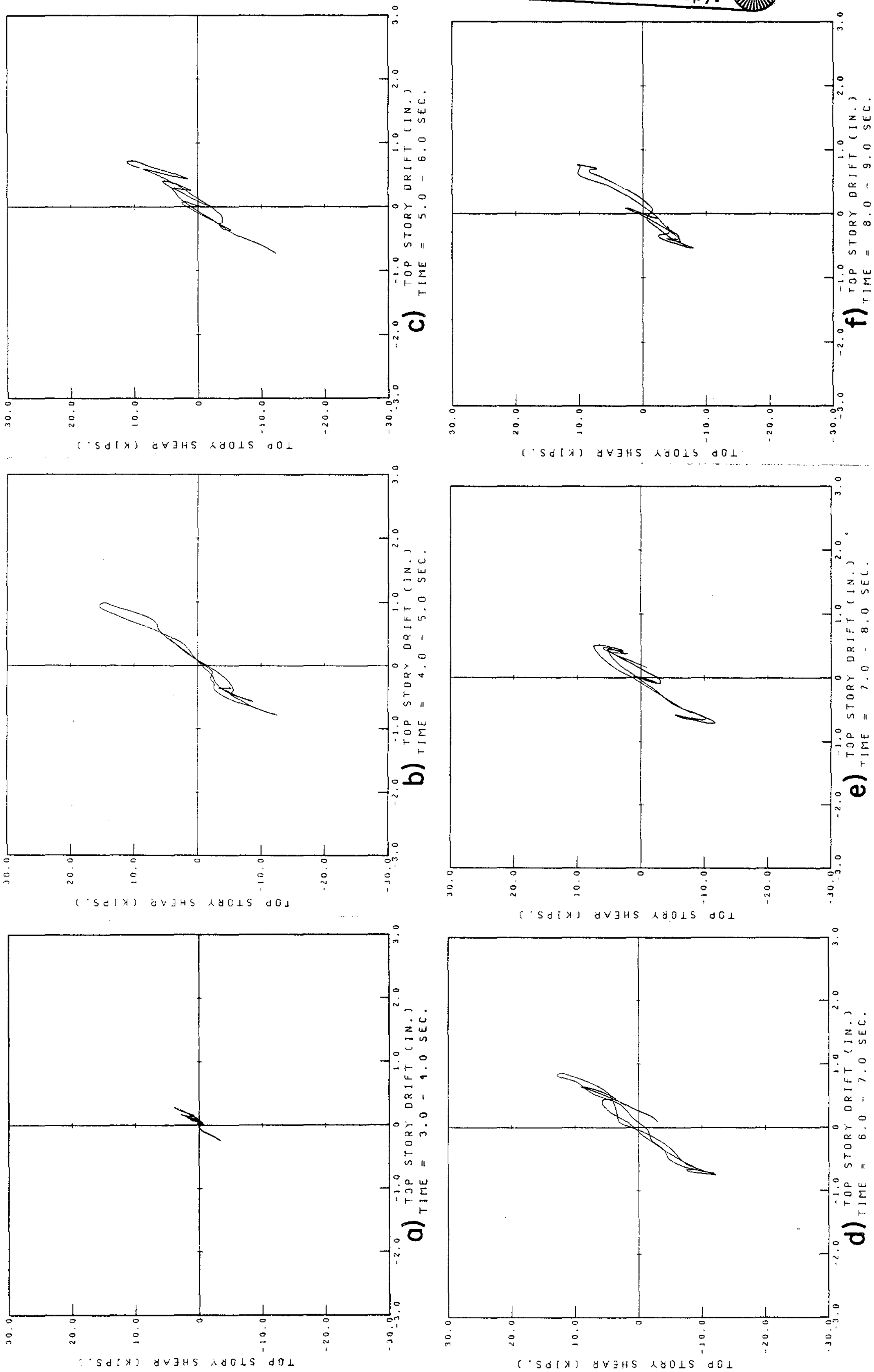

FIG. 5.32 TOP STORY SHEAR VS. DRIFT RELATIONSHIP DURING STRONGEST SHAKING ON RUN W3

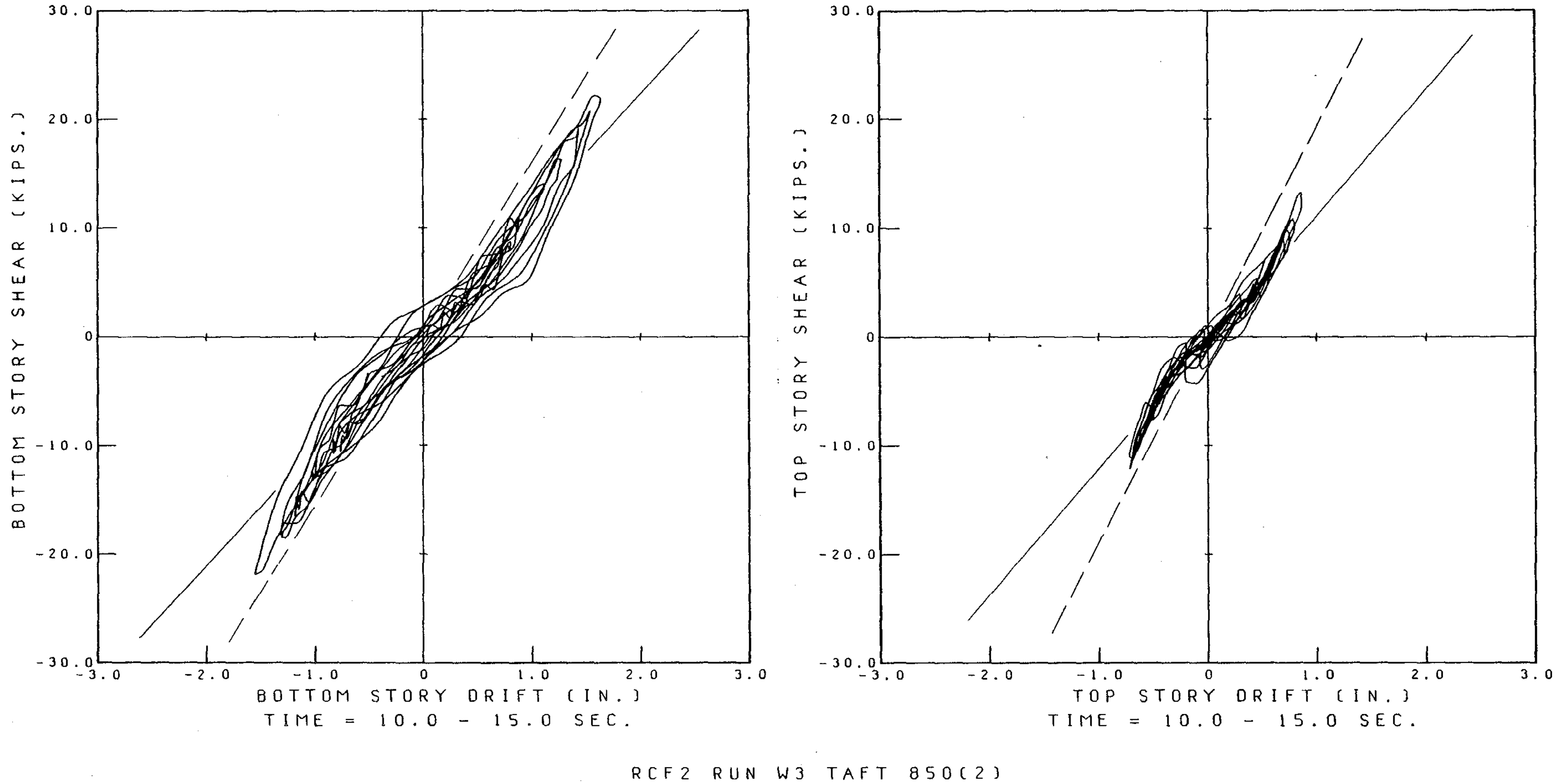

FIG. 5.33 COMPARISON BETWEEN BOTTOM AND TOP STORY BEHAVIOR DURING PART OF RUN W3

Reproduced from best available copy.

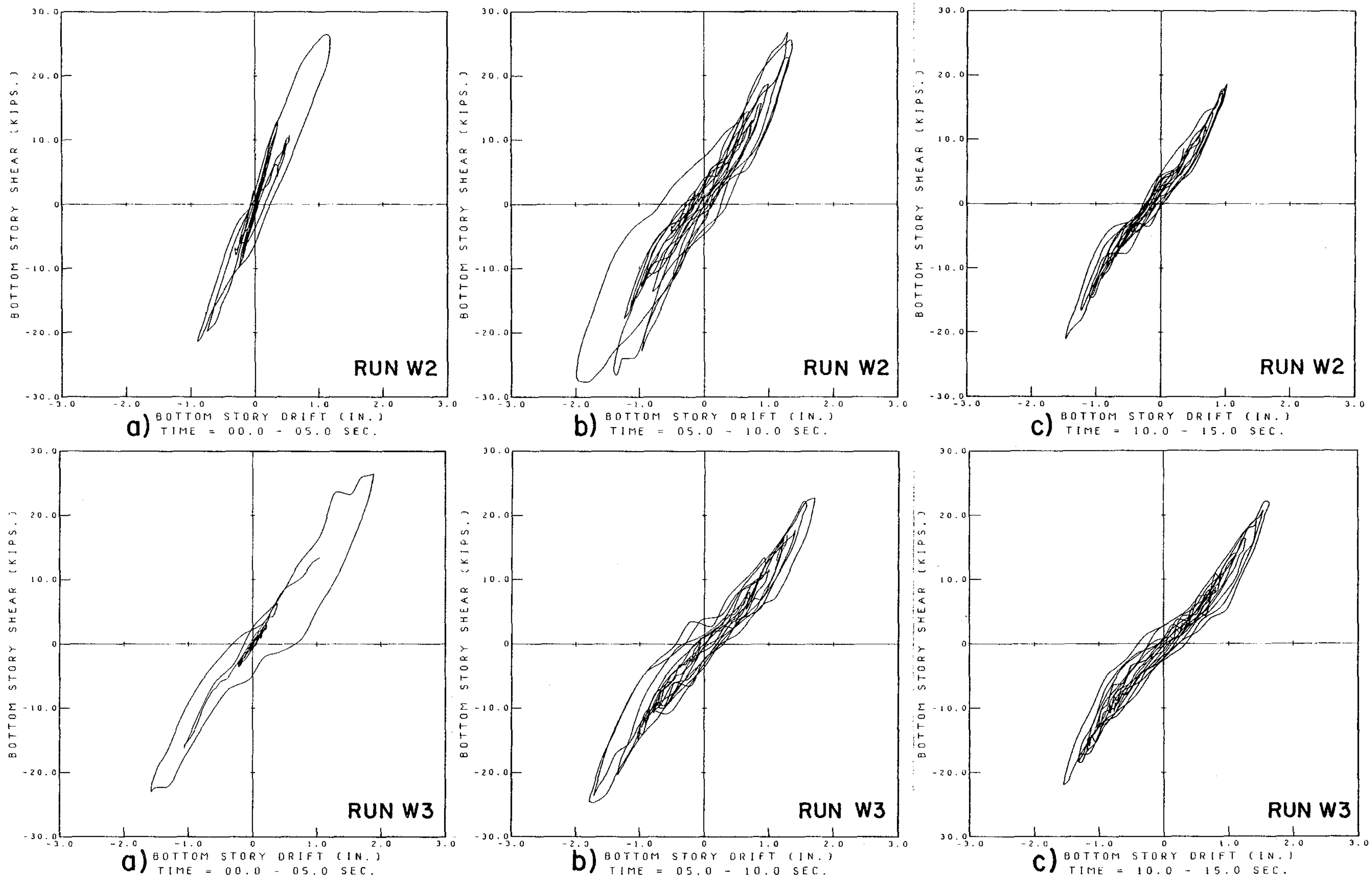

FIG. 5.34 RCF2 BOTTOM STORY PERFORMANCE DURING RUNS W2 AND W3

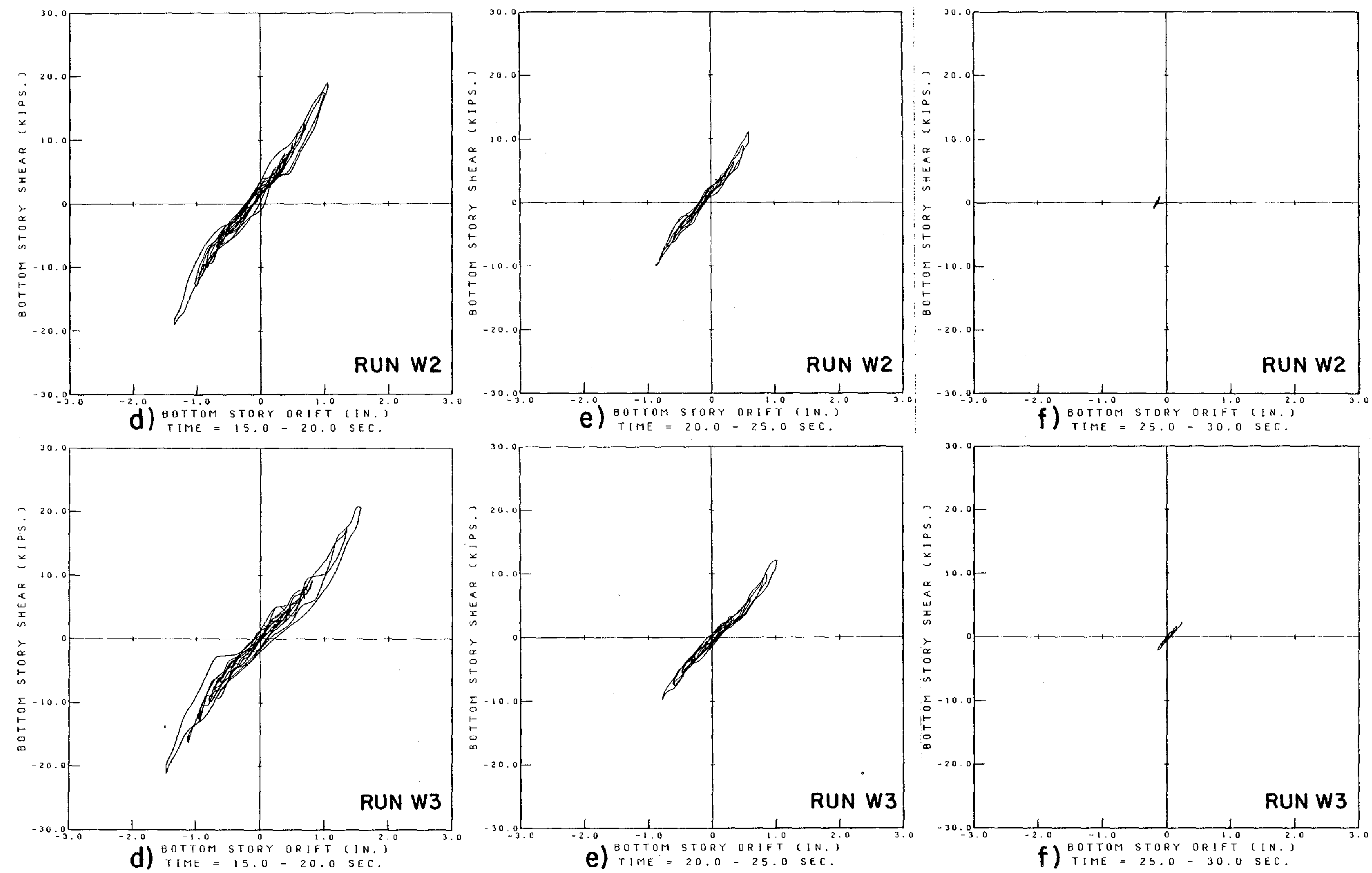

FIG. 5.34(CONT.) RCF2 BOTTOM STORY PERFORMANCE DURING RUNS W2 AND W3

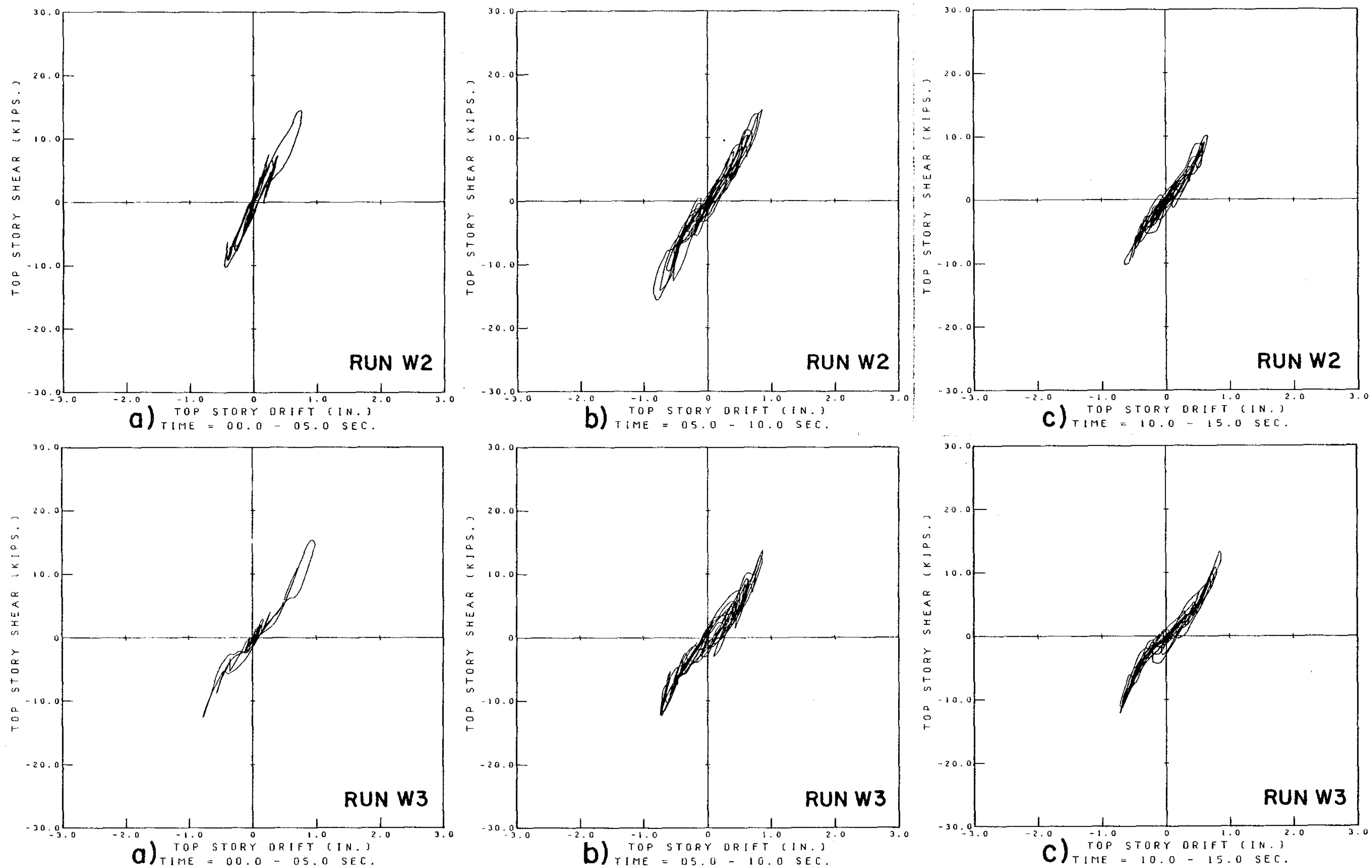

FIG. 5.35 RCF2 TOP STORY PERFORMANCE DURING RUNS W2 AND W3

Reproduced from best available copy.

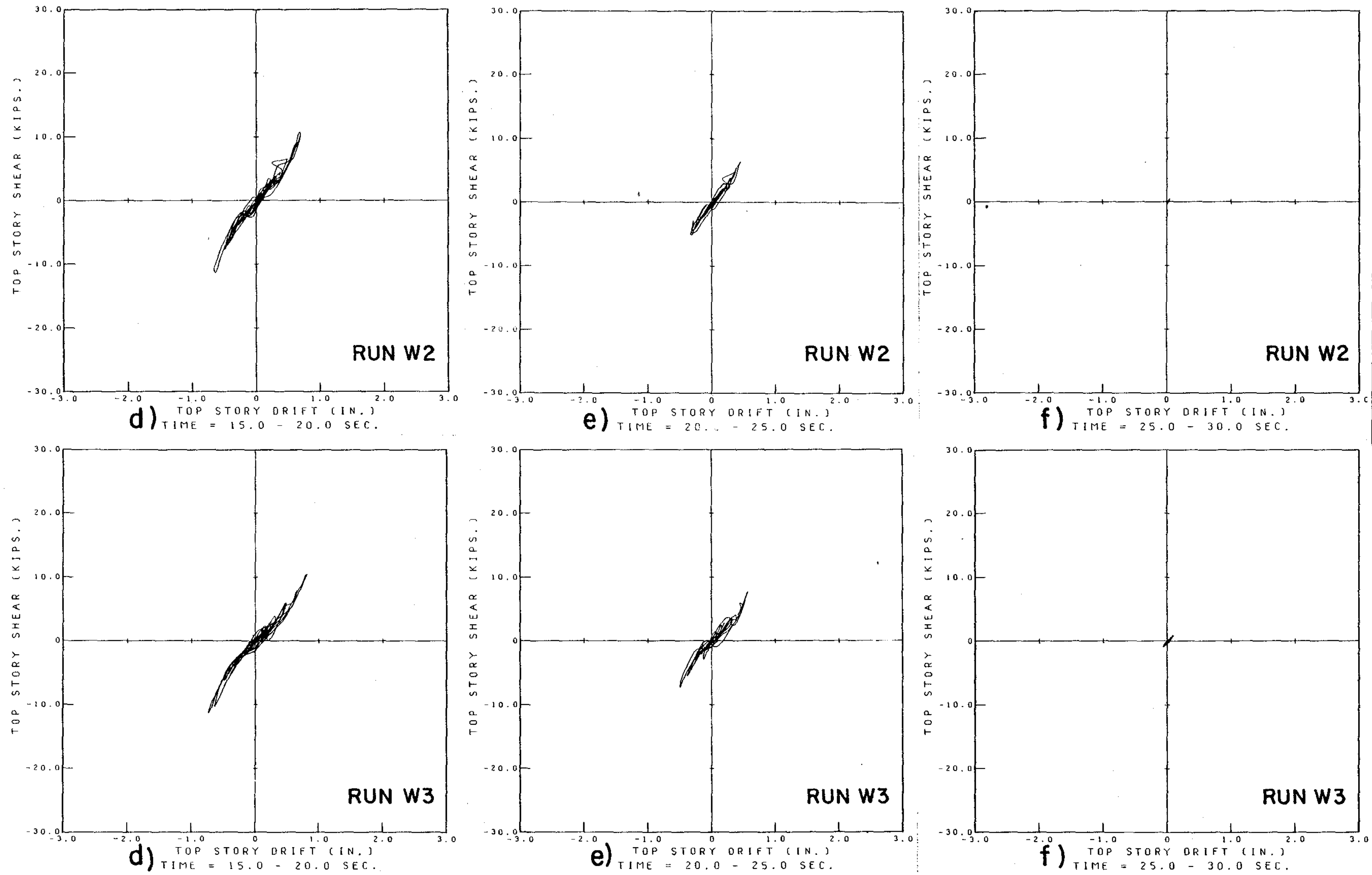

FIG. 5.35 (CONT.) RCF2 TOP STORY PERFORMANCE DURING RUNS W2 AND W3

6. SUMMARY OF CONCLUSIONS

6.1 Initial Remarks

In accordance with the objectives of this investigation, the different phases of a particular research program on the seismic response of reinforced concrete buildings were critically evaluated. As a result, a number of significant conclusions were obtained, and presented at the end of each chapter.

In order to provide an overall view of what has been learned through the different studies, these conclusions are restated and summarized in the next sections. However, it is important to emphasize that caution must be exercised in the interpretation of the results presented, since in many cases they are a consequence of the particular characteristics of the structural system under study, and therefore, they are applicable only to systems with similar characteristics. For example, test findings about the response behavior of RCF2 cannot be freely extrapolated to predict behavior of structures in which nonstructural elements could play an important role in the response, even if all the other conditions are similar.

Finally, the results presented are used to point out areas in which more research needs to be done, to increase the "state of the art" knowledge on seismic response of structural systems.

6.2 Restatement of Conclusions

The most important findings of this investigation, which were listed in preceding chapters of this report, have been selected and restated in the following paragraphs.

6.2.1 Design of Test Specimen

In this study the objective was to simulate a "real life" building, designed in accordance with the current seismic resistant Code specifications.

Due to physical limitations in the testing equipment, to economic considerations, and for testing convenience and safety, important modifications had to be made on the prototype building to obtain the actual test specimen.

In spite of these modifications, it was possible to maintain in the test structure the most significant structural characteristics of the prototype. In particular the global stiffness, strength, and vibratory properties were satisfactorily preserved, thus guaranteeing that the response of the test structure adequately reflected that of the prototype.

6.2.2 Selection of Seismic Excitation

There exist many possibilities of simulating seismic excitation using the shaking table system. In this study, it has been shown that by adequate, modification (by scaling in time and/or amplitude) of existing seismic records, it is feasible to generate table input signals which are representative of ground motions corresponding to seismic events of specified intensity on a diversity of local soil conditions.

However, it is necessary to be aware of the limitations imposed by the earthquake simulator system, such as, for example, the fact that only one horizontal direction of motion can be simulated together with the vertical, and that the table-specimen interface obviously affects the way in which the seismic energy is input into the structure.

6.2.3 Structural Response

The data obtained during the shaking table tests provide extremely valuable information about the response of the structural specimen under study, but it must be acknowledged that its quality and usefulness is directly related to the data acquisition characteristics and the instrumentation set-up on the specimen. This is a point which has not been thoroughly discussed in this study, but it is nevertheless worth mentioning.

In addition, as already expressed, it is very important to take into account that the results obtained from such data are representative of the structural system under study, when subjected to the conditions simulated on the shaking table. In other words, the extrapolation of results to other structural configurations and/or other excitations is a very delicate operation, and should be done with special care.

6.2.4 Experimental Results versus "State of the Practice"

In the case under study, the test specimen, whose design complied with strict Code requirements for seismic safety, showed excellent behavior during a succession of very strong simulated seismic motions. However, some of these Code requirements proved to be inconsistent with the seismic experience. In particular, the ultimate design lateral forces specified by the Code were shown to be disproportionally low, as compared with the inertia forces developed on the specimens during the tests. The "good" performance of RCF2 was due to the reinforcement detailing requirements of the Code which exclude the possibility of non-ductile behavior.

Similarly, the calculated results obtained using standard, Code-related analysis techniques, proved to be conservative and simplistic, with respect to the corresponding test results. This is particularly evident in the estimation of structural strength, stiffness and deformation capacity (ductility) which are the most critical factors in the seismic response of structures.

6.3 Final Remarks

The results obtained during the earthquake simulator testing proved to be extremely valuable for the realistic study of the seismic behavior of structural systems under seismic excitation. The importance of this kind of experiments resides in the fact that they constitute a test not only of the specimen under study but also of all the techniques and philosophies involved in its development and of the available theories to explain its behavior.

In the case of RCF2, the test results pointed out important drawbacks of widely used techniques to predict structural performance under lateral loads, and deficiencies in the current Code specification of the seismic demands on the structure.

The complexity of the response of reinforced concrete buildings when subjected to earthquake loads was also evident from the experimental results. Clearly, there is no simple answer to the problem of prediction of seismic response of reinforced concrete structures, and a considerable effort should be made in the study of important aspects of this problem, like the action-deformation characteristics at the section, member, and structural levels, in terms of realistic descriptions of the material properties and of the seismic excitation.

LIST OF REFERENCES

1. Hidalgo, P. and Clough, R., "Earthquake Simulator Study of a Reinforced Concrete Frame," Earthquake Engineering Research Center Report No. 74-13, December 1974.

2. Clough, R. and Gidwani, J., "Reinforced Concrete Frame 2: Seismic Testing and Analytical Correlation," Earthquake Engineering Research Center Report No. 76-15, June 1976.

3. Clough, R. and Hidalgo, P., "Earthquake Test Behavior of a Two-Story Reinforced Concrete Frame," Proceedings, 5th European Conference on Earthquake Engineering, Istanbul, Turkey, September 22-25, 1975.

4. Clough, R., "Predicting the Earthquake Response of Reinforced Concrete Structures," American Concrete Institute, Symposium, Vol. SP53-3, 1977, pp. 367-380.

5. Gidwani, J., "Local Hysteretic Behavior of Reinforced Concrete Column Sections Subject to Earthquake Loading," M. Eng. Thesis, Department of Civil Engineering, University of California, Berkeley, Spring 1978.

6. Clough, R. and Oliva, M., "Inelastic Frame Behavior During Shaking Table Tests," presented to the Symposium on Nonlinear Behavior of Reinforced and Prestressed Concrete Structures, Houston, Texas, November 1978.

7. Rea, D. and Penzien, J., "Structural Research using an Earthquake Simulator," Proc. of the Structural Engineer's Association of California Conference, Monterey, California, October 1972.

8. American Concrete Institute, "Building Code Requirements for Reinforced Concrete, (ACI 318-63)," Detroit, Michigan, June 1963.

9. International Conference of Building Officials, "Uniform Building Code, 1970 Edition, Volume I," Pasadena, California, 1970.

10. American Concrete Institute, "Building Code Requirements for Reinforced Concrete (ACI 318-71)," Detroit, Michigan, 1970.

11. International Conference of Building Officials "Uniform Building Code, 1979 Edition," California, 1979.

12. Structural Engineers Association of California, Seismology Committee, "Recommended Lateral Force Requirements and Commentary," San Francisco, California, 1975.

13. Wilson, E., Hollings, J. and Dovey, H., "Three Dimensional Analysis of Building Systems (Extended Version)," Earthquake Engineering Research Center Report No. 75-13, April 1975.

14. Sudhakar, A., Powell, G., Orr, G. and Wheaton, R., "ULARC ... Small Displacements Elasto-Plastic Analysis of Plane Frames," Computer Program available from National Information Service for Earthquake Engineering, University of California, Berkeley.

15. Mahin, S. and Bertero, V., "RCCOLA ... A Computer Program for Reinforced Concrete Column Analysis," User's Manual and Documentation, Department of Civil Engineering, University of California, Berkeley, August 1977.

16. Bolt, B. et al., "Geological Hazards," Springer Verlag, New York, 1975.

17 Nigam, N. and Jennings, P., "SPECEQ/SPECUQ: Digital Calculation of Response Spectra from Strong-Motion Earthquake Records," A Computer Program Distributed by NISEE/Computer Applications, California Institute of Technology, Pasadena, California, June 1968.

18. Seed, H. et al., "Site-Dependent Spectra for Earthquake-Resistant Design," Earthquake Engineering Research Center Report No. 74-12, 1974.

19. Idriss, I., "Characteristics of Earthquake Ground Motions," Proc. of the ASCE Geotechnical Engineering Division Specialty Conference Earthquake Engineering and Soil Dynamics, Pasadena, California, June 1978.

20. Winter, G. and Nilson, A., "Design of Concrete Structures," 8th Edition, McGraw-Hill, New York, 1972.

21. Crandall, S. "Random Vibrations," Technology Press of the Massachusetts Institute of Technology, Cambridge, Massachusetts, 1963.

22. Clough, R. and Penzien, J., "Dynamics of Structures," McGraw-Hill, New York, 1975.

23. Mahin, S. and Bertero, V., Problems in Establishing and Predicting Ductility in Aseismic Design," paper submitted for publication and presentation at the International Symposium on Earthquake Structural Engineering, St. Louis, August 1976.

24. Popov, E., "Introduction to Mechanics of Solids," Prentice Hall, New Jersey, 1968.

APPENDIX A

DESIGN OF ORIGINAL TEST STRUCTURE
(PROTOTYPE)

Preceding page blank

A.1 Analysis

A.1.1 Loads

Assume the weight of reinforced concrete to be 0.150 kip/cu.ft.

a) Dead Load

Dead Load	Bottom Story	Top Story
Slab 4 in. thickness	0.050 kip/sq.ft.	0.050 kip/sq.ft.
Ceiling (10 lb./cu.ft. x 1.2 in.)	0.001 kip/sq.ft.	0.001 kip/sq.ft.
Floor (10 lb./cu.ft. x 1.2 in.)	0.001 kip/sq.ft.	———
Roofing	———	0.010 kip/sq.ft.
Exterior walls (on transverse girders*)		
Hollow brick wall	0.200/kip/ft.	———
Glass	0.007/kip/ft.	———
Permanent partitions (on longitudinal girders*)	0.140 kip/ft.	———

Weight of columns and girders for both stories:

Assume for both stories 9.50 kips

b) Live Load

	Bottom Story	Top Story
	0.050 kip/sq.ft.	0.020 kip/sq.ft.

The live load at the top story will not be considered in the vertical load to be acting at the same time as the earthquake loads.

c) Earthquake Loads

Consider the total dead load

Top story 0.061 kip/sq.ft. x 17 ft. = 24.9 kip

* The term transverse girders will be used to denote the girders along the axes perpendicular to the ground motion direction. Longitudinal girders will be the ones along the axes parallel to the ground motion direction.

Bottom story 0.052 kip/sq.ft. x 17 ft. x 24 ft. = 21.2 kip

0.207 kip/ft. x 24 ft. x 2 = 9.9 kip

0.140 kip/ft. x 17 ft. x 2 = 4.8 kip

Columns and girders = 9.5 kip

$W = 70.3$ kip

Base Shear $V = ZKCW$

$Z = 1$ Zone No. 3

$K = 0.67$ Ductile moment frame resisting the total required lateral force

$C = 0.10$ Two-story building

$V = (0.67)\ (0.10)\ (70.3) = 4.7$ kips

$V = 2.35$ kips per frame

Uniform distribution = 1.175 kips Top story

1.175 kips Bottom story

d) <u>Distribution of loads on the girders</u>

Use ACI 318-63 Appendix A. Method 3

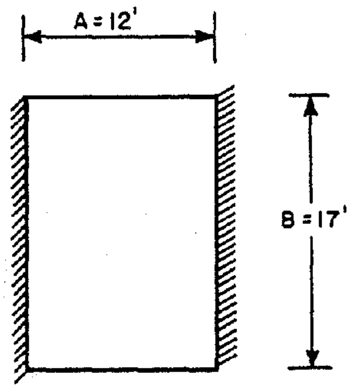

$\frac{A}{B} = 0.70 \qquad w_A = 0.95\ w$

$w_B = 0.05\ w$

Uniform distributed load on each longitudinal girder

$$w_L = 0.95\ w \times 12\ \text{ft} = 11.4\ w$$

On each transverse girder

$$w_T = 0.05\ w \times 8.5\ \text{ft} = 0.425\ w$$

but this load shall not be less than that of an area bounded by the intersection of 45° lines from the corners. The equivalent uniform load per linear foot is

$$w_T = \frac{w \times 12 \text{ ft.}}{3} = 4\ w$$

However this value will not be used since the building will be analyzed in the direction of the ground motion only.

i) Uniformly distributed loads on the longitudinal girders.

Assume a 8 in. x 16 in. section (slab thickness included)

$$w \text{ (own weight)} = 0.150 \times \frac{8 \times 12}{144} = 0.100 \text{ kip/ft.}$$

<u>Bottom Story</u>

Dead load $w_D = 11.4 \times 0.052 + 0.14 + 0.10 = 0.832$ kip/ft.

Live load $w_L = 11.4 \times 0.050 = 0.570$ kip/ft.

<u>Top Story</u>

Dead load $w_D = 11.4 \times 0.061 + 0.10 = 0.794$ kip/ft.

Live load $w_L = 11.4 \times 0.020 = 0.228$ kip/ft.

When live load is present at the same time as earthquake loads

$$W_{LE} = 0 \text{ kip/ft.}$$

ii) Uniformly distributed loads on the transverse girders (only to compute the additional axial load acting on the columns)

Assume a 8 in. x 16 in. section (slab thickness included)

w (own weight) = 0.100 kip/ft.

<u>Bottom Story</u>

Dead load $w_D = 0.425 \times 0.052 + 0.207 + 0.10 = 0.329$ kip/ft.

Live load $w_L = 0.425 \times 0.050 = 0.021$ kip/ft.

<u>Top Story</u>

Dead load $w_D = 0.425 \times 0.061 + 0.10 = 0.126$ kip/ft.

Live load $w_L = 0.425 \times 0.020 = 0.0085$ kip/ft.

When live load is present at the same time as earthquake loads

$$w_{LE} = 0 \text{ kip/ft.}$$

e) Load cases to be considered

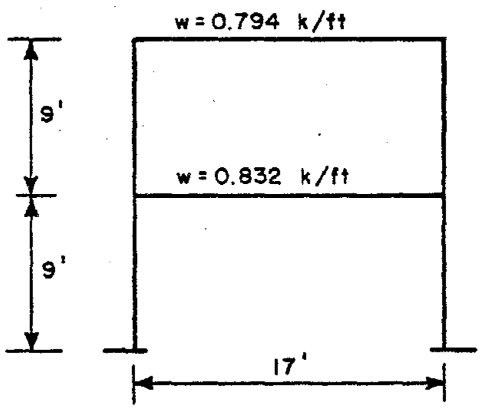

Dead Load (D)

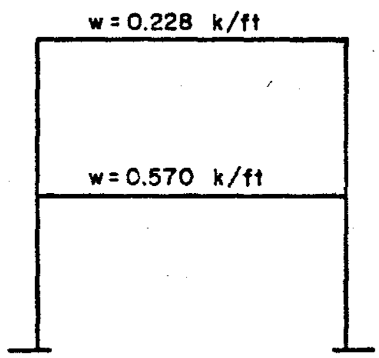

Live Load (L)

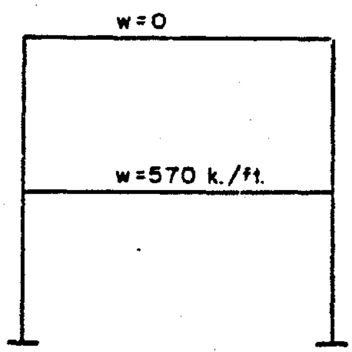

Live Load combined
with Earthquake Load
(LE)

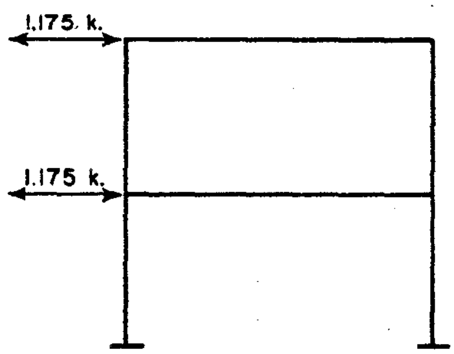

Earthquake Load
(E)

A.1.2 Moment Diagrams

To compute the relative stiffnesses assume 8 in. x 12 in. sections for the columns.

$$I_{COL} = \frac{1}{12}\,(8)\;(12)^3 = 1152\text{ in.}^4$$

$$K_o = \frac{I}{L} = 10.7\text{ in.}^3$$

For the girder let us consider a T-beam action. The maximum flange width allowed by the ACI Code (ACI 318-71 Section 8.72) is one fourth of the span length, that is 51 in.

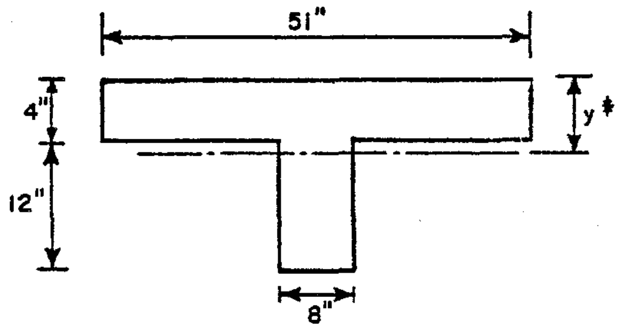

$$y^* = \frac{(43)(4)(2) + (8)(16)(8)}{(43)(4) + (8)(16)} = 4.56\text{ in.}$$

$$I_{GIR} = \frac{1}{12}\,(43)(4)^3 + (43)(4)(2.56)^2 + \frac{1}{12}\,(8)(16)^3 + (8)(16)(3.44)^2 = 5602\text{ in.}^4$$

$$K_G = \frac{I}{L} = 27.5\text{ in.}^3$$

Therefore

$$K_G = 2.57\,K_o \qquad \frac{1}{2}\,K_G = 1.29\,K_o \qquad \frac{3}{2}\,K_G = 3.87\,K_o$$

The moment diagram values were computed using moment distribution. Values are expressed in ft-kip and the moments indicated in the diagram on the following page are assumed to be positive.

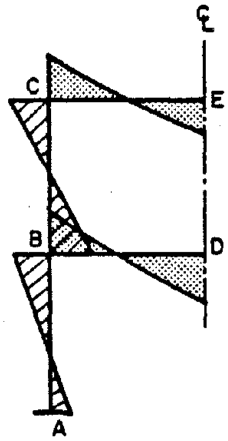

SECTION	DEAD LOAD D	LIVE LOAD L	LIVE LOAD EQ. LE	EARTQ. LOAD E
EC	18.94	4.72	-1.22	0
CE	9.76	3.52	1.22	±2.96
CB	9.76	3.52	1.22	±2.96
BC	8.62	4.73	3.86	±2.29
BD	13.62	8.69	8.19	±7.15
DB	16.48	11.91	12.41	0
BA	5.00	3.96	4.33	±4.86
AB	2.50	1.99	2.17	±5.70

A.1.3 Combination of Loads for Required Strength

The ACI Code (Sec. 9.3) requires the design to be made for the following ultimate strength conditions

$$U_{A1} = 1.4\ D + 1.7\ L$$

$$U_{A2} = 0.75\ (1.4D + 1.7\ LE + 1.87\ E)$$

$$U_{A3} = 0.9\ D + 1.43\ E$$

The UBC Code (Sec. 2630) requires

$$U_{B1} = 1.40\ (D + LE + E)$$

$$U_{B2} = 0.9\ D + 1.25\ E$$

When these values were computed U_{A1} and U_{B1} proved to govern the design for strength, and are shown below for the different sections.

a) Flexural Moments. (Values in Ft-kip; sign as indicated in A.1.2)

	COLUMNS				GIRDERS			
	Bottom Story		Top Story		Bottom Story		Top Story	
	AB	BA	BC	CB	BD	DB	CE	EC
U_{A1}	6.88	13.73	20.09	19.64	33.84	43.40	19.64	34.54
U_{B1}	14.50	19.90	20.60	19.55	40.60	40.50	19.55	24.80

b) Shear Force. (Values in kips; sign corresponds to positive flexural moments)

	COLUMNS		GIRDERS	
	Bottom Story	Top Story	Bottom Story	Top Story
U_{A1}	2.29	4.52	18.14	12.75
U_{B1}	3.82	4.35	17.85	9.93

c) Axial Force. (Values in kips; positive values denote tension, negative denote compression)

In these computations the shear transmitted by both the longitudinal and transverse girder has been considered.

	COLUMNS		GIRDERS	
	Bottom Story	Top Story	Bottom Story	Top Story
U_{A1}	-39.14	-15.04	+2.23	-4.52
U_{B1}	-35.78	-12.05	+0.53	-4.35

A.2 Design for Strength Conditions

A.2.1 Basic Assumptions

Materials Intermediate Grade Steel $f_y = 40$ ksi

$E_s = 29000$ ksi

Concrete $f'_c = 4$ ksi

$E_c = 57000 \sqrt{4000} = 3610$ ksi

Sections Columns 8 in. x 12 in.

Girders 8 in. x 16 in. (14 in. slab included)

A.2.2 Bottom Story Column

Slenderness effect (ACI Section 10.11). Consider most unfavorable direction (transverse direction)

$\ell_u = 9$ t., $\quad k = 1.4, \quad r = 0.30$ (8 in.) = 2.4 in.

$$\frac{k\ell_u}{r} = 1.4 \frac{(9)(12)}{2.4} = 63 > 22$$

$c_m = 1.0$ M (dead load alone) = 7.0 ft-kip

$$\beta_d = \frac{7.0}{19.90} = 0.351$$

$$I_g = \frac{1}{12} (12)\ 8^3 = 512 \text{ in.}^4$$

$$EI = \frac{E_c\ I_g}{2.5} \cdot \frac{1}{(1 + \beta_d)} = \frac{3610 \times 512}{2.5 \times 1.351} = 549 \times 10^3 \text{ in.}^2\text{-kip}$$

$$P_c = \frac{\pi^2\ EI}{(k\ \ell_u)^2} = \frac{\pi^2 \times 549 \times 10^3}{(1.4 \times 9 \times 12)^2} = 238 \text{ kip}$$

$$\phi \text{ factor: } \frac{h - d' - d_s}{h} = \frac{12 - 4.8}{12} = 0.60 < 0.70$$

Then $\phi = 0.70$

$$\delta = C_m / (1 - \frac{P_u}{\phi\ P_c}) = 1./(1- \frac{39.14}{0.70 \times 238}) = 1.31$$

Balance Condition

$$P_B = \phi(0.85\ f'_c\ b\ k_1\ C_b)$$

$$P_B = 0.70\ (0.85)^2\ 4 \times 8\ \frac{87000\ (9.6)}{127000}$$

$$P_B = 106 \text{ kips} > 39 \text{ kips}$$

Therefore the ultimate capacity is controlled by tensile yielding of the steel.

<u>Design for U_{B1}</u>

$M = 19.90$ ft-kip $\quad M_c = 1.31 \times 19.90 = 26.1$ ft-kip

$P = 35.78$ kip

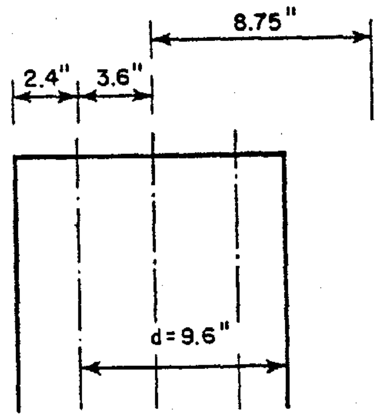

$$P_u = \phi\left[0.85\ f'_c bd\left\{-p + 1 - \frac{e'}{d} + \sqrt{\left(1 - \frac{e'}{d}\right)^2 + ep\left[m'\left(1 - \frac{d'}{d}\right) + \frac{e'}{e}\right]}\right\}\right]$$

$e = \frac{26.10}{35.78}\ 12 = 8.75$ in. $\quad e' = 3.60 + 8.75 = 12.35$ in.

$d = 9.6$ in. $\quad d' = 2.4$ in. $\quad b = 8$ in.

$$m' = m - 1 = \frac{f_y}{0.85\ f'_c} - 1 = 10.76$$

<u>Limits of reinforcement</u> (ACI Section A.6.1)

Minimum $\quad A_s = 0.01\ bd = 0.768\ \text{in.}^2$

Maximum $\quad A_s = 0.06\ bd = 4.61\ \text{in.}^2$

<u>Consider 4#7</u> $\quad A_s = A'_s = 1.20\ \text{in.}^2,\ p = \frac{A_s}{bd} = 0.0156$

$p_u = 56.6$ kips $\quad > 35.78$ kips

In fact, 2#6 are enough, but the top story column will need 2#7 and it is preferable to design the bottom story column with at least the same strength as the top story.

Check for U_{A1} Condition

$M = 13.73$ ft-kip $\qquad M_c = 1.31 \times 13.73 = 18$ ft-kip

$P = 39.14$ kip

$e = \frac{18}{39.14}\,12 = 5.52$ in. $\qquad e' = 3.60 + 5.52 = 9.12$ in.

$P_u = 85.27$ kips $\quad > 39.14$ kips

Check Condition U_{A3}: large moment and small axial load

$$U_{A3} = 0.9\ D + 1.43\ E$$

$M = 11.47$ ft-kip $\qquad M_c = 1.31 \times 11.47 = 15.05$ ft-kip

$P = 19.05$ kip

$e = \frac{15.05}{19.05} \times 12 = 9.50$ in. $\qquad e' = 13.1$ in.

$P_u = 49.85$ kips $\quad > 19.05$ kips

It has to be mentioned that since

$$P_e \leqslant 0.4\ P_B = 42.4 \text{ kip}$$

this column could have also been designed as a flexural member (ACI)

Design for Shear (ACI Chapter 11)

$\phi = 0.85 \qquad V = 3.82$ kip $\qquad M = 19.90$ ft-kip $\qquad P = 35.78$ kip

Minimum web reinforcement for columns (UBC 2630, ACI A.6)

Minimum bar size: #3

Maximum spacing: 4 in. $\quad$ #3 @ 4 in.

Nominal shear stress

$$v_u = \frac{V_u}{\phi\ b_w d} = \frac{3820}{0.85 \cdot 8 \cdot 9.6} = 58.5 \text{ psi}$$

Shear carried by concrete

$$\rho_w = \frac{A_s}{b_w d} = 0.0156$$

$$M_m = M_u - N_u \frac{4h-d}{8} = 19.90 \times 12 - 35.78 \frac{48-9.6}{8} = 67 \text{ in.-kip}$$

$$v_c = 1.9\sqrt{4000} + 2500 \times 0.0156 \times \frac{3.82 \times 9.6}{67} = 141.5 \text{ psi } \underline{\text{governs}}$$

$$\text{or } v_c = 3.5\sqrt{4000} = 221 \text{ psi}$$

$$\text{or } v_c = 2(1 + 0.0005 \times \frac{35780}{8 \times 12}) \sqrt{4000} = 150 \text{ psi}$$

$$\text{or } v_c = 3.5\sqrt{4000}\sqrt{1 + 0.002 \times \frac{35780}{8 \times 12}} = 292 \text{ psi}$$

Therefore

$$v_u < 0.50\, v_c$$

and according to ACI Code we would not need to use shear reinforcement. However we will use the minimum quantity prescribed by UBC Section 2630.

Within 18 in. from the face of each joint, the spacing of the stirrups will be reduced to 2 in.

A.2.3 <u>Top Story Column</u>

Slenderness effect

$$\frac{k\ell u}{r} = 63 > 22$$

M (dead load alont) = 12.06 ft-kip

$$\beta_d = \frac{12.06}{20.60} = 0.587$$

$$EI = 549 \times 10^3 \frac{1.35}{1.59} = 465 \times 10^3 \text{ in.}^2\text{-kip}$$

$$P_c = 238 \frac{1.35}{1.59} = 202 \text{ kips}$$

$\phi = 0.70 \qquad P_u = 15.04$ kips

$$\delta = 1./(1 - \frac{15.04}{0.70 \times 202}) = 1.12$$

Balanced Condition $\qquad P_B = 106$ kip > 15 kips

Then the ultimate capacity is controlled by tension.

Limits of reinforcement

Use 4#7 $\quad A_s = A'_s = 1.20$ in.^{2} $\quad p = 0.0156$

Design for U_{A1}

$M = 20.09$ ft-kip $\qquad M_c = 1.12 \times 20.09 = 22.5$ ft-kip

$P = 15.04$ kip

$e = \frac{22.5}{15.04} \times 12 = 18$ in. $\qquad e' = 21.6$ in.

$P_u = 19.9$ kips > 15.04 kips

Check for U_{B1}

$M = 20.60$ ft-kip $\qquad M_c = 1.12 \times 20.60 = 23$ ft-kip

$P = 12.05$ ft-kip

$e = \frac{23}{12.05} \times 12 = 23$ in. $\qquad e' = 26.6$ in.

$P_u = 13.5$ kips > 12.05 kips

Check Condition U_{A2}

$$U_{A2} = 1.05\ D + 1.28\ LE + 1.4E$$

$M = 17.21$ ft-kip $\qquad M_c = 1.12 \times 17.21 = 19.3$ ft-kip

$P = 9.18$ kip

$e = \frac{19.3}{9.18}(12) = 25.2$ in. $\qquad M_c = 1.12 \times 17.21 = 19.3$ ft-kip

$P_u = 12.6$ kip > 9.18 kip

Design for Shear

$\phi = 0.85 \qquad V = 4.52$ kip $\qquad M = 20.09$ ft-kip $\qquad P = 15.04$ kip

Minimum web reinforcement #3 @ 4 in.

Nominal shear stress

$$v_u = \frac{4520}{0.85 \times 8 \times 9.6} = 69.2 \text{ psi}$$

Shear carried by concrete

$M_m = 20.09 \times 12 - 15.04 \times 4.8 = 169$ in.-kip

$v_c = 1.9\sqrt{4000} + 2500 \times 0.0156 \frac{4.52 \times 9.6}{169} = 130$ psi governs.

Therefore $v_u < v_c$ and we can use the minimum shear reinforcement

$$A_v = 50 \frac{b_w s}{f_y} = 50 \frac{8 \times 4}{40000} = 0.040 \text{ in.}^2$$

The #3 bar specified is enough

Within 18 in. from the face of each joint, the spacing of the stirrups will be reduced to 2 in.

A.2.4 Bottom Story Girder

Midspan

U_{A1}: $M = 43.40$ ft-kip $\qquad V = 0 \qquad P = 23$ kip (tension)

Column face

U_{A1}: $M = 33.84$ ft-kip $\qquad V = 18.14$ kip $\qquad P = 2.23$ kip (tension)

U_{B1}: $M = 40.60$ ft-kip $\qquad V = 17.85$ kip $\qquad P = 0.53$ kip (tension)

<u>ϕ factor</u> (axial tension) $\phi = 0.90$

<u>Influence of axial tension</u>

A_g (T beam) $= 8 \times 16 + 43 = 300$ in.^{2}

stress $= \dfrac{2330}{300} = 7.8$ psi small enough to be neglected

<u>Limits of reinforcement</u> (ACI Section A.5)

Minimum $\quad P = \dfrac{200}{f_y} = 0.005$

$$A_s = 0.005 \times 8 \times 13.6 = 0.543 \text{ in.}^2$$

Maximum

Balanced Condition $\quad p_B = \dfrac{0.85\ k_1\ f'_c}{f_y} \dfrac{87000}{87000 + f_y} = 0.0495$

$$A_s = 0.50 \times 0.0495 \times 8 \times 13.6 = 2.69 \text{ in.}^2$$

<u>Midspan</u>

Depth of neutral axis

$$y^* = 1.18 \frac{A_s\ f_y}{k_1\ b\ f'_c}$$

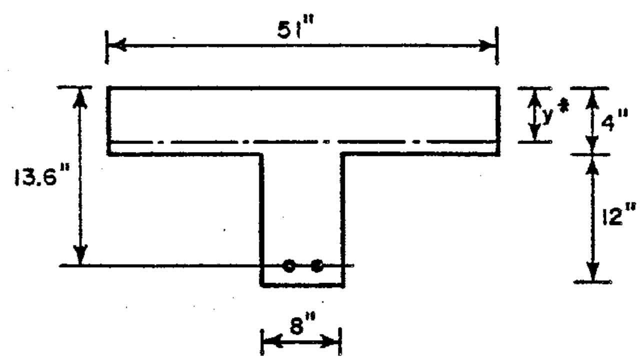

Assume 2#7, $A_s = 1.20$ in.^{2}

$$y^* = 1.18 \frac{1.20 \times 40}{0.85 \times 51 \times 4} = 0.33 \text{ in.} < 4 \text{ in.}$$

Top reinforcement

$$A = \frac{2 \times 2.4 \times 51}{4} = 61.2 \text{ in.}^2 \qquad f_s = 24 \text{ ksi}$$

<u>Design for shear</u>

$\phi = 0.85$

Minimum web reinforcement <u>#3 @ 6 in</u>.

Nominal shear stress

$$v_u = \frac{12750}{0.85 \times 8 \times 13.6} = 138 \text{ psi}$$

Shear carried by concrete

$$v_c = 2\sqrt{4000}\ (1 + 0.0005\ \frac{4520}{8 \times 16}) = 129 \text{ psi governs}$$

Shear reinforcement

$$A_v = \frac{(138 - 129) \times 8 \times 6}{40000} = 0.011 \text{ in.}^2$$

Therefore the minimum reinforcement is enough.

Within 34 in. from the face of the columns, the spacing of the stirrups will be reduced to 3 in.

A.3 <u>Serviceability Requirements</u>

Use ACI Section 9.5

Minimum thickness of girders $= \dfrac{17 \times 12}{16} = 12.75$ in.

$$\phi = 0.90 - \frac{4.52}{51.2} 0.20 = 0.88$$

Influence of axial compression (UBC 2619 b)

$$P_B = \phi \; [0.85 \; f'_c \; b \; k_1 \frac{87000 \; d}{87000 + f_y}]$$

$$k_1 = 0.85 \qquad b = 8 \text{ in.} \qquad d = 13.6 \text{ in.}$$

$$P_B = 189 \text{ kip} \; > \; P_u = 4.52 \text{ kip}$$

Then the axial compression effect may be disregarded.

Limits of reinforcement

Same as for the bottom story girder

Midspan

The depth of the neutral axis is smaller than the slab thickness. Use same procedure as in the bottom story girder.

Consider 2#6 as bottom reinforcement $A_s = 0.88 \text{ in.}^2$

$$M_u = 34.8 \text{ ft-kip} \; > \; 34.53 \text{ ft-kip}$$

Column face

Neglect compression steel; besides A_s is approximately equal to A'_s.

Consider 4#4 as top reinforcement $A'_s = 0.80 \text{ in.}^2$

$$M_u = 30.5 \text{ ft-kip} \; > \; 19.64 \text{ ft-kip}$$

Distribution of flexural reinforcement

Bottom reinforcement. Same as for bottom story girder

$$z = 86 \text{ kip/in.} \; < \; 175 \text{ kip/in.}$$

Minimum bar size: #3

Maximum Spacing: $\frac{d}{2}$, Use 6 in. <u>#3 @ 6 in.</u>

Nominal shear stress

$$v_u = \frac{V_u}{\phi\ b_w\ d} = \frac{18140}{0.85 \times 8 \times 13.6} = 196 \text{ psi}$$

Shear carried by concrete (axial tension is present)

$$v_c = 2\sqrt{4000}\ (1-0.002\ \frac{2230}{8 \times 16}) = 122 \text{ psi}$$

Shear reinforcement

$$A_v = \frac{(v_u - v_c)\ b_w\ s}{f_y} = \frac{74 \times 8 \times 6}{40000} = 0.089 \text{ in.}^2$$

Then the minimum reinforcement is enough.

Within 34 in. from the face of the columns, the spacing of the stirrups will be reduced to 3 in.

A.2.5 <u>Top Story Girder</u>

<u>Midspan</u>

U_{A1}: M = 34.53 ft-kip V = 0 P = 4.52 kip (comp.)

<u>Column face</u>

U_{A1}: M - 19.64 ft-kip V = 12.75 kip P = 4.52 kip (comp.)

U_{B1}: M = 19.55 ft-kip V = 9.93 kip P = 4.35 kip (comp.)

<u>ϕ factor</u> (ACI Section 9.2.1.2)

$$\frac{h - d' - d_s}{h} = \frac{16 - 4.8}{16} = 0.70$$

$$0.10\ f'_c\ A_g = 0.10 \times 4 \times 128 = 51.2 \text{ kips}$$

Then a rectangular beam with width b = 51 in. can be considered. Compression steel. Consider p - p' = o and the compression steel not to reach f_y at ultimate moment. Therefore the effect of compression steel will be neglected

$$M_u = \phi \times A_s \times f_y \left(d - \frac{A_s f_y}{2 \times 0.85 f'_c b}\right)$$

$\phi = 0.90$, $f_y = 40000$, $f'_c = 4000$, $d = 13.6$ in., $b = 51$ in.

Consider 2#7 as bottom reinforcement, $A_s = 1.20$ in.^{2}

$$M_u = 48.5 \text{ ft-kip} > 43.40 \text{ ft-kip}$$

Column face

Neglect compression reinforcement and use same formula as above with b = 8 in.

Consider 6#4 as top reinforcement $A'_s = 1.20$ in.^{2}

$$M_u = 45.9 \text{ ft-kip} > 40.60 \text{ ft-kip}$$

Distribution of flexural reinforcement (ACI Section 10.6)

Bottom reinforcement

$$A = \frac{2 \times 2.4 \times 8}{2} = 19.2 \text{ in.}^2 \qquad f_s = 0.60 \times 40 = 24 \text{ ksi}$$

$$z = 24 \sqrt[3]{2.4 \times 19.2} = 86 \text{ kip/in.} < 175 \text{ kip/in.}$$

Top reinforcement

$$A = \frac{2 \times 2.4 \times 51}{6} = 40.8 \text{ in.}^2 \qquad f_s = 24 \text{ ksi}$$

$$z = 24 \sqrt[3]{2.4 \times 40.8} = 111 \text{ kip/in.} < 175 \text{ kip/in}$$

Design for shear

$\phi = 0.85$

Minimum web reinforcement for girders

Preceding page blank

APPENDIX B

DESIGN OF TEST STRUCTURES RCF1 AND RCF2

Preceding page blank

B.1 Reduction of Size

The original test structure size was reduced using a length scale equal to 0.707.

If the term "prototype" is used to designate the original test structure and "model" the actual one, the following ratios between model and prototype apply:

Length ratio	= 0.707	
Area ratio	= 0.50	
Strain ratio	= 1.0	
Stress ratio	= 1.0	(Assumed)
Concentrated force ratio	= 0.50	
Gravity ratio	= 1.0	(Assumed)
Acceleration ratio	= 1.0	(to have inertia forces scaled by 0.50)

Therefore, the model dimensions are obtained by multiplying the prototype dimensions by 0.707. The reinforcing steel areas should be reduced by 0.50. This reduction as achieved in the following way

Prototype		Model	
# bar	A_s (in.^{2})	# bar	A_s (in.^{2})
7	0.60	5	0.31
6	0.44	4	0.20
4	0.20	3	0.11
3	0.11	2	0.05

Since the reduction is not exact, the strength of the different members has been checked in B.3.

The slab and the transverse girders at both stories were not designed for the prototype. The slab thickness for the model was scaled by the factor 0.707 but its reinforcement was designed directly for the actual test conditions (the slab carried no extra load but its own weight in the actual test structure.) The same can be said for the transverse girders. The final dimensions and reinforcement used in the test are shown in Figures 2.2 and 2.3.

B.2 Loads to be added in the actual test structure to reproduce original conditions

The actual test structure did not include the walls, partitions, roofing, ceiling, floor and other non-structural elements that contribute to the dead load. Besides the distance between the two longitudinal frames was made as short as possible without affecting the T-beam action in the floor diaphrgm. As has been noted before (See A.1.2) the contributing width of the slab is 51 in. for the prototype which corresponds to 36 in. in the model. Therefore, the distance between the frames in the model was 3 ft.

Due to these facts it was necessary to add mass at each floor in the actual test structure; this was accomplished by attaching concrete block that transmitted their weight directly to the longitudinal girders. The evaluation of these masses follows. It was carried out without considering the mass of the columns.

Original Test Structure

Top story dead load

Slab, ceiling, roofing	0.061 x 24 x 17	24.89 kip
Girders: longitudinal	0.100 x 18 x 2	
transverse	0.100 x 22.67 x 2	8.13 kip
	Total =	33.02 kip

Top story live load		0 kip
Bottom story dead load		
Slab, ceiling, floor	0.052 x 24 x 17	21.22 kip
Girders		8.13 kip
Walls	0.207 x 22.67 x 2	9.38 kip
Partitions	0.140 x 16 x 2	4.48 kip
	Total =	43.21 kip

Bottom story live load

	0.050 x 24 x 17	20.40 kip

Actual Test Structure. Each story

Slab	0.24 x 6 x 12.71 x 0.15	2.75 kip
Girders: longitudinal	0.34 x 12.71 x 0.15 x 2	
transverse	0.34 x 5.04 x 0.15 x 2	1.81 kip
	Total =	4.56 kip

It was originally decided to reproduce in the model all the dead load plus 25% of the live load at the bottom story. Then the following masses would have to be added

Top story: 0.50 (33.02) - 4.56 = 11.95 kips

Bottom story: 0.50 (43.21 + 0.25 x 20.40) - 4.56 = 19.60 kips

Then, concrete blocks weighing 4 kips (8 in. x 5 ft x 8 ft) were designed and constructed. Three of these blocks would be attached to the top floor and five to the bottom floor.

However it was afterwards decided to reduce the number of concrete blocks to two at the top story and four at the bottom; this final condition of loads is shown in Figure 2.2. Considering the measured weights of the blocks (8.25 kip at the top story and 16.16 kips at the bottom story) this condition was equivalent to consider no live load in the actual test structure and the following reductions in the dead load:

Top story	$\frac{8.25 + 4.56}{0.50 \times 33.02}$	= 0.78	22% reduction
Bottom story	$\frac{16.16 + 4.56}{0.50 \times 43.21}$	= 0.96	4% reduction

B.3 <u>Strength design verification</u>

a) <u>Bottom and top story columns</u>

Prototype has 4#7 $A_s = A'_s = 1.20$ in.^{2}

Model has 4#5 $A_s = A'_s = 0.62$. This corresponds to

$A_s = A'_s = 1.24$ in.^{2} in the prototype.

For the shear strength a reduction from #3 bars ($A_s = 0.11$ in.^{2}) to #2 bars ($A_s = 0.05$ in.^{2}) will be used. Since the shear reinforcement was decided from a minimum requirement which exceeded by a considerable amount the quantity necessary according to the Code formulas, no problem is presented by this reduction. The same is valid for all the following sections.

b) <u>Bottom story girder</u>

Midspan

Prototype has 2#7 $A_s = 1.20$ in.^{2}

Model has 2#5 $A_s = 0.62$ in.^{2}. No problem

Column face

Prototype has 6#4 $A'_s = 1.20$ in.^{2}

Model has 6#3 $A'_s = 0.66$ in.^{2}. This is equivalent to have 1.32 in.^{2} in the prototype.

c) <u>Top story girder</u>

Midspan

Prototype has 2#6 $A_s = 0.88$ in.^{2}

Model has 2#4 $A_s = 0.40$ in.^{2}. This corresponds to $A_s = 0.80$ in.^{2} in prototype. Check for condition U_{A1} gives

$$M_u = 31.7 \text{ ft-kip} < 34.53 \text{ ft-kip}$$

Therefore this condition represents a slightly under-reinforced model

Column face

Prototype has 4#4 $A'_s = 0.80$ in.^{2}

Model has 4#3 $A'_s = 0.44$ in.^{2}. This is equivalent to $A'_s = 0.88$ in.^{2} in the prototype.

Preceding page blank

APPENDIX C

IDEAL MODEL: DERIVATION OF ANALYTICAL CHARACTERISTICS

Preceding page blank

C.1 General

The different properties assigned to the ideal model for analysis purposes have been derived from those of the prototype structure applying the appropriate scaling ratios. These are shown in Table 2.2.

The units employed throughout the appendix are:

force : kips

length : inches

time : seconds

C.2 Geometry

1) Overall dimensions:

They are shown in Figures 2.1 (Prototype) and 2.3 (Ideal model)

2) Section properties:

The flange widths of the girders comply with the ACI and UBC Code requirements. The rotational moment of inertia J has been computed using

$$J = \sum \beta_i \, b_i \, c_i^3$$

where b_i and c_i are the longest and shortest dimension of rectangular component i, and β_i is a shape factor obtained from Reference [24]. The dimensions of the prototype and of the ideal model (within parenthesis) are shown.

a) Column

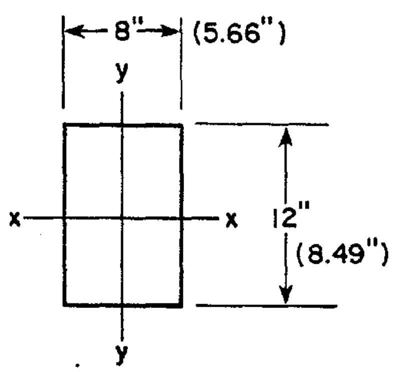

	PROTOTYPE	IDEAL MODEL
$A (in.^2)$	96.0	48.0
$I_{xx} (in.^4)$	1152.0	288.0
$I_{yy} (in.^4)$	512.0	128.0
$J (in.^4)$	1230.0	307.5

b) Longitudinal girders

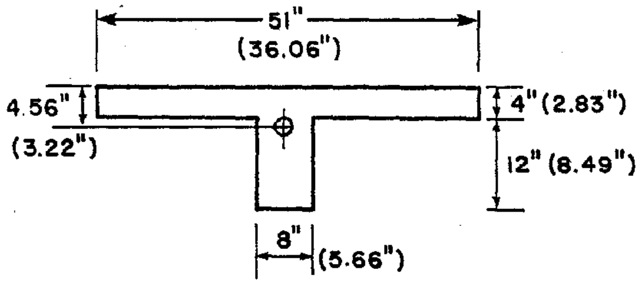

	PROTOTYPE	IDEAL MODEL
A	300.0	150.0
I_{XX}	5602.0	1400.0
J	2200.0	550.0

c) Transverse girders

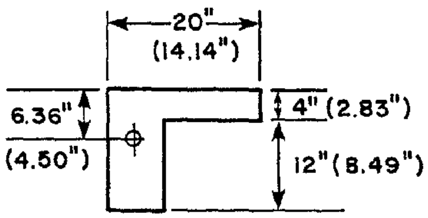

	PROTOTYPE	IDEAL MODEL
A	176.0	88.0
I_{xx}	3406.0	851.5
J	1536.0	384.0

The shear area for the girders has been taken as the area of their web, $A_v = 8 \times 16 = 128$ in.^{2} for prototype and 64 in.^{2} for model.

C.3 Inertial properties

The unit weight of the concrete is assumed to be 0.15 kip/ft^3. The contribution of the girders and columns is taken into account in the computation of the translational and rotational mass of each floor. No live load is considered acting on the structure.

	BOTTOM STORY		TOP STORY	
	PROTOTYPE	IDEAL MODEL	PROTOTYPE	IDEAL MODEL
Weight (k)	47.72	23.86	34.89	17.45
TR.MASS $\frac{k\text{-}sec^2}{in.}$	.123	.0618	.090	.0451
ROT.MASS $k\text{-}sec^2\text{-}in.$	1033.	258.	1557.	389.

C.4 Elastic modulus

According to the ACI and UBC Codes, $E_c = 57000\sqrt{4000} = 3605$ ksi for both the prototype and the ideal model.

C.5 Section cracking moments

The cracking moments M_{CR} corresponding to the girders and columns of the structure are computed using

$$f_R = \frac{M_{CR}}{I_g} \cdot y_t - \frac{P}{A_g}$$

therefore

$$M_{CR} = (f_R + \frac{P}{A_g}) \cdot \frac{I_g}{y_t}$$

where

f_R = tensile strength of concrete = $7.5\sqrt{f'_c}$ (psi)

I_g = gross central moment of inertia of the section

A_g = gross area

y_t = central distance of most stressed fiber (in tension)

P = axial load on section (compression is positive), correspond- to dead load. It is neglected for the girders.

Therefore, for $f_R = 7.5\sqrt{4000} = 474$ psi $= .474$ ksi the following values are obtained

	PROTOTYPE	IDEAL MODEL
Long girders		
M_{CR}+(k-in.)	232.11	82.07
M_{CR}-	582.31	205.91
Columns		
Bottom M_{CR}	132.31	46.78
Top M_{CR}	108.45	38.35

C.6 Transformed cracked properties of longitudinal girders

The moment of inertia of the transformed cracked sections are computed according to the following scheme

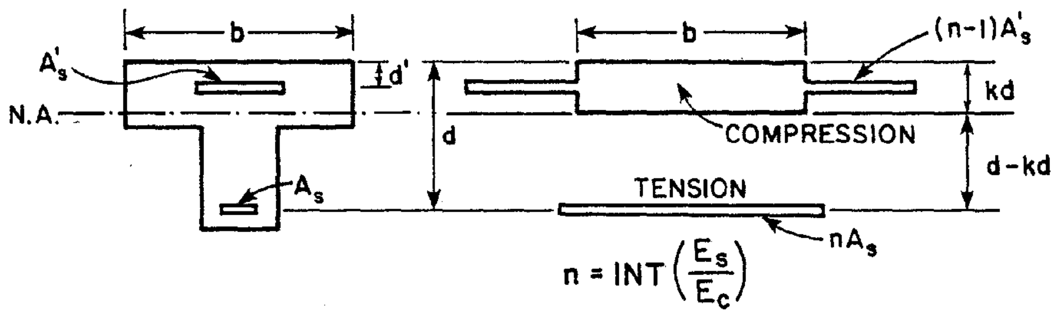

The value of kd is determined equating the first moment of the tension and compression areas with respect to the assumed position of the N.A. the equation obtained (for N.A below top reinforcement) is

$$b\,\frac{(kd)^2}{2} + (n-1)\,A'_s\,(kd-d') - n\,A_s\,(d-kd) = 0$$

This expression should be appropriately modified if the neutral axis is above the top reinforcement. The cracked moment of intertia results then:

$$I_{ct} = \frac{1}{3}\,b\,(kd)^3 + (n-1)\,A'_s\,(kd-d')^2 + nA_s\,(d-kd)^2$$

for $n = INT(\frac{29000}{3605}) = 8$

and the section characteristics shown in Figure 2.5, the following values are obtained, where positive curvature corresponds to compression of the top fibers

	PROTOTYPE	IDEAL MODEL
Bottom Story Girder		
I_{ct}^{+} (in.^{4})	1388.4	347.1
I_{ct}^{-}	1049.6	262.4
Top Story Girder		
I_{ct}^{+}	1040.0	260.0
I_{ct}^{-}	742.0	185.5

C.7 Lateral loads for elastoplastic analysis

The distribution of lateral loads along the height of the structure(s) is assumed to be proportional to the inertia forces associated with the first mode of vibration.

Thus, if the first mode shape is

$$\underline{\Phi}_1 = \begin{Bmatrix} \phi_{1T} \\ \phi_{1B} \end{Bmatrix}$$

the associated inertia force vector would be

$$f(t) = \begin{Bmatrix} f_T(t) \\ f_B(t) \end{Bmatrix} = \begin{Bmatrix} m_T\phi_{1T} \\ m_B\phi_{1B} \end{Bmatrix} p(t)$$

where p(t) is a scalar function of time

Therefore, if the force acting on the bottom story level is f_B, the corresponding force on the bottom floor is

$$f_T = \frac{m_T\ \phi_{1T}}{m_B\ \phi_{1B}} \cdot f_B$$

For the approximate value

$$\underline{\phi_1} = \begin{Bmatrix} 1.0 \\ 0.6 \end{Bmatrix}$$

and for $m_B = .0572 \frac{\text{k-sec}^2}{\text{in.}}$; $m_T = 0.0352$ the following relationship is obtained.

$$f_T = 1.03 \; f_B$$

C.8 Equivalent concentrated gravity loads for elastoplastic analysis.

The distributed loads acting on the girders of the ideal model had to be replaced by equivalent concentrated loads, since this is the only type of loading that can be handled by the program ULARC.

The criterion used to determine the equivalent loads consists in replacing the distributed loads by a statically equivalent system of concentrated forces which produce the same collapse load as the distributed load.

The plastic moment of the girders is assumed to be uniform along the length; and the location of the equivalent concentrated loads correspond to the position of the concrete block supports on the test stucture.

The load factor for a fixed-end beam subjected to uniform loadings is determined as follows

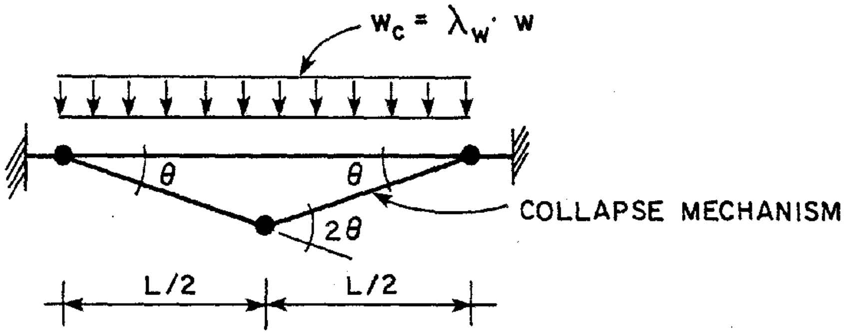

External work $W_E = \frac{1}{4} w_c \; L^2 \theta$

Internal work $W_I = 4M_p \theta$

and from $W_E = W_I$, it is obtained,

$$w_c = \lambda_w \cdot w = \frac{16\ M_p}{L^2}$$

and the load multiplier is

$$\lambda_w = \frac{16\ M_p}{w_c L^2}$$

For the case of the concentrated loads the procedure is similar:

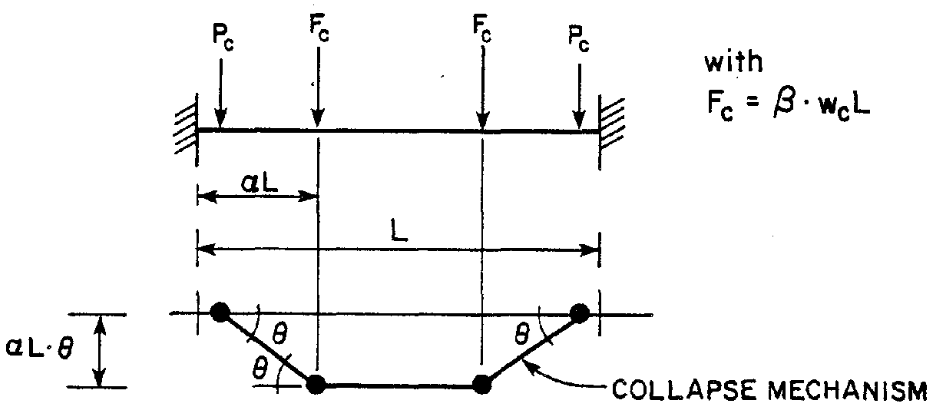

To have statically equivalent loading

$$2P_c + 2F_c = w_c L$$

$$\text{then, } P_c = \frac{w_c L - 2F_c}{2} = \frac{w_c L}{2}(1 - 2\beta)$$

At collapse,

$$W_E = 2F_c \cdot \alpha L\theta = 2\alpha\beta w_c L^2 \theta$$

$$W_I = 4M_p \theta$$

equating external and internal work

$$w_{coll} = \lambda_F w = \frac{2M_p}{\alpha\beta L^2}$$

Therefore

$$\lambda_F = \frac{2M_p}{\alpha\beta w L^2}$$

Hence, in order to have the same collapse load than in the distributed load case

$$\lambda_F = \lambda_W$$

or

$$\frac{16M_p}{w_L{}^2} = \frac{2M_p}{\alpha\beta w L^2}$$

from where

$$\alpha\beta = \frac{1}{8}$$

α is selected according to the geometric characteristics of the test structure

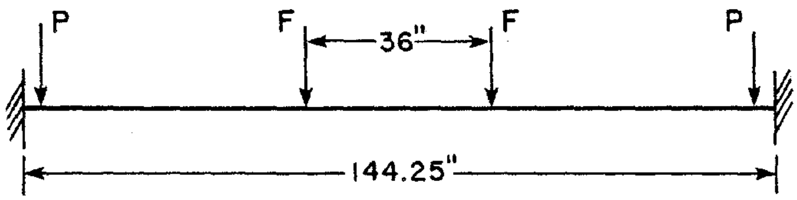

$$\alpha L = \frac{144.25 - 36}{2} = 54.125 \text{ in.}$$

then

$$\alpha = \frac{54.125}{144.25} \doteq 0.375$$

therefore

$$\beta = \frac{1}{8\alpha} = \frac{1}{8}$$

hence

$$F = \frac{1}{3} wL$$

and

$$P = \frac{1}{2}(1 - \frac{2}{3})wL = \frac{1}{6} wL$$

The equivalent loads used in analysis were obtained from the distributed loads shown in Figure 2.5, taking into consideration the column's own weight.

APPENDIX D

TEST STRUCTURE: DERIVATION OF ANALYTICAL CHARACTERISTICS

Preceding page blank

D.1 General

The methods employed to idealize the test structure for analytical purposes are the same as those used in the case of the ideal model (Chapter 2 and Appendix C.)

D.2 Geometry

The overall dimensions of RCF2 are shown in Figure 2.2, the section characteristics in Figure 2.5. The section geometric properties are listed below

a) Columns

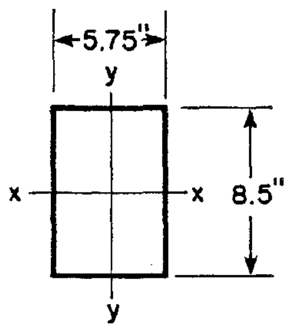

$A(\text{in.}^2) = 48.88$

$I_{xx}(\text{in.}^4) = 294.27$

$I_{yy}(\text{in.}^4) = 134.66$

$J(\text{in.}^4) = 313.5$

b) Longitudinal girders

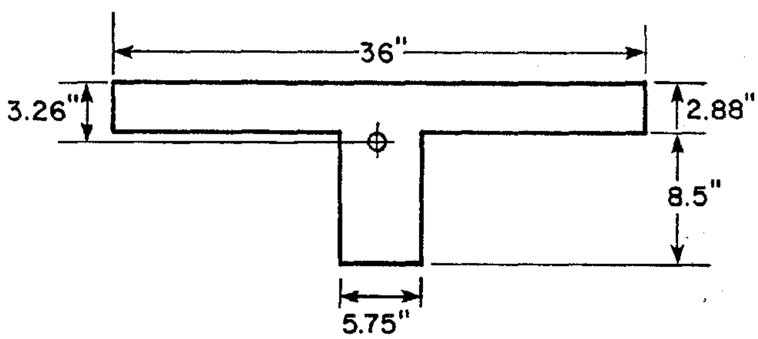

$A = 152.56$

$I_{xx} = 144.36$

$J = 588.7$

c) Transverse girders

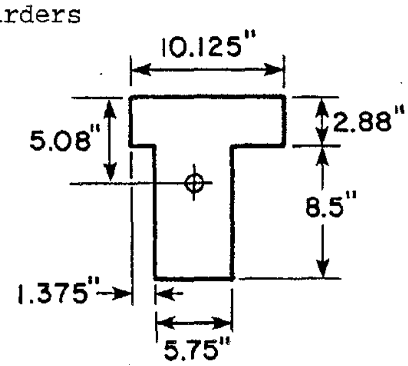

$A = 78.037$

$I_{xx} = 905.73$

$J = 378.55$

D.3 Inertial properties

Assuming a unit weight for the concrete of 0.15 kip/ft^3, the weight of the different components is:

ITEM	WEIGHT (kips)
Slab (each)	2.75
Longitudinal girder	0.576
Transverse girder	0.305
Columns (per unit length)	.00425 kip/in.
Concrete blocks and attachments	
bottom story	16.32
top story	8.42

Based on these values and on the geometry of the specimen, the inertia properties result:

	BOTTOM STORY	TOP STORY
WEIGHT(k)	21.98	13.51
TR. MASS($\frac{k\text{-}sec^2}{in.^2}$)	0.0572	.0351
ROT. MASS($k\text{-}sec^2\text{-}in.$)	92.01	61.94

D. 4 Loads on girders (dead load only)

From ACI 318-63, for the demensions of the slab

$$A = 3 \text{ ft}; \; B = 12.02 \text{ ft},$$

$\frac{A}{B} = 0.25$, and the slab behaves in one-way action,

transmitting all its weight to the longitudinal girders.

The distributed loads (using center-to-center dimensions) on the girders result then:

longitudinal girders	$w = 0.0135$ k/in.
transvers girders	$w = 0.0085$ k/in.

In addition, the concrete blocks produce "concentrated" loads, in each support, of 4.1 kips for the bottom story girder, and 2.1 kips for the top story girder.

D. 5 Section cracking moments

Using the same expression as for the prototype and the ideal model, the following values are obtained

Longitudinal girders:

$M_{CR}^{+} = 84.17$ (k-in.)

$M_{CR}^{-} = 209.38$

Columns:

Bottom story $M_{cr} = 46.04$

Top story $M_{cr} = 38.0$

EARTHQUAKE ENGINEERING RESEARCH CENTER REPORTS

NOTE: Numbers in parenthesis are Accession Numbers assigned by the National Technical Information Service; these are followed by a price code. Copies of the reports may be ordered from the National Technical Information Service, 5285 Port Royal Road, Springfield, Virginia, 22161. Accession Numbers should be quoted on orders for reports (PB --- ---) and remittance must accompany each order. Reports without this information were not available at time of printing. Upon request, EERC will mail inquirers this information when it becomes available.

EERC 67-1 "Feasibility Study Large-Scale Earthquake Simulator Facility," by J. Penzien, J.G. Bouwkamp, R.W. Clough and D. Rea - 1967 (PB 187 905)A07

EERC 68-1 Unassigned

EERC 68-2 "Inelastic Behavior of Beam-to-Column Subassemblages Under Repeated Loading," by V.V. Bertero - 1968 (PB 184 888)A05

EERC 68-3 "A Graphical Method for Solving the Wave Reflection-Refraction Problem," by H.D. McNiven and Y. Mengi - 1968 (PB 187 943)A03

EERC 68-4 "Dynamic Properties of McKinley School Buildings," by D. Rea, J.G. Bouwkamp and R.W. Clough - 1968 (PB 187 902)A07

EERC 68-5 "Characteristics of Rock Motions During Earthquakes," by H.B. Seed, I.M. Idriss and F.W. Kiefer - 1968 (PB 188 338)A03

EERC 69-1 "Earthquake Engineering Research at Berkeley," - 1969 (PB 187 906)A11

EERC 69-2 "Nonlinear Seismic Response of Earth Structures," by M. Dibaj and J. Penzien - 1969 (PB 187 904)A08

EERC 69-3 "Probabilistic Study of the Behavior of Structures During Earthquakes," by R. Ruiz and J. Penzien - 1969 (PB 187 886)A06

EERC 69-4 "Numerical Solution of Boundary Value Problems in Structural Mechanics by Reduction to an Initial Value Formulation," by N. Distefano and J. Schujman - 1969 (PB 187 942)A02

EERC 69-5 "Dynamic Programming and the Solution of the Biharmonic Equation," by N. Distefano - 1969 (PB 187 941)A03

EERC 69-6 "Stochastic Analysis of Offshore Tower Structures," by A.K. Malhotra and J. Penzien - 1969 (PB 187 903)A09

EERC 69-7 "Rock Motion Accelerograms for High Magnitude Earthquakes," by H.B. Seed and I.M. Idriss - 1969 (PB 187 940)A02

EERC 69-8 "Structural Dynamics Testing Facilities at the University of California, Berkeley," by R.M. Stephen, J.G. Bouwkamp, R.W. Clough and J. Penzien - 1969 (PB 189 111)A04

EERC 69-9 "Seismic Response of Soil Deposits Underlain by Sloping Rock Boundaries," by H. Dezfulian and H.B. Seed 1969 (PB 189 114)A03

EERC 69-10 "Dynamic Stress Analysis of Axisymmetric Structures Under Arbitrary Loading," by S. Ghosh and E.L. Wilson 1969 (PB 189 026)A10

EERC 69-11 "Seismic Behavior of Multistory Frames Designed by Different Philosophies," by J.C. Anderson and V. V. Bertero - 1969 (PB 190 662)A10

EERC 69-12 "Stiffness Degradation of Reinforcing Concrete Members Subjected to Cyclic Flexural Moments," by V.V. Bertero, B. Bresler and H. Ming Liao - 1969 (PB 202 942)A07

EERC 69-13 "Response of Non-Uniform Soil Deposits to Travelling Seismic Waves," by H. Dezfulian and H.B. Seed - 1969 (PB 191 023)A03

EERC 69-14 "Damping Capacity of a Model Steel Structure," by D. Rea, R.W. Clough and J.G. Bouwkamp - 1969 (PB 190 663)A06

EERC 69-15 "Influence of Local Soil Conditions on Building Damage Potential during Earthquakes," by H.B. Seed and I.M. Idriss - 1969 (PB 191 036)A03

EERC 69-16 "The Behavior of Sands Under Seismic Loading Conditions," by M.L. Silver and H.B. Seed - 1969 (AD 714 982)A07

EERC 70-1 "Earthquake Response of Gravity Dams," by A.K. Chopra - 1970 (AD 709 640)A03

EERC 70-2 "Relationships between Soil Conditions and Building Damage in the Caracas Earthquake of July 29, 1967," by H.B. Seed, I.M. Idriss and H. Dezfulian - 1970 (PB 195 762)A05

EERC 70-3 "Cyclic Loading of Full Size Steel Connections," by E.P. Popov and R.M. Stephen - 1970 (PB 213 545)A04

EERC 70-4 "Seismic Analysis of the Charaima Building, Caraballeda, Venezuela," by Subcommittee of the SEAONC Research Committee: V.V. Bertero, P.F. Fratessa, S.A. Mahin, J.H. Sexton, A.C. Scordelis, E.L. Wilson, L.A. Wyllie, H.B. Seed and J. Penzien, Chairman - 1970 (PB 201 455)A06

EERC 70-5 "A Computer Program for Earthquake Analysis of Dams," by A.K. Chopra and P. Chakrabarti - 1970 (AD 723 994)A05

EERC 70-6 "The Propagation of Love Waves Across Non-Horizontally Layered Structures," by J. Lysmer and L.A. Drake 1970 (PB 197 896)A03

EERC 70-7 "Influence of Base Rock Characteristics on Ground Response," by J. Lysmer, H.B. Seed and P.B. Schnabel 1970 (PB 197 897)A03

EERC 70-8 "Applicability of Laboratory Test Procedures for Measuring Soil Liquefaction Characteristics under Cyclic Loading," by H.B. Seed and W.H. Peacock - 1970 (PB 198 016)A03

EERC 70-9 "A Simplified Procedure for Evaluating Soil Liquefaction Potential," by H.B. Seed and I.M. Idriss - 1970 (PB 198 009)A03

EERC 70-10 "Soil Moduli and Damping Factors for Dynamic Response Analysis," by H.B. Seed and I.M. Idriss - 1970 (PB 197 869)A03

EERC 71-1 "Koyna Earthquake of December 11, 1967 and the Performance of Koyna Dam," by A.K. Chopra and P. Chakrabarti 1971 (AD 731 496)A06

EERC 71-2 "Preliminary In-Situ Measurements of Anelastic Absorption in Soils Using a Prototype Earthquake Simulator," by R.D. Borcherdt and P.W. Rodgers - 1971 (PB 201 454)A03

EERC 71-3 "Static and Dynamic Analysis of Inelastic Frame Structures," by F.L. Porter and G.H. Powell - 1971 (PB 210 135)A06

EERC 71-4 "Research Needs in Limit Design of Reinforced Concrete Structures," by V.V. Bertero - 1971 (PB 202 943)A04

EERC 71-5 "Dynamic Behavior of a High-Rise Diagonally Braced Steel Building," by D. Rea, A.A. Shah and J.G. Bouwkamp 1971 (PB 203 584)A06

EERC 71-6 "Dynamic Stress Analysis of Porous Elastic Solids Saturated with Compressible Fluids," by J. Ghaboussi and E. L. Wilson - 1971 (PB 211 396)A06

EERC 71-7 "Inelastic Behavior of Steel Beam-to-Column Subassemblages," by H. Krawinkler, V.V. Bertero and E.P. Popov 1971 (PB 211 335)A14

EERC 71-8 "Modification of Seismograph Records for Effects of Local Soil Conditions," by P. Schnabel, H.B. Seed and J. Lysmer - 1971 (PB 214 450)A03

EERC 72-1 "Static and Earthquake Analysis of Three Dimensional Frame and Shear Wall Buildings," by E.L. Wilson and H.H. Dovey - 1972 (PB 212 904)A05

EERC 72-2 "Accelerations in Rock for Earthquakes in the Western United States," by P.B. Schnabel and H.B. Seed - 1972 (PB 213 100)A03

EERC 72-3 "Elastic-Plastic Earthquake Response of Soil-Building Systems," by T. Minami - 1972 (PB 214 868)A08

EERC 72-4 "Stochastic Inelastic Response of Offshore Towers to Strong Motion Earthquakes," by M.K. Kaul - 1972 (PB 215 713)A05

EERC 72-5 "Cyclic Behavior of Three Reinforced Concrete Flexural Members with High Shear," by E.P. Popov, V.V. Bertero and H. Krawinkler - 1972 (PB 214 555)A05

EERC 72-6 "Earthquake Response of Gravity Dams Including Reservoir Interaction Effects," by P. Chakrabarti and A.K. Chopra - 1972 (AD 762 330)A08

EERC 72-7 "Dynamic Properties of Pine Flat Dam," by D. Rea, C.Y. Liaw and A.K. Chopra - 1972 (AD 763 928)A05

EERC 72-8 "Three Dimensional Analysis of Building Systems," by E.L. Wilson and H.H. Dovey - 1972 (PB 222 438)A06

EERC 72-9 "Rate of Loading Effects on Uncracked and Repaired Reinforced Concrete Members," by S. Mahin, V.V. Bertero, D. Rea and M. Atalay - 1972 (PB 224 520)A08

EERC 72-10 "Computer Program for Static and Dynamic Analysis of Linear Structural Systems," by E.L. Wilson, K.-J. Bathe, J.E. Peterson and H.H.Dovey - 1972 (PB 220 437)A04

EERC 72-11 "Literature Survey - Seismic Effects on Highway Bridges," by T. Iwasaki, J. Penzien and R.W. Clough - 1972 (PB 215 613)A19

EERC 72-12 "SHAKE-A Computer Program for Earthquake Response Analysis of Horizontally Layered Sites," by P.B. Schnabel and J. Lysmer - 1972 (PB 220 207)A06

EERC 73-1 "Optimal Seismic Design of Multistory Frames," by V.V. Bertero and H. Kamil - 1973

EERC 73-2 "Analysis of the Slides in the San Fernando Dams During the Earthquake of February 9, 1971," by H.B. Seed, K.L. Lee, I.M. Idriss and F. Makdisi - 1973 (PB 223 402)A14

EERC 73-3 "Computer Aided Ultimate Load Design of Unbraced Multistory Steel Frames," by M.B. El-Hafez and G.H. Powell 1973 (PB 248 315)A09

EERC 73-4 "Experimental Investigation into the Seismic Behavior of Critical Regions of Reinforced Concrete Components as Influenced by Moment and Shear," by M. Celebi and J. Penzien - 1973 (PB 215 884)A09

EERC 73-5 "Hysteretic Behavior of Epoxy-Repaired Reinforced Concrete Beams," by M. Celebi and J. Penzien - 1973 (PB 239 568)A03

EERC 73-6 "General Purpose Computer Program for Inelastic Dynamic Response of Plane Structures," by A. Kanaan and G.H. Powell - 1973 (PB 221 260)A08

EERC 73-7 "A Computer Program for Earthquake Analysis of Gravity Dams Including Reservoir Interaction," by P. Chakrabarti and A.K. Chopra - 1973 (AD 766 271)A04

EERC 73-8 "Behavior of Reinforced Concrete Deep Beam-Column Subassemblages Under Cyclic Loads," by O. Küstü and J.G. Bouwkamp - 1973 (PB 246 117)A12

EERC 73-9 "Earthquake Analysis of Structure-Foundation Systems," by A.K. Vaish and A.K. Chopra - 1973 (AD 766 272)A07

EERC 73-10 "Deconvolution of Seismic Response for Linear Systems," by R.B. Reimer - 1973 (PB 227 179)A08

EERC 73-11 "SAP IV: A Structural Analysis Program for Static and Dynamic Response of Linear Systems," by K.-J. Bathe, E.L. Wilson and F.E. Peterson - 1973 (PB 221 967)A09

EERC 73-12 "Analytical Investigations of the Seismic Response of Long, Multiple Span Highway Bridges," by W.S. Tseng and J. Penzien - 1973 (PB 227 816)A10

EERC 73-13 "Earthquake Analysis of Multi-Story Buildings Including Foundation Interaction," by A.K. Chopra and J.A. Gutierrez - 1973 (PB 222 970)A03

EERC 73-14 "ADAP: A Computer Program for Static and Dynamic Analysis of Arch Dams," by R.W. Clough, J.M. Raphael and S. Mojtahedi - 1973 (PB 223 763)A09

EERC 73-15 "Cyclic Plastic Analysis of Structural Steel Joints," by R.B. Pinkney and R.W. Clough - 1973 (PB 226 843)A08

EERC 73-16 "QUAD-4: A Computer Program for Evaluating the Seismic Response of Soil Structures by Variable Damping Finite Element Procedures," by I.M. Idriss, J. Lysmer, R. Hwang and H.B. Seed - 1973 (PB 229 424)A05

EERC 73-17 "Dynamic Behavior of a Multi-Story Pyramid Shaped Building," by R.M. Stephen, J.P. Hollings and J.G. Bouwkamp - 1973 (PB 240 718)A06

EERC 73-18 "Effect of Different Types of Reinforcing on Seismic Behavior of Short Concrete Columns," by V.V. Bertero, J. Hollings, O. Küstü, R.M. Stephen and J.G. Bouwkamp - 1973

EERC 73-19 "Olive View Medical Center Materials Studies, Phase I," by B. Bresler and V.V. Bertero - 1973 (PB 235 986)A06

EERC 73-20 "Linear and Nonlinear Seismic Analysis Computer Programs for Long Multiple-Span Highway Bridges," by W.S. Tseng and J. Penzien - 1973

EERC 73-21 "Constitutive Models for Cyclic Plastic Deformation of Engineering Materials," by J.M. Kelly and P.P. Gillis 1973 (PB 226 024)A03

EERC 73-22 "DRAIN - 2D User's Guide," by G.H. Powell - 1973 (PB 227 016)A05

EERC 73-23 "Earthquake Engineering at Berkeley - 1973," (PB 226 033)A11

EERC 73-24 Unassigned

EERC 73-25 "Earthquake Response of Axisymmetric Tower Structures Surrounded by Water," by C.Y. Liaw and A.K. Chopra 1973 (AD 773 052)A09

EERC 73-26 "Investigation of the Failures of the Olive View Stairtowers During the San Fernando Earthquake and Their Implications on Seismic Design," by V.V. Bertero and R.G. Collins - 1973 (PB 235 106)A13

EERC 73-27 "Further Studies on Seismic Behavior of Steel Beam-Column Subassemblages," by V.V. Bertero, H. Krawinkler and E.P. Popov - 1973 (PB 234 172)A06

EERC 74-1 "Seismic Risk Analysis," by C.S. Oliveira - 1974 (PB 235 920)A06

EERC 74-2 "Settlement and Liquefaction of Sands Under Multi-Directional Shaking," by R. Pyke, C.K. Chan and H.B. Seed 1974

EERC 74-3 "Optimum Design of Earthquake Resistant Shear Buildings," by D. Ray, K.S. Pister and A.K. Chopra - 1974 (PB 231 172)A06

EERC 74-4 "LUSH - A Computer Program for Complex Response Analysis of Soil-Structure Systems," by J. Lysmer, T. Udaka, H.B. Seed and R. Hwang - 1974 (PB 236 796)A05

EERC 74-5 "Sensitivity Analysis for Hysteretic Dynamic Systems: Applications to Earthquake Engineering," by D. Ray 1974 (PB 233 213)A06

EERC 74-6 "Soil Structure Interaction Analyses for Evaluating Seismic Response," by H.B. Seed, J. Lysmer and R. Hwang 1974 (PB 236 519)A04

EERC 74-7 Unassigned

EERC 74-8 "Shaking Table Tests of a Steel Frame - A Progress Report," by R.W. Clough and D. Tang - 1974 (PB 240 869)A03

EERC 74-9 "Hysteretic Behavior of Reinforced Concrete Flexural Members with Special Web Reinforcement," by V.V. Bertero, E.P. Popov and T.Y. Wang - 1974 (PB 236 797)A07

EERC 74-10 "Applications of Reliability-Based, Global Cost Optimization to Design of Earthquake Resistant Structures," by E. Vitiello and K.S. Pister - 1974 (PB 237 231)A06

EERC 74-11 "Liquefaction of Gravelly Soils Under Cyclic Loading Conditions," by R.T. Wong, H.B. Seed and C.K. Chan 1974 (PB 242 042)A03

EERC 74-12 "Site-Dependent Spectra for Earthquake-Resistant Design," by H.B. Seed, C. Ugas and J. Lysmer - 1974 (PB 240 953)A03

EERC 74-13 "Earthquake Simulator Study of a Reinforced Concrete Frame," by P. Hidalgo and R.W. Clough - 1974 (PB 241 944)A13

EERC 74-14 "Nonlinear Earthquake Response of Concrete Gravity Dams," by N. Pal - 1974 (AD/A 006 583)A06

EERC 74-15 "Modeling and Identification in Nonlinear Structural Dynamics - I. One Degree of Freedom Models," by N. Distefano and A. Rath - 1974 (PB 241 548)A06

EERC 75-1 "Determination of Seismic Design Criteria for the Dumbarton Bridge Replacement Structure, Vol. I: Description, Theory and Analytical Modeling of Bridge and Parameters," by F. Baron and S.-H. Pang - 1975 (PB 259 407)A15

EERC 75-2 "Determination of Seismic Design Criteria for the Dumbarton Bridge Replacement Structure, Vol. II: Numerical Studies and Establishment of Seismic Design Criteria," by F. Baron and S.-H. Pang - 1975 (PB 259 408)A11 (For set of EERC 75-1 and 75-2 (PB 259 406))

EERC 75-3 "Seismic Risk Analysis for a Site and a Metropolitan Area," by C.S. Oliveira - 1975 (PB 248 134)A09

EERC 75-4 "Analytical Investigations of Seismic Response of Short, Single or Multiple-Span Highway Bridges," by M.-C. Chen and J. Penzien - 1975 (PB 241 454)A09

EERC 75-5 "An Evaluation of Some Methods for Predicting Seismic Behavior of Reinforced Concrete Buildings," by S.A. Mahin and V.V. Bertero - 1975 (PB 246 306)A16

EERC 75-6 "Earthquake Simulator Study of a Steel Frame Structure, Vol. I: Experimental Results," by R.W. Clough and D.T. Tang - 1975 (PB 243 981)A13

EERC 75-7 "Dynamic Properties of San Bernardino Intake Tower," by D. Rea, C.-Y. Liaw and A.K. Chopra - 1975 (AD/A008 406) A05

EERC 75-8 "Seismic Studies of the Articulation for the Dumbarton Bridge Replacement Structure, Vol. I: Description, Theory and Analytical Modeling of Bridge Components," by F. Baron and R.E. Hamati - 1975 (PB 251 539)A07

EERC 75-9 "Seismic Studies of the Articulation for the Dumbarton Bridge Replacement Structure, Vol. 2: Numerical Studies of Steel and Concrete Girder Alternates," by F. Baron and R.E. Hamati - 1975 (PB 251 540)A10

EERC 75-10 "Static and Dynamic Analysis of Nonlinear Structures," by D.P. Mondkar and G.H. Powell - 1975 (PB 242 434)A08

EERC 75-11 "Hysteretic Behavior of Steel Columns," by E.P. Popov, V.V. Bertero and S. Chandramouli - 1975 (PB 252 365)A11

EERC 75-12 "Earthquake Engineering Research Center Library Printed Catalog," - 1975 (PB 243 711)A26

EERC 75-13 "Three Dimensional Analysis of Building Systems (Extended Version)," by E.L. Wilson, J.P. Hollings and H.H. Dovey - 1975 (PB 243 989)A07

EERC 75-14 "Determination of Soil Liquefaction Characteristics by Large-Scale Laboratory Tests," by P. De Alba, C.K. Chan and H.B. Seed - 1975 (NUREG 0027)A08

EERC 75-15 "A Literature Survey - Compressive, Tensile, Bond and Shear Strength of Masonry," by R.L. Mayes and R.W. Clough - 1975 (PB 246 292)A10

EERC 75-16 "Hysteretic Behavior of Ductile Moment Resisting Reinforced Concrete Frame Components," by V.V. Bertero and E.P. Popov - 1975 (PB 246 388)A05

EERC 75-17 "Relationships Between Maximum Acceleration, Maximum Velocity, Distance from Source, Local Site Conditions for Moderately Strong Earthquakes," by H.B. Seed, R. Murarka, J. Lysmer and I.M. Idriss - 1975 (PB 248 172)A0

EERC 75-18 "The Effects of Method of Sample Preparation on the Cyclic Stress-Strain Behavior of Sands," by J. Mulilis, C.K. Chan and H.B. Seed - 1975 (Summarized in EERC 75-28)

EERC 75-19 "The Seismic Behavior of Critical Regions of Reinforced Concrete Components as Influenced by Moment, Shear and Axial Force," by M.B. Atalay and J. Penzien - 1975 (PB 258 842)A11

EERC 75-20 "Dynamic Properties of an Eleven Story Masonry Building," by R.M. Stephen, J.P. Hollings, J.G. Bouwkamp and D. Jurukovski - 1975 (PB 246 945)A04

EERC 75-21 "State-of-the-Art in Seismic Strength of Masonry - An Evaluation and Review," by R.L. Mayes and R.W. Clough 1975 (PB 249 040)A07

EERC 75-22 "Frequency Dependent Stiffness Matrices for Viscoelastic Half-Plane Foundations," by A.K. Chopra, P. Chakrabarti and G. Dasgupta - 1975 (PB 248 121)A07

EERC 75-23 "Hysteretic Behavior of Reinforced Concrete Framed Walls," by T.Y. Wong, V.V. Bertero and E.P. Popov - 1975

EERC 75-24 "Testing Facility for Subassemblages of Frame-Wall Structural Systems," by V.V. Bertero, E.P. Popov and T. Endo - 1975

EERC 75-25 "Influence of Seismic History on the Liquefaction Characteristics of Sands," by H.B. Seed, K. Mori and C.K. Chan - 1975 (Summarized in EERC 75-28)

EERC 75-26 "The Generation and Dissipation of Pore Water Pressures during Soil Liquefaction," by H.B. Seed, P.P. Martin and J. Lysmer - 1975 (PB 252 648)A03

EERC 75-27 "Identification of Research Needs for Improving Aseismic Design of Building Structures," by V.V. Bertero 1975 (PB 248 136)A05

EERC 75-28 "Evaluation of Soil Liquefaction Potential during Earthquakes," by H.B. Seed, I. Arango and C.K. Chan - 1975 (NUREG 0026)A13

EERC 75-29 "Representation of Irregular Stress Time Histories by Equivalent Uniform Stress Series in Liquefaction Analyses," by H.B. Seed, I.M. Idriss, F. Makdisi and N. Banerjee - 1975 (PB 252 635)A03

EERC 75-30 "FLUSH - A Computer Program for Approximate 3-D Analysis of Soil-Structure Interaction Problems," by J. Lysmer, T. Udaka, C.-F. Tsai and H.B. Seed - 1975 (PB 259 332)A07

EERC 75-31 "ALUSH - A Computer Program for Seismic Response Analysis of Axisymmetric Soil-Structure Systems," by E. Berger, J. Lysmer and H.B. Seed - 1975

EERC 75-32 "TRIP and TRAVEL - Computer Programs for Soil-Structure Interaction Analysis with Horizontally Travelling Waves," by T. Udaka, J. Lysmer and H.B. Seed - 1975

EERC 75-33 "Predicting the Performance of Structures in Regions of High Seismicity," by J. Penzien - 1975 (PB 248 130)A03

EERC 75-34 "Efficient Finite Element Analysis of Seismic Structure - Soil - Direction," by J. Lysmer, H.B. Seed, T. Udaka, R.N. Hwang and C.-F. Tsai - 1975 (PB 253 570)A03

EERC 75-35 "The Dynamic Behavior of a First Story Girder of a Three-Story Steel Frame Subjected to Earthquake Loading," by R.W. Clough and L.-Y. Li - 1975 (PB 248 841)A05

EERC 75-36 "Earthquake Simulator Study of a Steel Frame Structure, Volume II - Analytical Results," by D.T. Tang - 1975 (PB 252 926)A10

EERC 75-37 "ANSR-I General Purpose Computer Program for Analysis of Non-Linear Structural Response," by D.P. Mondkar and G.H. Powell - 1975 (PB 252 386)A08

EERC 75-38 "Nonlinear Response Spectra for Probabilistic Seismic Design and Damage Assessment of Reinforced Concrete Structures," by M. Murakami and J. Penzien - 1975 (PB 259 530)A05

EERC 75-39 "Study of a Method of Feasible Directions for Optimal Elastic Design of Frame Structures Subjected to Earthquake Loading," by N.D. Walker and K.S. Pister - 1975 (PB 257 781)A06

EERC 75-40 "An Alternative Representation of the Elastic-Viscoelastic Analogy," by G. Dasgupta and J.L. Sackman - 1975 (PB 252 173)A03

EERC 75-41 "Effect of Multi-Directional Shaking on Liquefaction of Sands," by H.B. Seed, R. Pyke and G.R. Martin - 1975 (PB 258 781)A03

EERC 76-1 "Strength and Ductility Evaluation of Existing Low-Rise Reinforced Concrete Buildings - Screening Method," by T. Okada and B. Bresler - 1976 (PB 257 906)A11

EERC 76-2 "Experimental and Analytical Studies on the Hysteretic Behavior of Reinforced Concrete Rectangular and T-Beams," by S.-Y.M. Ma, E.P. Popov and V.V. Bertero - 1976 (PB 260 843)A12

EERC 76-3 "Dynamic Behavior of a Multistory Triangular-Shaped Building," by J. Petrovski, R.M. Stephen, E. Gartenbaum and J.G. Bouwkamp - 1976 (PB 273 279)A07

EERC 76-4 "Earthquake Induced Deformations of Earth Dams," by N. Serff, H.B. Seed, F.I. Makdisi & C.-Y. Chang - 1976 (PB 292 065)A08

EERC 76-5 "Analysis and Design of Tube-Type Tall Building Structures," by H. de Clercq and G.H. Powell - 1976 (PB 252 220) A10

EERC 76-6 "Time and Frequency Domain Analysis of Three-Dimensional Ground Motions, San Fernando Earthquake," by T. Kubo and J. Penzien (PB 260 556)A11

EERC 76-7 "Expected Performance of Uniform Building Code Design Masonry Structures," by R.L. Mayes, Y. Omote, S.W. Chen and R.W. Clough - 1976 (PB 270 098)A05

EERC 76-8 "Cyclic Shear Tests of Masonry Piers, Volume 1 - Test Results," by R.L. Mayes, Y. Omote, R.W. Clough - 1976 (PB 264 424)A06

EERC 76-9 "A Substructure Method for Earthquake Analysis of Structure - Soil Interaction," by J.A. Gutierrez and A.K. Chopra - 1976 (PB 257 783)A08

EERC 76-10 "Stabilization of Potentially Liquefiable Sand Deposits using Gravel Drain Systems," by H.B. Seed and J.R. Booker - 1976 (PB 258 820)A04

EERC 76-11 "Influence of Design and Analysis Assumptions on Computed Inelastic Response of Moderately Tall Frames," by G.H. Powell and D.G. Row - 1976 (PB 271 409)A06

EERC 76-12 "Sensitivity Analysis for Hysteretic Dynamic Systems: Theory and Applications," by D. Ray, K.S. Pister and E. Polak - 1976 (PB 262 859)A04

EERC 76-13 "Coupled Lateral Torsional Response of Buildings to Ground Shaking," by C.L. Kan and A.K. Chopra - 1976 (PB 257 907)A09

EERC 76-14 "Seismic Analyses of the Banco de America," by V.V. Bertero, S.A. Mahin and J.A. Hollings - 1976

EERC 76-15 "Reinforced Concrete Frame 2: Seismic Testing and Analytical Correlation," by R.W. Clough and J. Gidwani - 1976 (PB 261 323)A08

EERC 76-16 "Cyclic Shear Tests of Masonry Piers, Volume 2 - Analysis of Test Results," by R.L. Mayes, Y. Omote and R.W. Clough - 1976

EERC 76-17 "Structural Steel Bracing Systems: Behavior Under Cyclic Loading," by E.P. Popov, K. Takanashi and C.W. Roeder - 1976 (PB 260 715)A05

EERC 76-18 "Experimental Model Studies on Seismic Response of High Curved Overcrossings," by D. Williams and W.G. Godden - 1976 (PB 269 548)A08

EERC 76-19 "Effects of Non-Uniform Seismic Disturbances on the Dumbarton Bridge Replacement Structure," by F. Baron and R.E. Hamati - 1976 (PB 282 981)A16

EERC 76-20 "Investigation of the Inelastic Characteristics of a Single Story Steel Structure Using System Identification and Shaking Table Experiments," by V.C. Matzen and H.D. McNiven - 1976 (PB 258 453)A07

EERC 76-21 "Capacity of Columns with Splice Imperfections," by E.P. Popov, R.M. Stephen and R. Philbrick - 1976 (PB 260 378)A04

EERC 76-22 "Response of the Olive View Hospital Main Building during the San Fernando Earthquake," by S. A. Mahin, V.V. Bertero, A.K. Chopra and R. Collins - 1976 (PB 271 425)A14

EERC 76-23 "A Study on the Major Factors Influencing the Strength of Masonry Prisms," by N.M. Mostaghel, R.L. Mayes, R. W. Clough and S.W. Chen - 1976 (Not published)

EERC 76-24 "GADFLEA - A Computer Program for the Analysis of Pore Pressure Generation and Dissipation during Cyclic or Earthquake Loading," by J.R. Booker, M.S. Rahman and H.B. Seed - 1976 (PB 263 947)A04

EERC 76-25 "Seismic Safety Evaluation of a R/C School Building," by B. Bresler and J. Axley - 1976

EERC 76-26 "Correlative Investigations on Theoretical and Experimental Dynamic Behavior of a Model Bridge Structure," by K. Kawashima and J. Penzien - 1976 (PB 263 388)A11

EERC 76-27 "Earthquake Response of Coupled Shear Wall Buildings," by T. Srichatrapimuk - 1976 (PB 265 157)A07

EERC 76-28 "Tensile Capacity of Partial Penetration Welds," by E.P. Popov and R.M. Stephen - 1976 (PB 262 899)A03

EERC 76-29 "Analysis and Design of Numerical Integration Methods in Structural Dynamics," by H.M. Hilber - 1976 (PB 264 410)A06

EERC 76-30 "Contribution of a Floor System to the Dynamic Characteristics of Reinforced Concrete Buildings," by L.E. Malik and V.V. Bertero - 1976 (PB 272 247)A13

EERC 76-31 "The Effects of Seismic Disturbances on the Golden Gate Bridge," by F. Baron, M. Arikan and R.E. Hamati - 1976 (PB 272 279)A09

EERC 76-32 "Infilled Frames in Earthquake Resistant Construction," by R.E. Klingner and V.V. Bertero - 1976 (PB 265 892)A13

UCB/EERC-77/01 "PLUSH - A Computer Program for Probabilistic Finite Element Analysis of Seismic Soil-Structure Interaction," by M.P. Romo Organista, J. Lysmer and H.B. Seed - 1977

UCB/EERC-77/02 "Soil-Structure Interaction Effects at the Humboldt Bay Power Plant in the Ferndale Earthquake of June 7, 1975," by J.E. Valera, H.B. Seed, C.F. Tsai and J. Lysmer - 1977 (PB 265 795)A04

UCB/EERC-77/03 "Influence of Sample Disturbance on Sand Response to Cyclic Loading," by K. Mori, H.B. Seed and C.K. Chan - 1977 (PB 267 352)A04

UCB/EERC-77/04 "Seismological Studies of Strong Motion Records," by J. Shoja-Taheri - 1977 (PB 269 655)A10

UCB/EERC-77/05 "Testing Facility for Coupled-Shear Walls," by L. Li-Hyung, V.V. Bertero and E.P. Popov - 1977

UCB/EERC-77/06 "Developing Methodologies for Evaluating the Earthquake Safety of Existing Buildings," by No. 1 - B. Bresler; No. 2 - B. Bresler, T. Okada and D. Zisling; No. 3 - T. Okada and B. Bresler; No. 4 - V.V. Bertero and B. Bresler - 1977 (PB 267 354)A08

UCB/EERC-77/07 "A Literature Survey - Transverse Strength of Masonry Walls," by Y. Omote, R.L. Mayes, S.W. Chen and R.W. Clough - 1977 (PB 277 933)A07

UCB/EERC-77/08 "DRAIN-TABS: A Computer Program for Inelastic Earthquake Response of Three Dimensional Buildings," by R. Guendelman-Israel and G.H. Powell - 1977 (PB 270 693)A07

UCB/EERC-77/09 "SUBWALL: A Special Purpose Finite Element Computer Program for Practical Elastic Analysis and Design of Structural Walls with Substructure Option," by D.Q. Le, H. Peterson and E.P. Popov - 1977 (PB 270 567)A05

UCB/EERC-77/10 "Experimental Evaluation of Seismic Design Methods for Broad Cylindrical Tanks," by D.P. Clough (PB 272 280)A13

UCB/EERC-77/11 "Earthquake Engineering Research at Berkeley - 1976," - 1977 (PB 273 507)A09

UCB/EERC-77/12 "Automated Design of Earthquake Resistant Multistory Steel Building Frames," by N.D. Walker, Jr. - 1977 (PB 276 526)A09

UCB/EERC-77/13 "Concrete Confined by Rectangular Hoops Subjected to Axial Loads," by J. Vallenas, V.V. Bertero and E.P. Popov - 1977 (PB 275 165)A06

UCB/EERC-77/14 "Seismic Strain Induced in the Ground During Earthquakes," by Y. Sugimura - 1977 (PB 284 201)A04

UCB/EERC-77/15 "Bond Deterioration under Generalized Loading," by V.V. Bertero, E.P. Popov and S. Viwathanatepa - 1977

UCB/EERC-77/16 "Computer Aided Optimum Design of Ductile Reinforced Concrete Moment Resisting Frames," by S.W. Zagajeski and V.V. Bertero - 1977 (PB 280 137)A07

UCB/EERC-77/17 "Earthquake Simulation Testing of a Stepping Frame with Energy-Absorbing Devices," by J.M. Kelly and D.F. Tsztoo - 1977 (PB 273 506)A04

UCB/EERC-77/18 "Inelastic Behavior of Eccentrically Braced Steel Frames under Cyclic Loadings," by C.W. Roeder and E.P. Popov - 1977 (PB 275 526)A15

UCB/EERC-77/19 "A Simplified Procedure for Estimating Earthquake-Induced Deformations in Dams and Embankments," by F.I. Makdisi and H.B. Seed - 1977 (PB 276 820)A04

UCB/EERC-77/20 "The Performance of Earth Dams during Earthquakes," by H.B. Seed, F.I. Makdisi and P. de Alba - 1977 (PB 276 821)A04

UCB/EERC-77/21 "Dynamic Plastic Analysis Using Stress Resultant Finite Element Formulation," by P. Lukkunapvasit and J.M. Kelly - 1977 (PB 275 453)A04

UCB/EERC-77/22 "Preliminary Experimental Study of Seismic Uplift of a Steel Frame," by R.W. Clough and A.A. Huckelbridge 1977 (PB 278 769)A08

UCB/EERC-77/23 "Earthquake Simulator Tests of a Nine-Story Steel Frame with Columns Allowed to Uplift," by A.A. Huckelbridge - 1977 (PB 277 944)A09

UCB/EERC-77/24 "Nonlinear Soil-Structure Interaction of Skew Highway Bridges," by M.-C. Chen and J. Penzien - 1977 (PB 276 176)A07

UCB/EERC-77/25 "Seismic Analysis of an Offshore Structure Supported on Pile Foundations," by D.D.-N. Liou and J. Penzien 1977 (PB 283 180)A06

UCB/EERC-77/26 "Dynamic Stiffness Matrices for Homogeneous Viscoelastic Half-Planes," by G. Dasgupta and A.K. Chopra - 1977 (PB 279 654)A06

UCB/EERC-77/27 "A Practical Soft Story Earthquake Isolation System," by J.M. Kelly, J.M. Eidinger and C.J. Derham - 1977 (PB 276 814)A07

UCB/EERC-77/28 "Seismic Safety of Existing Buildings and Incentives for Hazard Mitigation in San Francisco: An Exploratory Study," by A.J. Meltsner - 1977 (PB 281 970)A05

UCB/EERC-77/29 "Dynamic Analysis of Electrohydraulic Shaking Tables," by D. Rea, S. Abedi-Hayati and Y. Takahashi 1977 (PB 282 569)A04

UCB/EERC-77/30 "An Approach for Improving Seismic - Resistant Behavior of Reinforced Concrete Interior Joints," by B. Galunic, V.V. Bertero and E.P. Popov - 1977 (PB 290 870)A06

UCB/EERC-78/01 "The Development of Energy-Absorbing Devices for Aseismic Base Isolation Systems," by J.M. Kelly and D.F. Tsztoo - 1978 (PB 284 978)A04

UCB/EERC-78/02 "Effect of Tensile Prestrain on the Cyclic Response of Structural Steel Connections, by J.G. Bouwkamp and A. Mukhopadhyay - 1978

UCB/EERC-78/03 "Experimental Results of an Earthquake Isolation System using Natural Rubber Bearings," by J.M. Eidinger and J.M. Kelly - 1978 (PB 281 686)A04

UCB/EERC-78/04 "Seismic Behavior of Tall Liquid Storage Tanks," by A. Niwa - 1978 (PB 284 017)A14

UCB/EERC-78/05 "Hysteretic Behavior of Reinforced Concrete Columns Subjected to High Axial and Cyclic Shear Forces," by S.W. Zagajeski, V.V. Bertero and J.G. Bouwkamp - 1978 (PB 283 858)A13

UCB/EERC-78/06 "Inelastic Beam-Column Elements for the ANSR-I Program," by A. Riahi, D.G. Row and G.H. Powell - 1978

UCB/EERC-78/07 "Studies of Structural Response to Earthquake Ground Motion," by O.A. Lopez and A.K. Chopra - 1978 (PB 282 790)A05

UCB/EERC-78/08 "A Laboratory Study of the Fluid-Structure Interaction of Submerged Tanks and Caissons in Earthquakes," by R.C. Byrd - 1978 (PB 284 957)A08

UCB/EERC-78/09 "Model for Evaluating Damageability of Structures," by I. Sakamoto and B. Bresler - 1978

UCB/EERC-78/10 "Seismic Performance of Nonstructural and Secondary Structural Elements," by I. Sakamoto - 1978

UCB/EERC-78/11 "Mathematical Modelling of Hysteresis Loops for Reinforced Concrete Columns," by S. Nakata, T. Sproul and J. Penzien - 1978

UCB/EERC-78/12 "Damageability in Existing Buildings," by T. Blejwas and B. Bresler - 1978

UCB/EERC-78/13 "Dynamic Behavior of a Pedestal Base Multistory Building," by R.M. Stephen, E.L. Wilson, J.G. Bouwkamp and M. Button - 1978 (PB 286 650)A08

UCB/EERC-78/14 "Seismic Response of Bridges - Case Studies," by R.A. Imbsen, V. Nutt and J. Penzien - 1978 (PB 286 503)A10

UCB/EERC-78/15 "A Substructure Technique for Nonlinear Static and Dynamic Analysis," by D.G. Row and G.H. Powell - 1978 (PB 288 077)A10

UCB/EERC-78/16 "Seismic Risk Studies for San Francisco and for the Greater San Francisco Bay Area," by C.S. Oliveira - 1978

UCB/EERC-78/17 "Strength of Timber Roof Connections Subjected to Cyclic Loads," by P. Gülkan, R.L. Mayes and R.W. Clough - 1978

UCB/EERC-78/18 "Response of K-Braced Steel Frame Models to Lateral Loads," by J.G. Bouwkamp, R.M. Stephen and E.P. Popov - 1978

UCB/EERC-78/19 "Rational Design Methods for Light Equipment in Structures Subjected to Ground Motion," by J.L. Sackman and J.M. Kelly - 1978 (PB 292 357)A04

UCB/EERC-78/20 "Testing of a Wind Restraint for Aseismic Base Isolation," by J.M. Kelly and D.E. Chitty - 1978 (PB 292 833)A03

UCB/EERC-78/21 "APOLLO - A Computer Program for the Analysis of Pore Pressure Generation and Dissipation in Horizontal Sand Layers During Cyclic or Earthquake Loading," by P.P. Martin and H.B. Seed - 1978 (PB 292 835)A04

UCB/EERC-78/22 "Optimal Design of an Earthquake Isolation System," by M.A. Bhatti, K.S. Pister and E. Polak - 1978 (PB 294 735)A06

UCB/EERC-78/23 "MASH - A Computer Program for the Non-Linear Analysis of Vertically Propagating Shear Waves in Horizontally Layered Deposits," by P.P. Martin and H.B. Seed - 1978 (PB 293 101)A05

UCB/EERC-78/24 "Investigation of the Elastic Characteristics of a Three Story Steel Frame Using System Identification," by I. Kaya and H.D. McNiven - 1978

UCB/EERC-78/25 "Investigation of the Nonlinear Characteristics of a Three-Story Steel Frame Using System Identification," by I. Kaya and H.D. McNiven - 1978

UCB/EERC-78/26 "Studies of Strong Ground Motion in Taiwan," by Y.M. Hsiung, B.A. Bolt and J. Penzien - 1978

UCB/EERC-78/27 "Cyclic Loading Tests of Masonry Single Piers: Volume 1 - Height to Width Ratio of 2," by P.A. Hidalgo, R.L. Mayes, H.D. McNiven and R.W. Clough - 1978

UCB/EERC-78/28 "Cyclic Loading Tests of Masonry Single Piers: Volume 2 - Height to Width Ratio of 1," by S.-W.J. Chen, P.A. Hidalgo, R.L. Mayes, R.W. Clough and H.D. McNiven - 1978

UCB/EERC-78/29 "Analytical Procedures in Soil Dynamics," by J. Lysmer - 1978

UCB/EERC-79/01 "Hysteretic Behavior of Lightweight Reinforced Concrete Beam-Column Subassemblages," by B. Forzani, E.P. Popov and V.V. Bertero - April 1979(PB 298 267)A06

UCB/EERC-79/02 "The Development of a Mathematical Model to Predict the Flexural Response of Reinforced Concrete Beams to Cyclic Loads, Using System Identification," by J. Stanton & H. McNiven - Jan. 1979(PB 295 875)A10

UCB/EERC-79/03 "Linear and Nonlinear Earthquake Response of Simple Torsionally Coupled Systems," by C.L. Kan and A.K. Chopra - Feb. 1979(PB 298 262)A06

UCB/EERC-79/04 "A Mathematical Model of Masonry for Predicting its Linear Seismic Response Characteristics," by Y. Mengi and H.D. McNiven - Feb. 1979(PB 298 266)A06

UCB/EERC-79/05 "Mechanical Behavior of Lightweight Concrete Confined by Different Types of Lateral Reinforcement," by M.A. Manrique, V.V. Bertero and E.P. Popov - May 1979(PB 301 114)A06

UCB/EERC-79/06 "Static Tilt Tests of a Tall Cylindrical Liquid Storage Tank," by R.W. Clough and A. Niwa - Feb. 1979 (PB 301 167)A06

UCB/EERC-79/07 "The Design of Steel Energy Absorbing Restrainers and Their Incorporation into Nuclear Power Plants for Enhanced Safety: Volume 1 - Summary Report," by P.N. Spencer, V.F. Zackay, and E.R. Parker - Feb. 1979(UCB/EERC-79/07)A09

UCB/EERC-79/08 "The Design of Steel Energy Absorbing Restrainers and Their Incorporation into Nuclear Power Plants for Enhanced Safety: Volume 2 - The Development of Analyses for Reactor System Piping,""Simple Systems" by M.C. Lee, J. Penzien, A.K. Chopra and K. Suzuki "Complex Systems" by G.H. Powell, E.L. Wilson, R.W. Clough and D.G. Row - Feb. 1979(UCB/EERC-79/08)A10

UCB/EERC-79/09 "The Design of Steel Energy Absorbing Restrainers and Their Incorporation into Nuclear Power Plants for Enhanced Safety: Volume 3 - Evaluation of Commercial Steels," by W.S. Owen, R.M.N. Pelloux, R.O. Ritchie, M. Faral, T. Ohhashi, J. Toplosky, S.J. Hartman, V.F. Zackay and E.R. Parker - Feb. 1979(UCB/EERC-79/09)A04

UCB/EERC-79/10 "The Design of Steel Energy Absorbing Restrainers and Their Incorporation into Nuclear Power Plants for Enhanced Safety: Volume 4 - A Review of Energy-Absorbing Devices," by J.M. Kelly and M.S. Skinner - Feb. 1979(UCB/EERC-79/10)A04

UCB/EERC-79/11 "Conservatism In Summation Rules for Closely Spaced Modes," by J.M. Kelly and J.L. Sackman - May 1979(PB 301 328)A03

UCB/EERC-79/12 "Cyclic Loading Tests of Masonry Single Piers; Volume 3 - Height to Width Ratio of 0.5," by P.A. Hidalgo, R.L. Mayes, H.D. McNiven and R.W. Clough - May 1979(PB 301 321)A08

UCB/EERC-79/13 "Cyclic Behavior of Dense Course-Grained Materials in Relation to the Seismic Stability of Dams," by N.G. Banerjee, H.B. Seed and C.K. Chan - June 1979(PB 301 373)A13

UCB/EERC-79/14 "Seismic Behavior of Reinforced Concrete Interior Beam-Column Subassemblages," by S. Viwathanatepa, E.P. Popov and V.V. Bertero - June 1979(PB 301 326)A10

UCB/EERC-79/15 "Optimal Design of Localized Nonlinear Systems with Dual Performance Criteria Under Earthquake Excitations," by M.A. Bhatti - July 1979(PB 80 167 109)A06

UCB/EERC-79/16 "OPTDYN - A General Purpose Optimization Program for Problems with or without Dynamic Constraints," by M.A. Bhatti, E. Polak and K.S. Pister - July 1979(PB 80 167 091)A05

UCB/EERC-79/17 "ANSR-II, Analysis of Nonlinear Structural Response, Users Manual," by D.P. Mondkar and G.H. Powell - July 1979(PB 80 113 301)A05

UCB/EERC-79/18 "Soil Structure Interaction in Different Seismic Environments," A. Gomez-Masso, J. Lysmer, J.-C. Chen and H.B. Seed - August 1979(PB 80 101 520)A04

UCB/EERC-79/19 "ARMA Models for Earthquake Ground Motions," by M.K. Chang, J.W. Kwiatkowski, R.F. Nau, R.M. Oliver and K.S. Pister - July 1979(PB 301 166)A05

UCB/EERC-79/20 "Hysteretic Behavior of Reinforced Concrete Structural Walls," by J.M. Vallenas, V.V. Bertero and E.P. Popov - August 1979(PB 80 165 905)A12

UCB/EERC-79/21 "Studies on High-Frequency Vibrations of Buildings - 1: The Column Effect," by J. Lubliner - August 1979 (PB 80 158 553)A03

UCB/EERC-79/22 "Effects of Generalized Loadings on Bond Reinforcing Bars Embedded in Confined Concrete Blocks," by S. Viwathanatepa, E.P. Popov and V.V. Bertero - August 1979

UCB/EERC-79/23 "Shaking Table Study of Single-Story Masonry Houses, Volume 1: Test Structures 1 and 2," by P. Gülkan, R.L. Mayes and R.W. Clough - Sept. 1979

UCB/EERC-79/24 "Shaking Table Study of Single-Story Masonry Houses, Volume 2: Test Structures 3 and 4," by P. Gülkan, R.L. Mayes and R.W. Clough - Sept. 1979

UCB/EERC-79/25 "Shaking Table Study of Single-Story Masonry Houses, Volume 3: Summary, Conclusions and Recommendations," by R.W. Clough, R.L. Mayes and P. Gülkan - Sept. 1979

UCB/EERC-79/26 "Recommendations for a U.S.-Japan Cooperative Research Program Utilizing Large-Scale Testing Facilities," by U.S.-Japan Planning Group - Sept. 1979(PB 301 407)A06

UCB/EERC-79/27 "Earthquake-Induced Liquefaction Near Lake Amatitlan, Guatemala," by H.B. Seed, I. Arango, C.K. Chan, A. Gomez-Masso and R. Grant de Ascoli - Sept. 1979(NUREG-CR1341)A03

UCB/EERC-79/28 "Infill Panels: Their Influence on Seismic Response of Buildings," by J.W. Axley and V.V. Bertero - Sept. 1979(PB 80 163 371)A10

UCB/EERC-79/29 "3D Truss Bar Element (Type 1) for the ANSR-II Program," by D.P. Mondkar and G.H. Powell - Nov. 1979 (PB 80 169 709)A02

UCB/EERC-79/30 "2D Beam-Column Element (Type 5 - Parallel Element Theory) for the ANSR-II Program," by D.G. Row, G.H. Powell and D.P. Mondkar - Dec. 1979(PB 80 167 224)A03

UCB/EERC-79/31 "3D Beam-Column Element (Type 2 - Parallel Element Theory) for the ANSR-II Program," by A. Riahi, G.H. Powell and D.P. Mondkar - Dec. 1979(PB 80 167 216)A03

UCB/EERC-79/32 "On Response of Structures to Stationary Excitation," by A. Der Kiureghian - Dec. 1979(PB 80166 929)A03

UCB/EERC-79/33 "Undisturbed Sampling and Cyclic Load Testing of Sands," by S. Singh, H.B. Seed and C.K. Chan - Dec. 1979(

UCB/EERC-79/34 "Interaction Effects of Simultaneous Torsional and Compressional Cyclic Loading of Sand," by P.M. Griffin and W.N. Houston - Dec. 1979

UCB/EERC-80/01 "Earthquake Response of Concrete Gravity Dams Including Hydrodynamic and Foundation Interaction Effects," by A.K. Chopra, P. Chakrabarti and S. Gupta - Jan. 1980(AD-A087297)A10

UCB/EERC-80/02 "Rocking Response of Rigid Blocks to Earthquakes," by C.S. Yim, A.K. Chopra and J. Penzien - Jan. 1980 (PB80 166 002)A04

UCB/EERC-80/03 "Optimum Inelastic Design of Seismic-Resistant Reinforced Concrete Frame Structures," by S.W. Zagajeski and V.V. Bertero - Jan. 1980(PB80 164 635)A06

UCB/EERC-80/04 "Effects of Amount and Arrangement of Wall-Panel Reinforcement on Hysteretic Behavior of Reinforced Concrete Walls," by R. Iliya and V.V. Bertero - Feb. 1980(PB81 122 525)A09

UCB/EERC-80/05 "Shaking Table Research on Concrete Dam Models," by A. Niwa and R.W. Clough - Sept. 1980(PB81 122 368)A06

UCB/EERC-80/06 "The Design of Steel Energy-Absorbing Restrainers and their Incorporation into Nuclear Power Plants for Enhanced Safety (Vol 1A): Piping with Energy Absorbing Restrainers: Parameter Study on Small Systems," by G.H. Powell, C. Oughourlian and J. Simons - June 1980

UCB/EERC-80/07 "Inelastic Torsional Response of Structures Subjected to Earthquake Ground Motions," by Y. Yamazaki April 1980(PB81 122 327)A08

UCB/EERC-80/08 "Study of X-Braced Steel Frame Structures Under Earthquake Simulation," by Y. Ghanaat - April 1980 (PB81 122 335)A11

UCB/EERC-80/09 "Hybrid Modelling of Soil-Structure Interaction," by S. Gupta, T.W. Lin, J. Penzien and C.S. Yeh May 1980(PB81 122 319)A07

UCB/EERC-80/10 "General Applicability of a Nonlinear Model of a One Story Steel Frame," by B.I. Sveinsson and H.D. McNiven - May 1980(PB81 124 877)A06

UCB/EERC-80/11 "A Green-Function Method for Wave Interaction with a Submerged Body," by W. Kioka - April 1980 (PB81 122 269)A07

UCB/EERC-80/12 "Hydrodynamic Pressure and Added Mass for Axisymmetric Bodies," by F. Nilrat - May 1980(PB81 122 343)A08

UCB/EERC-80/13 "Treatment of Non-Linear Drag Forces Acting on Offshore Platforms," by B.V. Dao and J. Penzien May 1980(PB81 153 413)A07

UCB/EERC-80/14 "2D Plane/Axisymmetric Solid Element (Type 3 - Elastic or Elastic-Perfectly Plastic) for the ANSR-II Program," by D.P. Mondkar and G.H. Powell - July 1980(PB81 122 350)A03

UCB/EERC-80/15 "A Response Spectrum Method for Random Vibrations," by A. Der Kiureghian - June 1980(PB81 122 301)A03

UCB/EERC-80/16 "Cyclic Inelastic Buckling of Tubular Steel Braces," by V.A. Zayas, E.P. Popov and S.A. Mahin June 1980(PB81 124 885)A10

UCB/EERC-80/17 "Dynamic Response of Simple Arch Dams Including Hydrodynamic Interaction," by C.S. Porter and A.K. Chopra - July 1980(PB81 124 000)A13

UCB/EERC-80/18 "Experimental Testing of a Friction Damped Aseismic Base Isolation System with Fail-Safe Characteristics," by J.M. Kelly, K.E. Beucke and M.S. Skinner - July 1980(PB81 148 595)A04

UCB/EERC-80/19 "The Design of Steel Energy-Absorbing Restrainers and their Incorporation into Nuclear Power Plants for Enhanced Safety (Vol 1B): Stochastic Seismic Analyses of Nuclear Power Plant Structures and Piping Systems Subjected to Multiple Support Excitations," by M.C. Lee and J. Penzien - June 1980

UCB/EERC-80/20 "The Design of Steel Energy-Absorbing Restrainers and their Incorporation into Nuclear Power Plants for Enhanced Safety (Vol 1C): Numerical Method for Dynamic Substructure Analysis," by J.M. Dickens and E.L. Wilson - June 1980

UCB/EERC-80/21 "The Design of Steel Energy-Absorbing Restrainers and their Incorporation into Nuclear Power Plants for Enhanced Safety (Vol 2): Development and Testing of Restraints for Nuclear Piping Systems," by J.M. Kelly and M.S. Skinner - June 1980

UCB/EERC-80/22 "3D Solid Element (Type 4-Elastic or Elastic-Perfectly-Plastic) for the ANSR-II Program," by D.P. Mondkar and G.H. Powell - July 1980(PB81 123 242)A03

UCB/EERC-80/23 "Gap-Friction Element (Type 5) for the ANSR-II Program," by D.P. Mondkar and G.H. Powell - July 1980 (PB81 122 285)A03

UCB/EERC-80/24 "U-Bar Restraint Element (Type 11) for the ANSR-II Program," by C. Oughourlian and G.H. Powell July 1980(PB81 122 293)A03

UCB/EERC-80/25 "Testing of a Natural Rubber Base Isolation System by an Explosively Simulated Earthquake," by J.M. Kelly - August 1980

UCB/EERC-80/26 "Input Identification from Structural Vibrational Response," by Y. Hu - August 1980(PB81 152 308)A05

UCB/EERC-80/27 "Cyclic Inelastic Behavior of Steel Offshore Structures," by V.A. Zayas, S.A. Mahin and E.P. Popov August 1980

UCB/EERC-80/28 "Shaking Table Testing of a Reinforced Concrete Frame with Biaxial Response," by M.G. Oliva October 1980(PB81 154 304)A10

UCB/EERC-80/29 "Dynamic Properties of a Twelve-Story Prefabricated Panel Building," by J.G. Bouwkamp, J.P. Kollegger and R.M. Stephen - October 1980

UCB/EERC-80/30 "Dynamic Properties of an Eight-Story Prefabricated Panel Building," by J.G. Bouwkamp, J.P. Kollegger and R.M. Stephen - October 1980

UCB/EERC-80/31 "Predictive Dynamic Response of Panel Type Structures Under Earthquakes," by J.P. Kollegger and J.G. Bouwkamp - October 1980(PB81 152 316)A04

UCB/EERC-80/32 "The Design of Steel Energy-Absorbing Restrainers and their Incorporation into Nuclear Power Plants for Enhanced Safety (Vol 3): Testing of Commercial Steels in Low-Cycle Torsional Fatigue," by P. Spencer, E.R. Parker, E. Jongewaard and M. Drory

UCB/EERC-80/33 "The Design of Steel Energy-Absorbing Restrainers and their Incorporation into Nuclear Power Plants for Enhanced Safety (Vol 4): Shaking Table Tests of Piping Systems with Energy-Absorbing Restrainers," by S.F. Stiemer and W.G. Godden - Sept. 1980

UCB/EERC-80/34 "The Design of Steel Energy-Absorbing Restrainers and their Incorporation into Nuclear Power Plants for Enhanced Safety (Vol 5): Summary Report," by P. Spencer

UCB/EERC-80/35 "Experimental Testing of an Energy-Absorbing Base Isolation System," by J.M. Kelly, M.S. Skinner and K.E. Beucke - October 1980(PB81 154 072)A04

UCB/EERC-80/36 "Simulating and Analyzing Artificial Non-Stationary Earthquake Ground Motions," by R.F. Nau, R.M. Oliver and K.S. Pister - October 1980(PB81 153 397)A04

UCB/EERC-80/37 "Earthquake Engineering at Berkeley - 1980," - Sept. 1980

UCB/EERC-80/38 "Inelastic Seismic Analysis of Large Panel Buildings," by V. Schricker and G.H. Powell - Sept. 1980 (PB81 154 338)A13

UCB/EERC-80/39 "Dynamic Response of Embankment, Concrete-Gravity and Arch Dams Including Hydrodynamic Interaction," by J.F. Hall and A.K. Chopra - October 1980(PB81 152 324)A11

UCB/EERC-80/40 "Inelastic Buckling of Steel Struts Under Cyclic Load Reversal," by R.G. Black, W.A. Wenger and E.P. Popov - October 1980(PB81 154 312)A08

UCB/EERC-80/41 "Influence of Site Characteristics on Building Damage During the October 3, 1974 Lima Earthquake," by P. Repetto, I. Arango and H.B. Seed - Sept. 1980(PB81 161 739)A05

UCB/EERC-80/42 "Evaluation of a Shaking Table Test Program on Response Behavior of a Two Story Reinforced Concrete Frame," by J.M. Blondet, R.W. Clough and S.A. Mahin